Harper Adams University

A Thesis Submitted for the Degree of Doctor of Philosophy at

Harper Adams University

Development of a predictive irrigation scheduling framework

Thesis submitted to the Harper Adams University for the degree of Doctor of Philosophy

Engineering Department

Olutobi Adeyemi

BEng. MSc.

2019

Harper Adams University

Abstract

Precision irrigation scheduling is critical for improving irrigation efficiency. However, to realize a robust precision irrigation scheduling workflow, adaptive decision support systems need to be incorporated and enabled as part of the workflow. Furthermore, these adaptive systems should be developed to align with the three key requirements of precision irrigation; measurement, monitoring and management.

The overall hypothesis of this research project was that data-driven models which are capable of predicting crop water requirements and the plant response to water supply can aid precision irrigation scheduling. There were three specific objectives which were formulated with the key requirements of precision irrigation in mind.

The first objective focused on the need to ensure the availability of quality data from soil moisture sensors in order to realize robust irrigation scheduling decisions. The performance of three dielectric soil moisture sensors was evaluated under varying conditions of soil texture, bulk density, temperature and salinity. Results indicated that calibration equations developed in the laboratory improved the accuracy of these sensors for all conditions.

The second objective focused on the development of data-driven dynamic models to aid the precision irrigation management of greenhouse cultivated lettuce plants. Dynamic models were developed for the prediction of the baseline temperatures and transpiration dynamics. Results indicated that the crop water stress index (CWSI) computed using the predicted baseline temperatures was significantly correlated with the theoretical CWSI and successfully distinguished the water status of lettuce plants receiving fractional irrigation amounts. The information contained in the residuals calculated from the measured and model predicted transpiration was exploited as a means of inferring the plant water status. This method successfully identified plants experiencing a shortage of water supply, achieving a sensitivity similar to stomatal conductance measurements.

The third objective focused on the development of dynamic neural network models for the prediction of the volumetric soil water content (VWC). The application of the models for predictive irrigation scheduling was also explored. The models successfully generated accurate one-day-ahead predictions of the VWC with minimal input data pre-processing. Using model-based simulations of the potato growing season, it was demonstrated that a water-saving ranging between 20 – 46% can be achieved when these models are used in a predictive irrigation scheduling system.

In conclusion, the study demonstrated the applicability of adaptive data-driven dynamic models for irrigation monitoring and management. The proposed adaptive models can be combined to realize a synergistic sustainable precision irrigation system.

Declaration

The thesis has been written by myself and describes the work carried out by myself unless otherwise stated. Information from other sources has been fully acknowledged and referenced in the text.

Olutobi Adeyemi

May 2019

Acknowledgments

Most of this research project has been successfully carried out thanks to the guidance, expertise and support of Dr. Tomas Norton. The continuous support of the other members of my supervisory team, Dr. Sven Peets and Dr. Ivan Grove has been incredibly precious. With their guidance and supervision, I was able to successfully conduct the experiments and modelling, and write the thesis.

The mathematical and modelling expertise of my colleague Yuvraj Domun had a huge impact on the success of this research. I also acknowledge the support provided by my colleagues, Mohammed, Ayoola, and Jeremiah. I am grateful to the staff of the engineering department for their support.

This work was possible with thanks to the funding provided by John Oldacre foundation.

I need to acknowledge all my family, in particular, my parents, parents-in-law, my sister Tosin and my brother Folabi. Their emotional and moral support is appreciated.

A lot of gratitude is for my lovely wife Tayo who has always supported me and my daughter Toyosi who constantly brings joy into my life.

List of Publications

The thesis is presented as a compilation style thesis where the chapters are formed from either published or submitted peer reviewed journal papers. Citations for the papers are given below together with their publication status at the time of thesis submission and the version of the manuscript presented within the thesis.

Chapter 1

Adeyemi, O., Grove, I., Peets, S., Norton, T., 2017. Advanced Monitoring and Management Systems for Improving Sustainability in Precision Irrigation. Sustainability 9, 1–29.

Chapter 1 is an updated version of the original publication.

Chapter 2

Adeyemi, O., Grove, I., Peets, S., Domun, Y., Norton, T. Peformance Evaluation of Three Dielectric Soil Moisture Sensors.

Submitted to the International Journal of Agricultural and Biological Engineering.

Chapter 3

Adeyemi, O., Grove, I., Peets, S., Domun, Y., Norton, T., 2018. Dynamic Modelling of the Baseline Temperatures for Computation of the Crop Water Stress Index (CWSI) of a Greenhouse Cultivated Lettuce Crop. Computers and Electronics in Agriculture 153, 102 – 114.

Published and the post-print version is presented in the thesis.

Chapter 4

Adeyemi, O., Grove, I., Peets, S., Domun, Y., Norton, T., 2018. Dynamic Modelling of Lettuce Transpiration for Water Status Monitoring. Computers and Electronics in Agriculture 155, 50 – 57.

Published and the post-print version is presented in the thesis.

Chapter 5

Adeyemi, O., Grove, I., Peets, S., Domun, Y., Norton, T., 2018. Dynamic Neural Network Modelling of Soil Moisture Content for Predictive Irrigation Scheduling. Sensors 18, 3408.

Published and the post-print version is presented in the thesis. The post-print version included in the thesis is presented with an amended in-text citation to ensure a uniform citation style within the thesis.

For all publications, the experiments, data analysis, modelling and write-up was conducted by myself (Olutobi Adeyemi). Sven Peets, Tomas Norton and Ivan Grove reviewed the manuscripts and suggested corrections. Yuvraj Domun contributed to version control of the source code applied in the modelling and code reviews.

Table of Contents

List of Figures

Chapter 5

List of Tables

Chapter 1 Introduction and literature review

Abstract

Globally, the irrigation of crops is the largest consumptive user of fresh water. Water scarcity is increasing worldwide, resulting in tighter regulation of its use for agriculture. This necessitates the development of irrigation practices that are more efficient in the use of water but do not compromise crop quality and yield. Precision irrigation already achieves this goal, in part. The goal of precision irrigation is to accurately supply the crop water need in a timely manner and as spatially uniformly as possible. However, to maximize the benefits of precision irrigation, additional technologies need to be enabled and incorporated into agriculture. This review discusses how incorporating adaptive decision support systems into precision irrigation management will enable significant advances in increasing the efficiency of current irrigation approaches. From the literature review, it is found that precision irrigation can be applied in achieving the environmental goals related to sustainability. The demonstrated economic benefits of precision irrigation in field-scale crop production is however minimal. It is argued that a proper combination of soil, plant and weather sensors providing real-time data to an adaptive decision support system provides an innovative platform for improving sustainability in irrigated agriculture. The review also shows that adaptive decision support systems integrated with data-driven models are able to adequately account for the time-varying nature of the soil-plant-atmosphere system. The review also shows that model-based decision support systems are able to consider operational limitations and agronomic objectives in arriving at optimal irrigation decisions. It is concluded that significant improvements in crop yield and water savings can be achieved by incorporating data-driven predictive models into precision irrigation decision support tools. Further improvements in water savings can also be realized by including deficit irrigation as part of the overall irrigation management strategy. Nevertheless, future research is needed for identifying crop response to regulated water deficits, developing improved soil moisture and plant sensors, and developing self-learning crop simulation frameworks that can be applied to evaluate adaptive decision support strategies related to irrigation.

1 Introduction

Globally, 70% of water use is applied in irrigation of crops, making irrigation the largest consumptive user of fresh water (Knox et al., 2012). Over 80% of freshwater withdrawals in developing countries is applied in irrigation (Hedley et al., 2014). Irrigated agriculture provides 40% of the world's food from less than 20% of the cultivated area highlighting the importance of irrigation in global food security (Turral et al., 2010).

Irrigated crop production globally extends over 275 million hectares, with an estimated annual increase of 1.3% (Hedley et al., 2014). Global climate change may further increase irrigation water demand due to a greater variation in annual precipitation amounts (Döll, 2002). Postel (1998) suggested that irrigation will provide 46% of the global crop water requirement by 2025, which was computed as 28% in 1995, resulting in a decline of rain-fed agriculture. Food production in the developing world, notably in South, Southeast and East Asia, is at present heavily reliant on irrigation. The total irrigated area in Asia is 230 million ha, which represents over 70% of the global irrigated area. Of the 230 million ha of the irrigated land area, 60% is located in China and India (Turral et al., 2010). It is estimated that 75% of the grain production in China is dependent on irrigation (Hedley et al., 2014). Sarma (2016) noted that India uses as much as four times more water to produce one unit of a major food crop as compared to the USA and Europe. This implies that an improvement in water use efficiency in the developing world would conserve at least half of the water presently applied in irrigation.

It is estimated that a water volume of 2630 km^3 is abstracted yearly from surface and groundwater sources for irrigated crop production. The absence of surface water sources in a number of communities has further increased the pressure on groundwater resources. This has resulted in the over-abstraction of global groundwater sources which is calculated to be as much as 163 km^3 per annum (Hedley et al., 2014). A global shortage in freshwater sources is predicted unless action is taken to improve water management, savings and increase water use efficiency. This has necessitated greater regulatory demands for environmental protection of freshwater (De Fraiture and Wichelns, 2010). It is reported that only half of the total freshwater volume abstracted for irrigation globally reaches the targeted crops (Hedley et al., 2014). These have brought about the need to devise procedures to use the limited water more efficiently while maximizing crop yield and quality.

Conventional irrigation practice involves applying water uniformly over every part of the field without taking into account the spatial variability in soil and crop water needs; this consequently leads to over-irrigation in some parts of the field while other parts of the field are under irrigated (Daccache et al., 2014). The risks associated with over-irrigation include surface runoff, deep percolation, and leaching of nitrates and nutrients. Those associated with under-irrigation are more subjective and include a reduction in crop yields

and quality, as well as inefficient use of fertilizer and other supplemental inputs for crop production (Al-Karadsheh, 2002).

The irrigation process requires a high level of ‘precision’ in order to optimize the water input and crop response while minimizing adverse environmental impacts. Precision irrigation is an evolving field with active interest by both industry and academic researchers. It is conceptualized by some researchers as the use of efficient irrigation application systems, whereas others view it as the variable application of irrigation based on predefined maps or sensor feedback (Raine et al., 2007). Smith et al. (2010) suggested that ‘precision’ involves the accurate determination, quantification of crop water needs and the precise application of the optimal water volume at the required time. This implies that varying water application spatially is not the sole requirement for the achievement of ‘precision’ in the irrigation process. Hence, precision irrigation can be defined as the process of accounting for the field-scale spatial variability in crop water need and applying the right amount of water to match the spatial crop water need at the right time (Al-Karadsheh, 2002). The advantages associated with precision irrigation include increased crop yields, improved crop quality, improved water use efficiency/savings, reduction of energy costs and reduction of adverse environmental impacts (Shah and Das, 2012). Pierce (2010) viewed precision irrigation as a tool for improving sustainability in irrigated agriculture in terms of improved irrigation water use efficiency and improved environmental quality of irrigated fields.

The balance of several core aspects is however important for the successful implementation of a robust precision irrigation system. Implementing a precision irrigation system involves efforts on real-time monitoring of crop and soil conditions, scheduling irrigation and control of the irrigation application equipment. Research has been mainly focused on the sensing and control aspects of precision irrigation with much advancements in the last decade (Shah and Das, 2012). Research is limited, however, in the development of appropriate irrigation scheduling tools for the precision irrigation process (DeJonge et al., 2007). Irrigation scheduling is the process by which a producer determines when to apply irrigation and the amount of irrigation water to apply (Ali and Talukder, 2001). Hornbuckle et al. (2009) suggested that the irrigation scheduling endeavor should be treated as an all-encompassing decision support system for irrigation management. A robust decision support system is important in the successful implementation of precision irrigation. The need for a decision support system capable of real-time management decisions of when, where and how much to irrigate while also considering uncertainty in climatic inputs, the time-varying nature of cropping systems, as well as equipment and operational limitations cannot be overemphasized. Rhodig and Hillyer (2013) noted that the development of an optimal decision support tool for precision irrigation will involve the combination of appropriate modelling and management tools.

The decision support tools available for precision irrigation management are presently inflexible and difficult to adapt to varying cropping scenarios (Evans and King, 2012).
In recent years, there has been a number of in-depth reviews on precision irrigation (e.g. (O'Shaughnessy and Rush, 2014; Shah and Das, 2012; Smith et al., 2010)), and the intention here is not to repeat the areas they addressed. Rather, the aim is to provide an in-depth technical analysis of the considerations necessary for the development of a practical and robust decision support system for precision irrigation in order to improve sustainable irrigated agriculture. To that end, this review will focus on the following critical aspects of precision irrigation: (1) monitoring considerations; (2) present limitations and state of the art in decision support; and (3) opportunities for improving sustainability. Brief sections on the concept of spatial variability and the control of water application in precision irrigation will, however, be included.

2 Spatial Variability: The long-term challenge of irrigated agriculture

The underlying argument for precision irrigation is the presence of within-field spatial variability that influences crop water demand. The spatial variability in crop water demand may have a direct influence on the crop yield, quality and the environmental quality of irrigated fields (Smith et al., 2009). The soil water presents the sole source of water available for direct plant uptake and therefore its spatial variability will have a direct influence on crop water demand. Soil and landscape characteristics like soil texture, topography, abiotic and management factors (e.g., compaction, tillage) and hydraulic properties vary spatially across a field (Smith et al., 2010). These have a direct influence on the water-holding capacity of the soil. Hedley and Yule (2009) reported that the spatial variation in the soil water retention characteristics was strongly correlated with the spatial variation in soil texture across a field, noting that areas with heavier soils within a field had a larger water-holding capacity in comparison to those with light textured soils. The advent of rapid non-invasive technologies for mapping soil properties, specifically electrical conductivity mapping, can reveal within-field variability that can guide in variable rate irrigation management. These have been successfully applied by Hedley and Yule (2009) and Daccache et al. (2014). A comprehensive overview of electrical conductivity mapping is presented in (Misra and Padhi, 2014; Kuhn et al., 2009)
The variability in yield across a field has also been found to be strongly correlated with the spatial variability in water available for crop use. The spatial variability in crop yield is a function of the interplay between water stress, nutrients, in addition to soil's physical and chemical properties (Thorp et al., 2008). The yield map can be correlated with the soil electrical conductivity (EC) map. These similarities can be explained through the spatial variability of soil properties that exists across a field. The water-holding capacity of the soil is a major factor affecting yield, and the yield map will likely show a strong correlation to soil EC (Lund et al., 2000). Irmak et al. (2001) noted that the spatial variability in soil water

retention characteristics played a dominant role in explaining the spatial yield variability observed in soybean. Martínez-Casasnovas et al. (2006) suggested yield mapping as an important tool in variable rate irrigation management.

A robust precision irrigation system will be able to meet the spatially varying crop water demand across a field at the right time. This requires accurate knowledge of the within-field variability. This is addressed by applying the concept of irrigation management zones/units in precision irrigation. The irrigation management zones are a group of homogeneous units with similar soil water retention characteristics (Hedley and Yule, 2009). It is however important that these management zones are large enough to be managed individually while remaining relatively homogeneous in order to reflect the spatial soil variation across the units. The delineation of irrigation management zones based on real-time sensor data has also been demonstrated. This is achieved by applying infrared thermometry/thermography to assess the spatial variation in crop canopy temperature across a field (Jones and Leinonen, 2003). The crop canopy temperature of a healthy transpiring crop will often be less than that of the ambient air. When crop transpiration is reduced as a result of water deficits, the crop canopy temperature is expected to increase. The characterization of crop water status as a function of the canopy and ambient temperature is the basis for using infrared thermometry/thermography as a mapping tool for precision irrigation (Jackson et al., 1981). Shaughnessy et al. (2014) and Evett et al. (2013) have successfully applied this procedure in generating dynamic maps to guide variable rate water application for field crops grown under a center pivot system. It should, however, be noted that infrared temperature measurements are usually taken over a short period, mostly at midday when the crop is expected to experience the highest evaporative demand. Hence, this method is well suited for crop production systems in which the soil moisture dynamics has relatively long time constants.

3 Spatial scales of irrigation management

Center-pivot, lateral move, and low energy precision application (LEPA) moving machines can be modified to apply spatially variable irrigation (Raine and Mccarthy, 2009). These systems are particularly suited to variable rate water application because of their current level of automation and large coverage area with a single lateral pipe. Fixed irrigation systems also have the potential to be deployed for variable rate water application as they can be very accurate and can be automated based on sensor feedback (Hedley et al., 2014). Implementing a spatially varied irrigation system requires an understanding of the characteristics of the irrigation application system deployed including the spatial scales covered by the water application equipment. The spatial scale associated with the

variability in crop water requirements and its impact on yield should also be identified (Raine and Mccarthy, 2009).

O'Shaughnessy and Rush (2014) suggested that the size and numbers of irrigation management zones that can be controlled in a precision irrigation strategy will determine the overall flexibility of the system. For moving application systems, the width of the management zone is dependent on the number of drops or nozzles within an individually controlled set (i.e., sprinklers controlled by a single solenoid valve) and the length will be dependent on the pattern of variability in the direction of the traveling sprinkler. The wind speed and the overlap from the wetted sprinkler patterns between management zones will also affect the accuracy of the water volume applied. Raine and Mccarthy (2009) noted that the spray diameter and overlap achieved by moving application systems make it impossible to target water applications on a single crop basis using these systems. Hedley et al. (2014) suggested that the economic benefits of spatially varied irrigation should be an important consideration even when the system is considered achievable from a technical standpoint. The spatial scales associated with moving and fixed irrigation systems are presented in Table 1. Smith et al. (2010) concluded that the spatial resolution of a precision irrigation system will be influenced by the spatial scales associated with the application system, the spatial resolution of the infield sensors and the spatial scales associated with the variability in crop water requirements.

Table 1. Spatial scales of fixed and moving irrigation systems.

System	Spatial Unit	Order of Magnitude of Spatial Scale (m^2)
Sprinkler - solid set	Wetted area of single sprinkler	100
Center-pivot, lateral move	Wetted area of single sprinkler	100
LEPA-bubbler	Furrow dyke	1
Traveling irrigator	Wetted area of sprinkler	5000
Drip	Wetted area of an emitter	1 to 10
Micro-spray	Wetted area of single spray	20

LEPA: low energy precision application. Source: (Raine and Mccarthy, 2009).

4 Control of water application in precision irrigation

The water application system used in the precision irrigation process must be able to control the water application volume applied per unit time to each defined irrigation management unit within a field (Pierce, 2010). The development of variable rate water application systems has been mostly focused on continuous move systems (Smith et al., 2010).

The control of water application on continuous move systems (center-pivot, linear move, boom and reel) is based on databases of spatially referenced data defining irrigation management units (Hedley and Yule, 2009). The volume of water applied to each management unit can be achieved by varying the application rate of sprinklers or controlling the ground speed of continuous move systems (Pierce, 2010).

The application rate of sprinklers is mostly varied through the pulse modulation of the sprinkler nozzles. This involves the application of normally opened solenoid valves to control flow through an individual or group of sprinkler heads. The solenoid turns the flow of water either on or off at a sprinkler location in order to achieve the desired application depth within a specified cycle time. The cycle time is the total number of switching (either to on or off phase) required by the solenoid valves during a pulse cycle (Evans et al., 2012). Evans et al. (2012) applied the pulse modulated sprinkler control on a linear move sprinkler system. Daccache et al. (2014) also applied a pulsed modulated sprinkler control on a boom and reel irrigation system. Field evaluation of both systems indicated a satisfactory performance over a range of water application rates. They, however, noted a problem with sprinkler overlap at the edge of the irrigation management units.

The variation in irrigation volume applied by a continuous move system can also be achieved by varying its travel speed. The sprinklers on the manifold of the irrigation system are usually operated at a specified flow rate and pressure. An increase in travel speed of the system reduces the application depth and a decrease in the travel speed increases the application depth (Hezarjaribi, 2008). This type of system cannot be applied in situations where variable application depths are needed along the length of the irrigation system (Evans et al., 2012). Al-Karadsheh (2002) evaluated the performance of speed control in achieving variable water application rate on a linear move system. The wetted diameter of the sprinklers was reported to be between 15.2–21.3 m. He reported that the system needed to travel a minimum distance of 16 m before the desired change in application volume could be reached. This suggests that this system is not suitable for use in applications where the management units are small in scale.

The adaptation of fixed irrigation systems for variable rate water application has been achieved (e.g., (Coates and Delwiche, 2008)). Variable water rate application in these systems is usually achieved either by individual nozzle or emitter control, or zone management (Pierce, 2010). A comprehensive review of such systems is presented in Pierce (2010). Miranda et al. (2005) described a distributed control system implemented

to achieve variable rate water application in a fixed irrigation system operating in predefined management zones. Their results indicated that the system was able to apply the irrigation volume required in each zone. Goumopoulos et al. (2014) also implemented a variable rate water application setup for a fixed irrigation system capable of zone-specific irrigation of strawberries. Individual nozzle control in a micro-sprinkler system has been demonstrated by Coates et al. (2013). They reported individual control of 54 nodes in a vineyard with the system. The nozzle connected to each node was capable of achieving a unique water application volume. They concluded that the water requirements of each defined zone in the vineyard can be individually met by the irrigation system. The authors reported a payback period of between 3.5–4.5 years for the system.

5 Monitoring

The routine or continuous monitoring of moisture fluxes in the soil-plant-atmosphere system is a fundamental aspect of managing crop production in irrigated agriculture. Monitoring can essentially be viewed as the application of various sensing technologies in determining and characterizing the spatiotemporal moisture dynamics and plant water use. These sensing methods can be classified under three broad headings: soil-based, weather-based and plant-based sensing (Steele et al., 1994). Soil-based sensing typically involves the use of sensors to determine the soil moisture content or potential. This information is then used to infer the amount of water available for plant use and its temporal dynamics. The weather-based sensing involves the use of the crop evapotranspiration to determine the temporal crop water use. The evapotranspiration is determined using climatic variables such as radiation, rainfall and wind speed (Allen et al., 1998; Leib et al., 2002). The plant-based sensing involves the determination of plant water status which is usually related to plant physiology. Measurements of canopy temperature, stomatal resistance, sap flow, leaf turgor pressure, stem diameter and leaf thickness are used to infer plant water status (Pardossi and Incrocci, 2011).

Recent advances in remote sensing has enhanced the possibility of monitoring the spatial nature of both soil and crop water status. Remote sensing encompasses non-contact technologies that are capable of sensing radiation reflected or emitted from agricultural fields. They are deployed using satellites, aerial platforms, and tractors (Mulla, 2013). These technologies have a high spatial resolution and are well suited for regional soil and crop water evaluation (Verstraeten et al., 2008). This review focuses on sensing technologies that can be applied in monitoring field-scale soil and crop water dynamics. A comprehensive review of remote sensing technologies applicable in precision agriculture is presented in (Mulla, 2013; Jones and Schofield, 2008).

5.1 Soil-based sensing

The knowledge of soil moisture fluxes comprising of the depletion and refill of soil water can be used to monitor crop water use hence making it a useful tool in irrigation scheduling and management decisions (Bellingham, 2009). Several methods have been developed for measuring soil moisture content; they are indirect methods which rely on the strong relationship between a particular property of the soil and the soil moisture content. Moreover, they are able to provide continuous monitoring and are non-destructive (Vereecken et al., 2014). In precision irrigation, the commonly applied method for monitoring the temporal dynamics of field-scale soil moisture is the dielectric-based method (Hedley and Yule, 2009). This is because of the ease of their deployment in large-scale soil moisture sensor networks (Romano et al., 2013). Thus, the proper deployment and management of this technology can optimize the sustainability of irrigated agriculture. Consequently, this section will outline a brief description of this method including a consideration of the factors affecting sensor performance. A detailed description of other state-of-the-art soil moisture sensing technologies is presented in (Romano, 2014; Zhu et al., 2012).

5.1.1 Dielectric soil moisture sensors

Dielectric soil moisture sensors operate by exploiting the dielectric properties of soil and its constituents (Phillips et al., 2014). The relative dielectric permittivity of a substance is used to describe the effect of an electromagnetic field on its molecular structure. It is a dimensionless constant greater than one, made up of a real and imaginary part (Topp, 2003). The apparent relative dielectric permittivity of soil, $\varepsilon'_{\mathrm{soil}}$ is a function of its constituents majorly being water, air, and solid particles. The relative dielectric permittivity of the other constituents except water has a negligible effect as they have small values in the range of 1–7. The one of water, $\varepsilon'_{\mathrm{water}}$ having a value of approximately 80 has the most remarkable effect. It is, therefore, possible to correlate the volumetric moisture content (VMC) to $\varepsilon'_{\mathrm{soil}}$ using empirical equations at a frequency range of between 50 MHz and 17 GHz. At this high-frequency range, $\varepsilon'_{\mathrm{soil}}$ is highly stable and it is usually referred to as the apparent dielectric permittivity of soil (Iaea, 2008).

A range of electromagnetic sensors exploits this property to provide a non-destructive in situ measurement of soil moisture contents. They include Time Domain Reflectometry (TDR) Sensors, Time Domain Transmission (TDT) Sensors and Capacitance Sensors. The Capacitance Sensors are commonly referred to as Frequency Domain Reflectometry Sensors (FDR). A detailed mathematical description of the operating principles of dielectric soil moisture sensors has been included in the supplementary materials.

5.1.2 Factors affecting the performance of dielectric soil moisture sensors

The accuracy of data from soil moisture sensors is important in the precision irrigation process. Over-estimation of soil moisture status may lead to a delay in irrigation scheduling decisions and consequently affect crop yield and quality. Underestimation of soil moisture status, on the other hand, may lead to the application of irrigation too often or when not required by the crops. This will result in water/energy wastage and adverse environmental effects.

Dielectric soil moisture sensors measure the soil moisture content for the soil volume corresponding to their sphere of influence. The various factors affecting the performance of dielectric soil moisture sensors include bulk electrical conductivity (salinity), soil texture, bulk density, and temperature. A variation in any of these factors around the sphere of influence of the dielectric sensor will have an effect on its performance. These properties vary with location and depth in a soil profile and it is important to take them into account when calibrating dielectric soil moisture sensors (Geesing et al., 2004). These sensors often rely on site-specific calibration, but they often come with 'universal' calibrations which can be used where absolute accuracy is not required. The accuracy of calibration equations supplied by manufacturers of these sensors are usually between a range of ±4 - 2% VMC when applied in non-saline soils (Adeyemi et al., 2016). Site-specific calibration equations which are developed by comparing the sensor output to gravimetrically derived soil moisture content can be applied when a higher level of accuracy is required (Rowlandson et al., 2013). In addition, for capacitance type probes, it is essential that the probe access tubes are fitted correctly without air gaps to ensure robust soil water measurements. A summary of research on factors affecting the performance of dielectric sensors is presented in Table 2. A detailed technical description of factors affecting the performance of dielectric sensors can be found in (Nemali et al., 2007; Saito et al., 2009).

Table 2. Factors affecting the performance of various Dielectric soil moisture sensors

Authors	EM Sensor Type	Factors Affecting Measurement Investigated	Comments
Benor et al. (2013)	TDR	Bulk Electrical Conductivity (EC)	Errors in VMC estimation encountered with high EC
Böhme et al. (2013)	FDR	Soil Organic Content, Soil Texture and Bulk Density	Variation in soil organic content introduced errors in VMC estimation
Kristoph-Dietrich et al. (2012)	FDR	Soil Organic Content, Soil Texture and Bulk Density	Variation in soil organic content introduced errors in VMC estimation in wetlands
Nemali et al. (2007)	FDR	Pore Electrical Conductivity and Temperature	High EC and temperature introduced errors in VMC estimation in soilless substrates
Kelleners et al. (2005)	TDR and FDR	Frequency Dependence of Dielectric Permittivity	Errors in VMC estimation with FDR due to low operating frequency. No errors encountered with TDR
Keshavarzi et al. (2015)	TDR	Soil Organic Content	Increase in organic content resulted in an underestimation of VMC
Varble and Chávez (2011)	TDR, TDT, and FDR	Bulk Electrical Conductivity and Temperature	Increase in Bulk EC caused errors in VMC estimation in the three sensors. The TDR and FDR sensor measurements were influenced by soil temperature fluctuations

5.2 Proximal sensing and mapping of soil moisture

The recent advances in rapid mapping and positioning technologies enable the spatial characterization of soil moisture retention properties to inform precision irrigation decisions. The electromagnetic induction (EM) technique is used in combination with accurate positioning systems to quantify soil moisture variability at resolutions less than 10 m. It also provides a highly accurate digital elevation map (DEM) (Hedley et al., 2014). The EM sensor maps the soil's apparent EC which is influenced by soil texture and moisture in non-saline soils (Vereecken et al., 2014). Those same factors correlate highly to the soil's water-holding capacity. Based on the EC maps, a targeted soil sampling can be conducted at different parts of the field. Topographic features that are likely to influence field-scale soil moisture dynamics are derived using the DEM (Hedley et al., 2013).

The EC maps enable the grouping of discrete units known as management units with similar available water-holding capacity (AWC) characteristics which can then be used in selecting soil moisture monitoring sites. This has been demonstrated by (Evans et al., 2012; Pan et al., 2013). The data from soil moisture sensors located in the management units can also be used in generating dynamic application maps based on a relationship between the soil moisture depletion and the mapped EC values. These application maps serve as an input into the precision irrigation control system. Hedley and Yule (2009) applied soil moisture sensors and an EC map in generating dynamic water status maps for a 35.2 ha irrigated maize field. Daccache et al. Daccache et al. (2014) applied a similar method in producing dynamic soil moisture maps for various fields.

The electric resistivity tomography technique can also be applied in deriving the EC map of a field. Hedley et al. (2014) reported that the method has a good vertical resolution but it cannot be deployed on a moving platform for rapid non-invasive mapping. It has been applied by Kelly et al. (2011) in positioning soil moisture sensors to support irrigation decisions.

The ground-penetrating radar (GPR) can also be applied in monitoring the field-scale soil moisture status (Romano, 2014). It can be mounted on a vehicle or moving irrigation system for mapping soil moisture in a field. The GPR is however affected by high clay content, is not amenable to automation and requires further development to improve its viability in precision irrigation applications (Bogena et al., 2007).

The deployment of soil moisture sensors in management units defined by these mapping techniques enables the dynamic updates of soil moisture maps which can aid variable rate water application.

5.3 Weather-based sensing

Weather-based sensing involves the use of climatic variables in determining evapotranspiration (ET) which is indicative of the crops' daily water use. Evaporation accounts for the direct evaporation of water to the air from the soil surface or canopy interception of either precipitation or applied irrigation. Transpiration accounts for the uptake of water by a plant and the subsequent loss of water as vapor through stomata in its leaves, required for metabolic cooling of the leaf to maintain photosynthesis without the leaf overheating (Allen et al., 1998). Evapotranspiration (ET) is generally viewed as a combination of the evaporation of water from the soil, evaporation from the canopy surface and plant transpiration (Pereira et al., 2014).

The evaporation and transpiration process occur simultaneously and are often difficult to distinguish. The predominance of each of these processes, however, varies at different crop growth stages. At the initial crop growth stage, water is lost mainly in form of evaporation from the soil surface. As the development of the crop progresses, transpiration becomes the major medium of water loss to the atmosphere (Verstraeten et al., 2008).

The ET process is largely dependent on solar radiation, vapor pressure deficit of the atmosphere at any given time and wind speed. It is also influenced by soil water content, the rate at which water can be taken up from the soil by the plant roots and crop characteristics (type, variety and growth stage) (Pereira et al., 2014). A further discussion on the evapotranspiration process is presented in (Allen et al., 1998; Pereira et al., 2014).

The temporal dynamics of evapotranspiration on hourly or daily timescales is appropriate for quantifying crop water use in the precision irrigation process. As such, a brief overview on monitoring techniques which can provide ET data at an hourly or daily resolution on a local scale is presented.

The United Nations Food and Agriculture Organization Penman–Monteith (FAO-PM) equation presents a procedure for computing hourly or daily ET values using standard climatological measurements of solar radiation, air temperature, humidity and wind speed made at a height of 2 m above a fully transpiring grass surface (Allen et al., 1998). These data can be obtained from automatic weather stations installed on a specific field or from a metrological network. The equation provides a basis from which reference ET (ET from the well-watered grass surface) for different time periods can be calculated and to which ET from other crops can be computed using crop coefficients, K_c (Howell and Evett, 2004). The crop coefficients are specific to each crop and crop canopy cover, which is dependent on the crop growth stage. The K_c curve defined for a crop over its growth stage is generalized for regions with similar climates. The K_c is however dependent on the canopy dynamics including cover fraction, leaf area index and greenness which may vary across regions with similar climates (Farg et al., 2012). This introduces errors in ET estimates derived using the standard FAO-PM crop coefficient approach. The FAO-PM

method presents a relatively easy procedure for determining the temporal dynamics of crop water use. The crop coefficient used in determining the actual ET of a particular crop, however, needs to be estimated at each growth stage. It is noted in Allen et al. (1998) that reference ET can be overestimated by as much as 20% during conditions of low evaporative demand.

Remote sensing provides a means of overcoming the shortcomings of the FAO-PM crop coefficient approach of estimating crop ET by providing real-time feedback on daily crop water use as influenced by actual crop canopy dynamics, local climatic conditions and field spatial variability (Hunsaker et al., 2003). The remotely sensed Normalised Difference Vegetation Index (NDVI) computed from crop canopy reflectance measurements in the red and near-infrared (NIR) wavelengths has been found to be a useful tool in computing accurate crop coefficients for a broad range of crops (Hunsaker et al., 2005). Singh et al. (2013) has demonstrated the use of the calculated reference ET and the remotely sensed NDVI in estimating the water use of cotton. A similar procedure has also been demonstrated by Farg et al. (2012) for estimating the daily water use of wheat.

The surface renewal analysis method presents an opportunity for assessing the real-time temporal dynamics of crop water use. The Surface Renewal (SR) method is used to determine the sensible heat which can then be applied to the energy balance equation to determine the latent heat (i.e., ET) (Mengistu and Savage, 2010). It is based on analysing the temperature time series generated from monitoring the change in heat content of air parcels that interact with the crop canopy. When an air parcel comes in contact with the crop canopy, the air temperature remains constant for a brief time period known as the quiescent period. The temperature of the air parcel, however, increases after this time period as energy is transferred to it from the crop canopy. The increase in temperature continues until the air parcel is replaced by cooler air from the atmosphere. At this time, the temperature of the air shows a sharp drop (Shapland et al., 2012). A high-frequency trace of this temperature renewal event exhibits a ramp-like function. Applying structure function theory to the ramp function enables the determination of the sensible heat flux. The instrumentation requirement for an SR system is minimal, consisting of small diameter fine wire thermocouples or a two-dimensional sonic anemometer and a high-frequency data acquisition system (2 Hz to 10 Hz) (Mengistu and Savage, 2010). Standard climatological measurements are also required to obtain the other parameters in the energy balance equation.

The SR technique requires that measurements are taken at a minimum height above the crop canopy. It is assumed that the canopy is homogeneous and able to absorb all the momentum transferred to it by the ambient airflow (Castellví and Snyder, 2009). This assumption introduces errors in ET estimates over fields with variable canopy structures. Castellví and Snyder (2010) concluded that the technique can be applied for estimating

ET from short and dense canopy crops as they are mostly decoupled from the environment. The technique also requires calibration using an eddy covariance system or a lysimeter. This may limit its practicality for farm-scale deployment. The SR methodology proposed by Castellvi (2004), however, does not require calibration. Rosa and Tanny (2015), Shapland et al. (2012), Rosa et al. (2013) have reported highly accurate hourly ET estimates from various crops using a surface renewal analysis system.

Lysimeters are extensively applied in monitoring the real-time temporal dynamics of the crop ET. They are tanks buried in the ground and filled with either disturbed or undisturbed soil in which crops can be grown under natural conditions to measure the amount of water lost by ET. It enables the accurate determination of the components of the soil water balance and it is considered a method of determining ET directly. The lysimeter is the standard against which other ET measurement methods are validated (Ramírez-Builes and Harmsen, 2011). There are two types of lysimeters; the non-weighing commonly referred to as the drainage lysimeter and the weighing lysimeter.

The drainage lysimeter operation is based on the principle of mass conservation in the soil water balance (Tomlinson, 1996). It calculates the ET amount for a given time period as the result of the subtraction of the drainage water from the sum of all the water input into the lysimeter and soil water change (Zhang et al., 2011). The drainage water is usually collected at the bottom of the lysimeter. Since drainage is a slow process, this type of system can only be applied in studies involving long time periods, limiting its use to research.

The Weighing Lysimeter is capable of measuring ET with higher temporal resolutions. It can determine ET with the accuracy of a few tenths of a millimeter and for time periods as short as a minute (Sun et al., 2008). In the weighing lysimeter, water loss from crop and soil surface is calculated directly from the change of mass of the entire system. The recorded mass change can be converted to ET in the units of water depth. The mass of the system is usually measured using mechanical scales or electronic load cells (Yang et al., 2000). Weighing lysimeters present an opportunity to monitor the water use of crops in real-time and over short time periods. This is especially attractive for protected crop cultivation systems where the crop water dynamics experience short time constants in order of minutes (Van Iersel et al., 2013). This technology can also be applied as part of a decision support system aimed at maintaining precise crop water deficits owing to its high accuracy. The use of weighing lysimeters for real-time irrigation scheduling in greenhouses has been demonstrated in Beeson (2011) and Prehn et al. (2010).

The real-time plant transpiration dynamics can be monitored using sap-flow sensors. Sap-flow sensors include a heater and temperature probes which are inserted into stems or branches. The sensors use heat as a tracer for sap-flow by taking advantage of the

negative correlation between the sensor probe temperature and sap-flow heat absorption (Verstraeten et al., 2008).

Different sap-flow measurement principles exist. For instance, the stem heat balance sensor consists of a flexible heating element which applies heat to the plant stem, a series connection of thermocouple embedded in a cork band that measures the radial temperature gradient, and a thermocouple pair that measures the temperature gradients upstream and downstream of the sap flow in the stem (Smith and Allen, 1996). The stem heat balance can be applied to plant stems as small as 4mm in diameter (Verstraeten et al., 2008). The heat pulse method is applicable to woody stems with diameters larger than 30mm. The velocity of a heat pulse applied by a heater into the sap flow is used to determine the mass flow rate of the sap (Verstraeten et al., 2008). The method makes use of a pair of heat pulse probes installed above the heater (downstream probes) and another pair of heat pulse probes (upstream probes) installed below the heater. The heat pulse probes measure the velocity of the heat pulse as it is transported by the sap flow (Smith and Allen, 1996). In the thermal dissipation method, method a sensor consisting of an upper probe containing a heater element and a thermocouple is inserted into the plant stem and a lower probe containing a thermocouple referenced to the upper probe. When heat is applied to the stem by the heating element, the temperature difference, ΔT between the two probes is dependent on the sap flow rate. A faster sap flow rate results in greater heat loss decreasing the value of ΔT (Chabot et al., 2005).

Sap-flow measurements are point based techniques, requiring extrapolation of transpiration rates from plant points to the entire field. This is an easy procedure when considering similar crops at similar growth stages with a high level of homogeneity as transpiration rates are likely not to vary among such plants. The sap flow method is a cheaper alternative to lysimeter experiments for real-time monitoring and gives insight into the physiological factors controlling transpiration (Wilson et al., 2001). Sap-flow sensors require specialized technical labour for their operation. It should also be noted that this method measures only the transpiration and cannot be deployed on plants at early growth stages due to the small diameter of their stems.

5.4 Plant-based sensing

The importance of plant-based monitoring becomes emphasized when studying the effect of water deficit on plants and its relation to plant water status. The temporal dynamics of crop water use can be monitored using a number of plant-based methods. They include methods that require direct contact with the plant and those that require only proximal contact with the plants (Jones, 2014). The contact sensors are useful in monitoring the temporal dynamics of the plant water status while the proximal sensors are capable of

assessing the spatial nature of crop water status across a field and hence well suited for the precision irrigation process (Smith et al., 2010). A good understanding of the various aspects of plant water status and plant drought physiology is important in the successful application of these systems. A comprehensive review of plant-based sensing methods applicable to irrigation management is presented in Jones (2004). Plant-based sensing systems measure either the plant water content, plant water potential or the plant physiological response to moisture deficits. A summary of various plant-based sensing systems is presented in Table 3. It should be noted that many of these require skilled labour and considerable management time for their operation.

Table 3. Summary of plant-based monitoring methods.

Plant-Based Measurement	Advantage	Disadvantage
Plant water potential methods		
Leaf turgor pressure sensors (Ruger et al., 2010; Zimmermann et al., 2013)	Capable of real-time measurements and can characterize leaf water dynamics	Point-based and requires scaling to canopy level
Plant water content methods		
Leaf thickness sensors (Seelig et al., 2012)	Relatively cheap and can be automated	Leaf thickness not sensitive to changes in plant water status. Sensors also largely inaccurate. Low spatial resolution
Stem diameter variation (Conejero et al., 2011; Livellara et al., 2011)	Sensitive to water deficits and can be automated	Limited by diurnal hysteresis. Low spatial resolution
Plant response to water deficits		
Xylem cavitation (Shifeng et al., 2008)	Sensitive to the onset of water stress and moderately cheap instrumentation	Only useful during drying and inadequate characterization of cavitation-water status relationship. Low spatial resolution
Sap flow (Chabot et al., 2005; Uddin et al., 2014)	Highly accurate method capable of quantifying plant transpiration	Point-based technique requiring replication to improve spatial resolution. Irrigation thresholds difficult to define. Also requires considerable time and expertise in its operation
Thermal sensing (proximal) (Çolak et al., 2015; Meron et al., 2010)	Simple procedure with high spatial and temporal resolution	Largely empirical and difficult to implement in humid climates

5.4.1 Thermal sensing

Plant canopy temperature is a widely accepted variable indicative of plant water status. The stomata control evaporative cooling of the leaves based on soil water status and prevailing environmental conditions. It closes due to increased water deficits and a reduction in plant transpiration causing an increase in plant canopy temperature (Blonquist et al., 2009). The measurement of the crop canopy temperature by infrared thermometry which is then normalized using an index such as the crop water stress index (CWSI) can be used in determining the plant water status and its response to water deficits (Jones, 2004).

The CWSI is a well-established method of accounting for the variation in canopy temperature as a function of prevailing microclimatological conditions and water deficits (Leinonen and Jones, 2004). It relates the difference in the crop canopy temperature measured using infrared thermometry to the air temperature as a function of atmospheric vapor deficit (Erdem et al., 2010). This temperature difference is then related to an upper and lower temperature baseline to determine a water stress index. The upper baseline represents a non-transpiring crop and the lower baseline represents a fully transpiring crop under the same prevailing environmental condition (Shaughnessy et al., 2014). The CWSI is a dimensionless value of between 0 and 1, with a value of 0 indicating a well-watered crop and a value of 1 indicating a severely water-stressed crop (Erdem et al., 2010).

Biotic factors can also induce stress in a plant thus affecting transpiration rate, crop water use and canopy temperature. These biotic factors also affect leaf color and morphology which in turn affects the optical properties of the crop canopy (Sankaran et al., 2010). In order to successfully apply infrared thermometry as a tool for assessing plant water status, it is important to differentiate between abiotic (such as water stress) and biotic stresses (such as plant diseases and pest infestation). Multiband optical sensors could be applied in detecting various crop diseases and crop infestation within a field by computing vegetation indices based on canopy reflectance measurements (O'Shaughnessy and Rush, 2014). This has been applied by Garcia-Ruiz et al. (2013) for detecting citrus greening and by Yang et al. (2009) for detecting infestation of green bugs and aphids in wheat. It may be useful to outfit precision irrigation systems with these sensors.

The main advantage of thermal sensing for precision irrigation application is related to the non-contact and real-time capability of the system. Infrared thermometry and thermography provide the opportunity to map the spatial variation in crop water status which can guide in variable rate irrigation management. The use of thermal sensing for guiding zone-specific water application has been demonstrated as noted in Section 2.

A major problem faced in applying the thermal sensing approach is the establishment of the baseline temperatures. In climates in which the air humidity is often high, variations in wind speed and net radiation introduce significant errors in the estimation of the lower limit

baseline temperature (Jones et al., 1997). A number of studies have been conducted to develop procedures for enhancing the possibility of applying measurements of crop canopy temperature in inferring plant water status in humid regions. Jones (1999) provides an excellent summary of these research efforts. They include the use of well-watered plots to substitute for empirical non-water stressed baselines, although these well-watered plots are rarely available in practice. The use of artificial reference surfaces for measuring baseline temperatures has been proposed but it is reported that these artificial reference surfaces differ significantly in thermal and radiative properties in comparison to real leaves. A modelling approach to simulating the canopy resistance of well-watered plants has also been investigated but this is limited by the difficulties encountered in correctly modelling stomata behavior and hence canopy resistance. The possibility of including a wide range of metrological data including net radiation and vapor pressure deficit in deriving CWSI models for humid climates has also been investigated. The mathematical complexity typical of the models, however, limit their practical application.

Another problem commonly encountered in applying infrared measurements of canopy temperature in inferring plant water status is the inclusion of soil temperature and other background temperature including the sky and stems in the measured canopy temperature. This usually leads to errors in estimation of the canopy temperature as the soil and background temperature are usually many degrees different from the canopy temperature Meron et al. (2010) and Jones (1999) proposed the use of narrow acceptance angle infrared sensors that can be positioned to view only single leaves as a solution to this problem. It has however been found that the temperature estimates of single leaves determined by this method is mostly not representative of the temperature of the plant canopy. A dense deployment of infrared sensors may seem an alternative but this may be prohibitive in terms of cost for practical applications.

The advancements in the field of thermal imagery and the recent availability of low-cost thermal cameras have presented the possibility of overcoming the problems associated with the inclusion of soil and background temperatures in the measured canopy temperature. Thermal imagery allows for the average temperature of a defined area to be obtained and also the separation of background temperature from the area of interest. The temperature of a large number of individual leaves making up a canopy can be included in an image while the soil and background temperature can be discarded by applying automated image processing techniques (Leinonen and Jones, 2004). Gonzalez-Dugo et al. (2013) have demonstrated the use of thermal imagery in mapping the crop water status in a commercial orchard in Spain. They also demonstrated the rapid mapping of field-scale crop water status by deploying thermal imaging equipment on an unmanned aerial vehicle (UAV).

Plant-based sensing methods including thermal sensing only provide information on the need for irrigation and provide no information on the volume of irrigation application needed. They are used in combination with soil-based and weather-based sensing for this reason (Smith et al., 2009).

6 Decision support

A decision support system for irrigation management and scheduling provides a framework for incorporating various tools and techniques for arriving at irrigation decisions. The widespread commercial adoption of precision irrigation will be predicated on the development of robust and optimal decision support systems (Smith et al., 2009). A number of decision support systems schedule irrigation at predefined intervals and apply predefined irrigation volumes. They do not incorporate any form of sensor feedback on plant water status, soil water status and climatic variables (Lozoya et al., 2014). This 'open-loop' strategy is largely designed based on heuristics and historical data. Mareels et al. (2005) suggested that this is an inefficient approach often leading to overwatering and waste of fertilizer and other supplemental crop inputs.

Closed-loop irrigation strategies aim to irrigate: when the soil moisture content reaches a certain threshold (Dabach et al., 2013; Liu et al., 2012; Vellidis et al., 2008); when plant sensors indicate a certain stress threshold (Erdem et al., 2010; Osroosh et al., 2015; Shaughnessy et al., 2012) or with feedback from crop simulation models with the aim of attaining a certain yield, crop physiological response or economic objective (McCarthy et al., 2014). These closed-loop irrigation strategies have been shown to improve water use efficiency in the production of horticultural crops under protected environments. Environmental conditions in such production systems can be controlled based on plant feedback which eliminates the stochastic plant response often encountered in field-scale crop production (Bennis et al., 2008). Belayneh et al. (2013) implemented a wireless sensor network of soil moisture sensors for closed-loop irrigation control in a pot-in-pot nursery. A significant reduction in water use was achieved by the system. The authors also reported a 2.7-year payback period for the system. Chappell et al. (2013) reported water savings of 83% for a closed-loop irrigation control system implemented in a protected crop production system. They noted that there was less occurrence of plant diseases in the nursery due to the elimination of over-watering. Saavoss et al. (2016) reported a 65% increase in profit due to the implementation of a wireless sensor network-based closed-loop control system in a nursery. The authors noted that the increase in profit was due to an improvement in crop quality and yield resulting from the precise control of irrigation applications.

In field-scale crop production, the crop needs vary over time and space due to both biotic and abiotic factors (Al-Karadsheh, 2002). McCarthy et al. (2013) noted that in these crop

production systems, closed-loop strategies are unable to account for unknown crop dynamics, the stochastic nature of climatic variables and crop response, and the time-varying nature of the soil-plant-atmosphere system. This last point is especially due to crop growth, crop management and infestation of pests and diseases. The closed-loop systems are also unable to consider equipment and other operational limitations. McCarthy et al. (2010) concluded that an optimal decision support system must be 'adaptive' with the ability to accommodate the temporal and spatial variability within the field. The decision support system must also have the capability of modifying irrigation decisions in response to crop physiology, uncertainties in climatic inputs, soil, irrigation systems and water supply limitations, economic considerations and the quality of sensor feedback.

6.1 Adaptive decision support

The characteristics of a cropping system vary over time. Within a cropped system, the properties that will typically vary within and between seasons include crop growth, soil properties (due to the addition of nutrients and other management processes) and climate. This will have a direct influence on the irrigation timing and volume required for optimal crop growth (Smith et al., 2010).

An adaptive decision support system is able to continuously re-adjust the irrigation scheduling algorithm in order to retain the desired performance of the irrigation system (McCarthy et al., 2010). The adaptive decision support system is able to utilize historical or real-time sensor data to arrive at irrigation timing and volume that adequately accounts for the temporal and spatial variability in the field (McCarthy et al., 2010). In control theory, an adaptive control system is generally accepted as a control system able to adjust its controller parameters based on sensor feedback from a process, such that the controlled process behaves in a desirable way (Smith et al., 2010). McCarthy et al. (2014) noted that an adaptive decision support system for irrigation may either be sensor-based if they use direct sensor measurements for the irrigation strategy or model-based if they use a calibrated process model to aid irrigation decisions.

The development of adaptive decision support systems presents an opportunity to improve sustainability in precision irrigation through improved water use and crop productivity. They will also enhance synergistic applications of data available from soil, plant and weather sensors to arrive at optimal irrigation scheduling decisions (McCarthy et al., 2014).

In this section, a discussion on the state-of-the-art in adaptive decision support systems is presented. The opportunities these systems present in improving sustainability in irrigated agriculture are also discussed. A comprehensive overview on the application of advanced process control to irrigation, details on methods of operation and a consideration of

fundamental control concepts as they apply to irrigation scheduling can be found in (McCarthy et al., 2013).

6.1.1 Mechanistic models

A number of irrigation decision support systems are based on complex physical models which closely resemble the actual physical system (Dabach et al., 2011; Rezaei et al., 2017). They are able to incorporate the physiological and morphological representation of the plant into the decision support tool. Barnard and Bauerle (2015) described an irrigation scheduling system based on the spatially explicit biophysical model, MAESTRA (Multi-Array Evaporation Stand Tree Radiation A), which couples the within-canopy photosynthesis and stomatal conductance. Data on leaf temperature, canopy aerodynamics, and environmental variables are used as inputs into the model to predict the plant transpiration. They reported that the model-based tool applied between 18%–56% more water than a sensor-based method for scheduling irrigation in four species. They, however, noted that the model-based approach produced greater tree growth. Asher et al. (2013) described a mechanistic model capable of inferring crop water requirements. The model employs leaf temperature data as input for determining the crop aerodynamic characteristics which is then used in the Penman–Monteith equation for calculating the actual crop ET. A major drawback of these mechanistic models is that they include static parameters which, once identified, are assumed to remain constant over the cropping season. This is rarely so in practice as the cropping system varies over time due to both biotic and abiotic factors. Mechanistic models usually require large input requirements which widely limits their applicability to research (Young and Garnier, 2006).

6.1.2 Simulations

Crop simulation models based on first principle physical models of crop phenology, soil physics, and hydrology can be applied in simulating the crop response to irrigation and cropping system management (Hsiao et al., 2009; Raes et al., 2009; Steduto et al., 2009). These simulation models provide the opportunity to evaluate the benefit of several precision irrigation strategies as they eliminate the need for time-consuming field experiments (Jones et al., 2003). They can be interfaced with real-time sensor feedback from soil or plant sensors and weather data to determine daily irrigation requirements of crops. They can also be used in predicting the yield impact of an irrigation strategy. This is achieved by employing weather data in computing a daily soil moisture balance and assessing the impact of soil moisture deficits on crop growth (Jones et al., 2003). DeJonge et al. (2007) investigated the effect of variable rate irrigation management on corn production in Iowa using the CERES-maize model. Corn yield was compared for a period of 28 years under simulated scenarios of no irrigation, scheduled uniform irrigation and precision irrigation. They reported no significant difference in corn yield and water use between the uniform irrigation and precision irrigation scenarios. Thorp et al. (2008)

described a methodology for applying the Decision Support System for Agrotechnology Transfer (DSSAT) crop growth model in analyzing variable-rate management practices including irrigation on crop growth and yield. The platform enabled the evaluation of precision irrigation strategies on crop performance in predefined management zones. The system is however incapable of real-time decision support and can only be applied using historical data.

McCarthy et al. (2010) proposed a simulation framework, VARIwise, capable of real-time decision support in precision irrigation. The simulation framework is capable of incorporating real-time data input from field sensors in arriving at irrigation decisions. The combination of different sensor inputs into the simulation framework enables adaptive decision support with the system being able to re-adjust irrigation decisions based on plant feedback and also explore optimal control strategies.

Simulation models for use in irrigation decision support require extensive calibration and validation to establish model accuracy. The limitation in data available for this endeavor often limits the use of the platforms to specific crops (McCarthy et al., 2014).

6.1.3 Artificial intelligence

Artificial intelligence presents the potential of solving problems in precision irrigation which are complex, non-linear and ill-defined (Hardaha et al., 2012). Artificial intelligence algorithms are able to emulate the human decision-making process when applied to a particular problem domain. They have been deployed for implementing adaptive decision support in irrigation in form of artificial neural networks, fuzzy logic and expert systems with mixed success to date (Prasad and Babu, 2007; Tsang and Jim, 2016).

Artificial neural networks

Artificial neural networks (ANN) are non-linear mapping structures employed in modelling when the underlying data relationship is not well defined. ANN are able to identify and learn correlations between input data and corresponding target output values. They are able to predict the outcome of new independent data sets making them a useful tool in predictive modelling (Kasslin et al., 1992). ANN are well suited for the irrigation decision support problem that can often be complex and stochastic in nature. These networks are also adaptive in nature and are able to continuously learn in order to provide optimal solutions to target problems in dynamic systems.

Karasekreter et al. (2013) implemented an ANN for scheduling irrigation in a strawberry orchard using soil moisture and its physical properties as model inputs. The system was able to achieve water savings of 20.5% and an energy saving of 23.9%. ANN's, however, require large datasets for training and are unable to give physical insights into the dynamics of a system. This makes their use limited when it is desirable to give a physical interpretation to a process.

6.1.4 Fuzzy logic

Fuzzy logic is an artificial intelligence algorithm that can be used to model a process and relate it to human experience in arriving at decisions. A fuzzy logic system is made up of a set used to classify input data into membership classes, a decision rule that is applied to each set which culminates in a human-like decision output from the system (Mousa and Abdullah, 2014). A detailed description of the process is given in Prakashgoud and Desai (2013).

Mousa and Abdullah (2014) successfully applied a fuzzy logic model in scheduling irrigation in drip and sprinkler irrigation systems using ET, soil moisture data and crop growth stage as model inputs. Prakashgoud and Desai (2013) employed a fuzzy logic system using soil moisture data, leaf wetness, and climatological data as model inputs in order to implement irrigation scheduling decisions. The system was capable of maintaining soil moisture thresholds in the specified range. Giusti and Marsili-Libelli (2015) described an adaptive irrigation decision support system implemented with fuzzy logic. The system incorporates a predictive model of the soil moisture and an inference system for maintaining the soil moisture within an acceptable threshold. The system was reported to adapt irrigation decisions to rainfall uncertainty and produced water savings of 13.55% over a simulation period of 168 days.

The accuracy of fuzzy logic systems is largely tied to an in-depth knowledge of the physical system. They also lack an inner mechanistic structure with the domain of applicability limited to the range of training data used in setting them up. Delgoda et al. (2016) suggested that the points mentioned makes decision making with a fuzzy system an ad hoc process limiting its application in adaptive decision support.

6.1.5 Expert systems

An expert system is a tool able to emulate the reasoning process a human expert would employ in a decision-making process in his/her field of expertise. It captures the human decision-making expertise and heuristics representing it in a series of rules and facts (Plant et al., 1992). An expert system typically consists of a knowledge base component and an inference engine that acts as a reasoning tool (Singh and Sharma, 2014). Expert systems are especially suited to dynamic problems that are of a complex nature. They are also well suited to dealing with incomplete and uncertain data (Rani and Rajesh, 2013). This makes them well suited for irrigation decision support which often requires the input of experts to arrive at optimal decisions.

Expert systems applied in irrigation decision support can be classified as either ‘expert systems proper’ or hybrid expert systems. A detailed review on the application of expert systems in irrigation decision support is presented in (Mohan and Arumugam, 1997; Rani and Rajesh, 2013). The ‘expert systems proper’ class of irrigation decision support tools schedule irrigation based on soil moisture and climatic data. They are unable to consider

the time-varying nature of the cropping system (crop growth, disease, and pest infestation) to arrive at optimal irrigation decisions. They are also unable to account for the stochastic nature of climatic variables and are not well suited for real-time applications (Mohan and Arumugam, 1997).

Hybrid expert systems which are also referred to as model-based expert systems combine algorithmic techniques and a knowledge-based component in solving problems relevant to its application domain. Its advantage in irrigation is that optimal irrigation decision can be made by combining expert knowledge with data feedback from infield sensors, data-driven models and crop simulation models (Rani et al., 2011). Thomson and Ross (1996) described a model-based expert system designed for decision support in irrigation management. The system employs feedback from soil moisture sensors to adjust the input of a crop simulation model, PNUTGRO (Peanut crop growth simulation model) and also incorporates the capability of sensor feedback validation. The system was reported to maintain soil moisture at the defined thresholds. Goumopoulos et al. (2014) developed an expert system-based adaptive decision support platform for zone-specific irrigation of strawberry plants. The system includes a wireless sensor network of soil, climate and plant sensors providing feedback for the decision support system. It also includes a machine learning process capable of inferring new rules and extending the knowledge base from logged data sets. The system was reported to reduce irrigation water consumption by around 20%. A hybrid expert system based on real-time soil moisture data with the capability of incorporating plant models is described in Kohanbash et al. (2013).

The performance of an expert system is largely dependent on the effectiveness of the knowledge acquisition process. An error in this process will drastically affect the system reliability and its performance.

6.1.6 Learning control

Learning control decision support strategies control a process using sensor feedback, without defining a model for the response of the process (McCarthy et al., 2013). One method of sensor-based control is iterative learning control.

Iterative learning control can be applied in systems with ill-defined models that operate repetitively and assume the same initial condition after each iteration. It is well suited to the irrigation problem as irrigation scheduling and application is a repetitive problem over the crop season. The time-varying nature of the soil–plant–atmosphere system can also be viewed as an ill-defined problem. The strategy is also able to improve system performance by eliminating the effects of a repeating disturbance with undefined dynamics. Applied to irrigation, this may be a measured crop response that reoccurs as a consequence of irrigation. The temporal changes in crop water use and weather conditions are not considered (McCarthy et al., 2013).

McCarthy et al. (2010) noted that a drawback of the iterative learning approach may be the inefficient description of the process response resulting from the slow system dynamics of the cropping system in response to irrigation events. This results from the evaluation of the effect of only one irrigation volume on plant response at any water application event. They suggested that this drawback may be eliminated by applying the process of Iterative Hill Climbing Control. This learning control strategy employs an adaptive varied identification process. A range of irrigation volumes is applied at each irrigation event to a number of test cells on the field. The response in the test cell that best matches the desired system performance is identified as the optimal irrigation process. They reported that the Iterative Hill Climbing Control procedure was capable of maximizing cotton yield when used with a combination of plant and soil sensors to provide feedback for the identification process. Their conclusions were however based on results from a simulation study and a field-based validation of the procedure was not reported. The results of the learning control procedure are based solely on sensor measurements and may be largely affected by sensor drift as a model of the crop response is not developed from the identification process. This method can be considered more of a "brute force" approach than a scientifically based approach to scheduling irrigation.

6.1.7 Data-driven models

Data-driven modelling employs statistical and machine learning models that are able to learn from data in order to make predictions pertaining to the response of a process. These models are able to explore the spatial and temporal information contained in data in order to define a function that describes the input/output relationship of a process (Zhang et al., 2018). They do not rely on a physical model of the process. In many cases, these statistical and machine learning models have been shown to achieve a robust predictive performance (Payero and Irmak, 2006; Young and Garnier, 2006).
These methods have been successfully applied in the advanced process industry as part of adaptive decision systems (Das et al., 2012; Sharma et al., 2010). Data-driven models have also been used in irrigation decision support. Navarro-Hellín et al. (2016) presented a regression model for predicting the weekly irrigation needs of a plantation using climatic and soil data as inputs. In Delgoda et al. (2014), the authors applied a multivariate linear dynamic model for predicting the soil moisture deficit. Their model employed climatic and soil moisture data as inputs. The authors reported that the model was able to generate robust predictions of the soil moisture deficit without the need to explicitly specify the soil's hydraulic properties. Goldstein et al. (2018) applied a gradient boosted regression model for predicting the weekly irrigation volumes for an olive oil orchard. The model was able to provide insights into the variables that strongly influenced the orchard's irrigation dynamics.

The success achieved by data-driven methodologies in the process control industry, and also recently in irrigation decision support suggests that these methods can be further exploited for use in adaptive decision support systems applicable to precision irrigation. They are able to overcome the limitations encountered by mechanistic models. The models can be updated online using feedback from real-time sensor data enabling them to adapt to the time-varying nature of the cropping system. They also have minimal input requirements as they are able to learn the variables which have a strong influence on the response of a process.

6.1.8 Model predictive control

Model predictive control (MPC) is an industrial control approach employed in decision support for large-scale multivariable problems with multiple constraints. It has been successfully implemented in the food industry, petrochemical industry and power generation among others (Saleem et al., 2013). Model predictive control employs a plant model and optimization algorithm to calculate plant inputs in order to achieve a future value of a performance criterion. The system performance is predicted over a finite horizon subject to constraints on both the inputs and outputs of the plant (Lozoya et al., 2014). An in-depth review on the theory of model predictive control and its application in various industries is presented in (Froisy, 2006; Qin and Badgwell, 2003)

In the case of irrigation, applying a soil moisture balance model, the plant input will be the irrigation amount, the plant output will be the soil moisture deficit, and both crop ET and precipitation values will be considered as disturbances as they cannot be controlled. A prediction of future input values and disturbances is required in an MPC system in order to determine the optimal system output (Delgoda et al., 2014). This highlights the need for the incorporation of weather forecast data into the MPC framework for irrigation decision support.

Model predictive control appears to be well suited to the domain of irrigation decision support. The irrigation problem has input constraints in terms of optimal irrigation volume and output constraints in terms of soil moisture thresholds and the desired plant response to water deficits (Saleem et al., 2013). Ooi et al. (2008), Lozoya et al. (2014) and Saleem et al. (2013) described a model predictive control framework for irrigation scheduling based on a soil moisture balance model. They employed a data-driven modelling procedure to generate a grey box model of the soil–plant–atmosphere system with a network of soil moisture sensors providing real-time feedback to the control algorithm. They all reported the ability of the MPC platform to sufficiently predict crop irrigation needs and also observations of significant water savings. The authors of the discussed systems, however, fail to account for the stochastic nature of rainfall and crop water use in the system dynamics. Delgoda et al. (2014) noted that an adequate consideration of the

uncertainty in rainfall and ET inputs into the water balance model employed in the MPC framework will improve the capability of the MPC system.

Delgoda et al. (2016) addressed the drawbacks noted in the above MPC frameworks by employing disturbance affine feedback control, an uncertainty modelling technique widely applied in MPC to account for the stochastic nature of rainfall and crop water use. A low order model of soil moisture dynamics is included in the system to enable the online calculation of model parameters, hence accounting for the time-varying nature of the soil-plant-atmosphere system. The authors reported an optimal performance of the system in humid regions where considerable uncertainties in climatic variables exist.

6.2 Commercial sensor applications in adaptive decision support

Manufacturers of sensors and a number of system integrators are showing considerable interest in developing innovative tools that will further optimize irrigation water use.

A sensor integration project is described by AgSmarts, Memphis, USA. Moving irrigation systems are equipped with sensors which provide data on crop growth stage and soil profile. Aquaspy soil moisture sensors (Aquaspy, San Diego,CA, USA) positioned in various parts of the field also provide data on soil moisture status which is applied in irrigation timing and calculation of irrigation volumes. These irrigation decisions are automatically adjusted based on the varying water requirements at each crop growth stage (“Take the Guesswork Out of Irrigation | AquaSpy Home – AquaSpy”).

Omica, Italy has deployed a wireless sensor network of Libelium environmental and soil moisture sensors (Libelium, Zaragoza, Spain) on a maize farm in Italy to support irrigation decisions. The sensors are interfaced to a geo-referenced decision support system which enables zone-specific irrigation management. The system is able to predict crop yield based on irrigation timing and application volumes combined with historical yield data. This can then be applied in optimizing the decision support system towards achieving a desired crop yield goal.

Most decision support systems presently produced for commercial use provide on/off irrigation control based on specified thresholds and plant/crop sensor feedback. The incorporation of predictive models into these systems will enhance the possibility of improving irrigation water use and crop yield (“Precision Farming to control irrigation and improve fertilization strategies on corn crops | Libelium).

7 Opportunities for improving sustainability

Sustainability is premised on the principle of meeting the needs of the present generation without compromising the ability of future generations to meet their own needs. Sustainable agriculture is focused on developing farming practices that are safe and do not have an adverse impact on the environment (Alberola et al., 2008).

Pretty (1995) suggested that sustainable agriculture integrates the main goals of environmental health and economic profitability. The efficient and effective use of water is considered the main driver for improving sustainability in irrigated agriculture. This will involve the use of less water for irrigating crops and also preserving the quality of water sources. Conventional irrigation practices apply water uniformly over a field resulting in a high volume of water use. Over-irrigation may also result from this practice which causes leaching of nitrates and nutrients into groundwater sources. An important consideration would also be the use of less energy for operating water pumps and irrigation application equipment. Soil erosion continues to be a serious threat to sustainability in irrigated agriculture. This can be eliminated by applying precise irrigation volumes to reduce surface runoff.

Precision irrigation presents a promising platform for improving sustainability in irrigated agriculture. This is especially hinged on the possibility of eliminating the adverse environmental impacts related to conventional irrigation practices with the adoption of precision irrigation. The economic profitability of the adoption of precision irrigation is, however, a very important point to consider. This will be manifested in terms of improved crop yields and increased water savings including the associated reduction in energy consumption resulting from the optimal matching of irrigation inputs to the spatial and temporal water demands of the crop, thus reducing costs (Smith et al., 2010).

Precision irrigation is predicated on the hypothesis that the crop water requirements vary spatially and temporally across a field. In heterogeneous crops such as fruit orchards, this variability is also due to physiological factors such as leaf area and fruit load (Fernández, 2014). It is assumed that varying water application across the field to meet this spatiotemporal crop water need will improve crop yield and reduce the costs of associated inputs. Smith et al. (2010) noted that the evidence to support this hypothesis in commercial crop production is not readily found in literature.

Evans and King (2012) reviewed much of the work prior to that date focused on analysing the improvements in crop yield and water savings achievable with precision irrigation and suggested that the greatest savings are likely to occur in humid climates by the increased utilization of stored moisture and in-season precipitation. Results from simulation- and field-based case studies they reviewed showed water savings of 0% to 26% for well-watered crop production employing precision irrigation strategies. No significant improvements in crop yields resulting from the adoption of precision irrigation were reported. They concluded that in arid and semi-arid regions, precision irrigation is more suited to maximize net return rather than yield and it may have greater potential in reducing irrigation water use in humid climates when irrigating to maximally utilize in-season precipitation. They further noted that the economic benefit of adopting precision irrigation for field-scale crop production is limited. This is because the cost of equipment, maintenance and management are much greater than the revenue improvements

achieved as a result of improved yield and water savings. The payback period of implementing the technology may also exceed the useful life of the water application equipment, typically placed at 15 years. A payback period ranging from 5 to 20 years is reported in Smith et al. (2010) for the adoption of precision irrigation for crop production in New Zealand.

Evans et al. (2013) reviewed the adoption trends of spatially varied irrigation in the USA covering a period of 20 years. They noted that about only 200 of the 175,000 moving irrigation systems in the USA were fitted with variable rate water application technology. They suggested higher net returns on investment as a stimulus for the adoption of spatially varied irrigation by growers. Growers that had adopted the technology reported no significant savings in water and energy use in non-limiting water situations. They noted that in more than 20 years of research pertaining to variable rate irrigation management, the economic benefit was yet to be demonstrated. This was attributed to the marginal water savings (5%–15%) which is insufficient to realize a payback for the initial investment in the water application technology. They concluded that an economic strategy that optimizes net return rather than total returns for the technology should be adopted as a long-term investment goal.

Heeren et al. (2016) conducted a simulation study to assess the reductions in pumping costs through the adoption of spatially varied irrigation in 49,224 center-pivot irrigated fields in Nebraska, USA. The study focused on applying variable rate water applications in mining undepleted available water. They noted that the reduction in pumping costs achieved from the adoption of this technology in all fields may be negligible in comparison to the cost of variable rate water application equipment. They concluded that the adoption of this technology will be economically justifiable only with an increase in energy costs.

An economic evaluation of spatially varied irrigation applications is presented in Lee (2016). The study assessed energy savings resulting from pumping lesser volumes of water for irrigation on a 67-acre field in Wyoming. The cost of installing the variable rate water application equipment on the field was reported as $29,513 with a useful equipment life of 15 years. The yearly return for the equipment based on energy savings achieved was computed as $1816.71, which equates to a payback period of 16.25 years. This suggests that a payback will only be realized for the technology outside the useful life of the equipment.

Precision irrigation offers the benefit of providing water conservation benefits by avoiding over-irrigation and the associated adverse environmental impacts (Evans and King, 2012). Sadler et al. (2005) discussed water conservation strategies where precision irrigation can potentially reduce the total water applied and improve the environmental quality of irrigated fields. They suggested that programming zero irrigation amounts to non-cropped areas will improve water conservation using precision irrigation. They also noted that adjusting spatial water application based on the infiltration rate of the soil and soil water

storage capacity will reduce the occurrence of surface runoff and soil erosion. Surface runoff and leaching were identified as the major avenues for loss of nutrients from the soil. They suggested the occurrence of this can be eliminated by spatial application of precise irrigation volumes based on the soil water-holding characteristics. They presented several case studies in which the adoption of precision irrigation has been demonstrated to enhance the environmental quality of irrigated fields. They concluded that precision irrigation has the capability of improving water use efficiencies while reducing the adverse environmental impacts associated with conventional irrigation practices.

The results from the above studies show that precision irrigation is a proven tool for improving sustainability in irrigated agriculture in terms of enhancing environmental health. Its economic justification in terms of significant yield improvements and water savings is however limited.

Evans and King (2012) suggested that the lack of significant improvements in yield response when employing precision irrigation may result from the fact that the yield response to the water curve near maximum yield (100% ET) is almost flat, with small changes in water applied using precision irrigation having little effect on yield. The majority of these precision irrigation studies have used only soil data for irrigation management. The local microclimate and crop genetics may, however, have a direct influence on the yield response of the crops.

Soil moisture status may also not provide a complete indication of crop water status, rather the plant may be the best indicator of water availability. The decision support systems employed by current precision irrigation systems assume that the soil–plant–atmosphere system never varies with time. The characteristics of the crop, soil, and climate vary within the season, altering the timing and optimal amount of irrigation volume required at any irrigation application event.

It is argued that the incorporation of multiple sensed variables (plant, soil and weather data) will enhance the possibility of arriving at optimal irrigation decisions and hence an improvement in economic outcomes. This should be integrated with a decision support system that has the capability to adapt to the time-varying nature of the cropping system. The decision support system should also have the capacity to ‘learn’ in order to improve its performance based on experience and a target crop production function. This review discusses how this can be achieved by exploiting improvements in monitoring and management considerations.

7.1 Monitoring Considerations

A precision irrigation system is designed to apply water at a differential rate in response to the temporal and spatial variation in crop water need across a field. This process is supported by a number of sensors providing data to a real-time decision support system. These sensors include weather stations, soil moisture sensors, environmental sensors,

plant sensors and thermal sensors which may be integrated into a wireless sensor network. A careful design of these sensing systems including a consideration of factors affecting their performance is crucial in realizing the goal of improved water use through precision irrigation.

Dielectric soil moisture sensors sense the water content of the immediate soil in their zone of influence. The zone of influence reported for most commercial dielectric soil moisture sensors corresponds to a cylindrical measurement volume of 1.5 L (Evett et al., 2006). It is therefore important to install the sensors in areas representative of the soil moisture available for plant use. The normal practice employed by most users is to place the sensors in the driest regions of the field or in the regions comprising of a soil profile with the lowest available water-holding capacity (Li et al., 2014). Adopting this approach will most likely lead to wetter regions in the field receiving more frequent irrigation which will consequently result in over-irrigation. A more efficient approach is to define irrigation management zones and place a number of sensors in each management zone to give the average soil moisture estimate. This may, however, be limited by cost.

A structured installation profile is also necessary in order to capture soil water movement and availability. It is recommended that sensors should be installed at each soil horizon along the plant rooting zone (Chávez et al., 2011). An accepted convention is the installation of sensors at three to four depths along the rooting zone (1 per 25% of total rooting depth). The sensor located on the uppermost soil profile is able to detect precipitation events, the sensor in the deepest part of the profile is able to detect drainage and the other sensors located midway in the soil profile are able to capture soil moisture dynamics useful in supporting irrigation scheduling decisions (University of Florida, 2007). The variation in soil properties at the different rooting depths should also be taken into account. With an increasing knowledge of the site, it is usually possible to install the sensors at two depths and still adequately capture the soil moisture dynamics. The soil moisture sensors should also be deployed using soil-specific calibration equations to enable accurate estimates of soil moisture content.

The actual crop evapotranspiration can vary spatially and temporally under conditions of unrestricted water supply. These variations can be the result of several factors including differences in crop genetics, plant density, weed competition, pest intensity, nutrient availability and stage of growth (Evans and King, 2012). Addressing the variation in ET across a field may result in significant water savings.

The accurate measurement of evapotranspiration is crucial in arriving at optimal irrigation decisions (Mengistu and Savage, 2010). The FAO-PM procedure for calculating ET which is applied in many precision irrigation systems relies on information from weather stations applied in calculating a reference ET which is adjusted for specific crops using crop coefficients. This calculated ET is assumed to be uniform for every part of the field. This will, however, result in the application of inaccurate irrigation volumes to replace crop

water use, owing to the spatial nature of the actual ET. The application of the NDVI technique in determining site-specific crop coefficients provides a platform for overcoming this challenge. The surface renewal analysis procedure also presents a promising tool for quantifying the actual crop ET. It is, however, best suited to homogeneous, short and dense canopies. For protected crop cultivation, lysimeters can be applied in accurately quantifying the temporal dynamics of crop water use (Sun et al., 2008).

Plant-based measurements provide the best indication of plant water status as they provide a direct measure of the plants' response to soil moisture availability and climatic demand. An efficient plant-based monitoring system should, however, respond sensitively to the slightest change in water deficits.

Measurements of leaf water potential and sap flow are contact methods which give direct information on plant water status but their spatial resolution is limited as many samples are required to effectively monitor the dynamics of field-scale plant water status (Kacira et al., 2002). Infrared thermometry has provided a robust platform for assessing plant water status. The CWSI calculated from the infrared measurements of crop canopy temperature can adequately quantify field-scale crop water status with high spatial and temporal resolution. This presents a robust and cost-effective tool for use in precision irrigation. Its application in humid regions is however marred with difficulties.

A systems engineering approach can be applied in overcoming the difficulties encountered with applying the CWSI in humid climates. A mathematical model derived using this approach may adequately simulate the real-time dynamics of the baseline temperatures required for computing the index.

A summary of the technology gaps and refinements necessary in monitoring tools in order to achieve robust precision irrigation management is presented in Smith et al. (2010). They include the limited volume of influence, high cost and the need to improve the measurement accuracy of soil moisture sensors. The refinements recommended include the development of low-cost soil measurement sensors with a wider volume of influence, low cost and resilient wireless communication networks able to link spatially deployed soil moisture sensors and the development of smart calibration software in order to improve the accuracy of soil moisture sensors. The technology gaps identified in plant sensing technology include the limited knowledge of irrigation thresholds and quantity, and low spatial resolution. The refinements recommended include the integration of plant-based sensing with soil moisture sensing tools in order to determine irrigation volumes, calibration of infra-red thermography against physiologically explicit plant measurements in order to determine critical thresholds and the deployment of IR thermography tools on low altitude UAVs to further enhance spatial coverage.

A combination of multiple sensor inputs deployed at a density that captures spatial and temporal variability is therefore likely to yield the most robust and accurate solution for precision irrigation. This will ensure that the decision support system is robust to data

availability, gaps, and deficiencies. This will include data from soil, weather and plant sensors (Smith et al., 2010). An important consideration will also include developing cost-effective and user-friendly tools which will enhance the adoption of these adaptive systems by farmers.

7.2 Management considerations

Management can perhaps be viewed as the most vital aspect of a precision irrigation system. Management acts as an interface between monitoring and decision support, culminating into irrigation decisions. This enables the implementation of vital management decisions of when and where to apply irrigation and also the irrigation volumes to be applied. The decision support system is perhaps the management backbone of a precision irrigation system and its proper implementation is vital for improving sustainability in irrigated agriculture.

The adaptive decision support tools discussed have the capability of improving crop yield and water savings when deployed as part of a precision irrigation system. Smith et al. (2010) noted that the simulation of adaptive decision support strategies can be used in identifying optimal irrigation scheduling decisions. A simulation tool capable of representing a range of field conditions at different spatial and temporal scales is considered ideal. Such a simulation framework is presented in McCarthy et al. (2010). Model-based decision support systems using feedback from multiple sensors may present a platform for arriving at optimal water applications. MPC appears to be ideally suited for achieving the aim of improving sustainability in irrigated agriculture. A decision support system based on MPC employs an optimization algorithm to implement an input strategy with the best performance.

McCarthy et al. (2013) noted that MPC implemented for a precision irrigation system could involve the use of real-time data from field sensors to calibrate a crop or soil model and then optimizing this calibrated model to arrive at optimal irrigation scheduling decisions. A combination of data from soil moisture sensors, thermal sensors and weather sensors would be appropriate for MPC. The data from the sensors would most likely be required daily, as measurements are not required at a high temporal resolution to calibrate the model. A dense deployment of these sensors is however required to account for the spatial nature of field-scale crop water use. The thermal sensors may be mounted on a moving platform for spatial data collection across the field.

Equipment availability, irrigation system capacity and other operational considerations can be incorporated as system-level constraints in an MPC-based decision support system. These constraints can be considered to arrive at future irrigation scheduling decisions (McCarthy et al., 2013).

MPC uses a model's prediction to determine the optimum irrigation application timing and volume. When combined with a soft sensing system, variables that are not directly

measured can be controlled and optimized. This presents the possibility of applying decision support systems based on MPC in realizing a desired crop yield and also a water-saving goal (Qin and Badgwell, 2003).

Data-driven decision support systems that employ real-time sensor data to update a statistical or machine learning model also present a vehicle for improved irrigation scheduling decisions. Such systems are able to adapt to the time-varying response of the cropping system and are able to learn robust functions that describe the response of the crop to water availability.

Data-driven systems will also mostly require minimal input requirements. As an example, Sánchez et al. (2012) demonstrated that the crop transpiration of greenhouse crops can be predicted using the solar radiation, vapour pressure deficit, and air temperature as inputs into a data-driven dynamic model. Their model consistently outperformed a mechanistic model that required extensive instrumentation and explicit modelling of the crops stomata response. The limited instrumentation required by such data-driven models makes them attractive for use in irrigation decision support. Furthermore, the limited complexity associated with their implementation suggests that growers with limited knowledge of crop physiology can easily apply them for irrigation purposes.

There has been considerable research into water use procedures that can achieve improved water savings in irrigated agriculture, particularly deficit irrigation. Deficit irrigation (DI) is an irrigation strategy in which a crop is exposed to a level of water stress at certain growth stages in its development (regulated deficit irrigation) or throughout its growth season. The growth stage in which the plant is subjected to water stress is predetermined as a drought tolerant stage. The goal of deficit irrigation is that there will be little adverse effect on yield and irrigation water can be conserved (Kirda, 2002). Evans and King (2012) suggested deficit irrigation as a tool for improving water use in precision irrigation. They noted that it can be applied in maximizing net returns and conserve large amounts of water in arid and semi-arid regions.

It is, however, important to investigate the response of different crops to water deficits including timing tolerances in order to develop optimal deficit irrigation strategies that can be integrated into the precision irrigation decision support framework. It is also important to investigate the economics of yield reduction associated with deficit irrigation strategies. O'Shaughnessy and Rush (2014) suggested that implementing deficit irrigation as part of precision irrigation management will involve the continuous assessment of crop stress and growth stage throughout the growing season. This will be instrumental in avoiding temporary severe stress which could result in an uneconomic reduction in crop yield or quality.

The high cost of the component technologies of precision irrigation including soil, plant and weather sensors, decision support systems and variable rate water application systems is presently a constraint to the wide-scale adoption of this technology by farmers

(Sadler et al., 2005). The minimal yield improvements and water savings currently achieved through field-scale precision irrigation may not justify the initial capital investment required for its adoption. As freshwater resources become scarcer, it is expected that more premium will be placed on water abstracted for irrigated agriculture. Regulatory agencies may also require farmers to continuously demonstrate the efficient use of water. These factors may promote the adoption of precision irrigation by farmers (Berbel et al., 2007).

A conceptual model-based decision support system that uses the full range of plant, weather and soil data for irrigation management is illustrated in Figure 1. It involves the integration of various sensing systems, dynamic modelling, machine learning, and model predictive control into an adaptive decision support system for precision irrigation.

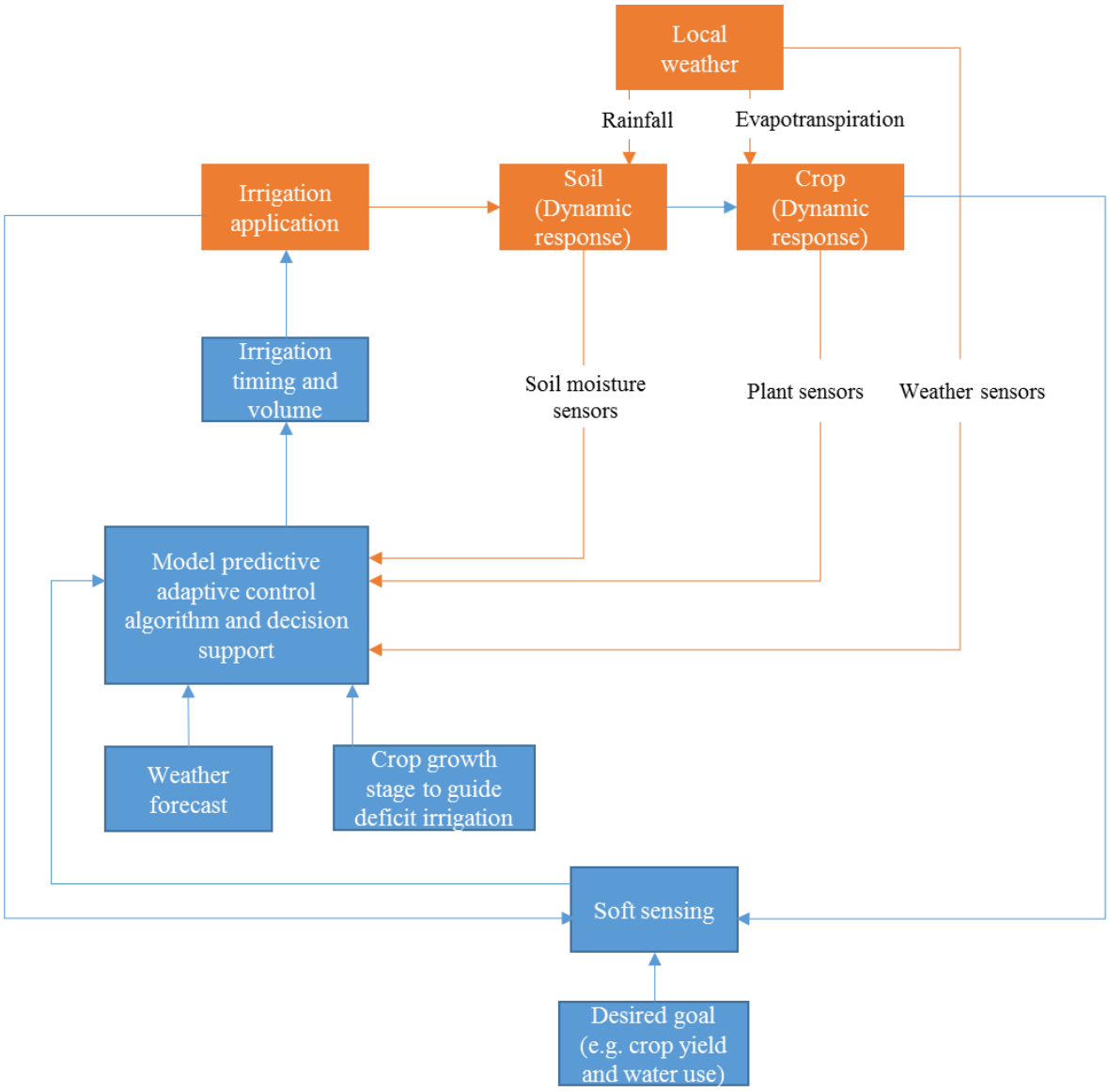

Figure 1. Conceptual model-based decision support system for precision irrigation. Elements in blue represent novel ideas synthesized from the review and elements in orange are from the decision support system presented in McCarthy et al. (2010).

8 Conclusions

Technological innovations that can improve sustainability in irrigated agriculture form an important vehicle for actualizing the optimal use of limited water resources. Precision irrigation has been demonstrated as such an innovation, though presently the economic benefit related to the adoption of this technology at field-scale crop production is minimal. This is because the potential for yield improvements and water savings may not cover the cost of technology required for its implementation.

The application of adaptive control techniques to irrigation decision support and improvements in monitoring tools has the capability of dealing with the time-varying and stochastic nature of the soil–plant–atmosphere system while also considering operational limitations in arriving at optimal irrigation decisions. This ultimately presents a platform for actualizing the environmental and economic goals of sustainability in irrigated agriculture. A robust design of monitoring tools including a proper combination of soil, weather and plant sensors is however vital for the proper operation of an adaptive decision support system. The decision support system should be able to account for the varying crop water requirements within season as a result of both biotic and abiotic factors. The decision support system should also consider agronomic objectives to ensure the optimal irrigation strategy is delivered by the precision irrigation system.

The high cost of sensors and the requirement for dense deployment in order to obtain data at high spatial resolutions is presently a constraint. The large dataset required for the calibration of crop simulation models is also another significant problem. Future research needs include the development of cost-effective soil moisture sensors with wider spheres of influence, identification of irrigation thresholds for plant-based sensors and the development of self-learning crop simulation models that are able to infer relationships from a limited data set. The field evaluation of adaptive decision support systems would also be beneficial in quantifying their sustainability improvement potential.

References

A. Irmak, J. W. Jones, W. D. Batchelor, J. O. Paz, 2001. Estimating Spatially Variable Soil Properties for Application of Crop Models in Precision Farming. Trans. ASAE 44. https://doi.org/10.13031/2013.6424

Adeyemi, O., Norton, T., Grove, I., Peets, S., 2016. Performance Evaluation of Three Newly Developed Soil Moisture Sensors, in: CIGR-AgEng Conference. Aarhus, pp. 1–10.

Al-Karadsheh, E., 2002. Precision Irrigation: New strategy irrigation water management. Conf. Int. Agric. Res. Dev. 1–7.

Alberola, C., Lichtfouse, E., Navarrete, M., Debaeke, P., Souchère, V., 2008. Agronomy for sustainable development. Ital. J. Agron. 3, 77–78. https://doi.org/10.1051/agro

Ali, M.H., Talukder, M.S.U., 2001. Methods or Approaches of Irrigation Scheduling – An Overview. J. Inst. Eng. 28, 11–23.

Allen, R., Pereira, L.S., Raes, D., Smith, M., 1998. FAO Irrigation and Drainage Paper No.56, FAO. https://doi.org/10.1016/j.eja.2010.12.001

Asher, J. Ben, Yosef, B.B., Volinsky, R., 2013. Ground-based remote sensing system for irrigation scheduling. Biosyst. Eng. 114, 444–453. https://doi.org/10.1016/j.biosystemseng.2012.09.002

Barnard, D.M., Bauerle, W.L., 2015. Species-specific irrigation scheduling with a spatially explicit biophysical model: A comparison to substrate moisture sensing with insight into simplified physiological parameterization. Agric. For. Meteorol. 214–215, 48–59. https://doi.org/10.1016/j.agrformet.2015.08.244

Beeson, R.C., 2011. Weighing lysimeter systems for quantifying water use and studies of controlled water stress for crops grown in low bulk density substrates. Agric. Water Manag. 98, 967–976. https://doi.org/10.1016/j.agwat.2011.01.005

Belayneh, B.E., Lea-Cox, J.D., Lichtenberg, E., 2013. Costs and benefits of implementing sensor-controlled irrigation in a commercial pot-in-pot container nursery. Horttechnology 23, 760–769.

Bellingham, B.K., 2009. Method for Irrigation Scheduling Based on Soil Moisture Data Acquisition, in: The 2009 Irrigation District Conference. pp. 1–17.

Bennis, N., Duplaix, J., Enéa, G., Haloua, M., Youlal, H., 2008. Greenhouse climate modelling and robust control. Comput. Electron. Agric. 61, 96–107. https://doi.org/10.1016/j.compag.2007.09.014

Benor, M., Levy, G.J., Mishael, Y., Nadler, A., 2013. Salinity Effects on the Fieldscout TDR 300 Soil Moisture Meter Readings. Soil Sci. Soc. Am. J. 77, 412. https://doi.org/10.2136/sssaj2012.0294n

Berbel, J., Calatrava, J., Garrido, a., 2007. Water pricing and irrigation: a review of the European experience. Irrig. water pricing gap between theory Pract. 295–327.

Blonquist, J.M., Norman, J.M., Bugbee, B., 2009. Automated measurement of canopy stomatal conductance based on infrared temperature. Agric. For. Meteorol. 149, 2183–2197. https://doi.org/10.1016/j.agrformet.2009.10.003

Bogena, H.R., Huisman, J. a., Oberdörster, C., Vereecken, H., 2007. Evaluation of a low-cost soil water content sensor for wireless network applications. J. Hydrol. 344, 32–42. https://doi.org/10.1016/j.jhydrol.2007.06.032

Böhme, B., Becker, M., Diekkrüger, B., 2013. Calibrating a FDR sensor for soil moisture monitoring in a wetland in Central Kenya. Phys. Chem. Earth 66, 101–111. https://doi.org/10.1016/j.pce.2013.09.004

Castellvi, F., 2004. Combining surface renewal analysis and similarity theory: A new approach for estimating sensible heat flux. Water Resour. Res. 40. https://doi.org/10.1029/2003WR002677

Castellví, F., Snyder, R.L., 2010. A comparison between latent heat fluxes over grass using a weighing lysimeter and surface renewal analysis. J. Hydrol. 381, 213–220. https://doi.org/10.1016/j.jhydrol.2009.11.043

Castellví, F., Snyder, R.L., 2009. On the performance of surface renewal analysis to estimate sensible heat flux over two growing rice fields under the influence of regional advection. J. Hydrol. 375, 546–553. https://doi.org/10.1016/j.jhydrol.2009.07.005

Chabot, R., Bouarfa, S., Zimmer, D., Chaumont, C., Moreau, S., 2005. Evaluation of the sap flow determined with a heat balance method to measure the transpiration of a sugarcane canopy. Agric. Water Manag. 75, 10–24. https://doi.org/10.1016/j.agwat.2004.12.010

Chappell, M., Dove, S.K., van Iersel, M.W., Thomas, P.A., Ruter, J., 2013. Implementation of wireless sensor networks for irrigation control in three container nurseries. Horttechnology 23, 747–753.

Chávez, J.L., Varble, J.L., Andales, A.A., 2011. Performance Evaluation of Selected Soil Moisture Sensors, in: Proceedings of the 23rd Annual Central Plains Irrigation Conference. Burlington, pp. 29–38.

Coates, R.W., Delwiche, M.J., 2008. Site-specific water and chemical application by wireless valve controller network. Am. Soc. Agric. Biol. Eng. Annu. Int. Meet. 8, 5032–5052.

Coates, R.W., Delwiche, M.J., Broad, A., Holler, M., 2013. Wireless sensor network with irrigation valve control. Comput. Electron. Agric. 96, 13–22. https://doi.org/10.1016/j.compag.2013.04.013

Çolak, Y.B., Yazar, A., Çolak, İ., Akça, H., Duraktekin, G., 2015. Evaluation of Crop Water Stress Index (CWSI) for Eggplant under Varying Irrigation Regimes Using Surface and Subsurface Drip Systems. Agric. Agric. Sci. Procedia 4, 372–382. https://doi.org/10.1016/j.aaspro.2015.03.042

Conejero, W., Mellisho, C.D., Ortuño, M.F., Moriana, a., Moreno, F., Torrecillas, a., 2011. Using trunk diameter sensors for regulated deficit irrigation scheduling in early maturing peach trees. Environ. Exp. Bot. 71, 409–415. https://doi.org/10.1016/j.envexpbot.2011.02.014

Dabach, S., Lazarovitch, N., Šimůnek, J., Shani, U., 2013. Numerical investigation of irrigation scheduling based on soil water status. Irrig. Sci. https://doi.org/10.1007/s00271-011-0289-x

Dabach, S., Lazarovitch, N., Šimůnek, J., Shani, U., 2011. Numerical investigation of irrigation scheduling based on soil water status. Irrig. Sci. 27–36. https://doi.org/10.1007/s00271-011-0289-x

Daccache, A., Knox, J.W., Weatherhead, E.K., Daneshkhah, A., Hess, T.M., 2014. Implementing precision irrigation in a humid climate - Recent experiences and on-

going challenges. Agric. Water Manag. 147, 135–143. https://doi.org/10.1016/j.agwat.2014.05.018

Das, A., Maiti, J., Banerjee, R.N., 2012. Process monitoring and fault detection strategies: a review. Int. J. Qual. Reliab. Manag. 29, 720–752. https://doi.org/10.1108/02656711211258508

De Fraiture, C., Wichelns, D., 2010. Satisfying future water demands for agriculture. Agric. Water Manag. 97, 502–511. https://doi.org/10.1016/j.agwat.2009.08.008

DeJonge, K.C., Kaleita, A.L., Thorp, K.R., 2007. Simulating the effects of spatially variable irrigation on corn yields, costs, and revenue in Iowa. Agric. Water Manag. 92, 99–109. https://doi.org/10.1016/j.agwat.2007.05.008

Delgoda, D., Malano, H., Saleem, S.K., Halgamuge, M.N., 2016. Irrigation control based on model predictive control (MPC): Formulation of theory and validation using weather forecast data and AQUACROP model. Environ. Model. Softw. 78, 40–53. https://doi.org/10.1016/j.envsoft.2015.12.012

Delgoda, D., Saleem, S.K., Malano, H., Halgamuge, M.N., 2014. Root zone soil moisture prediction models based on system identification: Formulation of the theory and validation using field and AQUACROP data. Agric. Water Manag. 163, 344–353. https://doi.org/10.1016/j.agwat.2015.08.011

Döll, P., 2002. Impact of climate change and variability on irrigation requirements: A global perspective. Clim. Change 54, 269–293. https://doi.org/10.1023/A:1016124032231

Erdem, Y., Arin, L., Erdem, T., Polat, S., Deveci, M., Okursoy, H., Gültaş, H.T., 2010. Crop water stress index for assessing irrigation scheduling of drip irrigated broccoli (Brassica oleracea L. var. italica). Agric. Water Manag. 98, 148–156. https://doi.org/10.1016/j.agwat.2010.08.013

Evans, R.G., Iversen, W.M., Kim, Y., 2012. Integrated Decision Support, Sensor Networks, and Adaptive Control for Wireless Site-Specific Sprinkler Irrigation. Adv. Irrig. 28, 377–387.

Evans, R.G., King, B.A., 2012. Site-specific sprinkler irrigation in a water-limtied future. Adv. Irrig. 55, 493–504.

Evans, R.G., LaRue, J., Stone, K.C., King, B.A., 2013. Adoption of site-specific variable rate sprinkler irrigation systems. Irrig. Sci. 31, 871–887. https://doi.org/10.1007/s00271-012-0365-x

Evett, S.R., Colaizzi, P.D., Howell, T.A., 2013. Wireless Sensor Network Effectively Controls Center Pivot Irrigation of Sorghum. Appl. Eng. Agric. 29, 853–864. https://doi.org/10.13031/aea.29.9921

Evett, S.R., Tolk, J. a., Howell, T. a., 2006. TDR Laboratory Calibration in Travel Time, Bulk Electrical Conductivity, and Effective Frequency. Vadose Zo. J. 5, 1020–1029. https://doi.org/10.2136/vzj2006.0062

Farg, E., Arafat, S.M., Abd El-Wahed, M.S., El-Gindy, A.M., 2012. Estimation of

Evapotranspiration ET c and Crop Coefficient K c of Wheat, in south Nile Delta of Egypt Using integrated FAO-56 approach and remote sensing data. Egypt. J. Remote Sens. Sp. Sci. 15, 83–89. https://doi.org/10.1016/j.ejrs.2012.02.001

Fernández, J.E., 2014. Plant-based sensing to monitor water stress: Applicability to commercial orchards. Agric. Water Manag. 142, 99–109. https://doi.org/10.1016/j.agwat.2014.04.017

Froisy, J.B., 2006. Model predictive control — Building a bridge between theory and practice. Comput. Chem. Eng. 30, 1426–1435. https://doi.org/10.1016/j.compchemeng.2006.05.044

Garcia-Ruiz, F., Sankaran, S., Maja, J.M., Lee, W.S., Rasmussen, J., Ehsani, R., 2013. Comparison of two aerial imaging platforms for identification of Huanglongbing-infected citrus trees. Comput. Electron. Agric. 91, 106–115. https://doi.org/10.1016/j.compag.2012.12.002

Geesing, D., Bachmaier, M., Schmidhalter, U., 2004. Field calibration of a capacitance soil water probe in heterogeneous fields. Aust. J. Soil Res. 42, 289–299. https://doi.org/10.1071/SR03051

Giusti, E., Marsili-Libelli, S., 2015. A Fuzzy Decision Support System for irrigation and water conservation in agriculture. Environ. Model. Softw. 63, 73–86. https://doi.org/10.1016/j.envsoft.2014.09.020

Goldstein, A., Fink, L., Meitin, A., Bohadana, S., Lutenberg, O., Ravid, G., 2018. Applying machine learning on sensor data for irrigation recommendations: revealing the agronomist's tacit knowledge. Precis. Agric. 19, 421–444. https://doi.org/10.1007/s11119-017-9527-4

Gonzalez-Dugo, V., Zarco-Tejada, P., Nicolás, E., Nortes, P.A., Alarcón, J.J., Intrigliolo, D.S., Fereres, E., 2013. Using high resolution UAV thermal imagery to assess the variability in the water status of five fruit tree species within a commercial orchard. Precis. Agric. 14, 660–678. https://doi.org/10.1007/s11119-013-9322-9

Goumopoulos, C., O'Flynn, B., Kameas, A., 2014. Automated zone-specific irrigation with wireless sensor/actuator network and adaptable decision support. Comput. Electron. Agric. 105, 20–33. https://doi.org/10.1016/j.compag.2014.03.012

Hardaha, M.K., Chouhan, S.S., Ambast, S.K., 2012. Application of Artificial Neural Network in Prediction of Response of Farmers Water Management Decisions on Wheat Yield. J. Indian Water Resour. Soc. 32, 1–12.

Hedley, C., Yule, I., 2009. Soil water status mapping and two variable-rate irrigation scenarios. Precis. Agric. 10, 342–355. https://doi.org/10.1007/s11119-009-9119-z

Hedley, C.B., Knox, J.W., Raine, S.R., Smith, R., 2014. Water: Advanced Irrigation Technologies. Encycl. Agric. Food Syst. 5, 378–406. https://doi.org/http://dx.doi.org/10.1016/B978-0-444-52512-3.00087-5

Hedley, C.B., Roudier, P., Yule, I.J., Ekanayake, J., Bradbury, S., 2013. Soil water status

and water table depth modelling using electromagnetic surveys for precision irrigation scheduling. Geoderma 199, 22–29. https://doi.org/10.1016/j.geoderma.2012.07.018

Hedley, C.B., Yule, I.J., 2009. A method for spatial prediction of daily soil water status for precise irrigation scheduling. Agric. Water Manag. 96, 1737–1745. https://doi.org/10.1016/j.agwat.2009.07.009

Heeren, D.M., Martin, D., Mateos, L., 2016. Pumpage Reduction by using Variable Rate Irrigation to Mine Undepleted Soil Water. Trans. ASABE 59, 1285–1298.

Hezarjaribi, A., 2008. Site-specific irrigation : Improvement of application map and a dynamic steering of modified centre pivot irrigation system. Federal Agricultural Research Centrer Braunschweig Germany.

Hornbuckle, J.W., Car, N.J., Christen, E.W., Stein, T., Williamson, B., 2009. IrriSatSMS Irrigation water management by satellite and SMS - A utilisation framework, CRC for Irrigation Futures Technical Report No. 01/09 CSIRO Land and Water Science Report No. 04/09.

Howell, T., Evett, S., 2004. The Penman-Monteith Method, USDA-Agricultural Research Service Conservation & Production Research Laboratory.

Hsiao, T.C., Heng, L., Steduto, P., Rojas-Lara, B., Raes, D., Fereres, E., 2009. Aquacrop-The FAO crop model to simulate yield response to water: III. Parameterization and testing for maize. Agron. J. 101, 448–459. https://doi.org/10.2134/agronj2008.0218s

Hunsaker, D., Barnes, E., Clarke, T., Fitzgerald, G., Pinter Jr, P., 2005. Cotton irrigation scheduling using remotely sensed and FAO-56 basal crop coefficients. Trans. ASAE 48, 1395–1407.

Hunsaker, D.J., Pinter, P.J., Barnes, E.M., Kimball, B.A., 2003. Estimating cotton evapotranspiration crop coefficients with a multispectral vegetation index. Irrig. Sci. 22, 95–104. https://doi.org/10.1007/s00271-003-0074-6

Iaea, 2008. Field estimation of soil water content: A practical guide to methods, instrumentation and sensor technology. At. Energy 131. https://doi.org/10.2489/jswc.64.4.116A

Jackson, R.D., Idso, S.B., Reginato, R.J., Pinter, P.J., 1981. Canopy temperature as a crop water stress indicator. Water Resour. Res. https://doi.org/10.1029/WR017i004p01133

Jones, H.G., 2014. Plants and Microclimate, Third Edit. ed. Cambridge University Press, New York.

Jones, H.G., 2004. Irrigation scheduling: Advantages and pitfalls of plant-based methods. J. Exp. Bot. 55, 2427–2436. https://doi.org/10.1093/jxb/erh213

Jones, H.G., 1999. Use of thermography for quantitative studies of spatial and temporal variation of stomatal conductance over leaf surfaces. Plant, Cell Environ. 22, 1043–1055. https://doi.org/10.1046/j.1365-3040.1999.00468.x

Jones, H.G., 1999. Use of infrared thermometry for estimation of stomatal conductance as

a possible aid to irrigation scheduling. Agric. For. Meteorol. 95, 139–149. https://doi.org/10.1016/S0168-1923(99)00030-1

Jones, H.G., Aikman, D., McBurney, T.A., 1997. Improvements to infra-red thermometry for irrigation scheduling in humid climates. Acta Hortic.

Jones, H.G., Leinonen, I., 2003. Thermal Imaging for the Study of Plant Water Relations. J. Agric. Meteorol. 59, 205–217. https://doi.org/10.2480/agrmet.59.205

Jones, H.G., Schofield, P., 2008. Thermal and other remote sensing of plant stress. Gen. Appl. Plant Physiol. 34, 19–32.

Jones, J.W., Hoogenboom, G., Porter, C.H., Boote, K.J., Batchelor, W.D., Hunt, L.A., Wilkens, P.W., Singh, U., Gijsman, A.J., Ritchie, J.T., 2003. The DSSAT cropping system model. Eur. J. Agron. 18, 235–265. https://doi.org/10.1016/S1161-0301(02)00107-7

Kacira, M., Ling, P.P., Short, T.H., 2002. Establishing Crop Water Stress Index (Cwsi) Threshold Values for Early, Non-Contact Detection of Plant Water Stress. Trans. ASAE 45, 775–780. https://doi.org/10.13031/2013.8844

Karasekreter, N., Başçiftçi, F., Fidan, U., 2013. A new suggestion for an irrigation schedule with an artificial neural network. J. Exp. Theor. Artif. Intell. 25, 93–104. https://doi.org/10.1080/0952813X.2012.680071

Kasslin, M., Kangas, J., Simula, O., 1992. Artificial Neural Networks. Artif. Neural Networks 1531–1534. https://doi.org/10.1016/B978-0-444-89488-5.50152-4

Kelleners, T.J., Robinson, D. a, Shouse, P.J., Ayars, J.E., Skaggs, T.H., 2005. Frequency dependence of the complex permittivity and its impact on dielectric sensor calibration in soils. Soil Sci. Soc. Am. J. 69, 67–76.

Kelly, B.F.J., Acworth, R.I., Greve, A.K., 2011. Better placement of soil moisture point measurements guided by 2D resistivity tomography for improved irrigation scheduling. Soil Res. 49, 504–512. https://doi.org/10.1071/SR11145

Keshavarzi, M., Ojaghlou, H., Nazemi, A., Ashraf, S., Ababaei, B., 2015. Effect of soil texture and organic matter on the accuracy of Time domain reflectometry method for estimating soil moisture, in: Soil and Water Pollution. pp. 368–373.

Kirda, C., 2002. Deficit irrigation scheduling based on plant growth stages showing water stress tolerance. Irrig. Sci. 3–10.

Knox, J.W., Kay, M.G., Weatherhead, E.K., 2012. Water regulation, crop production, and agricultural water management-Understanding farmer perspectives on irrigation efficiency. Agric. Water Manag. 108, 3–8. https://doi.org/10.1016/j.agwat.2011.06.007

Kohanbash, D., Kantor, G., Martin, T., Crawford, L., 2013. Wireless sensor network design for monitoring and irrigation control: User-centric hardware and software development. Horttechnology 23, 725–734.

Kristoph-Dietrich, K., Nkosinathi, M., Ramchand, O., 2012. Comparison of Laboratory and

Field Calibration of a Soil-Moisture Capacitance Probe for Various Soils. J. Irrig. Drain. 138, 416–423. https://doi.org/10.1061/(ASCE)IR

Kuhn, J., Brenning, A., Wehrhan, M., Koszinski, S., Sommer, M., 2009. Interpretation of electrical conductivity patterns by soil properties and geological maps for precision agriculture. Precis. Agric. 10, 490–507. https://doi.org/10.1007/s11119-008-9103-z

Lee, B.B., 2016. Economic Evaluation of Variable Rate Irrigation Center Pivot Technology. Rural Connect. 15–16.

Leib, B.G., Hattendorf, M., Elliott, T., Matthews, G., 2002. Adoption and adaptation of scientific irrigation scheduling: Trends from Washington, USA as of 1998. Agric. Water Manag. 55, 105–120. https://doi.org/10.1016/S0378-3774(01)00191-3

Leinonen, I., Jones, H.G., 2004. Combining thermal and visible imagery for estimating canopy temperature and identifying plant stress. J. Exp. Bot. 55, 1423–1431. https://doi.org/10.1093/jxb/erh146

Li, T., Hao, X., Kang, S., 2014. Spatiotemporal Variability of Soil Moisture as Affected by Soil Properties during Irrigation Cycles. Soil Sci. Soc. Am. J. 78, 598–608. https://doi.org/10.2136/sssaj2013.07.0269

Liu, H., Yang, H., Zheng, J., Jia, D., Wang, J., Li, Y., Huang, G., 2012. Irrigation scheduling strategies based on soil matric potential on yield and fruit quality of mulched-drip irrigated chili pepper in Northwest China. Agric. Water Manag. 115, 232–241. https://doi.org/10.1016/j.agwat.2012.09.009

Livellara, N., Saavedra, F., Salgado, E., 2011. Plant based indicators for irrigation scheduling in young cherry trees. Agric. Water Manag. 98, 684–690. https://doi.org/10.1016/j.agwat.2010.11.005

Lozoya, C., Mendoza, C., Mejía, L., Quintana, J., Mendoza, G., Bustillos, M., Arras, O., Solís, L., 2014. Model predictive control for closed-loop irrigation, in: IFAC Proceedings Volumes (IFAC-PapersOnline). pp. 4429–4434. https://doi.org/10.3182/20140824-6-ZA-1003.02067

Lund, E.D., Christy, C.D., Drummond, P.E., 2000. Using yield and soil electrical conductivity (EC) maps to derive crop production performance information., in: 5th International Conference on Precision Agriculture. pp. 1–10.

Mareels, I., Weyer, E., Ooi, S.K., Cantoni, M., Li, Y., Nair, G., 2005. Systems engineering for irrigation systems: Successes and challenges. Annu. Rev. Control 29, 191–204. https://doi.org/10.1016/j.arcontrol.2005.08.001

Martínez-Casasnovas, J.A., Bigorda, D.V., Ramos, M.C., 2006. Irrigation management zones for precision viticulture according to intra-field variability. Environment 523–530.

McCarthy, A.C., Hancock, N.H., Raine, S.R., 2014. Development and simulation of sensor-based irrigation control strategies for cotton using the VARIwise simulation framework. Comput. Electron. Agric. 101, 148–162.

https://doi.org/10.1016/j.compag.2013.12.014
McCarthy, A.C., Hancock, N.H., Raine, S.R., 2013. Advanced process control of irrigation: The current state and an analysis to aid future development. Irrig. Sci. 31, 183–192. https://doi.org/10.1007/s00271-011-0313-1
McCarthy, A.C., Hancock, N.H., Raine, S.R., 2010. VARIwise: A general-purpose adaptive control simulation framework for spatially and temporally varied irrigation at sub-field scale. Comput. Electron. Agric. 70, 117–128. https://doi.org/10.1016/j.compag.2009.09.011
Mengistu, M., Savage, M., 2010. Surface renewal method for estimating sensible heat flux. Water SA 36, 9–18.
Meron, M., Tsipris, J., Orlov, V., Alchanatis, V., Cohen, Y., 2010. Crop water stress mapping for site-specific irrigation by thermal imagery and artificial reference surfaces. Precis. Agric. 11, 148–162. https://doi.org/DOI 10.1007/s11119-009-9153-x
Miranda, F.R., Yoder, R.E., Wilkerson, J.B., Odhiambo, L.O., 2005. An autonomous controller for site-specific management of fixed irrigation systems. Comput. Electron. Agric. 48, 183–197. https://doi.org/10.1016/j.compag.2005.04.003
Misra, R.K., Padhi, J., 2014. Assessing field-scale soil water distribution with electromagnetic induction method. J. Hydrol. 516, 200–209. https://doi.org/10.1016/j.jhydrol.2014.02.049
Mohan, S., Arumugam, N., 1997. Expert system applications in irrigation management: an overview. Comput. Electron. Agric. 17, 263–280. https://doi.org/10.1016/S0168-1699(97)01309-4
Mousa, A.K., Abdullah, M.N., 2014. Fuzzy based Decision Support Model for Irrigation System Management. Int. J. Comput. Appl. 104, 14–20.
Mulla, D.J., 2013. Twenty five years of remote sensing in precision agriculture: Key advances and remaining knowledge gaps. Biosyst. Eng. 114, 358–371. https://doi.org/10.1016/j.biosystemseng.2012.08.009
Navarro-Hellín, H., Martínez-del-Rincon, J., Domingo-Miguel, R., Soto-Valles, F., Torres-Sánchez, R., 2016. A decision support system for managing irrigation in agriculture. Comput. Electron. Agric. 124, 121–131. https://doi.org/10.1016/j.compag.2016.04.003
Nemali, K.S., Montesano, F., Dove, S.K., van Iersel, M.W., 2007. Calibration and performance of moisture sensors in soilless substrates: ECH2O and Theta probes. Sci. Hortic. (Amsterdam). 112, 227–234. https://doi.org/10.1016/j.scienta.2006.12.013
O'Shaughnessy, S.A., Rush, C., 2014. Precision Agriculture: Irrigation. Encycl. Agric. Food Syst. 4, 521–535. https://doi.org/10.1016/B978-0-444-52512-3.00235-7
Ooi, S.K., Mareels, I., Cooley, N., Dunn, G., Thoms, G., 2008. A systems engineering approach to viticulture on-farm irrigation, in: IFAC Proceedings Volumes (IFAC-

PapersOnline). IFAC, pp. 9569–9574. https://doi.org/10.3182/20080706-5-KR-1001.0936

Osroosh, Y., Troy Peters, R., Campbell, C.S., Zhang, Q., 2015. Automatic irrigation scheduling of apple trees using theoretical crop water stress index with an innovative dynamic threshold. Comput. Electron. Agric. 118, 193–203. https://doi.org/10.1016/j.compag.2015.09.006

Pan, L., Adamchuk, V.I., Martin, D.L., Schroeder, M. a., Ferguson, R.B., 2013. Analysis of soil water availability by integrating spatial and temporal sensor-based data. Precis. Agric. 14, 414–433. https://doi.org/10.1007/s11119-013-9305-x

Pardossi, A., Incrocci, L., 2011. Traditional and New Approaches to Irrigation Scheduling in Vegetable Crops. Horttechnology 21, 309–313.

Payero, J.O., Irmak, S., 2006. Variable upper and lower crop water stress index baselines for corn and soybean. Irrig. Sci. 25, 21–32. https://doi.org/10.1007/s00271-006-0031-2

Pereira, L.S., Allen, R.G., Smith, M., Raes, D., 2014. Crop evapotranspiration estimation with FAO56: Past and future. Agric. Water Manag. 147, 4–20. https://doi.org/10.1016/j.agwat.2014.07.031

Phillips, A.J., Newlands, N.K., Liang, S.H.L., Ellert, B.H., 2014. Integrated sensing of soil moisture at the field-scale: Measuring, modeling and sharing for improved agricultural decision support. Comput. Electron. Agric. 107, 73–88. https://doi.org/10.1016/j.compag.2014.02.011

Pierce, F.J., 2010. Precision Irrigation. Landbauforsch. Völkenrode 45–55.

Plant, R.E., Horrocks, R.D., Grimes, D.W., Zelinski, L.J., 1992. CALEX/COTTON: An Integrated Expert System Application for Irrigation Scheduling. Am. Soc. Agric. Eng. ASAE 35, 1833–1838.

Postel, S.L., 1998. Water for Food Production : Will There Be Enough in 2025 ? crucial to meeting future food needs. Bioscience 48, 629–637.

Prakashgoud, P., Desai, B.L., 2013. Intelligent Irrigation Control System by Employing Wireless Sensor NetworksPatil. Int. J. Comput. Appl. 79, 33–40.

Prasad, G., Babu, A., 2007. PANI*: An Expert System for Irrigation Management. Georg. Electron. Sci. J. 1, 40–44.

Precision Farming to control irrigation and improve fertilization strategies on corn crops | Libelium [WWW Document], n.d. URL http://www.libelium.com/precision-farming-to-control-irrigation-and-improve-fertilization-strategies-on-corn-crops/ (accessed 1.17.17).

Prehn, A., Owen, J., Warren, S., Bilderback, T., Albano, J.P., dammeri Schneid, C.C., 2010. Comparison of Water Management in Container-Grown Nursery Crops using Leaching Fraction or Weight-Based On Demand Irrigation Control 1 28, 117–123.

Pretty, J.N., 1995. Participatory learning for sustainable agriculture. World Dev. 23, 1247–

1263. https://doi.org/10.1016/0305-750X(95)00046-F

Qin, J., Badgwell, T., 2003. A survey of industrial model predictive control technology. Control Eng. Pract. 11, 733–764.

Raes, D., Steduto, P., Hsiao, T.C., Fereres, E., 2009. Aquacrop-The FAO crop model to simulate yield response to water: II. main algorithms and software description. Agron. J. 101, 438–447. https://doi.org/10.2134/agronj2008.0140s

Raine, S., Mccarthy, A.C., 2009. Managing spatial and temporal variability in irrigated agriculture through adaptive control. Aust. J. Multi-Disciplinary Eng. 7, 79–90.

Raine, S.R., Meyer, W.S., Rassam, D.W., Hutson, J.L., Cook, F.J., 2007. Soil-water and solute movement under precision irrigation: Knowledge gaps for managing sustainable root zones. Irrig. Sci. 26, 91–100. https://doi.org/10.1007/s00271-007-0075-y

Ramírez-Builes, V., Harmsen, E., 2011. Water Vapor Flux in Agroecosystems Methods and Models Review, www.intechopen.com. https://doi.org/10.5772/585

Rani, M.N., Rajesh, T., 2013. Expert System with Special Reference to Agriculture. Int. J. Recent Technol. Eng. 2, 85–89.

Rani, P.M.N., Rajesh, T., Saravanan, R., 2011. Expert Systems in Agriculture : A Review. Int. J. Sci. Technol. Eng. 3, 59–71.

Rezaei, M., Pue, J. De, Seuntjens, P., Joris, I., Cornelis, W., 2017. Environmental Modelling & Software Quasi 3D modelling of vadose zone soil-water fl ow for optimizing irrigation strategies : Challenges , uncertainties and ef fi ciencies. Environ. Model. Softw. 93, 59–77.

Rhodig, L., Hillyer, C., 2013. Energy and Water Savings from Optimal Irrigation Management and Precision Application. ACEEE Summer Study Energy Effic. Ind. 1–12.

Romano, N., 2014. Soil moisture at local scale: Measurements and simulations. J. Hydrol. 516, 6–20. https://doi.org/10.1016/j.jhydrol.2014.01.026

Romano, N., D'Urso, G., Severino, G., Chirico, G.B., Palladino, M., Majone, B., Viani, F., Filippi, E., Bellin, a., Massa, a., Toller, G., Robol, F., Salucci, M., 2013. Wireless Sensor Network Deployment for Monitoring Soil Moisture Dynamics at the Field Scale. Procedia Environ. Sci. 19, 426–435. https://doi.org/10.1016/j.proenv.2013.06.049

Rosa, R., Dicken, U., Tanny, J., 2013. Estimating evapotranspiration from processing tomato using the surface renewal technique. Biosyst. Eng. 114, 406–413. https://doi.org/10.1016/j.biosystemseng.2012.06.011

Rosa, R., Tanny, J., 2015. Surface renewal and eddy covariance measurements of sensible and latent heat fluxes of cotton during two growing seasons. Biosyst. Eng. 136, 149–161. https://doi.org/10.1016/j.biosystemseng.2015.05.012

Rowlandson, T.L., Berg, A. a., Bullock, P.R., Ojo, E.R., McNairn, H., Wiseman, G., Cosh,

M.H., 2013. Evaluation of several calibration procedures for a portable soil moisture sensor. J. Hydrol. 498, 335–344. https://doi.org/10.1016/j.jhydrol.2013.05.021

Ruger, S., Netzer, Y., Westhoff, M., Zimmermann, D., Reuss, R., Ovadiya, S., Gessner, P., Zimmermann, G., Schwartz, A., Zimmermann, U., 2010. Remote monitoring of leaf turgor pressure of grapevines subjected to different irrigation treatments using the leaf patch clamp pressure probe. Aust. J. Grape Wine Res. 16, 405–412. https://doi.org/10.1111/j.1755-0238.2010.00101.x

Saavoss, M., Majsztrik, J., Belayneh, B., Lea-Cox, J., Lichtenberg, E., 2016. Yield, quality and profitability of sensor-controlled irrigation: a case study of snapdragon (Antirrhinum majus L.) production. Irrig. Sci. 34, 409–420. https://doi.org/10.1007/s00271-016-0511-y

Sadler, E.J., Evans, R.G., Stone, K.C., Camp, C.R., 2005. Opportunities for conservation with precision irrigation. J. Soil Water Conserv. 60, 371–378.

Saito, T., Fujimaki, H., Yasuda, H., Inoue, M., 2009. Empirical Temperature Calibration of Capacitance Probes to Measure Soil Water. Soil Sci. Soc. Am. J. 73, 1931–1937. https://doi.org/10.2136/sssaj2008.0128

Saleem, S.K.., Delgoda, D.., Ooi, S.K.., Dassanayake, K.B.., Yue, L.., Halmamuge, M.., Malano, H., 2013. Model Predictive Control for Real-Time Irrigation Scheduling, in: IFAC Conference on Modelling and Control in Agriculture, Horticulture and Post Harvest Industry. IFAC, Espoo, Finland, pp. 299–304. https://doi.org/10.3182/20130828-2-SF-3019.00062

Sánchez, J.A., Rodríguez, F., Guzmán, J.L., Arahal, M.R., 2012. Virtual sensors for designing irrigation controllers in greenhouses. Sensors 12, 15244–15266. https://doi.org/10.3390/s121115244

Sankaran, S., Mishra, A., Ehsani, R., Davis, C., 2010. A review of advanced techniques for detecting plant diseases. Comput. Electron. Agric. 72, 1–13. https://doi.org/10.1016/j.compag.2010.02.007

Sarma, A., 2016. Precision irrigation-a tool for sustainable management of irrigation water, in: Civil Engineering for Sustainable Development-Opportunities and Challenges.

Seelig, H.D., Stoner, R.J., Linden, J.C., 2012. Irrigation control of cowpea plants using the measurement of leaf thickness under greenhouse conditions. Irrig. Sci. 30, 247–257. https://doi.org/10.1007/s00271-011-0268-2

Shah, N.G., Das, I., 2012. Precision Irrigation : Sensor Network Based Irrigation. Probl. Perspect. Challenges Agric. Water Manag. 217–232.

Shapland, T.M., Snyder, R.L., Smart, D.R., Williams, L.E., 2012. Estimation of actual evapotranspiration in winegrape vineyards located on hillside terrain using surface renewal analysis. Irrig. Sci. 30, 471–484. https://doi.org/10.1007/s00271-012-0377-6

Sharma, A.B., Golubchik, L., Govindan, R., 2010. Sensor Faults : Detection Methods and Prevalence in Real-World Datasets. ACM Trans. Sens. Networks 6, 23.

https://doi.org/10.1145/1754414.1754419
Shaughnessy, S.A., Evett, S.R., Colaizzi, P.D., Howell, T.A., 2012. A crop water stress index and time threshold for automatic irrigation scheduling of grain sorghum. Agric. Water Manag. 107, 122–132. https://doi.org/10.1016/j.agwat.2012.01.018
Shaughnessy, S.A.O., Evett, S.R., Colaizzi, P.D., 2014. Infrared Thermometry as a Tool for Site-Specific Irrigation Scheduling, in: Proceedings of the 26th Annual Central Plains Irrigation Conference. pp. 136–145.
Shifeng, Y., Ye, Y., Jiankai, L., Xiuqing, W., 2008. Non-destructive Measurement on Crop Water Stress Based on Microcomputer. Proceeding ASABE 2008 Conf.
Singh, H., Sharma, N., 2014. Design and Development of Fuzzy Expert System for Potato Crop. Int. J. Emerg. Technol. Adv. Eng. 4, 278–283.
Singh, S.K., Dutta, S., Dharaiya, N., 2013. Estimation of Crop Evapotranspiration of Cotton using Remote Sensing Technique. Int. J. Environ. Eng. Manag. 4, 523–528.
Smith, D.M., Allen, S.J., 1996. Measurement of sap flow in plant stems. J. Exp. Bot. 47, 1833–1844. https://doi.org/10.1093/jxb/47.12.1833
Smith, R., Baillie, J., McCarthy, A., Raine, S.R., Baillie, C.P., 2010. Review of precision irrigation technologies and their application. Natl. Cent. ….
Smith, R.J., Baillie, J.N., Futures, I., 2009. Defining precision irrigation : A new approach to irrigation management, in: Irrigation and Drainage Conference. Victoria, Australia, pp. 18–21.
Steduto, P., Hsiao, T.C., Raes, D., Fereres, E., 2009. Aquacrop-the FAO crop model to simulate yield response to water: I. concepts and underlying principles. Agron. J. 101, 426–437. https://doi.org/10.2134/agronj2008.0139s
Steele, D.D., Stegman, E.C., Gregor, B.L., 1994. Field Comparison of Irrigation Scheduling Methods for Corn. Trans. Asae 37, 1197–1203.
Sun, G., Noormets, a., Chen, J., McNulty, S.G., 2008. Evapotranspiration estimates from eddy covariance towers and hydrologic modeling in managed forests in Northern Wisconsin, USA. Agric. For. Meteorol. 148, 257–267. https://doi.org/10.1016/j.agrformet.2007.08.010
Take the Guesswork Out of Irrigation | AquaSpy Home – AquaSpy [WWW Document], URL http://aquaspy.com/take-the-guesswork-out-of-irrigation/ (accessed 1.17.17).
Thomson, S.J., Ross, B.B., 1996. Model-based irrigation management using a dynamic parameter adjustment method. Comput. Electron. Agric. 14, 269–290. https://doi.org/10.1016/0168-1699(95)00033-X
Thorp, K.R., DeJonge, K.C., Kaleita, A.L., Batchelor, W.D., Paz, J.O., 2008. Methodology for the use of DSSAT models for precision agriculture decision support. Comput. Electron. Agric. 64, 276–285. https://doi.org/10.1016/j.compag.2008.05.022
Tomlinson, S.A., 1996. Weighing-Lysimeter Evapotranspiration for Two Sparse-Canopy Sites in Eastern Washington.

Topp, G.C., 2003. State of the art of measuring soil water content. Hydrol. Process. 17, 2993–2996. https://doi.org/10.1002/hyp.5148

Tsang, S.W., Jim, C.Y., 2016. Applying artificial intelligence modeling to optimize green roof irrigation. Energy Build. 127, 360–369. https://doi.org/10.1016/j.enbuild.2016.06.005

Turral, H., Svendsen, M., Faures, J.M., 2010. Investing in irrigation: Reviewing the past and looking to the future. Agric. Water Manag. 97, 551–560. https://doi.org/10.1016/j.agwat.2009.07.012

Uddin, J., Smith, R., Hancock, N., Foley, J., 2014. Evaluation of Sap Flow Sensors to Measure the Transpiration Rate of Plants during Canopy Wetting and Drying. J. Agric. Stud. 2, 105. https://doi.org/10.5296/jas.v2i2.6134

University of Florida, 2007. Field Guide to Proper Installation, Calibration, and Maintenance of Soil Moisture Sensor Control Systems in Residential Florida Landscapes, St. Johns River Water Management District.

Van Iersel, M.W., Chappell, M., Lea-Cox, J.D., 2013. Sensors for improved efficiency of irrigation in greenhouse and nursery production. Horttechnology 23, 735–746.

Varble, J.L., Chávez, J.L., 2011. Performance evaluation and calibration of soil water content and potential sensors for agricultural soils in eastern Colorado. Agric. Water Manag. 101, 93–106. https://doi.org/10.1016/j.agwat.2011.09.007

Vellidis, G., Tucker, M., Perry, C., Kvien, C., Bednarz, C., 2008. A real-time wireless smart sensor array for scheduling irrigation. Comput. Electron. Agric. 61, 44–50. https://doi.org/10.1016/j.compag.2007.05.009

Vereecken, H., Huisman, J. a., Pachepsky, Y., Montzka, C., van der Kruk, J., Bogena, H., Weihermüller, L., Herbst, M., Martinez, G., Vanderborght, J., 2014. On the spatio-temporal dynamics of soil moisture at the field scale. J. Hydrol. 516, 76–96. https://doi.org/10.1016/j.jhydrol.2013.11.061

Verstraeten, W.W., Veroustraete, F., Feyen, J., 2008. Assessment of Evapotranspiration and Soil Moisture Content Across Different Scales of Observation. Sensors 8, 70–117. https://doi.org/10.3390/s8010070

Wilson, K.B., Hanson, P.J., Mulholland, P.J., Baldocchi, D.D., Wullschleger, S.D., 2001. A comparison of methods for determining forest evapotranspiration and its components: Sap-flow, soil water budget, eddy covariance and catchment water balance. Agric. For. Meteorol. 106, 153–168. https://doi.org/10.1016/S0168-1923(00)00199-4

Yang, J., Li, B., Shiping, L., 2000. A large weighing lysimeter for evapotranspiration and soil-water-gr oundwater exchange studies. Hydrol. Process. 14, 1887–1897. https://doi.org/10.1002/1099-1085(200007)14:10<1887::AID-HYP69>3.0.CO;2-B

Yang, Z., Rao, M.N., Elliott, N.C., Kindler, S.D., Popham, T.W., 2009. Differentiating stress induced by greenbugs and Russian wheat aphids in wheat using remote

sensing. Comput. Electron. Agric. 67, 64–70. https://doi.org/10.1016/j.compag.2009.03.003

Young, P.C., Garnier, H., 2006. Identification and estimation of continuous-time, data-based mechanistic (DBM) models for environmental systems. Environ. Model. Softw. 21, 1055–1072. https://doi.org/10.1016/j.envsoft.2005.05.007

Zhang, J., Zhu, Y., Zhang, X., Ye, M., Yang, J., 2018. Developing a Long Short-Term Memory (LSTM) based model for predicting water table depth in agricultural areas. J. Hydrol. 561, 918–929. https://doi.org/10.1016/j.jhydrol.2018.04.065

Zhang, Y., Kang, S., Ward, E.J., Ding, R., Zhang, X., Zheng, R., 2011. Evapotranspiration components determined by sap flow and microlysimetry techniques of a vineyard in northwest China: Dynamics and influential factors. Agric. Water Manag. 98, 1207–1214. https://doi.org/10.1016/j.agwat.2011.03.006

Zhu, Q., Liao, K., Xu, Y., Yang, G., Wu, S., Zhou, S., 2012. Monitoring and prediction of soil moisture spatial – temporal variations from a hydropedological perspective : a review. Soil Res. 50, 625–637.

Zimmermann, U., Bitter, R., Marchiori, P.E.R., Rüger, S., Ehrenberger, W., Sukhorukov, V.L., Schüttler, A., Ribeiro, R.V., 2013. A non-invasive plant-based probe for continuous monitoring of water stress in real time: a new tool for irrigation scheduling and deeper insight into drought and salinity stress physiology. Theor. Exp. Plant Physiol. 25, 2–11. https://doi.org/10.1590/S2197-00252013000100002

Supplementary Material

1 Dielectric soil moisture sensors

The mode of operation of the Time Domain Reflectometry (TDR) Sensors, Time Domain Transmission (TDT) Sensors and Frequency Domain Reflectometry (FDR) Sensors is explained below

1.1 Time domain reflectometry (TDR) sensors

The TDR technique determines the apparent dielectric permittivity of soil by calculating the travel time of a reflected high frequency electromagnetic pulse (2-3GHz) in form of a fast-rise-step voltage through a waveguide of known length consisting of a coaxial cable connected to a pair of parallel probes of known length buried in the soil at the desired depth for soil moisture measurement (Romano, 2014). The pulse is reflected to the beginning of the probes and its travel distance is calculated as twice the length of the probe. A data acquisition and signal processing system is connected to the setup to analyse the waveform and determine the travel time from which the propagation velocity, v can be determined. Recent TDR probes mostly have the data acquisition and signal

processing electronics housed on top of the probes eliminating the use of coaxial cables. The propagation velocity, v is expressed as (Genuchten, 1986).

$$v = \frac{2l}{t} \quad (S1)$$

Where L is the length of the parallel probes, t is the travel time of the electromagnetic pulse and v is its propagation velocity. The dielectric permittivity, ε of a medium can be expressed in terms of the propagation velocity and the speed of light in a vacuum ($c = 3 \times 10^{8} ms^{-1}$) as

$$v = \frac{c}{\sqrt{\varepsilon}} \quad (S2)$$

Combining the above equations and setting $\varepsilon = K_a$, the apparent dielectric permittivity of soil, $K_a$is estimated by TDR as (Noborio, 2001)

$$K_a = \left(\frac{ct}{2l}\right)^2 \quad (S3)$$

The travel time of the pulse is determined by taking the first and second derivatives of the reflected waveform (Blonquist et al., 2005). The calculated apparent dielectric permittivity can be related to the volumetric moisture content (VMC) through empirical equations. A concept known as the dielectric mixing model is employed by some researchers to define a more physically based relationship between the dielectric permittivity measured by the TDR and the volumetric moisture content. It involves taking into account the dielectric permittivity of the individual components of soil, mainly air, water and solid particles to determine a composite dielectric permittivity of soil (Iaea, 2008). The influence of soil texture, salinity, temperature and soil bulk density on the measured volumetric moisture content is usually negligible. A high level of organic content in soil however introduces errors in the determination of moisture content by TDR (Noborio, 2001).

1.2 Time domain transmission (TDT) sensors

The TDT technique of estimating the apparent dielectric permittivity of soil is basically the same with the TDR technique (Blonquist et al., 2005).

The difference is that in TDT the pulse is generated at a much lower frequency (1-1.75GHz) and travels the length of the probe in one direction with no pulse reflection. The apparent dielectric permittivity, K_a is calculated with the factor of 2 omitted to indicate one way pulse travel (Evett & Schwartz, 2011)

$$K_a = \left(\frac{ct}{l}\right)^2 \quad (S4)$$

The performance characteristics have been reported so be similar to that of TDR (Blonquist et al., 2005).

1.3 Frequency domain reflectometry (FDR) sensors

The FDR technique also referred to as the capacitance technique measures the charge time of a capacitor inserted into soil with the soil acting as a dielectric medium (Romano, 2014). The measured charge time is related to the apparent dielectric permittivity of soil.

A capacitance soil moisture sensor is made up of a probe that forms a parallel plate capacitor which is connected to an oscillator circuit (Iaea, 2008). This connection forms an LC circuit. Most capacitance sensors are installed into the soil using an access tube system (Polyakov et al., 2005). When installed in the soil the changes in frequency of the oscillator system is dependent on the change in the dielectric properties of soil which in turn influences the capacitance of the system. Due to the high dielectric permittivity of water in comparison to the other constituents of soil, it has the largest influence on the capacitance of the system (Kelleners et al., 2005). The frequency of the system decreases as the apparent dielectric permittivity of the system increases due to an increase in system capacitance which corresponds to an increase in soil moisture content. The volumetric moisture content is related to the frequency change through empirical equations (Iaea, 2008).

The capacitance, C (F) of the access tube system is given as

$$C = g\varepsilon_a \quad (S5)$$

Where ε_a is the apparent dielectric permittivity of the system and g is a capacitance value dependent on the geometry of the system (Skierucha and Wilczek, 2010).

The resonant frequency, F (HZ) of the system is (Iaea, 2008)

$$F = [2\pi(L)^{0.5}]^{-1}\left(C^{-1} + C_b^{-1} + C_c^{-1}\right)^{0.5} \quad (S6)$$

C, is the capacitance (F) of the access tube system defined previously, C_b and C_c are the capacitance of the probe and the internal circuit elements and L, is the inductance (H) of the coil in the LC circuit. The frequency of the oscillator system is also largely dependent on the soil bulk electrical conductivity (EC) which is determined by soil texture, bulk density and salinity. The temperature dependence of the permittivity of water also makes

the system sensitive to changes in temperature. These problems can however be minimized using measurement frequencies greater than 50Hz. The frequency operation range of most capacitance sensors is usually between 20-100MHz although newer systems now operate at frequencies in the region of 300MHz (Romano, 2014).

References

Blonquist, J.M., Jones, S.B., Robinson, D. a., 2005. A time domain transmission sensor with TDR performance characteristics. J. Hydrol. 314, 235–245. https://doi.org/10.1016/j.jhydrol.2005.04.005

Evett, S.R., Schwartz, R.C., 2011. Discussion of “Soil Moisture Measurements: Comparison of Instrumentation Performances” by Ventura Francesca, Facini Osvaldo, Piana Stefano, and Rossi Pisa Paola. J. Irrig. Drain. Eng. 137, 466–468. https://doi.org/10.1061/(ASCE)IR.1943-4774.0000247

Genuchten, F.N.D. and M.T. Van, 1986. The time-domain reflectometry method for measuring soil water content and salinity. Geoderma 38, 237–250.

Iaea, 2008. Field estimation of soil water content: A practical guide to methods, instrumentation and sensor technology. At. Energy 131. https://doi.org/10.2489/jswc.64.4.116A

Kelleners, T.J., Robinson, D. a, Shouse, P.J., Ayars, J.E., Skaggs, T.H., 2005. Frequency dependence of the complex permittivity and its impact on dielectric sensor calibration in soils. Soil Sci. Soc. Am. J. 69, 67–76.

Noborio, K., 2001. Measurement of soil water content and electrical conductivity by time domain reflectometry: A review. Comput. Electron. Agric. 31, 213–237. https://doi.org/10.1016/S0168-1699(00)00184-8

Polyakov, V., Fares, a., Ryder, M.H., 2005. Calibration of a Capacitance System for Measuring Water Content of Tropical Soil. Vadose Zo. J. 4, 1004. https://doi.org/10.2136/vzj2005.0028

Romano, N., 2014. Soil moisture at local scale: Measurements and simulations. J. Hydrol. 516, 6–20. https://doi.org/10.1016/j.jhydrol.2014.01.026

Skierucha, W., Wilczek, A., 2010. A FDR sensor for measuring complex soil dielectric permittivity in the 10-500 MHz frequency range. Sensors 10, 3314–3329. https://doi.org/10.3390/s100403314

General objective of the study

The review clearly shows that the development of adaptive decision support systems to aid the precision irrigation management of crops will further enhance the sustainable use of limited water resources. This will be enabled by the availability of quality sensor data and robust data-driven models of crop response to water availability.

The need to consider the various factors affecting the performance of dielectric sensors when deployed to provide data to aid irrigation scheduling decisions has been highlighted. Previous studies in the literature have shown that site-specific calibration equations developed for these sensors will generally improve their performance. Nevertheless, sensor manufacturers consistently claim that they will perform optimally when the factory supplied calibration functions are used. This is especially commonplace with the release of new sensor models into the market.

Despite the advancements in the field of precision irrigation, research on the development of adaptive decision support tools is lacking. Consideration of the time-varying nature of the cropping system is an important aspect in the development of robust irrigation decision support systems. These systems will further benefit from the use of data-driven models for the prediction and fulfillment of crop water requirements. This will enable the system to adjust to external perturbations and learn from data in order to modify irrigation decisions based on the crop response. On this basis, it was hypothesized that data-driven models which are capable of predicting crop water requirements and the plant response to water supply can aid precision irrigation scheduling.

The general objective of this work was the development of novel data-driven models that are able to predict the crop water requirements while considering the time-varying nature of the cropping system. The application of such data-driven models for the prediction of irrigation timing and depth and the sustainability improvement potential of model-based predictive irrigation scheduling was demonstrated. The need to ensure the availability of quality data from soil moisture sensors to ensure robust irrigation decisions was also investigated. These objectives sum up the three key requirements of precision irrigation; measurement, monitoring, and management. Succinctly, measurement is viewed as the physical sensing of various attributes of the soil-plant-atmosphere continuum which relate to crop water use. Monitoring is the application of various modelling techniques to the sensor measurements in order to quantify the response of crops to water availability. Management is the synergy of the measurement and monitoring phase which informs the timing and amount of irrigation application.

The remaining chapters (i.e. 2-5) of the thesis are written as a series of papers. Thus, each chapter is presented with an abstract, and an extended introduction, and a result and discussion.

The specific objectives for each chapter are explained below.

Specific objectives

Chapter 2: Performance evaluation of three dielectric soil moisture sensors.

The objective in Chapter 2 was to develop soil-specific calibration equations for three soil moisture sensors to predict soil moisture in three different soil types. The effects of soil texture, bulk density, salinity and temperature on the performance of the sensors were also investigated.

Chapter 3: Dynamic modelling of the baseline temperatures for computation of the crop water stress index (CWSI) of a greenhouse cultivated lettuce crop.

The objective in Chapter 3 was to exhibit the potential of using a data-driven dynamic model to predict the baseline temperatures and demonstrate the applicability in calculating an empirical CWSI for a lettuce crop (*Lactuca sativa*) grown under greenhouse conditions. This model will be capable of accounting for the time-varying nature of the crop response to water availability.

Chapter 4: Dynamic modelling of lettuce transpiration for water status monitoring

The objective in Chapter 4 was to develop a novel data-driven dynamic model capable of predicting the transpiration rate of a lettuce crop (*Lactuca sativa*) grown under greenhouse conditions. The predicted transpiration rate is used as a tool for monitoring the water status of the lettuce plants and real-time detection of deviations from a defined water status state. This model will be capable of accounting for the time-varying nature of the crop response to water availability.

Chapter 5: Dynamic neural network modelling of soil moisture content for predictive irrigation scheduling.

The objective in Chapter 5 was to develop dynamic neural network models for the prediction of volumetric soil moisture content in three different soil types. The application of the dynamic neural network models in predictive irrigation scheduling was explored. The water savings potential of a dynamic neural network model-based predictive irrigation scheduling system was also demonstrated using simulations.

Chapter 2 Performance Evaluation of Three Dielectric Soil Moisture Sensors

Abstract

The various factors affecting the performance of dielectric soil moisture sensors include soil texture, bulk density, salinity, and temperature variations. It is therefore important to take these factors into account when deploying these sensors. This study evaluated the performance of three dielectric soil moisture sensors; GS 1 (Decagon Devices), Stevens Hydraprobe II (Stevens Water) and TDR 315 (Acclima Inc.) under laboratory conditions. Measured soil moisture contents on three sandy loam soils with contrasting particle composition (light, medium and heavier textured) were compared with corresponding values derived from gravimetric samples. The sensors were also evaluated under conditions of varying bulk density, temperature, and salinity. Results indicated that a linear calibration equation developed for the three sensors in the soils tested could improve their accuracy. The TDR 315 and Hydraprobe sensors underestimated soil moisture with an increase in compaction in the medium textured soil while the GS 1 sensor readings were slightly influenced. The results showed that the sensor outputs responded linearly to increasing temperature in the light and heavier textured soils, recording errors in soil moisture estimates over a 13°C temperature increase in the soils tested. An increase in salinity level in the light and heavier textured soils further increased the errors in the recorded soil moisture estimates. This was however not observed for the TDR 315 sensor when salinity was increased in the light textured soil. An empirical temperature compensation procedure substantially reduced the temperature effects on the sensor output in the soils tested. These sensors can be useful in monitoring soil moisture fluxes and in irrigation scheduling with laboratory-derived calibration and temperature compensation functions significantly improving their accuracy.

1 Introduction

Due to the reduced global availability of fresh water, it has become imperative to develop methods that improve water use in irrigated agriculture. A common approach is the use of soil moisture sensors that monitor the field scale volumetric water content (VWC). This enables growers to schedule irrigation when the soil moisture is depleted to a defined threshold which results in improved irrigation timing and application depths (Chávez et al., 2011).

The neutron probe has long been considered a reliable method of estimating soil moisture content, but the associated radioactive hazards, high cost and inability to automate data collection, limits its application in irrigation management (Lukanu and Savage, 2006). Dielectric soil moisture sensors provide a suitable means of continuously monitoring field scale soil moisture status. They take advantage of the high dielectric permittivity of water relative to other soil constituents to infer soil moisture content. The dielectric permittivity of soil is however influenced by other factors including soil texture, bulk density, salinity, and temperature, therefore a careful consideration of these factors is essential for the accurate determination of soil moisture content (Paige and Keefer, 2008).

The variability in the dielectric properties of different soil types and the influence of dry plant tissues make it necessary to calibrate dielectric sensors for every soil type (Polyakov et al., 2005). A number of researchers have conducted studies with dielectric sensors in various soil types and generally conclude that a soil specific calibration developed either in the field or laboratory will generally improve sensor accuracy (Kammerer et al., 2014; Keshavarzi et al., 2015; Mittelbach et al., 2012). Lukanu and Savage (2006) reported that variations in clay content and bulk density had an effect on the performance of a capacitance sensor; the Thetaprobe. Keshavarzi et al. (2015) reported a decrease in the measured VWC by a Time Domain Reflectometry (TDR) probe with an increase in percentage clay and organic matter content. Fares et al. (2011) also reported a similar decrease in measured volumetric water content by three different capacitance sensors in soils with high clay content.

In irrigated agriculture, there is a tendency for the soil salinity to increase due to the quality of irrigation water used, application of various nutrients to the soil in form of fertigation and fertilizer application (Thompson et al., 2007). The dielectric measurement of electromagnetic soil moisture sensors is widely affected by salinity which is closely linked to the soil bulk electrical conductivity especially at low operating frequencies less than 50 MHz. The effect of salinity on the operation of dielectric soil moisture sensors is a function of the dielectric losses in the imaginary part of the complex permittivity and it is positively dependent on the soil's ionic conductivity (Saito et al., 2008). The effect of salinity on dielectric measurements is usually masked at low temperatures (Bogena et al., 2007). Dielectric losses in soils due to salinity can, however, be ignored in soils with

conductivities less than 0.5 dsm^{-1} at low operating frequencies (Bosch, 2004). Thompson et al. (2007) reported an increase in volumetric moisture measurements of 7.5% for every increase of 1 dsm^{-1} increase in pore water electrical conductivity in a sandy loam soil and an increase of 4% in VWC measurement for every increase of 1 dsm^{-1} in pore-water electrical conductivity in a clay soil when using a capacitance sensor. They employed a scaled frequency calibration approach to compensate for the salinity effect but no remarkable improvement was reported. Saito et al. (2008) reported a 16.2% error in VWC estimates by two capacitance sensors in a sandy soil with pore water electrical conductivities of up to 31dsm^{-1}. An empirical calibration procedure reduced the error in the VWC estimates to around 1.1%. Benor et al. (2013) reported an underestimation of VWC by a TDR sensor in sand with an increase in salinity.

Temperature variations in the field affect the performance of electromagnetic soil moisture sensors. The influence of increasing temperature occur via the following mechanisms

- Decrease in the apparent dielectric permittivity of free water; usually predominant at a high moisture content in soils with low clay content.
- Increase in the dielectric measurement due to the release of bound water; usually predominant at a low moisture content in soils with high clay content.
- Increase in the dielectric measurement due to signal attenuation at high electrical conductivity with the influence of electrical conductivity positively dependent on soil temperature; usually predominant in soils with high salinity.

Czarnomski et al. (2005) reported an underestimation of VWC of about 0.1% for every 1°C increase in temperature by a capacitance probe installed in a sandy loam soil. Polyakov et al. (2005) evaluated a capacitance sensor in a clay soil and reported a 15% overestimation of VWC over a 45°C temperature range. Gong et al. (2003) reported an underestimation of VWC by a TDR sensor installed in a sandy loam soil at high moisture contents with increasing temperature. Theoretical approaches based on effective frequency and complex permittivity model for compensating for the effect of temperature and salinity on the accuracy of dielectric sensors have been successfully applied by Evett et al. (2006) and Schwartz et al. (2009). These methods improve the accuracy of the sensors but they require an extensive knowledge of electromagnetics and high-cost spectrum analyzing equipment limiting their use to research. Benson and Wang (2006) and Saito et al. (2009) have successfully applied empirical compensation procedures to reduce the influence of temperature on the accuracy of several dielectric soil moisture sensors.

Three dielectric soil moisture sensors are considered in this study; the GS 1 volumetric soil moisture sensor (Decagon Devices, Pullman, Washington, USA), the Hydraprobe II (Stevens Water, Portland, Oregon, USA) and the TDR 315 (Acclima Inc, Meridian, Idaho,

USA). The three sensors were recently released into the market and to the best of our knowledge, there are presently no peer-reviewed articles on their comparison. The sensors also have a different method of inferring the dielectric permittivity of the sensed media. Several researchers have previously evaluated the earlier version of the Hydraprobe. Merlin et al. (2007) reported that the Hydraprobe sensor's response differs significantly with soil type. An overestimation of around 3% VWC was reported for a 15°C temperature rise in a clay soil. Seyfried and Murdock (2004) reported similar observations in a loam soil. Bosch (2004) and Kammerer et al. (2014) reported an improvement in the Hydraprobe sensor's VWC estimates using laboratory derived calibration equations.

The purpose of this study is therefore to develop soil-specific calibrations for the three soil moisture sensors to predict soil moisture in three different soil types. The effects of soil texture, bulk density, salinity and temperature on the performance of the sensors are also investigated. In order to achieve this, experiments were designed to answer the following research questions

1. What empirical relationships adequately relate the output of the soil moisture sensors to the laboratory measured soil moisture content of different soil types from three different sites?
2. What improvement in sensor accuracy can be achieved by using laboratory-developed calibration equations in comparison to the default equations specified by the manufacturers?
3. To what extent do variations in bulk density due to the compaction levels encountered in the field affect the accuracy of the soil moisture sensors?
4. To what extent do temperature variations over the range encountered in the field soils affect the accuracy of the soil moisture sensors?
5. To what extent does variable salinity over the range encountered in the field soils affect the accuracy of the soil moisture sensors?
6. What improvement in sensor accuracy can be achieved by using laboratory derived empirical temperature corrections when sensors are used in soils with either high temperature or salinity?

2 Material and Methods

2.1 Sensors

The Hydraprobe II and GS 1 are both frequency domain sensors. In order to infer the VWC of the soil, the Hydraprobe II sensor measures the real dielectric permittivity of the soil while the GS 1 sensor measures the apparent dielectric permittivity (a combination of the real and imaginary part of the dielectric permittivity). The TDR 315 operates in the time domain and infers the soil's VWC from its measured apparent dielectric permittivity. The mode of operation of the sensors is further explained below.

2.1.1 GS 1 volumetric soil moisture sensor

The GS 1 volumetric soil moisture sensor is a capacitance sensor operating at a frequency of 70 MHz. The sensor applies an oscillating wave at the stated frequency to the soil to form a complete capacitor. The charge stored in the sensor probes after a predetermined time is directly proportional to the soil's apparent dielectric permittivity which can be related empirically to the volumetric water content of the soil. According to the manufacturer, the sensor's output is unaffected by variations in soil texture and has an accuracy of ±3% VWC in soils with EC of less than 8 dsm^{-1} and temperatures less than 50°C. The manufacturer also states that the accuracy can be increased to ±1% VWC using soil-specific calibration. The GS 1 sensor has a measurement region with a diameter of 11 cm. The GS 1 sensor outputs an analog voltage of between 0 - 5 V which can be related to the VWC of the soil using the manufacturer supplied calibration equation for mineral soils.

2.1.2 Hydraprobe II

The Hydraprobe II sensor, hereafter referred to as Hydraprobe, operates at a frequency of 50 MHz. The sensor calculates the amplitude ratio of reflected waves within its probes when installed in soil and applies a numerical solution of Maxwell's equation to calculate the real dielectric permittivity of the surrounding soil based on this. The real dielectric permittivity is then related empirically to the volumetric water content of the soil. According to the manufacturer, this procedure makes the probe immune to variations in soil texture, salinity, and temperature. The sensor has a measurement region with a diameter of 3 cm. The stated accuracy of the sensor is ±3% VWC in all soil types. The Hydraprobe is an SDI-12 sensor which outputs the raw VWC of the soil in water fraction by volume ($\mathrm{m}^3\mathrm{m}^{-3}$).

2.1.3 TDR 315

The TDR 315 operates at a wave propagation bandwidth of 3500 MHz. It measures the time taken by a reflected wave to travel through its probes which can be related to the apparent dielectric permittivity of the sensed soil medium.

The calculated apparent dielectric permittivity is related to the volumetric soil water content using propriety equation similar to the Topp's model (Topp et al., 1980). According to the manufacturer, this procedure makes the sensor immune to variations in soil texture, salinity, and temperature. The stated accuracy of the sensor is ±2% VWC in all soil types up to a maximum bulk EC of 5 dsm^{-1}. A temperature accuracy of ±1% VWC is reported by the manufacturer for a temperature range of 0 - 50°C. A measurement region with a diameter of 5 cm is reported for the sensor. The TDR 315 is an SDI-12 sensor which outputs the raw VWC of the soil in % water content.

Four of each of the respective sensor types were evaluated; making a total of twelve sensors (4 GS 1, 4 Hydraprobe, 4 TDR 315). The output of the GS 1 sensors was logged using a Campbell scientific CR 1000 datalogger (Campbell Scientific, Logan, Utah, USA) programmed with the manufacturer's default calibration equation for mineral soils. The output of the Hydraprobe and TDR 315 sensors was logged using an Acclima datasnap SDI-12 datalogger (Acclima Inc, Meridian, Idaho, USA). For the purpose of uniformity the output of all sensors are presented in units of water fraction by volume; $\mathrm{m^3 m^{-3}}$.

2.2 Soils

Soils were collected from the top 30 cm in three different sites in Harper Adams University, England (-2°25'39.06" W; 52°46'46.74" N) to represent a range of soil textures typical of the University's Farms. The physical properties of the soils are summarized in Table 1

Table 1. Physical properties of the soils tested

Site	Soil type	Sand %	Silt %	Clay %	Organic matter %	Dry bulk density $(\mathrm{gcm^{-3}})$	Field capacity $(\mathrm{m^3 m^{-3}})$	Permanent wilting point $(\mathrm{m^3 m^{-3}})$
Crabtree (CT)	Sandy loam (light textured)	79	9	12	2.7	1.19	0.114	0.06
Back of CERC (BOC)	Sandy loam (medium textured)	72	15	13	2.5	1.28	0.144	0.071
Blackbirtch (BB)	Sandy loam (heavier textured)	67	16	17	2.7	1.30	0.18	0.082

2.3 Experiments

Three experiments were performed. The first experiment established the relationships between the output of the sensors and the gravimetrically measured volumetric water content (VWC) for the various soils. The second experiment examined the relationships between the VWC estimate of the sensors and the gravimetrically measured VWC

estimates in a soil subjected to both a medium and high level of compaction similar to that experienced in the field. The third experiment examined the effect of soil temperatures on the output of the three sensors. Soil temperatures were varied within the range typically experienced in the field.

In all the experiments the performance of the calibration equations derived in the laboratory was compared with those supplied by the manufacturer.

2.3.1 Experiment 1

The laboratory calibrations were performed using the soils from the three sites at a room temperature of 22 ± 2°C. The laboratory calibration was based on the procedure proposed by Campbell et al. (2009). Soils collected from each field were air dried and passed through a 5mm sieve. They were then packed into 4 L containers (diameter 16 cm, height 19 cm) at the approximate field bulk density by adding equal volumes of soil in three layers. The water content of each container was altered by adding deionized water in increments of 400 ml to represent soil moisture contents from air dry to saturation. This produced soil moisture contents ranging from 0 – 0.45 $\mathrm{m^3 m^{-3}}$ in the three soils. The containers were wrapped with polythene to prevent surface evaporation and left for 48 hours in order for the soil moisture to equilibrate. A total of twelve replicates for each soil/soil moisture content combination were prepared. The twelve sensors were randomly assigned to the containers and the readings over 10 mins intervals were averaged. After each reading gravimetric samples were taken from the containers and oven dried a 105°C for 24 h. The volumetric water content was calculated by multiplying the gravimetric water content by the soil's bulk density and dividing by the density of pure water.

2.3.2 Experiment 2

The medium textured soil from BOC was used in this experiment. This is because all the soils had a similar range of dry bulk density and organic matter content. Therefore, the sensor response to variation in bulk density in the BOC soil will be similar to the response expected in the two other soils (Saini, 1966). Soils collected from the field were air dried and passed through a 5mm sieve. Adapting the methodology outlined by John et al. (1986), the soil was packed into 4 L calibration containers and compacted in three layers to a medium and high level of compaction similar to that experienced in the field by imposing a load of 2.1 KN and 3.5KN respectively using a tensile testing machine (Samuel Denison and Son Ltd, Leeds, UK). These values were calculated based on the Proctor compaction principle which is the laboratory standard for determining the maximum bulk density of soils (ASTM Standard D1557, 2009). The load imposed for the medium compaction level corresponds to 15 taps of the Proctor hammer while that for the high compaction level corresponds to 25 taps of the Proctor hammer based on the dimensions of the calibration container.

This produced an average bulk density of 1.35 gcm^{-3} in the moderately compacted soil and 1.42 gcm^{-3} in the highly compacted soil. Laboratory calibration equations were then developed for the soils at both compaction levels following the methodology outlined in Experiment 1.

2.3.3 Experiment 3

For this experiment, the light textured soil from CT and the heavier textured soil from BB was used. This is because the two soils had the largest difference in clay content which is the major factor influencing the temperature response of dielectric soil moisture sensors in both saline and non-saline soils (Kizito et al., 2008). Soils collected from each field was air dried and passed through a 5mm sieve. They were then packed into 4 L containers at the approximate field bulk density by adding equal volumes of soil in layers. Following the methodology proposed by Benson and Wang (2006), the soils were brought to five moisture levels by adding deionized water in increments of 400 ml. This produced soil moisture content ranging from 0.05 – 0.35 $\mathrm{m}^3\mathrm{m}^{-3}$ in the soils from CT and 0.05 – 0.39 $\mathrm{m}^3\mathrm{m}^{-3}$ in the soils from BB. The containers were then wrapped in polythene to prevent surface evaporation and left for 48 h for soil moisture to equilibrate. Each of the soil/soil moisture content combinations was then subjected to temperatures of 5, 15, 25 and 35°C in an incubator (Model ICI 180, Sanyo Electric Co, Osaka, Japan). The temperature of the soil was monitored with a thermocouple and at each temperature step, time was allowed for the soil temperature to equilibrate. A total of twelve replicates for each soil/soil moisture content combination was prepared. At each temperature step the averaged sensor readings were then logged over 10 mins intervals by randomly assigning each of the twelve sensors to a container. After the temperature variation procedure gravimetric samples were taken from the containers and oven dried at 105°C for 24 h.

To investigate the effect of variable salinity on the performance of the sensors a one-time addition of salts to soils from both sites was performed. The aim was to increase the bulk EC at saturation of each soil to values less than 12 dsm^{-1} which is the recommended limit for agricultural soils (Kizito et al., 2008). To achieve this 100 g of calcium chloride dihydrate was dissolved in 400 ml of deionized water and mixed thoroughly with air-dried soils from CT and BB. They were then air-dried prior to the addition of deionized water in increments of 400 ml in order to produce five different moisture levels in the soils. This produced bulk EC readings in the range of 0.4 dSm^{-1} to 5 dSm^{-1} in the soil from CT and 0.8 dSm^{-1} to 8.3 dSm^{-1} in the soils from BB. The bulk EC was measured using the TDR 315 sensor. Temperature variation tests on the soils were then conducted following the procedure outlined in the paragraph above.

2.4 Statistical analysis

Calibration equations using linear least squares regression were developed to relate laboratory derived gravimetric water content to the values measured by the sensors. Following recommendations by Varble and Chávez (2011), two statistical tests were used to evaluate the default manufacturers calibration equations and the laboratory-derived calibration equations. They include the mean bias error (MBE) and root mean square error (RMSE). A calibration equation with an MBE value of ±0.02 $\mathrm{m^3 m^{-3}}$ and RMSE value less than 0.035 $\mathrm{m^3 m^{-3}}$ was considered accurate. These values are chosen to reflect the measurement accuracy of 0.01 – 0.02 $\mathrm{m^3 m^{-3}}$ required in agricultural applications (Iaea, 2008).

In the temperature changing experiment, the performance of the sensors was evaluated by relating the sensor output to the temperature range investigated using linear least squares regression.

All statistical analysis was carried out using the JMP statistical package (SAS Institute, North Carolina, USA).

3 Results

3.1 Factory calibration evaluation

The statistical parameters for the laboratory evaluation of the sensors are listed in Table 2. Table 2 shows that under laboratory conditions the factory based calibration of the three sensors types achieved the required accuracy within the air dry to saturation range in the light textured soil (CT). Varble and Chávez (2011) reported similar results for a Decagon 5TE sensor evaluated in a sandy soil. The MBE values for the TDR 315's factory calibration in Table 2 show that the sensor underestimated volumetric water content (VWC) by an average of 0.034 $\mathrm{m^3 m^{-3}}$ in the heavier textured soil (BB) and an average of 0.023 $\mathrm{m^3 m^{-3}}$ in the medium textured soil (BOC). The highest errors in VWC estimates by TDR 315 were recorded in the heavier textured soil from low moisture content to high moisture content range ($P < 0.001$). The Hydraprobe sensor's factory calibration recorded the highest errors in VWC estimates in the heavier textured soil ($P<0.001$). The sensor underestimated VWC by an average of 0.047 $\mathrm{m^3 m^{-3}}$ in the heavier textured soil. The factory calibration of the GS 1 sensor was accurate in the light and medium textured soil. However, the calibration was not accurate in the heavier textured soil with an underestimation of VWC by an average of 0.021 $\mathrm{m^3 m^{-3}}$ and an RMSE of 0.05 $\mathrm{m^3 m^{-3}}$. During the laboratory evaluation, a maximum EC of 0.1 $\mathrm{dS m^{-1}}$ was recorded in the soil from CT, 0.19 $\mathrm{dS m^{-1}}$ in the soil from BOC and 0.35 $\mathrm{dS m^{-1}}$ in the soil from BB.

Table 2. Comparison of factory calibration based VWC (m^3m^{-3}) with laboratory measurements of VWC (m^3m^{-3}) for the different sensors and soils. BB is the heavier textured soil, BOC is the medium textured soil and CT is the light textured soil.

Sensor and soil type	R^2	MBE (m^3m^{-3})	RMSE (m^3m^{-3})
TDR 315			
BB	0.76	-0.034	0.05
BOC	0.85	-0.023	0.03
CT	0.91	-0.015	0.03
Hydraprobe			
BB	0.54	-0.047	0.06
BOC	0.91	-0.017	0.03
CT	0.94	-0.015	0.03
GS 1			
BB	0.81	-0.021	0.05
BOC	0.92	-0.006	0.03
CT	0.92	0.009	0.03

Figure 1 shows that a linear calibration equation provides a good fit for the data collected during the laboratory evaluation of all the three sensor types in the light, medium and heavier textured soils. Figure 1 indicates that the factory calibration equation of the TDR 315 sensor was accurate at lower moisture contents in the light textured soil and underestimated VWC at higher moisture contents. This was also the case for the Hydraprobe sensor. The GS1 sensor was accurate at lower moisture contents in the light textured soil but overestimated VWC at higher moisture content. Figure 1 also shows that

in the medium textured soil, the factory calibration of the Hydraprobe sensor underestimated VWC at both lower and higher moisture contents with the magnitude of underestimation increasing at higher moisture contents. This was also the case for the TDR315 sensor. It also shows that the factory calibration of the GS 1 sensor was more accurate at lower moisture contents than at higher moisture contents. It can also be seen that the three sensors perform with less accuracy in the heavier textured soil. The sensors all underestimate the VWC in the lower and higher moisture range. This is in agreement with the data presented in Table 2.

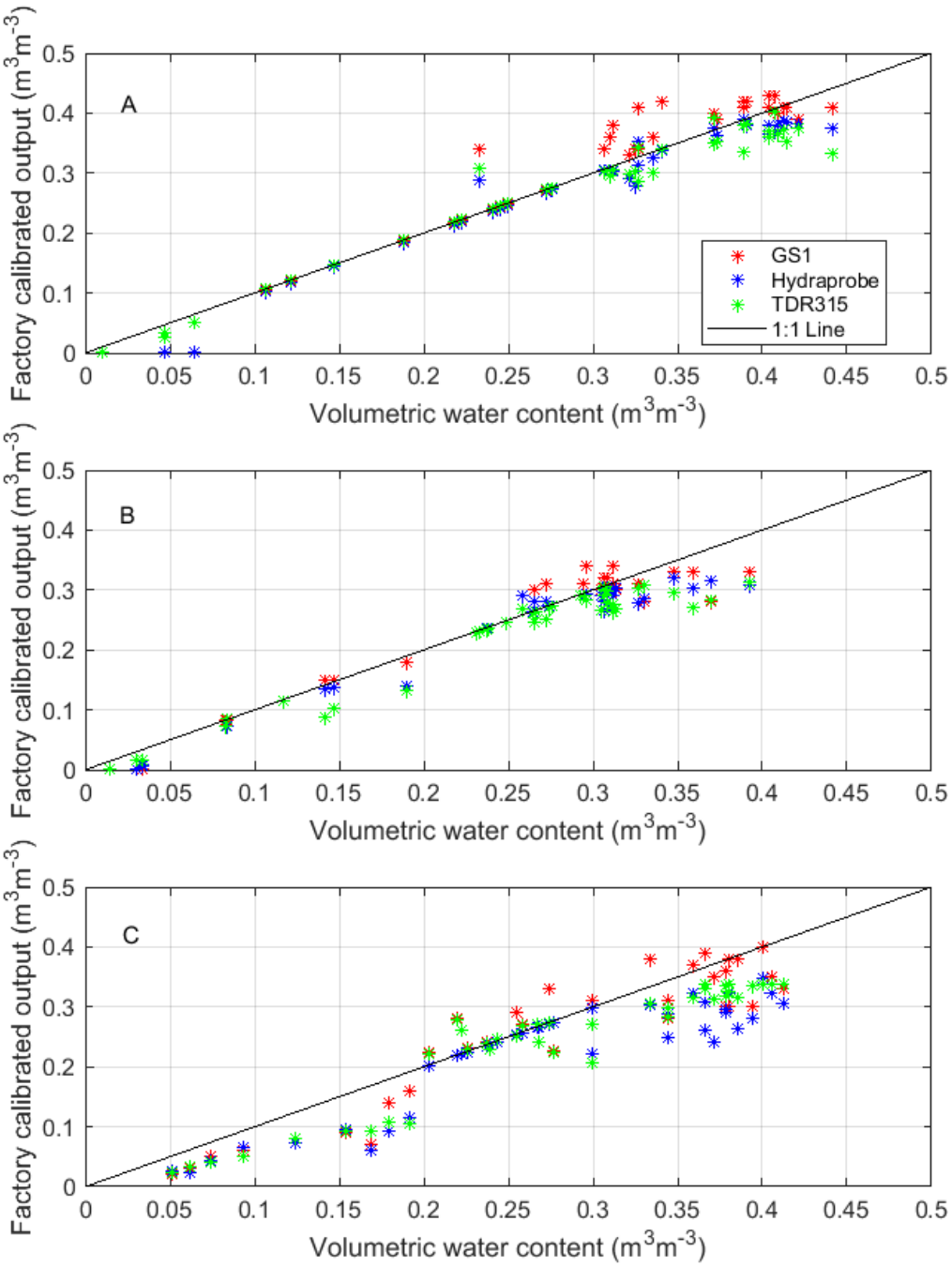

Figure 1. Comparison of the factory calibrated sensor output and laboratory measured water content (A) CT (B) BOC (C) BB. CT is the light textured soil, BOC is the medium textured soil and BB is the heavier textured soil.

3.2 Laboratory calibration evaluation

The soil specific calibration equations developed for the three sensors types in the laboratory improved the accuracies of the sensors as shown in Table 3. These calibration equations yielded lower levels of errors in all soil types ($P<0.001$) in comparison to when the factory calibrations were used. The RMSE and MBE were within statistical targets in

all tests except in the Hydraprobe and BB combination where the RMSE value recorded was 0.04 m^3m^{-3}.

Table 3. Comparison of laboratory calibration based VWC (m^3m^{-3}) with laboratory measurements of VWC (m^3m^{-3}) for the different sensors and soils. . BB is the heavier textured soil, BOC is the medium textured soil and CT is the light textured soil.

Sensor and soil type	R^2	MBE (m^3m^{-3})	RMSE (m^3m^{-3})
TDR 315			
BB	0.89	0	0.03
BOC	0.93	0	0.02
CT	0.94	0	0.03
Hydraprobe			
BB	0.84	0	0.04
BOC	0.94	0	0.02
CT	0.96	0	0.02
GS 1			
BB	0.85	0	0.03
BOC	0.93	0	0.02
CT	0.94	0	0.02

3.3 Sensor sensitivity to soil compaction

The three sensor types tested in the compacted medium textured soil recorded the highest errors in VWC estimation in the high compaction treatment ($P<0.05$). The statistical parameters for the comparison between factory calibrated sensor output and gravimetric water content have been inserted in Table 4. To ensure completeness, the

parameters for the non-compacted BOC soil from Table 2 are also listed. Table 4 shows that in the medium compacted soil, all sensors achieve a performance similar to that achieved in the non-compacted soil. Table 4 also shows that the magnitude of soil moisture underestimation by the TDR 315 and the Hydraprobe sensor increased in the highly compacted soil. An average underestimation of soil moisture by 0.035 $\mathrm{m^3m^{-3}}$ was recorded for the TDR 315 and an average underestimation of soil moisture by 0.027 $\mathrm{m^3m^{-3}}$ was recorded for the Hydraprobe sensor. The GS 1 sensor performed within statistical targets at high levels of compaction as indicated in Table 4.

Table 4. Comparison of factory calibration based VWC ($\mathrm{m^3m^{-3}}$) with laboratory measurements of VWC ($\mathrm{m^3m^{-3}}$) for the different sensors in the compacted medium textured soil (BOC).

Sensor and Soil	R^2	MBE ($\mathrm{m^3m^{-3}}$)	RMSE ($\mathrm{m^3m^{-3}}$)
TDR 315			
BOC Non-Compacted	0.85	-0.023	0.03
BOC Medium Compaction	0.85	-0.024	0.03
BOC High Compaction	0.77	-0.035	0.05
Hydraprobe			
BOC Non-Compacted	0.91	-0.017	0.03
BOC Medium Compaction	0.90	-0.019	0.03
BOC High Compaction	0.88	-0.027	0.03
GS 1			
BOC Non-Compacted	0.92	-0.006	0.03
BOC Medium Compaction	0.92	-0.008	0.03
BOC High Compaction	0.90	-0.01	0.03

Table 5 shows that the laboratory calibration equation developed for all the sensor types improves their predictions enabling them to perform within statistical targets in both the medium and highly compacted medium textured soil.

Table 5. Comparison of laboratory calibration based VWC ($\mathrm{m^3m^{-3}}$) with laboratory measurements of VWC ($\mathrm{m^3m^{-3}}$) for the different sensors in the compacted medium textured soil (BOC).

Sensor and Soil	$\mathrm{R^2}$	MBE ($\mathrm{m^3m^{-3}}$)	RMSE ($\mathrm{m^3m^{-3}}$)
TDR 315			
BOC Medium Compaction	0.93	0	0.02
BOC High Compaction	0.90	0	0.03
Hydraprobe			
BOC Medium Compaction	0.93	0	0.02
BOC High Compaction	0.92	0	0.03
GS 1			
BOC Medium Compaction	0.93	0	0.02
BOC High Compaction	0.92	0	0.03

3.4 Sensor sensitivity to soil temperature and salinity variations

The factory calibrated sensor output showed a significant linear response to an increase in temperature for all the soil/sensor combinations (the lowest $\mathrm{R^2}$=0.73) at all VWC values. The slopes of the linear regression between the factory calibrated output of the sensors and temperature at different VWC values in the non-saline soils are shown in Figure 2. Figure 2 shows that the slope of the linear response varied with VWC in every soil-sensor combination. It can be seen that the output of the TDR 315 probe in the light textured soil decreased with increasing temperature as indicated by the negative slope values. The rate of temperature effect increased with an increase in moisture, thus the highest effect 0.00207 $\mathrm{m^3m^{-3}{}^{\circ}C^{-1}}$ was observed at a moisture content of 0.3516 $\mathrm{m^3m^{-3}}$. The output of the GS 1 sensor in the light textured soil exhibited a positive response to increasing temperature. The rate of temperature effect increased with increasing moisture content,

thus the highest effect 0.0016 $\mathrm{m^3 m^{-3} {}^{\circ}C^{-1}}$ was observed at a moisture content of 0.3516 $\mathrm{m^3 m^{-3}}$. The Hydraprobe sensor's output also exhibited a positive response to increasing temperature in the light textured soil, the response was however similar at all moisture content values with an increase in sensor output of between 0.0003 - 0.0005 $\mathrm{m^3 m^{-3} {}^{\circ}C^{-1}}$ observed.

Figure 2 also shows that the output of the TDR 315 sensor exhibited a positive response to an increase in temperature in the heavier textured. The response was however similar at all moisture content values with an increase in sensor output of between 0.0003 - 0.0006 $\mathrm{m^3 m^{-3} {}^{\circ}C^{-1}}$ observed. The output of the Hydraprobe sensor exhibited a positive response to an increase in soil temperature in the heavier textured soil with the increase being more at medium moisture contents (highest response 0.00125 $\mathrm{m^3 m^{-3} {}^{\circ}C^{-1}}$). The GS 1 exhibited a negative dependence of sensor output to increasing temperature at high moisture content as indicated by the negative slope values in Figure 2 (highest response 0.0007 $\mathrm{m^3 m^{-3} {}^{\circ}C^{-1}}$). The sensor response to increasing temperature was however positive at low to medium moisture content values.

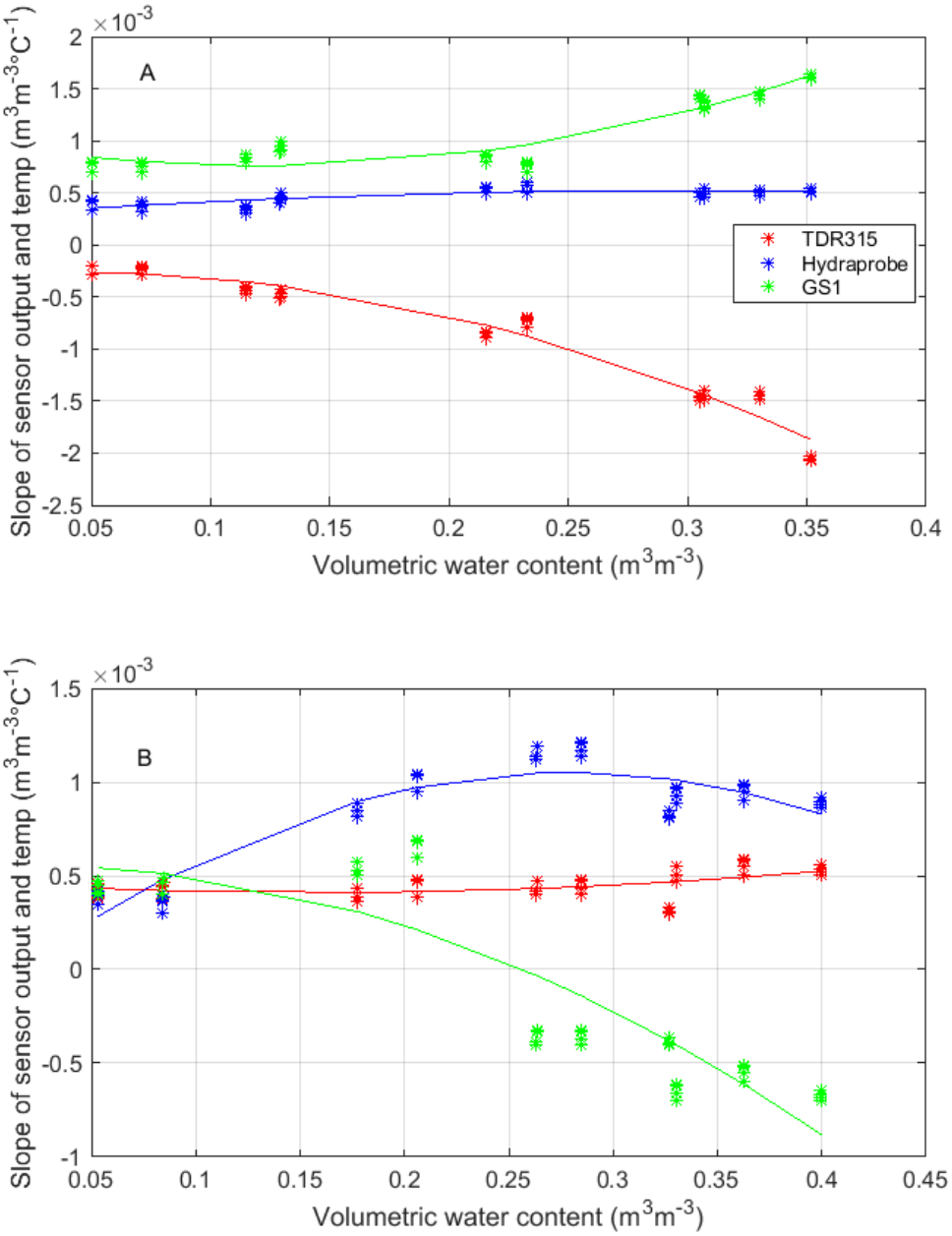

Figure 2. Dependence of the slope of the sensor output and temperature on water content in (A) CT non-saline (B) BB non-saline. CT is the light textured soil and BB is the heavier textured soil.

An increase in salinity in the light textured soil had a significant effect ($P<0.001$) on the average error in VWC estimates by the three sensor types when compared with the errors observed in the non-saline soil. The slopes of the linear regression between the factory calibrated output of the sensors and temperature at different VWC values in the saline soils are shown in Figure 3. Figure 3 shows that the output of the TDR 315 in the saline light textured soil exhibited a response similar to that observed in the non-saline light textured soil. It is interesting to see that the temperature dependence of the TDR 315 sensor output is generally less than that observed in the non-saline light textured soil. The

output of the Hydraprobe sensor exhibited a strong positive relationship with increasing soil temperature at all moisture content values (the lowest $\mathrm{R}^2 = 0.83$) in the saline light textured soil. The rate of increase in sensor output increased with an increase in moisture content, thus the highest response, 0.00418 $\mathrm{m}^3\mathrm{m}^{-3}{}^{\circ}\mathrm{C}^{-1}$ was observed at a moisture content of 0.3519 $\mathrm{m}^3\mathrm{m}^{-3}$. The output of the GS 1 sensor also exhibited a similar positive response to an increase in temperature in the saline light textured soil. The highest response, 0.0026 $\mathrm{m}^3\mathrm{m}^{-3}{}^{\circ}\mathrm{C}^{-1}$ was recorded at a moisture content value of 0.3519 $\mathrm{m}^3\mathrm{m}^{-3}$.

An increase in salinity in the heavier textured soil had a significant effect (P<0.001) on the average error in VWC estimates by the three sensor types when compared with the errors observed in the non-saline soil. Figure 3 shows that the VWC estimates by the three sensor types at all moisture content levels in the saline heavier textured soil were positively dependent on temperature (P<0.001). This is indicated by the positive slope values. Figure 3 also shows that the TDR 315 sensor output exhibited an increasingly positive response to temperature with an increase in volumetric water content. The highest response, 0.0048 $\mathrm{m}^3\mathrm{m}^{-3}{}^{\circ}\mathrm{C}^{-1}$ was observed at a moisture content value of 0.3877 $\mathrm{m}^3\mathrm{m}^{-3}$. The response of the Hydraprobe sensor was also increasingly positively dependent on temperature with an increase in VWC in the heavier textured saline soil (highest response 0.003 $\mathrm{m}^3\mathrm{m}^{-3}{}^{\circ}\mathrm{C}^{-1}$). A similar response of sensor output to increase in temperature was also observed in the GS 1 sensor tested in the heavier textured saline soil. The rate of increase in sensor output increased with increase in moisture content and the highest increase in sensor output observed was 0.0031 $\mathrm{m}^3\mathrm{m}^{-3}{}^{\circ}\mathrm{C}^{-1}$ at a moisture content value of 0.3877 $\mathrm{m}^3\mathrm{m}^{-3}$.

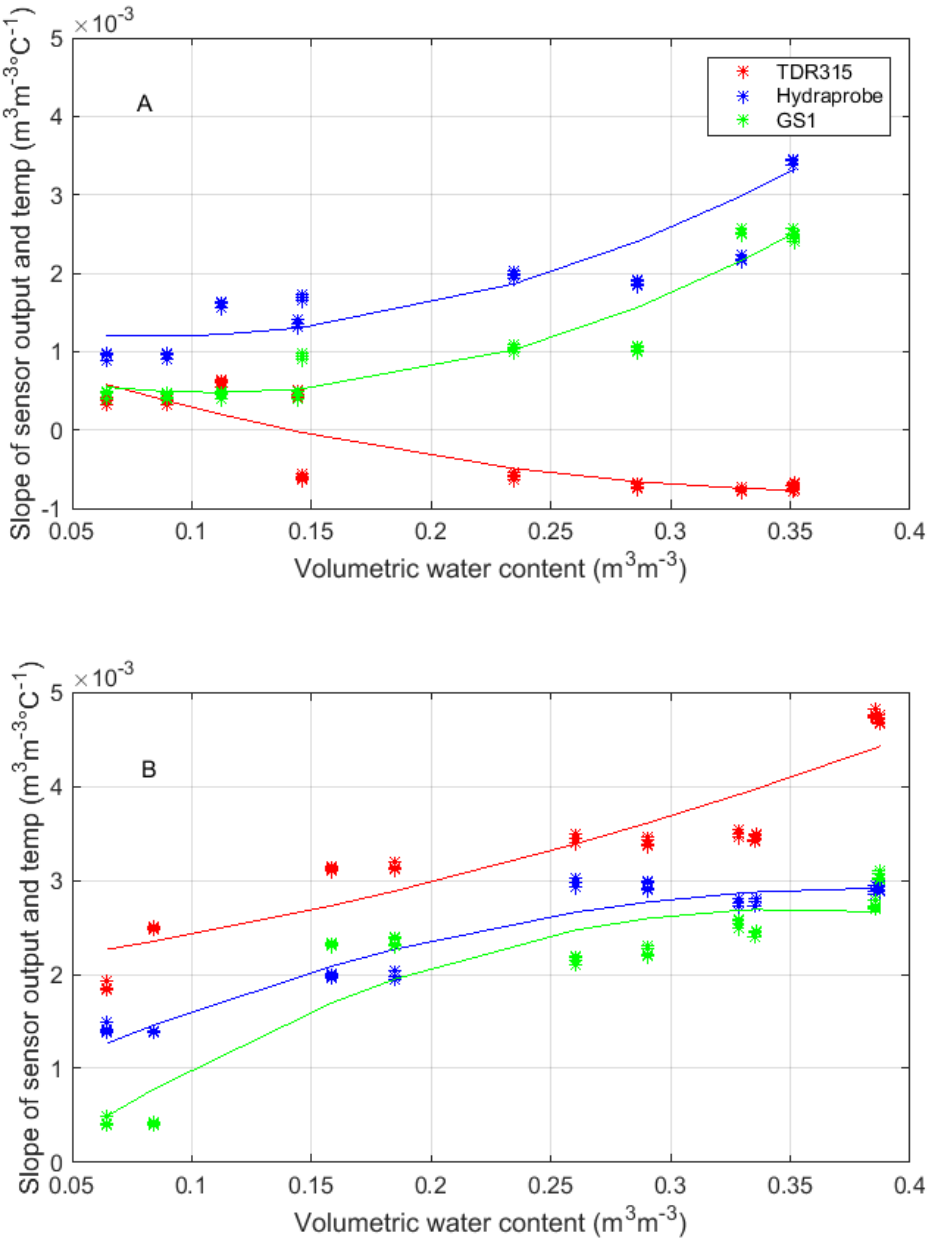

Figure 3. Dependence of the slope of the sensor output and temperature on water content in (A) CT saline and (B) BB saline soils. CT is the light textured soil and BB is the heavier textured soil.

3.5 Calibration with temperature compensation

An empirical method to correct for the influence of temperature on sensor output was developed adopting the procedure proposed by Saito et al. (2009). This method is based on the linear correlation that exists between the output of the three sensors types and temperature in all the soil/sensor combinations as shown by the slope values plotted in Figures 2 and 3.

The linear relationship illustrated can be expressed as

$$\theta_{fc} = aT + b \quad (1)$$

Where a and b are the slopes and intercept of the linear regression between the factory calibrated sensor output, θ_{fc} (m^3m^{-3}) and soil temperature, T (℃) at a known VWC value. The slope of the regression, a ($m^3m^{-3}℃^{-1}$) is a function of the actual soil water content, θ_a (m^3m^{-3}). Thus, a is expressed as

$$a = \frac{d\theta_{fc}}{dT} = f(\theta_a) \quad (2)$$

Integrating the above equation and setting θ_{fc}=θ_{lc} at $T = T_r$ gives:

$$\theta_{fc} = \theta_{lc} + f(\theta_a)(T - T_r) \quad (3)$$

In equation 3, θ_{lc} (m^3m^{-3}) is the laboratory calibrated water content (a function of θ_a), T_r (℃) is the temperature at which the laboratory calibration of the sensors was conducted and T (℃) is the soil temperature.

$f(\theta_a)$ expresses the dependency of a on θ_a as shown in Figures 2 and 3. It clear that a second order polynomial will fit the data points in Figures 2 and 3. This is expressed as

$$f(\theta_a) = c_1 + c_2\theta_a + c_3\theta_a^2 \quad (4)$$

Substituting equation 4 into 3 results in a calibration equation that describes the factory calibrated probe output, θ_{fc} as a function of the actual water content,θ_a, the soil temperature, T and the reference temperature at which the laboratory calibration was conducted, T_r (in this study T_r= 22°C).

An example application of the calibration equation with temperature correction on the heavier textured soil at 35°C is shown in Figure 4. It can be seen that the temperature compensated output of the three sensor types closely matches the 1:1 line indicating a high level of accuracy in VWC estimates. It can also be seen that both the factory and laboratory calibrated output without temperature compensation exhibit a high level of scatter around the 1:1 line.

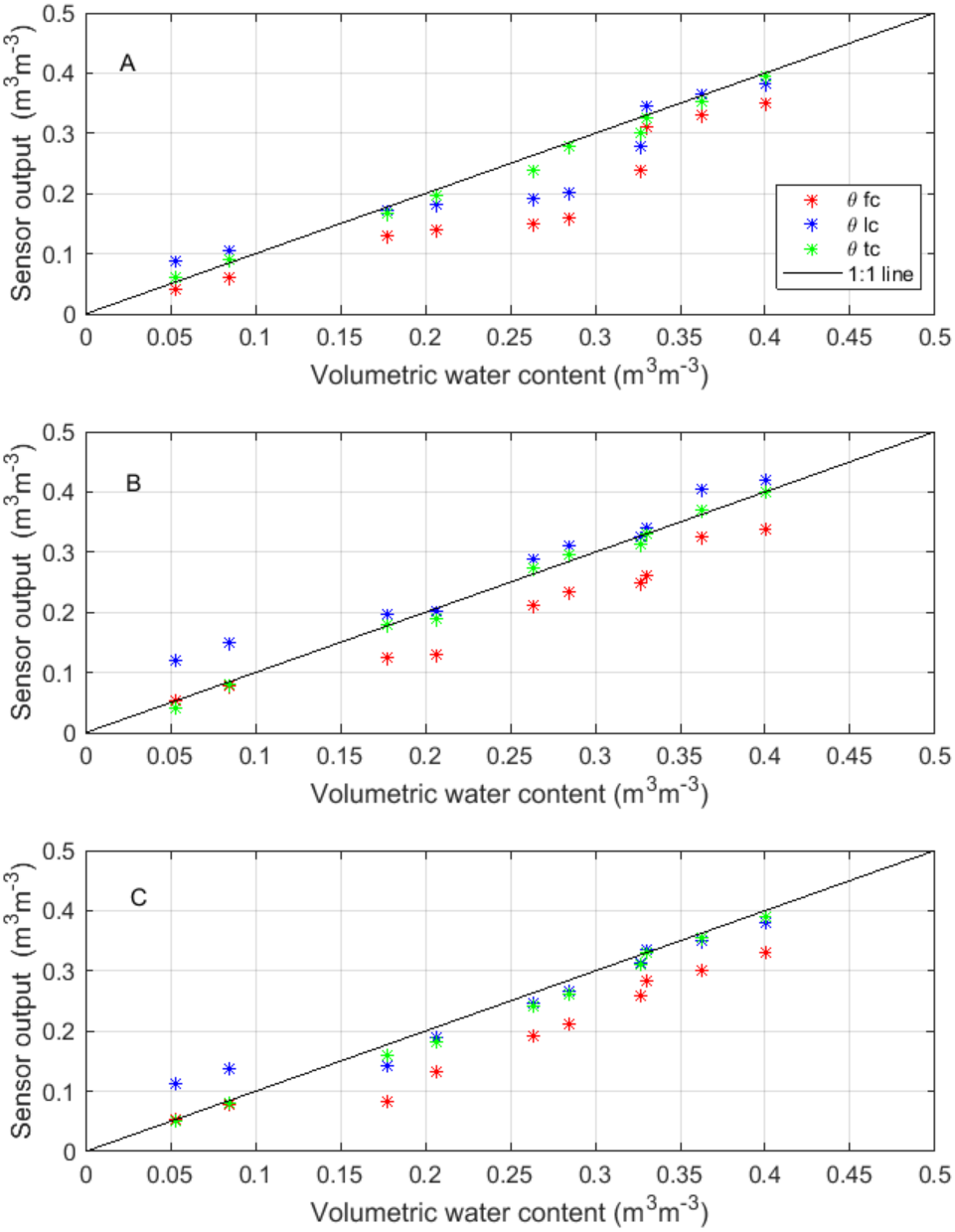

Figure 4. Comparison of the temperature corrected, laboratory and factory calibrated outputs of (A) TDR 315 (B) Hydraprobe and (C) GS 1 sensors in the heavier textured soil (BB) at 35°C. θ_{fc} is the factory calibrated water content, θ_{lc} is the laboratory calibrated water content and θ_{tc} is the temperature compensated water content.

Table 6 summarizes the calibration results obtained with all soil/sensor combinations at 35°C. The RMSE values obtained by the temperature corrected calibration equation are within statistical targets with the exception of the Hydraprobe and BB saline/non-saline combination. The RMSE values obtained by the temperature corrected equation are reduced compared to those obtained by the factory supplied equation and the laboratory equation without temperature compensation.

Table 6. Root mean square errors between actual and predicted water content obtained by all calibration equations applied on the tested soils at 35°C. BB is the heavier textured soil, BOC is the medium textured soil and CT is the light textured soil.

Sensor and soil type	RMSE (m^3m^{-3})		
	$\theta_a$vs θ_{fc}	$\theta_a$vs θ_{tc}	$\theta_a$vs θ_{lc}
TDR 315			
CT	0.04	0.03	0.04
BB	0.05	0.03	0.04
CT saline	0.04	0.03	0.04
BB saline	0.06	0.03	0.05
Hydraprobe			
CT	0.04	0.02	0.03
BB	0.08	0.04	0.07
CT saline	0.05	0.02	0.05
BB saline	0.12	0.04	0.10
GS 1			
CT	0.04	0.02	0.03
BB	0.06	0.03	0.05
CT saline	0.05	0.02	0.04
BB saline	0.07	0.03	0.06

4 Discussion

The factory calibration of the sensors evaluated achieved the required accuracy only in the light textured soil, and the GS 1 and Hydraprobe sensors tested in the medium textured soil. The factory calibration of the three sensor types consistently underestimated soil moisture in the heavier textured soil. This may be due to a large amount of bound water present in soils with high clay content. The dielectric permittivity of bound water is

lower than that of free water leading to an underestimation of soil water content by dielectric sensors. Polyakov et al. (2005) and Fares et al. (2011) reported similar results for capacitance sensors evaluated in heavier textured soils, and Keshavarzi et al. (2015) reported similar results for a TDR sensor. The factory calibration of the three sensors can be applied in light textured soils but for heavier soils, a laboratory calibration procedure is recommended.

The linear calibration developed in the laboratory improved the performance of the three sensor types in all the soils. This indicates that a laboratory calibration process is important for soil moisture sensors deployed in irrigation scheduling applications where slight inaccuracies in estimated soil moisture content may lead to the onset of plant water stress. Bosch (2004) and Merlin et al. (2007) reported similar conclusions for the earlier version of the Hydraprobe. Kizito et al. (2008) and Parsons and Bandaranayake (2009) reported that a linear laboratory calibration equation improved the accuracy of the predecessor of the G1 sensor, the EC-5 sensor. Varble and Chávez (2011) also reported similar findings for the predecessor of the TDR 315 sensor, the Acclima TDT sensor.

The linear laboratory calibration of the Hydraprobe sensor in the heavier textured soil did not completely eliminate the errors in soil moisture estimates. It, however, performed close to statistical targets indicating that the laboratory-derived calibration of the sensor can be applied in heavier textured soils as long as growers understand some errors may exist in soil moisture estimates ($\pm\ 0.04\ \mathrm{m^3 m^{-3}}$).

A high level of compaction in the medium textured soil increased the magnitude of soil moisture underestimation by both the TDR 315 and Hydraprobe sensors. Gong et al. (2003) reported an underestimation of soil moisture content by a TDR sensor with increasing bulk density in a medium textured soil. Czarnomski et al. (2005) however reported an overestimation of soil moisture content by a TDR sensor with an increase in bulk density in a medium textured forest soil. Polyakov et al. (2005) reported similar findings for a capacitance sensor evaluated in a medium textured tropical soil. The underestimation of soil moisture content by the TDR 315 sensor and the Hydraprobe sensor can be explained by the increase in the volume ratio of solid particles to air with an increase in soil bulk density. This causes an increase in the dielectric permittivity of the solid particles accompanied by a decrease in the dielectric permittivity of the soil water. This mechanism consequently leads to an underestimation of soil moisture content by dielectric sensors. An increase in the level of compaction had a negligible effect on the accuracy of the GS 1 sensor in the medium textured soil. The GS 1 sensor performed within statistical targets at all levels of compaction. Lukanu and Savage (2006) reported similar findings for a capacitance sensor evaluated in a medium textured soil. The similar performance of all sensor types in the non-compacted and medium compacted soils may

be as a result of the marginal increase in bulk density recorded. Campbell et al. (2009) reported that a 16.2% change in bulk density will result in a 1% change in the predicted volumetric water content. The percentage change in bulk density recorded (5.2 %) when going from a level of no compaction to a level of medium compaction is less than this value. The calibration equation developed in the laboratory reduced the errors in soil moisture estimate by all the sensors tested in the compacted soils. This leads to the conclusion that it is beneficial to calibrate soil moisture sensors at compaction levels similar to that experienced on the field soils where they are intended for deployment. Quality control checks should also be performed periodically on the soils to monitor the level of compaction and if necessary sensors should be recalibrated to account for any increase in bulk density observed.

Changes in soil temperature had an effect on the output of the three sensor types in all the soils tested. The TDR 315 sensor tested in the light textured soil exhibited a negative response to an increase in soil temperature. The most pronounced effect of soil temperature was observed at high moisture contents. This is because the dielectric permittivity of free water reduces with increasing temperature leading to an underestimation of soil moisture by the TDR sensor. Light textured soils such as the one evaluated in this study hold a large amount of free water. Gong et al. (2003) reported similar results for a TDR sensor evaluated in a light textured soil. The highest decrease in sensor output observed in this study corresponds to an underestimation of 0.027 $\mathrm{m^3 m^{-3}}$ over a 13°C increase in temperature relative to a reference temperature of 22°C used in this study. The underestimation in soil moisture by the TDR 315 sensor applied in the light textured soil may be considered negligible for most applications, however, a temperature compensation procedure may still be beneficial in applications where a high level of accuracy is desired. The GS 1 and Hydraprobe sensors exhibited a positive response to increase in temperature in the light textured soil. Kizito et al. (2008) reported a negative response of the EC-5 sensor to increase in temperature in light textured soils and a similar response was also reported by Merlin et al. (2007) for the earlier version of the Hydraprobe sensor. Bogena et al. (2007) however reported findings similar to this study for the EC-5 sensor. The highest response to temperature observed for the GS 1 sensor corresponds to an overestimation of soil moisture content by 0.02 $\mathrm{m^3 m^{-3}}$ while the highest response to temperature observed for the Hydraprobe sensor corresponds to an overestimation of soil moisture by 0.007 $\mathrm{m^3 m^{-3}}$ over a 13°C increase in soil temperature. These errors in soil moisture estimates by the GS 1 and Hydraprobe sensor are considered negligible in most applications.

The Hydraprobe and TDR 315 sensors tested in the heavier textured soil exhibited a positive response to an increase in temperature at all moisture contents. This may be due to the release of bound water in soils high in clay content with an increase in temperature.

The bound water effect will lead to an overestimation of soil moisture content with an increase in temperature. This is in agreement with the results presented by Benson and Wang (2006) and Seyfried and Murdock (2004). The temperature response of the TDR 315 sensor indicated an overestimation of soil moisture by 0.001 $\mathrm{m^3 m^{-3}}$, an overestimation of 0.016 $\mathrm{m^3 m^{-3}}$ by the Hydraprobe sensor, and an overestimation of 0.001 $\mathrm{m^3 m^{-3}}$ by the GS 1 sensor at medium moisture content over a 13°C increase in soil temperature. The range of soil moisture overestimation by the TDR 315, Hydraprobe and GS 1 sensors tested in the heavier textured soils may be considered negligible in most applications. The response of the Hydraprobe sensor to an increase in temperature leading to overestimation of soil moisture content was, however, more pronounced at medium moisture contents. This range of soil moisture is usually the most critical point for irrigation scheduling decisions leading to a conclusion that applying a temperature compensation procedure for this sensor when deployed in heavier textured soils will lead to an improvement in irrigation scheduling decisions.

The TDR 315 sensor exhibited a negative response to increasing temperature in the saline light textured soil. The decrease in the dielectric permittivity of free water with an increase in temperature still seemed to have a predominant effect on the output of the TDR 315 sensor. The highest temperature effect observed corresponds to a soil moisture underestimation of 0.01 $\mathrm{m^3 m^{-3}}$ which may be considered negligible for most applications. The Hydraprobe and GS 1 sensor exhibited a positive response to increasing temperature in the saline light textured soil. The temperature effect was positively dependent on soil moisture for both sensors suggesting the greater contribution of pore water to the bulk electrical conductivity of the light textured soil. Results also indicate that both sensors were more sensitive to increasing temperature in the saline light textured soil. This may be due to increased signal attenuation resulting from an increase in salinity and the low operating frequencies of both sensors. This is in agreement with the results presented by Saito et al. (2009) for various capacitance sensors. The highest temperature effect observed for the Hydraprobe correspond to a soil moisture overestimation of 0.053 $\mathrm{m^3 m^{-3}}$ while the highest effect observed for the GS 1 sensor corresponds to a soil moisture overestimation of 0.033$\mathrm{m^3 m^{-3}}$. This leads to a conclusion that a temperature compensation procedure is important when deploying low-frequency capacitance sensor under conditions of variable salinity in a light textured soil.

The three sensor types evaluated exhibited a positive response to increasing temperature when tested in the saline heavier textured soil. Results indicated that the sensors overestimated soil moisture at low VWC with the magnitude of overestimation larger at higher VWC. Benson and Wang (2006) presented similar results for a water content reflectometer evaluated in a saline clay soil. This is explained by the contribution of the highly charged clay particles to the bulk EC of the soil and the positive dependence of the

bulk soil EC on VWC. The magnitude of soil moisture overestimation by the three sensors was remarkably larger than statistical targets over a 13°C increase in temperature. The highest temperature effect observed corresponds to a soil moisture overestimation of 0.06 $\mathrm{m^3m^{-3}}$ by TDR 315, 0.04 $\mathrm{m^3m^{-3}}$ by Hydraprobe and 0.04 $\mathrm{m^3m^{-3}}$ by GS 1. This emphasizes the need for a temperature compensation procedure when deploying these sensors under conditions of variable salinity in a heavier textured soil. This is in line with the conclusions of Skierucha et al. (2012).

The applicability of a generalized regression procedure in developing temperature compensation equations for dielectric soil moisture sensors was pursued. The empirical temperature compensation procedure sufficiently reduced the error in soil moisture estimation in all the soil/sensor combinations as shown in Table 6. This suggests that the sensors can be used for irrigation scheduling under conditions of high salinity in the soil types tested when a temperature compensation calibration has been applied.

5 Conclusions

This research evaluated the performance of TDR 315, Hydraprobe and GS 1 soil moisture sensors, within air dry to saturation range of soil moisture contents, under laboratory conditions for three soils. Acceptable statistical targets for this test were set as an MBE value of ±0.02 $\mathrm{m^3m^{-3}}$ and an RMSE value less than 0.035 $\mathrm{m^3m^{-3}}$. Linear calibration equations were developed for the three sensors in all soils tested. The factory based calibration of the three sensors performed within the required accuracy in the light textured soil, and the GS 1 and Hydraprobe sensors tested in the medium textured soil. It, however, failed to achieve the required accuracy when the sensors were tested in the heavier textured soil.

The linear calibration equation developed in the laboratory reduced the error in soil moisture estimates by the three sensors in all the soils tested. The laboratory calibration did not, however, achieve the required accuracy with the Hydraprobe sensor tested in the heavier textured soil.

The TDR 315 and Hydraprobe sensors experienced errors in reporting soil moisture content at a high level of soil compaction and bulk density. The GS 1 sensor was however not sensitive to increasing soil bulk density due to compaction. Laboratory calibration equations developed for the sensors in the compacted soils reduced the errors in soil moisture estimate to values within statistical targets in the three sensors evaluated.

The output of the three soil moisture sensors exhibited a significant linear response to increasing temperature when tested in both the light and heavier textured soil. The TDR 315 sensor underestimated soil moisture with an increase in temperature while the Hydraprobe and GS 1 sensors overestimated soil moisture with an increase in temperature in the light textured soil. At low to medium moisture content, the three

sensors overestimated soil moisture with increasing temperature in the heavier textured soil. The magnitude of errors in soil moisture estimate by the three sensors increased with an increase in salinity level in the heavier textured soil. A similar result was recorded for the Hydraprobe and GS 1 sensors tested in the saline light textured soil. An empirical temperature compensation approach was, however, able to reduce the magnitude of the temperature dependence of the output of the three sensor types in all soils tested achieving RMSE values close to the statistical targets specified.

In summary, this study has demonstrated that laboratory developed calibration equations improved the accuracy of the evaluated soil moisture sensors. A temperature compensation procedure has also proven to further improve the accuracy of the sensors when deployed under conditions of variable temperature and salinity.

References

ASTM Standard D1557, 2009. Standard Test Methods for Laboratory Compaction Characteristics of Soil Using Modified Effort. ASTM International, West Conshohocken ,PA.

Benor, M., Levy, G.J., Mishael, Y., Nadler, A., 2013. Salinity Effects on the Fieldscout TDR 300 Soil Moisture Meter Readings. Soil Sci. Soc. Am. J. 77, 412. https://doi.org/10.2136/sssaj2012.0294n

Benson, C.H., Wang, X., 2006. Temperature-compensating calibration procedure for Water Content Reflectometers. Tdr 2006 Paper ID 50, 16 p.

Bogena, H.R., Huisman, J. A., Oberdörster, C., Vereecken, H., 2007. Evaluation of a low-cost soil water content sensor for wireless network applications. J. Hydrol. 344, 32–42. https://doi.org/10.1016/j.jhydrol.2007.06.032

Bosch, D.D., 2004. Comparison of Capacitance-Based Soil Water Probes in Coastal Plain Soils. Vadose Zo. J. 3, 1380–1389. https://doi.org/10.2136/vzj2004.1380

Campbell, C.S., Campbell, G.S., Cobos, D.R., Bissey, L.L., 2009. Calibration and evaluation of an improved low-cost soil moisture sensor, Decagon Devices Application Note.

Chávez, J.L., Varble, J.L., Andales, A.A., 2011. Performance Evaluation of Selected Soil Moisture Sensors, in: Proceedings of the 23rd Annual Central Plains Irrigation Conference. Burlington, pp. 29–38.

Czarnomski, N.M., Moore, G.W., Pypker, T.G., Licata, J., Bond, B.J., 2005. Precision and accuracy of three alternative instruments for measuring soil water content in two forest soils of the Pacific Northwest. Can. J. For. Res. 35, 1867–1876. https://doi.org/10.1139/x05-121

Evett, S.R., Tolk, J. A., Howell, T. A., 2006. TDR Laboratory Calibration in Travel Time, Bulk Electrical Conductivity, and Effective Frequency. Vadose Zo. J. 5, 1020–1029. https://doi.org/10.2136/vzj2006.0062

Fares, A., Abbas, F., Maria, D., Mair, A., 2011. Improved calibration functions of three capacitance probes for the measurement of soil moisture in tropical soils. Sensors (Basel). 11, 4858–74. https://doi.org/10.3390/s110504858

Gong, Y., Cao, Q., Sun, Z., 2003. The effects of soil bulk density, clay content and temperature on soil water content measurement using time-domain reflectometry. Hydrol. Process. 17, 3601–6314. https://doi.org/10.1002/hyp.1358

Iaea, 2008. Field estimation of soil water content: A practical guide to methods, instrumentation and sensor technology. At. Energy 131. https://doi.org/10.2489/jswc.64.4.116A

John, O.O., Raghavan, G.S. V, McKyes, E., Mehuys, G., 1986. Shear Strength Prediction of Compacted Soils with Varying Added Organic Matter Contents. Am. Soc. Agric. Eng. ASAE 29, 351–355.

Kammerer, G., Nolz, R., Rodny, M., Loiskandl, W., 2014. Performance of Hydra Probe and MPS-1 Soil Water Sensors in Topsoil Tested in Lab and Field. J. Water Resour. Prot. 6, 1207–1219.

Keshavarzi, M., Ojaghlou, H., Nazemi, A., Ashraf, S., Ababaei, B., 2015. Effect of soil texture and organic matter on the accuracy of Time domain reflectometry method for estimating soil moisture, in: Soil and Water Pollution. pp. 368–373.

Kizito, F., Campbell, C.S., Campbell, G.S., Cobos, D.R., Teare, B.L., Carter, B., Hopmans, J.W., 2008. Frequency, electrical conductivity and temperature analysis of a low-cost capacitance soil moisture sensor. J. Hydrol. 352, 367–378. https://doi.org/10.1016/j.jhydrol.2008.01.021

Lukanu, G., Savage, M.J., 2006. Calibration of a frequency-domain reflectometer for determining soil-water content in a clay loam soil. Water SA 32, 37–42. https://doi.org/10.4314/wsa.v32i1.5237

Merlin, O., Walker, J., Panciera, R., Young, R., 2007. Calibration of a Soil Moisture Sensor in Heterogeneous Terrain, in: MODSIM 2007 International Congress on Modelling and Simulation. Modelling and Simulation Society of Australia and New Zealand, pp. 2604–2610.

Mittelbach, H., Lehner, I., Seneviratne, S.I., 2012. Comparison of four soil moisture sensor types under field conditions in Switzerland. J. Hydrol. 430–431, 39–49. https://doi.org/10.1016/j.jhydrol.2012.01.041

Paige, G.B., Keefer, T.O., 2008. Comparison of field performance of multiple soil moisture sensors in a semi-arid rangeland. J. Am. Water Resour. Assoc. 44, 121–135. https://doi.org/10.1111/j.1752-1688.2007.00142.x

Parsons, L.R., Bandaranayake, W.M., 2009. Performance of a New Capacitance Soil Moisture Probe in a Sandy Soil. Soil Sci. Soc. Am. J. 73, 1378. https://doi.org/10.2136/sssaj2008.0264

Polyakov, V., Fares, A., Ryder, M.H., 2005. Calibration of a Capacitance System for Measuring Water Content of Tropical Soil. Vadose Zo. J. 4, 1004. https://doi.org/10.2136/vzj2005.0028

Saini, G.R., 1966. Organic Matter as a Measure of Bulk Density of Soil. Nature 210, 1295.

Saito, T., Fujimaki, H., Inoue, M., 2008. Calibration and Simultaneous Monitoring of Soil Water Content and Salinity with Capacitance and Four-electrode Probes. Am. J. Environ. Sci. 4, 683–692. https://doi.org/10.3844/ajessp.2008.683.692

Saito, T., Fujimaki, H., Yasuda, H., Inoue, M., 2009. Empirical Temperature Calibration of Capacitance Probes to Measure Soil Water. Soil Sci. Soc. Am. J. 73, 1931–1937. https://doi.org/10.2136/sssaj2008.0128

Schwartz, R.C., Evett, S.R., Bell, J.M., 2009. Complex Permittivity Model for Time Domain Reflectometry Soil Water Content Sensing: II. Calibration. Soil Sci. Soc. Am. J. 73, 898. https://doi.org/10.2136/sssaj2008.0195

Seyfried, M.S., Murdock, M.D., 2004. Measurement of Soil Water Content with a 50-MHz Soil Dielectric Sensor. Soil Sci. Soc. Am. J. 68, 394. https://doi.org/10.2136/sssaj2004.0394

Skierucha, W., Wilczek, A., Szypłowska, A., Sławiński, C., Lamorski, K., 2012. A TDR-Based Soil Moisture Monitoring System with Simultaneous Measurement of Soil Temperature and Electrical Conductivity. Sensors 12, 13545–13566. https://doi.org/10.3390/s121013545

Thompson, R.B., Gallardo, M., Fernandez, M.D., Valdez, L.C., Martinez-Gaitan, C., 2007. Salinity Effects on Soil Moisture Measurement Made with a Capacitance Sensor. Soil Sci Soc Am J 71, 1647–1657. https://doi.org/10.2136/sssaj2006.0309

Topp, G.C., Davis, J.L., Annan, A.P., 1980. Electromagnetic Determination of Soil Water Content: Measruements in Coaxial Transmission Lines. Water Resour. Res. 16, 574–582. https://doi.org/10.1029/WR016i003p00574

Varble, J.L., Chávez, J.L., 2011. Performance evaluation and calibration of soil water content and potential sensors for agricultural soils in eastern Colorado. Agric. Water Manag. 101, 93–106. https://doi.org/10.1016/j.agwat.2011.09.007

Chapter 3:

Dynamic Modelling of the Baseline Temperatures for Computation of the Crop Water Stress Index (CWSI) of a Greenhouse Cultivated Lettuce Crop

DOI: https://doi.org/10.1016/j.compag.2018.08.009

Chapter 3 Dynamic Modelling of the Baseline Temperatures for Computation of the Crop Water Stress Index (CWSI) of a Greenhouse Cultivated Lettuce Crop

Abstract

The crop water stress index (CWSI) has been shown to be a tool that could be used for non-contact and real-time monitoring of plant water status, which is a key requirement for the precision irrigation management of crops. However, its adoption for irrigation scheduling is limited because of the need to know the baseline temperatures which are required for its calculation. In this study, the canopy temperature of greenhouse cultivated lettuce plants which were maintained as either well-watered or non-transpiring was continuously monitored along with prevailing environmental conditions during a five-week period. This data was applied in developing a dynamic model that can be used for predicting the baseline temperatures. Input variables for the dynamic model included air temperature, shortwave irradiance, and air vapour pressure deficit measured at a 10 s interval. During a follow-up study, the dynamic model successfully predicted the baseline temperatures producing mean absolute errors (MAE) that varied between 0.17°C and 0.29°C, and root mean squared errors (RMSE) that varied between 0.21°C and 0.35°C when comparing model predictions with measured values. The model predicted baseline temperatures were applied in calculating an empirical CWSI for lettuce plants receiving one of two irrigation treatments. The empirical CWSI consistently differentiated between the irrigation treatments and was significantly correlated with the theoretical CWSI with correlation coefficient (r) values greater than 0.9. The dynamic model presented in this study requires easily measured input parameters for the prediction of the baseline temperatures. This eliminates the need to maintain artificial reference surfaces required in other empirical approaches for the CWSI calculation and also eliminates the need for computing the complex theoretical CWSI.

1 Introduction

Optimization of crop quality during protected crop cultivation requires finely tuned water management; here, protected crop cultivation refers to crops grown under fixed structures such as greenhouses and polytunnels. The improvement of crop quality is a major aim of protected crop cultivation in humid countries such as the UK (Monaghan et al., 2013). Imposing a certain degree of water stress in determined phenological periods has been found to improve crop quality in a number of crops including lettuce (Monaghan et al., 2017; Oh et al., 2010), strawberries (Weber et al., 2016), tomatoes (Kuscu et al., 2014; Shao et al., 2008). Monitoring tools that provide accurate information regarding plant water status would, therefore, be beneficial for scheduling and management of irrigation in protected crop cultivation (Adeyemi et al., 2017).

Plant canopy temperature (T_c) has long been considered as an indicator of plant water status (Tanner, 1963) based on the cooling effect of the transpiration process (Jones & Schofield, 2008). Therefore, as a remote monitoring solution, infra-red thermometry offers the potential of acquiring the surface temperature of plant canopies from which plant water status can be inferred (Jones & Leinonen, 2003). T_c is determined not only by the plant water status but also by prevailing environmental conditions including incoming shortwave irradiance, wind speed, air temperature and humidity (Jones et al., 1997).

To use T_c as an indicator of plant water status, it must be normalized to account for the varying environmental conditions (Agam et al., 2013). One of the most commonly used methods for normalizing T_c as an indicator of plant water status is the crop water stress index (CWSI) originally proposed by Jackson et al. (1981); Idso et al. (1981) in which the measured crop canopy temperature (T_c) is normalized using two baseline temperatures, both assumed to be achieved under the same environmental conditions as T_c; namely (a) the canopy temperature of a well-watered crop (T_{nws}); referred to as the non-water-stressed baseline temperature, and (b) the temperature of a non-transpiring canopy (T_{dry}); referred to as the upper limit baseline temperature. Ideally, the CWSI ranges from 0 to 1, where 0 represents a well-watered condition and 1 represents a non-transpiring, water-stressed condition, hence providing intuitive crop water status quantification as a simple tool for irrigation scheduling (King and Shellie, 2016).

Two forms of the CWSI are currently available. The first is the empirical CWSI, originally introduced by Idso et al. (1981). In their empirical approach to quantifying the CWSI, T_{nws} and T_{dry} were determined by developing a linear relationship for the canopy-air temperature difference and the vapour pressure deficit (VPD). It has however been shown that T_{nws} is crop growth stage dependent and also dependent on the agro climatic zone in which the crop is being grown (Jones, 1999). The stable weather conditions required for the application of the original approach to quantifying the CWSI is also seldom

encountered in humid regions where weather conditions are highly variable in the short term (Maes and Steppe, 2012). Artificial wet and dry reference surfaces have been successfully applied to estimate T_{nws} and T_{dry} under the same environmental conditions as T_c for the calculation of an empirical CWSI (Grant et al., 2007; Möller et al., 2007). These include the use of wet and dry filter papers, leaves sprayed with water and those covered with petroleum jelly, and plots maintained as well watered and water stressed. However, the required maintenance of these artificial surfaces limit their potential use for automation in a precision irrigation system including periods during which high frequency data acquisition is required (Maes and Steppe, 2012).

The use of theoretical equations of CWSI based on the energy balance model of Jackson et al. (1981) involves the combination of T_c and meteorological measurements to compute the CWSI. This approach eliminates the need to acquire separate measurements of T_{nws} and T_{dry}. It is however limited by the need to estimate net radiation and aerodynamic resistance, and also requires large model input parameters (Agam et al., 2013). The energy balance model proposed by Jones (1999) requires less model input parameters and the baseline temperatures computed using the model have been demonstrated to show excellent agreement with the measured temperatures of artificial reference leaf surfaces under minimal wind conditions (Fuentes et al., 2012). It has further been demonstrated as producing a robust quantification of the CWSI and eliminates the need for artificial reference surfaces (Ben-Gal et al., 2009). However, the model requires ancillary measurement to reliably estimate equation parameters including the boundary layer resistance to heat and water vapor which limits the potential of its application in commercial crop production.

Baseline temperature prediction models which have limited data requirements and straightforward calculation will, therefore, enhance the adoption of the CWSI as a practical irrigation monitoring tool. Maes and Steppe (2012) noted that this could be realized through improvements in the prediction of the baseline temperatures employed in the empirical CWSI approach. Including air temperature, solar radiation, wind speed and VPD as predictors in multiple linear regression models (MLR) has been found to improve the predictions of the baseline temperatures (Payero and Irmak, 2006). King and Shellie (2016) also reported improved predictions of the baseline temperatures using an artificial neural network (ANN), with air temperature, solar radiation, wind speed and VPD applied as input variables. The plant response will typically vary over the growth season due to crop growth and various adaptation processes (Boonen et al., 2000). Dhillon et al. (2014) showed that baseline temperature prediction models for tree crops varied as the season progressed. Hedley et al. (2014) noted that adaptive monitoring systems which are able to account for the temporal variability in plant response and water requirements would improve the performance of irrigation management tools. The ANN and MLR approaches

however fail to consider the time-varying nature of the plant systems as their model parameters are assumed to remain constant once identified.

Dynamic models provide a possible approach for accounting for the time-varying nature of the plant system in the prediction of the baseline temperatures. Dynamic models have been successfully applied in simplifying and modelling complex environmental and biological processes(Taylor et al., 2007; Young, 2006), predicting time-varying biological responses (Kirchsteiger et al., 2011; Quanten et al., 2006), and in many other irrigation decision support applications (Delgoda et al., 2016; Lozoya et al., 2016). To the best of our knowledge, a dynamic model has not ever been used to predict T_{nws} or T_{dry} for calculation of a CWSI. A dynamic model is particularly well suited for predicting T_{nws} and T_{dry} because the time varying nature of the system under study can be taken into account through and adaptive and online estimation of the model parameters. This means the model parameters are updated recursively using all new incoming data from the system. Predicting plant canopy temperature may involve an understanding of the timing of the opening and closing of the stomates (Al-Faraj et al., 2000). A dynamic model is however able to implicitly account for the stomatal response by the inclusion of the time delay associated with each model input parameter.

The objectives of this paper are to exhibit the potential of using a dynamic model to predict T_{nws} and T_{dry} (baseline temperatures) and demonstrate the applicability in calculating an empirical CWSI for a lettuce crop (*Lactuca sativa*) grown under greenhouse conditions. Performance of the dynamic model was evaluated by comparing the model predicted baseline temperatures with measured baseline temperatures. The calculated empirical CWSI values were also compared with theoretical CWSI values.

2 Theoretical background

2.1 Empirical CWSI

The empirical CWSI introduced by Idso et al. (1981) hereafter referred to as $\mathrm{CWSI_E}$, is defined as

$$\mathrm{CWSI_E} = \frac{T_C - T_{nws}}{T_{dry} - T_{nws}} \tag{1}$$

Where T_C (°C) is the actual canopy surface temperature under given environmental conditions, T_{dry} (°C) is the upper limit for canopy temperature and equates to the temperature of a non-transpiring canopy such as would occur if the stomata were completely closed as a result of drought, while T_{nws} (°C) is the non-water stressed baseline representing the typical canopy of a well-watered crop transpiring at maximum rate.

Therefore, the temperature of a plant transpiring without soil water shortage can be assumed to represent T_{nws} and the temperature of a plant canopy from which all transpiration has been blocked, for example using petroleum jelly, can be assumed to represent T_{dry}. This is similar to the methodology employed by Rojo et al. (2016) to calculate an empirical CWSI for grape and almond trees. In their study, T_{nws} and T_{dry} were measured using a well-watered tree and a simulated dry canopy.

2.2 Theoretical CWSI

The theoretical CWSI proposed by Jackson et al. (1981) hereafter referred to as $\mathrm{CWSI_T}$ is calculated as

$$\mathrm{CWSI_T} = \frac{(T_c - T_a) - (T_c - T_a)_{LL}}{(T_c - T_a)_{UL} - (T_c - T_a)_{LL}} \tag{2}$$

Where $T_c - T_a$ is the canopy-air temperature difference, $(T_c - T_a)_{LL}$ is the lower baseline representing a non-stressed canopy, transpiring at potential rate and $(T_c - T_a)_{UL}$ is the upper baseline representing a stressed, non-transpiring canopy. The lower and upper baselines are given as

$$(T_c - T_a)_{UL} = \frac{r_a I_c}{\rho_a c_p} R_n \tag{3}$$

$$(T_c - T_a)_{LL} = \frac{r_a I_c}{\rho_a c_p} \frac{\gamma(1 + r_{c,pot}/r_a)}{s + \gamma(1 + r_{c,pot}/r_a)} R_n - \frac{1}{s + \gamma\left(1 + r_{c,pot}/r_a\right)} \delta e \tag{4}$$

Where r_a is the aerodynamic resistance $(\mathrm{sm^{-1}})$, I_c is the interception coefficient, ρ_a is the air density $(\mathrm{kgm^{-3}})$, c_p is the specific heat capacity of air $(\mathrm{JKg^{-1}K^{-1}})$, R_n is the net radiation $(\mathrm{Wm^{-2}})$, s is the slope relating temperature with the saturation vapour pressure deficit $(\mathrm{PaK^{-1}})$, $r_{c,pot}$ is the canopy resistance at potential transpiration $(\mathrm{sm^{-1}})$, γ is the psychometric constant $(\mathrm{kPaK^{-1}})$, and δe is the vapour pressure deficit (kPa).

$\mathrm{CWSI_T}$ has been shown to provide a robust quantification of the water status of various crops (Osroosh et al., 2015; Shaughnessy et al., 2012; Yuan et al., 2004). It can be estimated using the canopy temperature as measured by infrared radiometers and appropriate environmental measurements, including aerodynamic and canopy resistances.

2.3 Dynamic response of the plant canopy temperature

The plant canopy can be viewed as a natural dynamic input/output system. The inputs (prevailing meteorological conditions) applied to the system causes the system to respond with an output (canopy temperature) (Al-Faraj et al., 2000). Under minimal wind speed (u, ms^{-1}) conditions, the dynamic response of the canopy temperature can be expressed in form of a first-order differential equation given as (Jones, 2014)

$$\frac{\mathrm{d}T_c(t)}{dt} + \left(\frac{\rho C_p}{\xi r_H}\right) T_c(t) = \left(\frac{\rho C_p}{\xi r_H}\right) T_a(t-\tau_a) + \left(\frac{1}{\xi}\right) R_n(t-\tau_r) - \left(\frac{\rho C_p}{\xi\gamma(r_C + r_H}\right)(e_C^* - e_a)(t-\tau_v) \quad (5)$$

With $\rho^* C_p^* l^* = \xi$

Where t is the time (s), $\tau_{(a,r,v)}$ are the advective time delays (s) associated with the air temperature, radiation and vapour pressure deficit inputs respectively, ρ is the air density ($\mathrm{Kg\ m^{-3}}$), C_p is the heat capacity of air ($\mathrm{J\ Kg^{-1}\ °C^{-1}}$), T_c is the canopy temperature (°C), T_a is the air temperature (°C), e_C^* is the saturated vapour pressure at canopy temperature (kPa), e_a is the vapour pressure of air (kPa), r_H is the aerodynamic resistance ($\mathrm{s\ m^{-1}}$), r_C is the canopy resistance ($\mathrm{s\ m^{-1}}$) , R_n is the net radiation ($\mathrm{Wm^{-2}}$) and γ is the psychrometric constant ($\mathrm{Pa\ °C^{-1}}$).

Using Laplace transform, Eq.(5) can be rewritten as (Al-Faraj et al., 2000)

$$(s+a)T_c(t) = aT_a(t-\tau_a) + bR_n(t-\tau_r) - c(e_c^* - e_a)\,(t-\tau_v) \quad (6)$$

Where

$s = d/dt$ is the time derivative operator

$a = [\rho C_p]/[\,\xi r_H]$ $(\mathrm{s^{-1}})$

$b = \xi^{-1}(\mathrm{m^2 °C W^{-1} s^{-1}})$

$c = [\rho C_p]/[\,\xi\gamma(r_c + r_H)](\mathrm{°C Pa^{-1} s^{-1}})$

The net radiation flux (R_n) absorbed by the crop can be systematically assumed to be equal to the net radiation measured above the crop, thus neglecting the radiation exchanged below the canopy and the ground. Thus, net radiation above the canopy is almost equal to the total shortwave irradiance R_{sw} ($\mathrm{Wm^{-2}}$) during the day (Cannavo et al., 2016).

The canopy-air vapor pressure difference in Eq. (6). can be expressed in terms of vapor pressure deficit of the ambient air as

$$e_c^* - e_a = (e_a^* - e_a) + \Delta \quad (7)$$

Where Δ $(\mathrm{k\ Pa°\ C^{-1}})$ is the slope of the curve relating the saturation vapor pressure to temperature which is assumed to be approximately constant over the range $\mathrm{T_c}$ to $\mathrm{T_a}$ (Jones, 2014).

Since Δ is a constant, Eq. (7) is expressed with respect to time as $(e_a^* - e_a)$ which is the VPD of the ambient air as a function of time.

Therefore, Eq. (5) can be expressed as a first-order continuous time multiple-input-single-output (MISO) transfer function model

$$T_c(t) = \frac{a}{s+a} T_a(t-\tau_a) + \frac{b}{s+a} R_{sw}(t-\tau_r) - \frac{c}{s+a} VPD(t-\tau_v) \quad (8)$$

The dynamic model in Eq. (8) has the canopy temperature (T_c) as the model output. The model inputs are the dynamic course of air temperature (T_a), shortwave irradiance (R_{sw}) and the air vapour pressure deficit (VPD). The physical meaningfully model parameters to be estimated are a, b and c which can be accomplished using a suitable system identification technique described in section 2.4. The identified parameters will be unique to the well-watered and non-transpiring canopies, and will also drive the dynamic response of their temperatures to the prevailing meteorological conditions.

2.4 Data-based mechanistic modelling approach

Data-based mechanistic (DBM) modelling is a dynamic modelling approach applicable to transfer function models (Young, 2006). It consists of two phases as illustrated in Figure 1. In the mechanistic phase, a model structure is formulated based on the physical knowledge of the process under consideration. In the data-based phase, time-series input/output data are exploited to estimate the physically meaningful model parameters and the advective time delay associated with each model input (Desta et al., 2004).

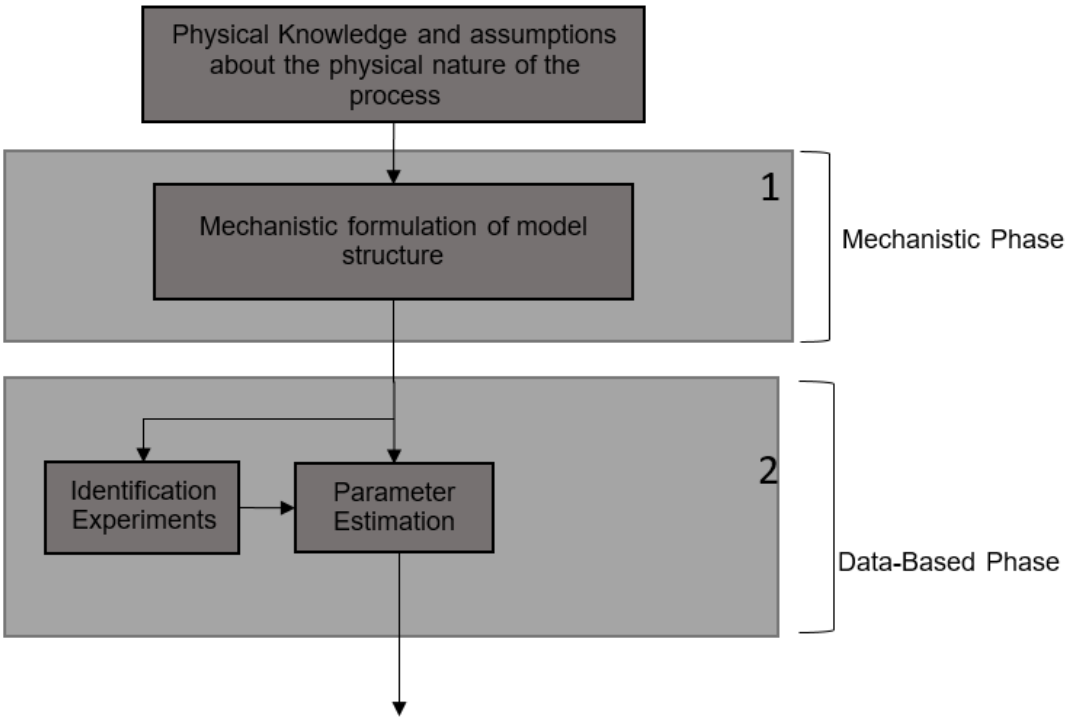

Figure 1. The Data-based mechanistic (DBM) modelling approach (Desta et al., 2004)

The DBM model can be formulated in the form of a MISO continuous-time transfer function written as

$$y(t) = \frac{B_1(s)}{A(s)}u_1(t-\partial_1) + \cdots + \frac{B_k(s)}{A(s)}u_k(t-\partial_k) + \frac{1}{C(s)}e(t) \quad (9)$$

In Eq. 9, $y(t)$ is the output which is T_c in this study, u_k are the set of k inputs into the system which are T_a, R_{sw} and VPD in this study, ∂_k are the advective time delays associated with each input and $e(t)$ is the noise signal considered as zero mean, white noise with Gaussian amplitude distribution and variance.

$A(s)$ and $B(s)$ are polynomials in the derivative operator $s = d/dt$ of the form

$$A(s) = s^n + y_1 s^{n-1} + \cdots y_{n-1}s + y_n \quad (10)$$

$$B(s) = x_0 s^m + x_1 s^{m-1} + \cdots x_{m-1}s + x_m \quad (11)$$

Where x, y are model parameters to be estimated for the $A(s)$ and $B_1(s) \ldots B_k(s)$ polynomials. The model structure is denoted by the triad $[n, m, \partial]$ where n represents the number of parameters in the $A(s)$ polynomial, m represents the number of parameters in each $B(s)$ polynomial and ∂ is the time delay associated with each input. By comparing Eq. (8) with Eq. (9-11), in the present study, the model parameters to be identified are a, b, c, n=1 (a in the denominators of Eq. 8) and m=1 for each input (a, b, c in the numerators of Eq.8). The time delays are τ_a, τ_r and τ_v.

The continuous time MISO transfer function model parameters and time delays are estimated from the experimental input/output time-series data using the recursive refined instrumental variable algorithm for continuous time systems (RIVC) (Taylor et al., 2007). This algorithm has been applied and validated for many practical applications (Young & Garnier, 2006). The RIVC optimally filters the data which ensures the estimation is statistically efficient and also generates the filtered derivatives of the input and output signals. The model estimated using the RIVC approach has statistically optimum properties due to the iterative and adaptive mode of solution used by the algorithm (Youssef et al., 2011).

3 Methodology

Plant canopy temperature and meteorological data for lettuce plants cultivated under greenhouse conditions were collected for the development and testing of the dynamic model.

The lettuce crop was selected for our study because of its highly sensitive response to water stress. Irrigation is also widely optimized to enhance the post-harvest quality of the crop (Monaghan et al., 2017). Some previous studies have reported the canopy temperature as a useful indicator of the plant water status of the lettuce crop (Qiu et al., 2009; Story and Kacira, 2015).

3.1 Plants and measurements

The canopy temperature of randomly selected lettuce plants was continuously measured for two five-week study periods.

At the start of the initial five-week study, eight plants were maintained as well-watered by adding irrigation volumes to fully replace daily water loss through crop evapotranspiration ($\mathrm{ET_C}$). The water loss through $\mathrm{ET_C}$ for all plants was measured using a load balance system (Model ALC, Acculab, Englewood, USA) with a $16\ kg$ capacity and $\pm 0.1\ g$ resolution. This set of plants were used for T_{nws} measurements. Petroleum jelly was applied on the leaves of eight other plants to completely inhibit transpiration, and this set of plants were used for T_{dry} measurements. Prior to the application of the petroleum jelly, these plants received irrigation volumes to fully replace $\mathrm{ET_C}$ water loss. The plants selected for T_{dry} measurements were replaced after three days with a new set of plants which had been receiving full irrigation volumes in order to ensure uniform development of the plant canopy.

During a follow up five-week study with a new set of lettuce plants receiving irrigation volumes to fully replace water loss through $\mathrm{ET_C}$, two days prior to the commencement of measurements, four replicate lettuce plants received one of two irrigation treatments supplying; 80% of $\mathrm{ET_C}$ and 40% of $\mathrm{ET_C}$. The treatments are hereafter referred to as 80ET and 40ET respectively. These sets of plants were used for T_c measurements for the calculation of the CWSI. This methodology was applied in order to ensure uniform development of the plant canopy. A total of ten plants were also maintained as well-watered and stressed for assessing the model prediction of the baseline temperatures.

The canopy temperature of each of the plants was continuously measured using Pyro NFC infrared (IR) sensors (Calex Electronic Limited, Bedfordshire, UK). The IR sensors operate at a spectral range of 8 – 14μm. The sensors were positioned approximately 30 - 50cm above the plant canopy and pointed in a nadir direction. The temperature sensing area was approximately 3 - 5cm to ensure only the plant canopy was in the view of the IR sensors. Readings from the IR sensors were recorded every 10 s.

Environmental variables measured at plant canopy level included ambient air temperature and relative humidity using a temperature and humidity probe (Model EE08, E+E Elektronik, Engerwitzdorf, Austria), and shortwave irradiance using a pyranometer sensor (Model SP-110, Apogee Instruments, Logan, Utah, USA). Wind speed was measured using a hot wire anemometer (Model AM – 4202, Lutron Electronics, London, UK) installed 10cm above the crop canopy. The VPD was calculated using temperature and relative humidity data following the equations outlined in Allen et al. (1998). Readings from the sensors were recorded every 10 s. All sensors were factory calibrated by their respective manufacturers.

Data from all the sensors were collected and stored using a CR1000 data acquisition system (Campbell Scientific, Logan, Utah, USA).

The leaf area index (LAI) values for the plants used for IR measurement were assessed using digital images captured with a mobile phone camera. The LAI values were then extracted from the digital images using the Easy leaf area software (Department of Plant Sciences, University of California). During the initial study period, leaf area measurement was conducted on six random plants every three days. The measurements were conducted prior to the application of petroleum jelly on the T_{dry} plants. During the follow up study leaf area measurement was conducted on six random plants, prior to the initiation of irrigation treatments.

3.2 Dynamic model development for the baseline temperatures

The DBM modelling approach was applied in developing the dynamic model of the baseline temperatures. This was achieved using all incoming time-series measurements of T_{nws}, T_{dry} and environmental variables recorded during the initial five week period, resulting in an approximate total of 302, 000 data points for each measured variable. The parameter estimation was constrained to a first-order model following Eq. (8), and the model parameters and the time delay associated with each input were identified using the recursive RIVC algorithm.

3.3 CWSI calculations

The CWSI proposed by Idso et al. (1981) was intended as a tool for detecting the water status of plants around noon which corresponds to the period of peak plant transpiration. However, an extended period of between 8:00 and 16:00 h was explored during this study.

$\mathrm{CWSI_E}$ was calculated for the 40ET and 80ET plants using their measured canopy temperature and the baseline temperatures predicted using the dynamic model. $\mathrm{CWSI_T}$ was also calculated for these plants using their measured canopy temperature and

ancillary meteorological measurements. The aerodynamic resistance, r_a was calculated following the equations of Thom and Oliver (1977) given as

$$r_a = \frac{4.72\left\{In\left[\frac{z-d}{z_o}\right]\right\}^2}{1+0.54u} \quad (12)$$

Where z is the measurement height (m), d the displacement height (m), z_o the roughness length (m), and u the windspeed (ms^{-1}). Values of z_o and d were derived from the plant height h (m) as $z_o = 0.13\,h$ and $d = 0.67\,h$. The canopy resistance at potential transpiration, $r_{c,pot}$ was determined for each of the evaluation days by adjusting its value until the lowest CWSI value on that day was zero (González-Dugo et al., 2006).

The CWSI values were computed using 15 mins average values of the measured canopy temperature and environmental variables.

3.4 Statistical analysis

Model evaluation was carried out by comparing the T_{nws} and T_{dry} values predicted by the dynamic model and the measured values using several goodness-of-fit statistical indicators. These included the coefficient of determination (R^2), the mean absolute error (MAE) and the root mean square error (RMSE). The coefficient of correlation (r) was applied in comparing $\mathrm{CWSI_E}$ with $\mathrm{CWSI_T}$.

The MAE and RMSE were calculated as (Chai and Draxler, 2014).

$$\mathrm{MAE} = \frac{1}{n}\sum_{i=1}^{n}|P_i - O_i| \quad (13)$$

$$\mathrm{RMSE} = \left[\frac{\sum_{i=1}^{n}(P_i - O_i)^2}{n}\right]^{0.5} \quad (14)$$

Where O_i and P_i are measured and predicted value at time i ($i = 1,2,\ldots\ldots n$) respectively. R^2 values close to 1 indicate that the model explains well the variance of observations, and MAE and RMSE values close to zero indicate good model predictions (González et al., 2015). r values close to 1 indicate a strong positive linear relationship between the compared variables.

4 Results and discussion

The recursive parameter identification for the development of the dynamic model was conducted using all incoming time-series of data collected during the initial five-week

study period. Data from four selected days during the follow-up study, however, seem to be sufficient to conduct the model evaluation as this data shows a contrast in the prevailing environmental conditions (Appendix A) and crop growth stage(Appendix B). These days are hereafter referred to as D1, D2, D3 and D4 respectively.

4.1 Dynamic modelling of the baseline temperatures

The measured canopy temperatures of each of the plants maintained as either T_{nws} or T_{dry} were usually within 1°C of each other. The average coefficient of variance was 1.8% for T_{nws} measurements and 2% for T_{dry} measurements. The average measured canopy temperature of the plants in each baseline temperature group was therefore applied in recursive parameter identification.

The dynamics of T_{nws} and T_{dry} were consistently described by a first order model as indicated in the transfer function model in Eq. (8). The standard errors associated with the recursive parameter estimates ranged from 4 % to 10 %. The model residuals also had a zero mean with a standard deviation less than $\pm$ 1°C. These low parameter standard errors and residuals give evidence in favour of the first order model. It was however observed that the recursively identified model parameters and the time delay associated with the model inputs varied temporally over the plant growth cycle. For this reason, the LAI was used to divide the models into four intervals as shown in Table 1. The intervals include LAI values less than 0.8, 0.8 to 1.6, 1.6 to 2.5 and above 2.5. For the division, it is easy to change the LAI into other time units such as days after planting. The LAI evolution over the study period and identified model parameters are presented in Appendix C.

Table 1. Model Identified for the different leaf area index (LAI) intervals

LAI interval	T_{nws}					T_{dry}				
	n	m	τ_a	τ_r	τ_v	n	m	τ_a	τ_r	τ_v
0.8 or lower	1	1	2	2	2	1	1	2	2	2
0.8 to 1.6	1	1	1	2	2	1	1	1	2	2
1.6 to 2.5	1	1	1	1	2	1	1	2	1	2
2.5 or higher	1	1	1	1	1	1	1	1	1	2

Taking plant growth into account when predicting baseline temperatures would greatly reduce the errors associated with the prediction as a result of the time-varying nature of the plant system. Payero and Irmak (2006) noted that plant growth affects the crop aerodynamic resistance, surface albedo and canopy resistance which affects the canopy temperature response and hence induces a change in established model parameters. The accuracy of regression models developed by the authors for predicting baseline temperatures for corn and soybean was greatly improved when they accounted for the evolution of the plant height.

4.2 Baseline temperature prediction

The comparisons between the model predicted and measured baseline temperatures are presented in Figure 2. The data points in Figure 2 are selected from D1 – D4 which corresponds to a day in each of the four LAI intervals used to divide the models (Appendix B). It is seen that the predicted T_{nws} are highly correlated with the measured T_{nws} values ($R^2 = 0.92$). The predicted T_{dry} values are also highly correlated with the measured T_{dry} values ($R^2 = 0.95$). Summary statistics on the comparison between the measured and model predicted baseline temperatures are also presented in Table 2.

Table 2. Results of the comparison between the measured and model predicted baseline temperatures

LAI interval	T_{nws}		T_{dry}	
	RMSE (°C)	MAE (°C)	RMSE (°C)	MAE (°C)
0.8 or lower	0.35	0.29	0.31	0.24
0.8 to 1.6	0.23	0.18	0.25	0.20
1.6 to 2.5	0.21	0.17	0.28	0.21
2.5 or higher	0.22	0.18	0.22	0.17

Table 2 shows the model performs with reasonable accuracy in each LAI interval, recording low MAE and RMSE values. This suggests that the dynamic model can account

for the time-varying response of the plant system and its influence on the canopy temperature response.

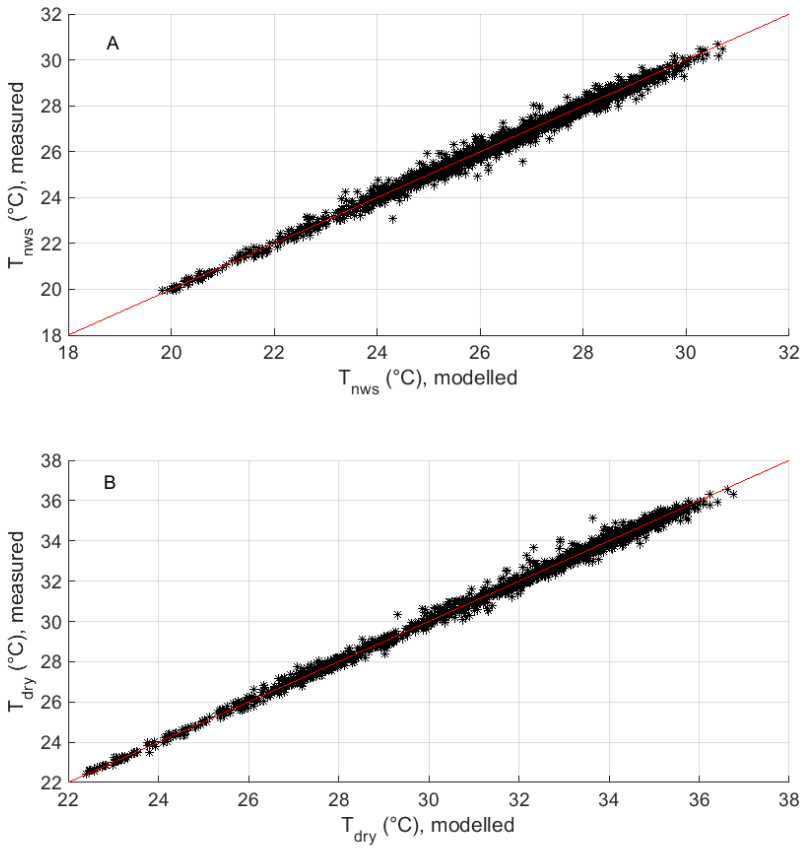

Figure 2. Comparison between the measured and modelled predicted baseline temperatures for the four model evaluation days (A) T_{nws} (B) T_{dry}

The dynamic response of the measured baseline temperatures along with prevailing shortwave irradiance and ambient air temperature for a sunny and cloudy day is presented in Figure 3. T_{dry} values are consistently higher than T_{nws} values which in turn maintain values lower than the ambient air temperature. It can also be seen that the fluctuations in the baseline temperature values closely follow the fluctuations in the incoming solar radiation. This is in agreement with results presented by Agam et al. (2013). The importance of considering the diurnal dynamics of the baseline temperatures was highlighted in a study by Payero and Irmak (2006). In their study, significant diurnal variations as high as 5°C was recorded for the baseline canopy and air temperature difference measured on corn and soybean crops. They attributed these variations to diurnal variations in the incoming solar radiation. They concluded that accounting for these diurnal variations and its effect on the canopy temperature dynamics will result in more accurate and realistic baseline temperature predictions. The empirical CWSI

approach proposed by Idso et al. (1981) assumes the baseline temperatures are constant often leading to erroneous values during cloudy periods. Agam et al. (2013) has shown that neglecting the influence of the prevailing environment on the baseline temperatures leads to a severe underestimation of CWSI values for stressed olive trees during periods of abrupt changes in radiation intensity.

It should be noted that the DBM modelling technique constitutes a data-driven approach in which the dynamic response of the baseline temperatures is parametrized for the specific ranges of environmental and crop conditions encountered during model development, and therefore the models are only applicable to the specific crop and environment for which they are developed. The methodology can, however, be adapted to any other location and crop grown under greenhouse conditions.

The high speed of the prevailing wind under field conditions results in turbulent and atmospheric and canopy exchanges which in turn alters the canopy energy balance. Hence, it may be important to consider the influence of the prevailing wind when developing dynamic models to estimate baseline temperatures for field grown crops.

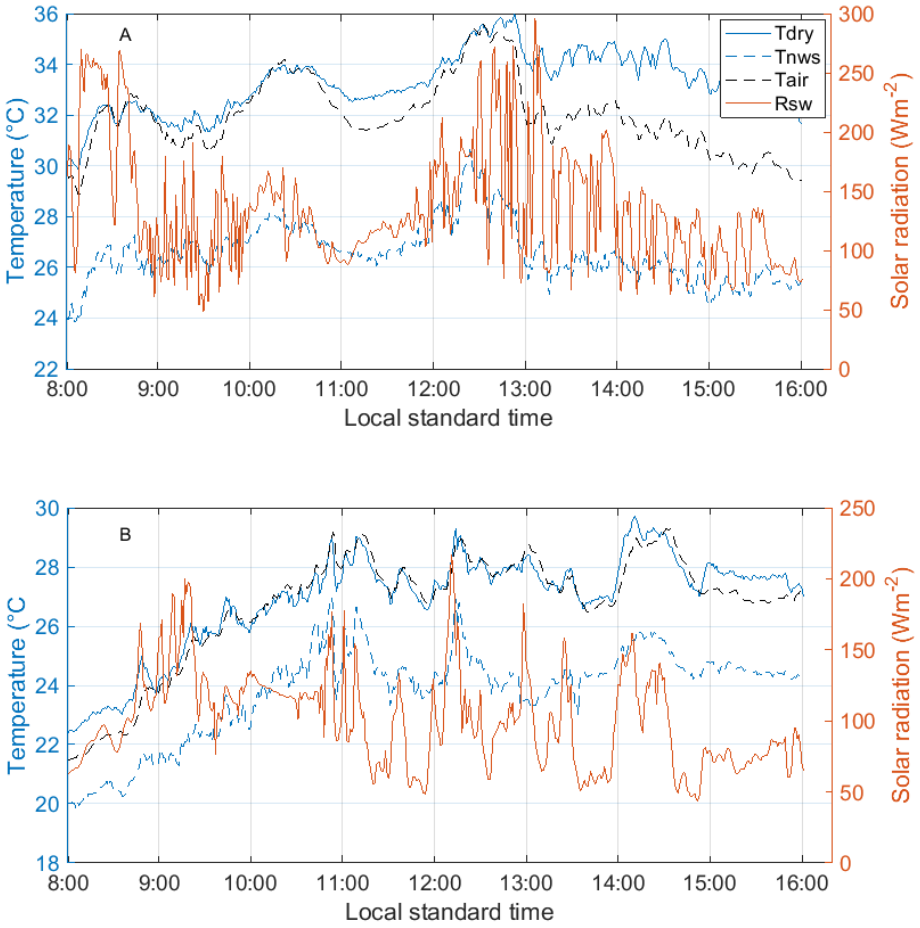

Figure 3. The diurnal dynamics of the baseline temperatures (T_{dry} and T_{nws}) along with the incoming shortwave irradiance (R_{sw}) and ambient air temperature (T_{air}). (A) Sunny day (B) Cloudy day

4.3 Comparison of the empirical and theoretical CWSI

A comparison of the $\mathrm{CWSI_E}$ and $\mathrm{CWSI_T}$ values calculated during the four model evaluation days for the 40ET and 80ET plants is presented in Figure 4. Both CWSI approaches are able to clearly separate the water status of the plants which explains the gaps in the plots. The CWSI values are significantly correlated ($p < 0.01$) during all days with r values greater than 0.9. These high correlation values are demonstrated during all crop growth stages in form of the LAI evolution.

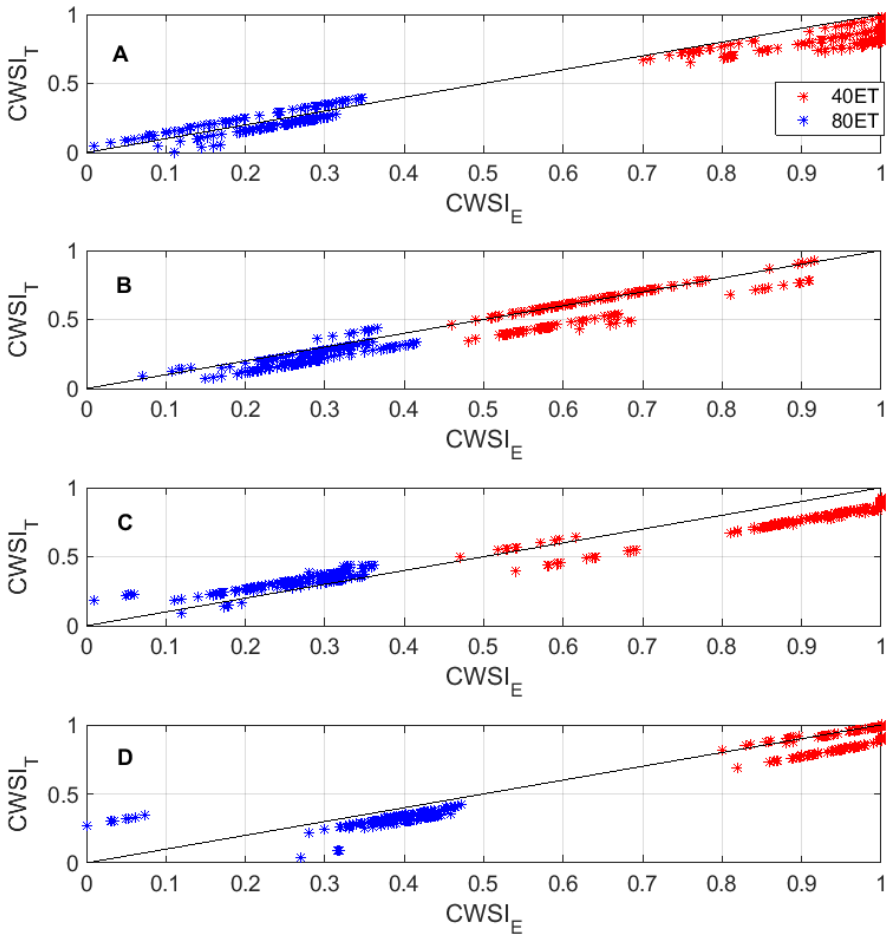

Figure 4. Comparison of empirical $(\mathrm{CWSI_E})$ and theoretical $(\mathrm{CWSI_T})$ crop water stress index during the model evaluation period (A) D1 (B) D2 (C) D3 (D) D4

The empirical CWSI approach demonstrated in this paper requires easily measured meteorological variables and crop canopy temperature for its computation. The high correlation between the empirical CWSI and the widely validated theoretical CWSI further suggests it can be deployed as part of an irrigation monitoring tool. This will eliminate the need for the computation of the crop canopy and aerodynamic resistance which is required for the computation of the theoretical CWSI. It also eliminates the need to physically maintain dry and wet reference surfaces which are required for the baseline temperature computation in other empirical CWSI approaches.

4.4 Daily dynamics of the crop water stress index

The diurnal dynamics $\mathrm{CWSI_E}$ calculated for the 40ET and 80ET plants were well differentiated during the four model evaluation days as shown in Figure 5. The CWSI recorded for the 80ET crops ranged between 0.1 – 0.4 while those of the 40ET plants consistently approached values ranging from 0.8 – 1 at noon which coincides with the

period of maximum atmospheric evaporative demand. The dynamics of the modelled baseline temperatures are also presented in Figure 6.

Agam et al. (2013) suggested that the diurnal course of CWSI of well-watered plants will maintain a relatively constant level while that of stressed plants will increase until early afternoon and decrease after that, following the dynamics of evaporative demand. Indeed the diurnal course of $\mathrm{CWSI_E}$ calculated for both 80ET and 40ET plants followed these patterns as shown in Figure 5. The cloudless conditions that are required for the application of the original empirical CWSI approach may not occur often enough during noon in humid climates such as UK (Jones, 1999). The ability of the empirical CWSI approach proposed in this paper to depict the plant water status of lettuce over an extended diurnal period should, however, make its application in practice more flexible. This is because the baseline temperature values applied in its calculation are predicted as a function of the prevailing environment, limiting the underestimation of CWSI of stressed plants during cloudy periods as shown by Agam et al. (2013). Furthermore, the results indicate that the CWSI calculated during diurnal periods different from the solar noon separates the water status of the stressed and well-watered plants, which will be particularly attractive for applications where there is a rapid change in the plant's water status due to limited container volume or substrate water holding capacity.

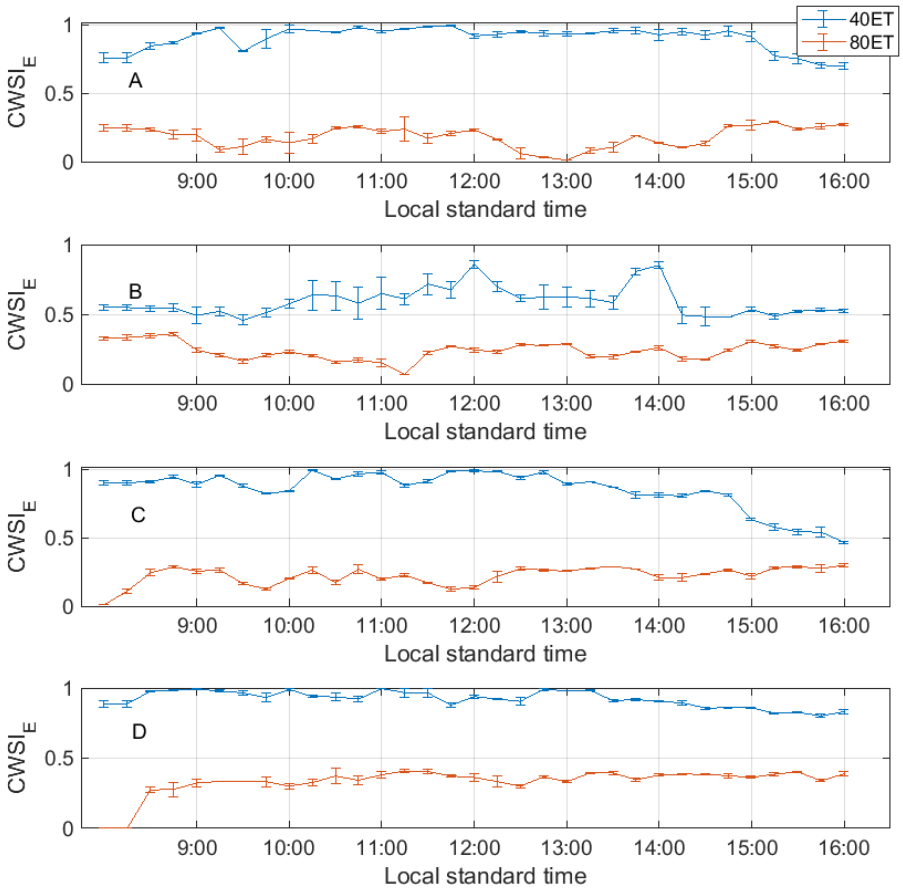

Figure 5. Diurnal dynamics of empirical crop water stress index (CWSI_E) during the model evaluation period (A) D1 (B) D2 (C) D3 (D) D4

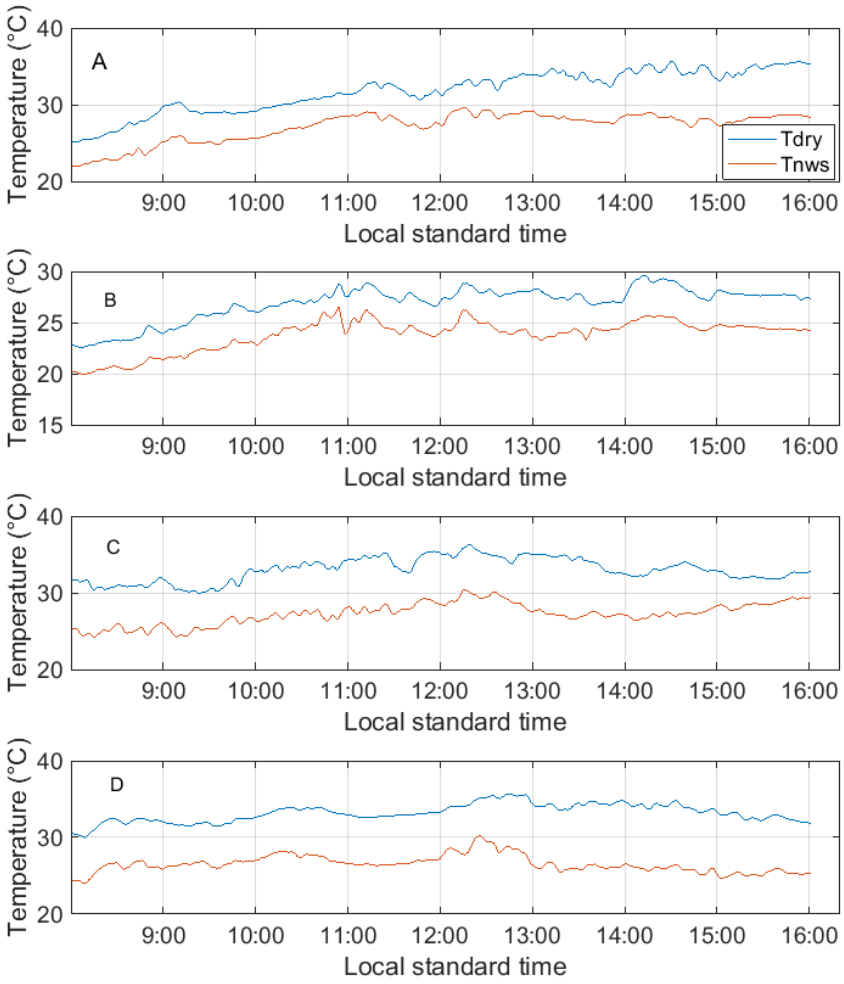

Figure 6. Diurnal dynamics of the baseline temperatures (T_{dry} and T_{nws}) during the model evaluation period (A) D1 (B) D2 (C) D3 (D) D4

It is however noted that while the empirical CWSI described in this paper can provide a useful indication of the need for irrigation, it is unable to estimate the amount of irrigation water that is needed. As such, this tool should be complemented with soil moisture measurements or estimations of $\mathrm{ET_C}$ in order to implement a robust irrigation decision support system.

5 Conclusions

In this paper, the feasibility of using a dynamic model to predict the baseline temperatures needed to calculate an empirical CWSI was demonstrated for the lettuce crop cultivated in a greenhouse. The dynamic response of the baseline temperatures was modelled as a function of shortwave irradiance, air temperature and VPD, and parameters of the model varied in response to crop growth. The empirical CWSI values computed using the dynamic model predicted baseline temperatures were significantly correlated with

theoretical CWSI values at all crop growth stages and successfully differentiated between two levels of irrigation treatment for the lettuce crop.

The dynamic modelling approach adopted in this study for predicting the baseline temperatures should enhance the application of the CWSI method for irrigation scheduling. It requires easily measured meteorological variables as input parameters, and it is able to account for the diurnal fluctuations in these variables in the baseline temperature prediction. It can also be applied in computing the CWSI over an extended diurnal period making its application more flexible. The requirement for the calculation of the aerodynamic resistances needed in the theoretical CWSI computation is eliminated. The need to maintain artificial reference surfaces applicable in other empirical CWSI approaches is also eliminated. The implementation of this model in a commercial greenhouse and model development for other high-value crops will be the focus of future research.

Appendices

Appendix A: Climatic conditions during model evaluation

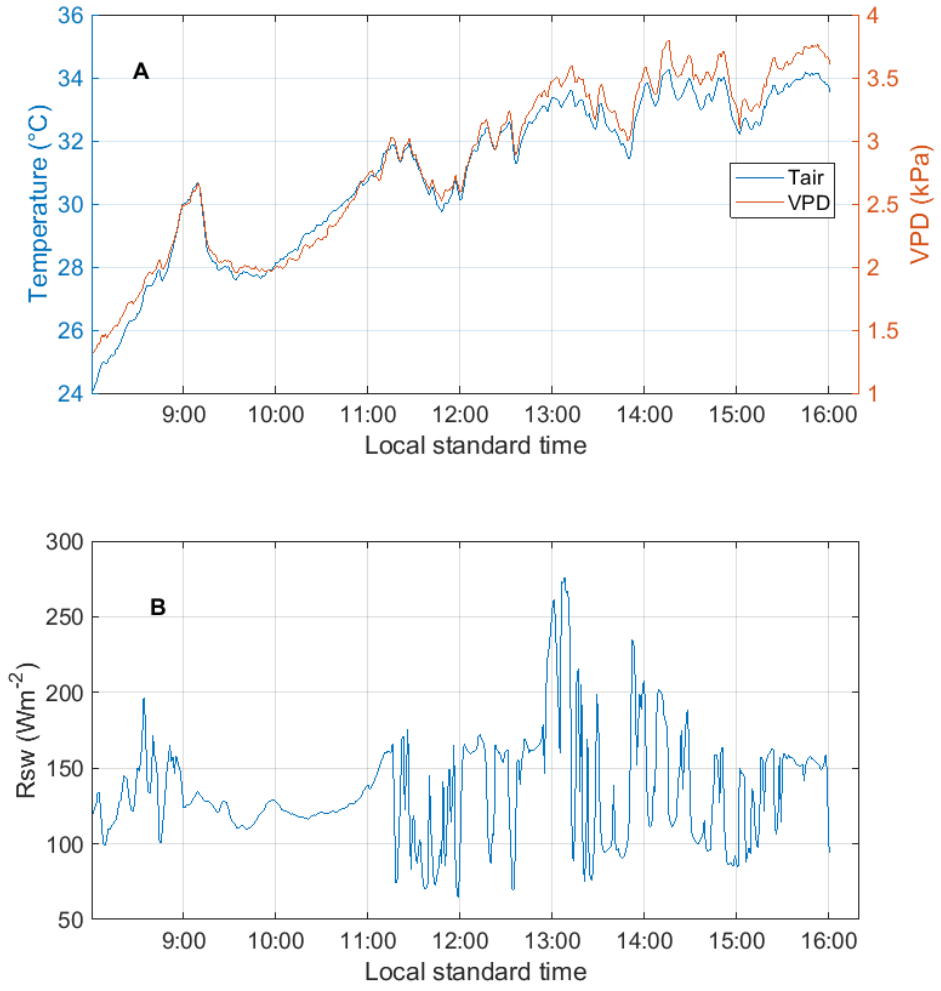

Figure A1. Climatic conditions during D1 (A) T_{air} (Air temperature) and VPD (Vapour pressure deficit) (B) R_{sw} (Incoming shortwave irradiance)

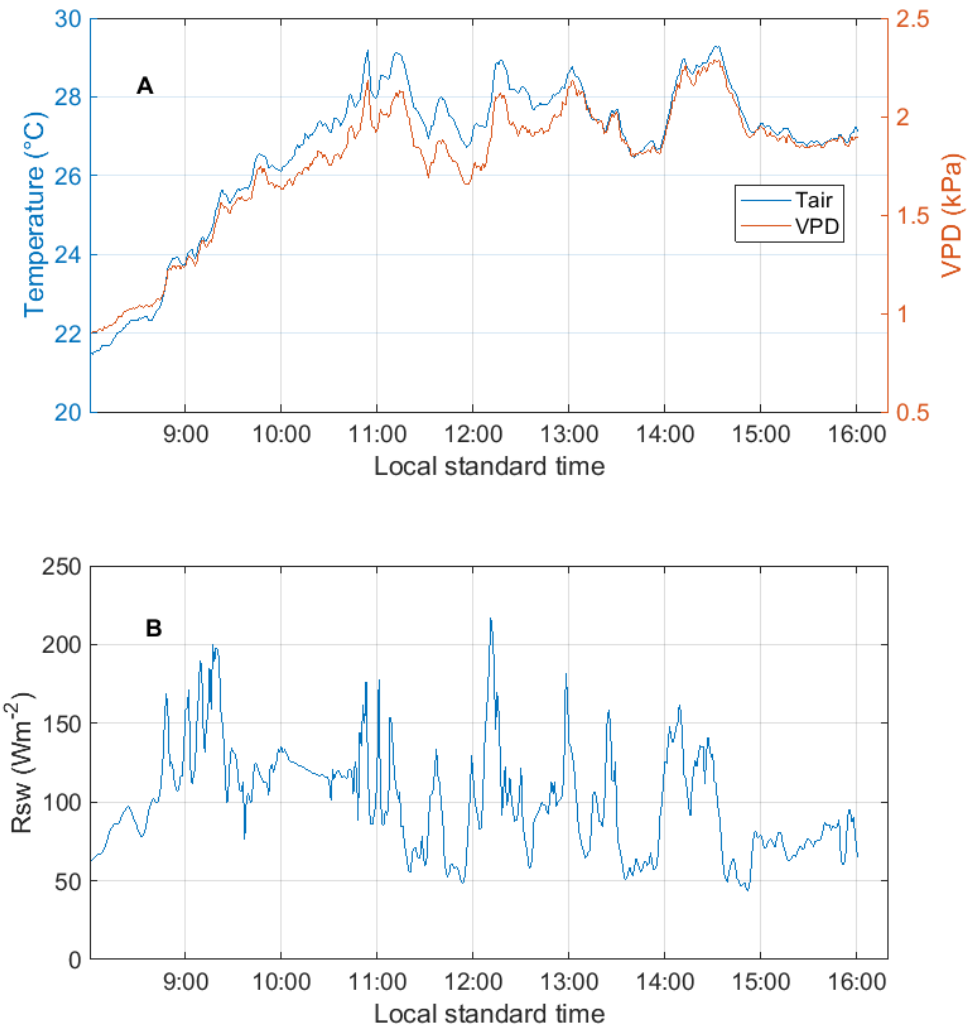

Figure A2. Climatic conditions during D2 (A) T_{air} (Air temperature) and VPD (Vapour pressure deficit) (B) R_{sw} (Incoming shortwave irradiance)

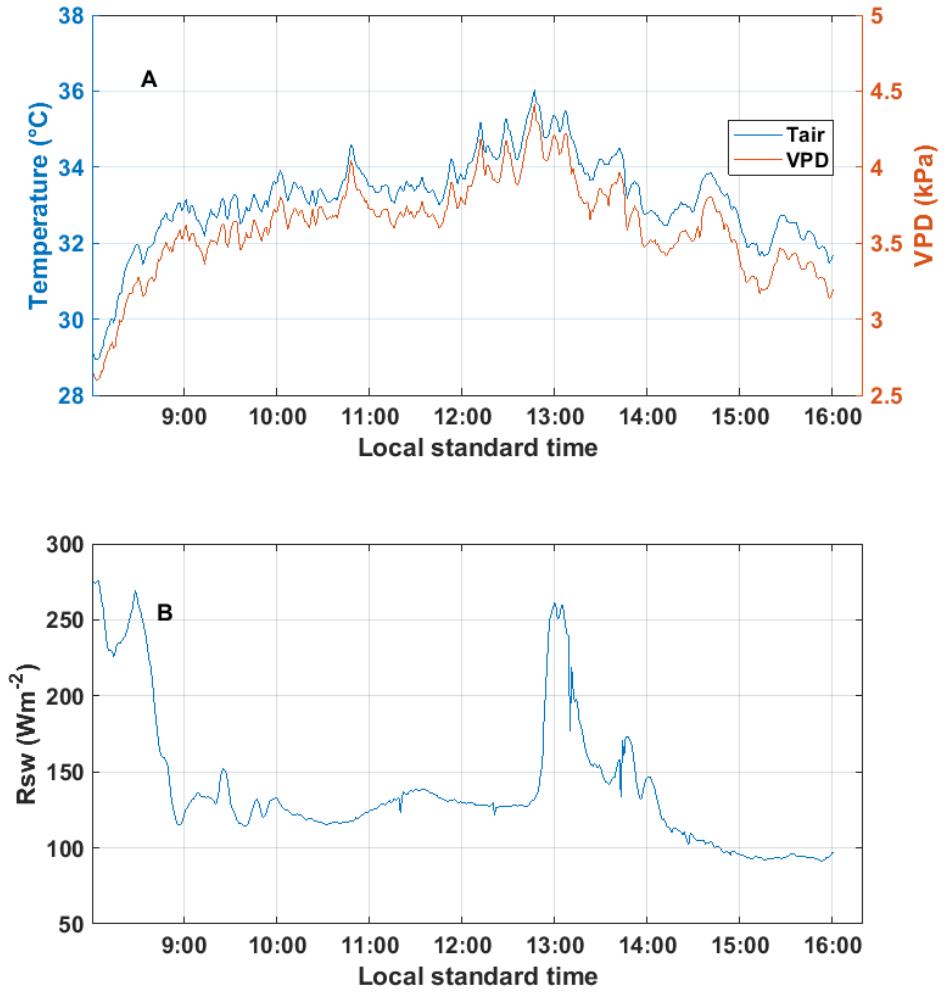

Figure A3. Climatic conditions during D3 (A) T_{air} (Air temperature) and VPD (Vapour pressure deficit) (B) R_{sw} (Incoming shortwave irradiance)

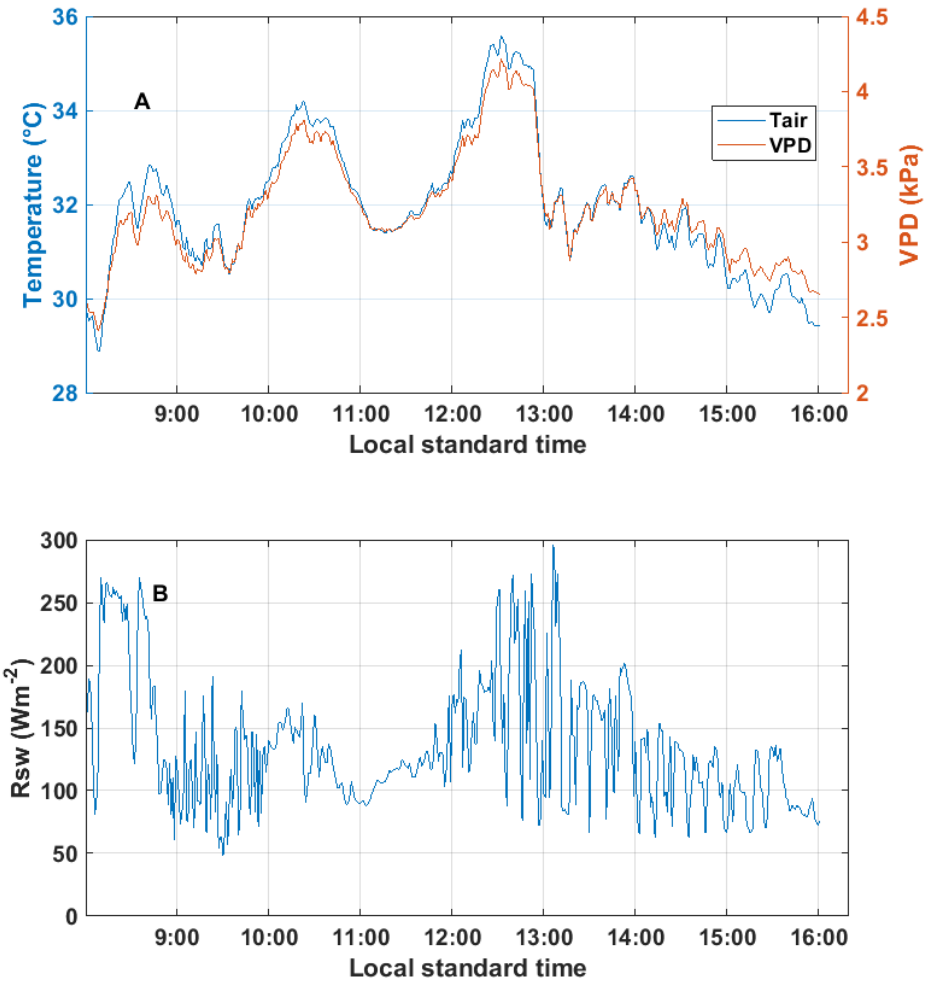

Figure A4. Climatic conditions during D4 (A) T_{air} (Air temperature) and VPD (Vapour pressure deficit) (B) R_{sw} (Incoming shortwave irradiance)

Appendix B: Crop growth stage during the model evaluation days

Table B1. Leaf area index (LAI) values (standard deviations in brackets) during the model evaluation days

LAI value	LAI interval	Model evaluation day
0.6 (0.03)	0.8 or lower	D1
1.3 (0.05)	0.8 to 1.6	D2
2.2 (0.15)	1.6 to 2.5	D3
4.2 (0.11)	2.5 or higher	D4

Appendix C: Model parameters as a function of LAI evolution

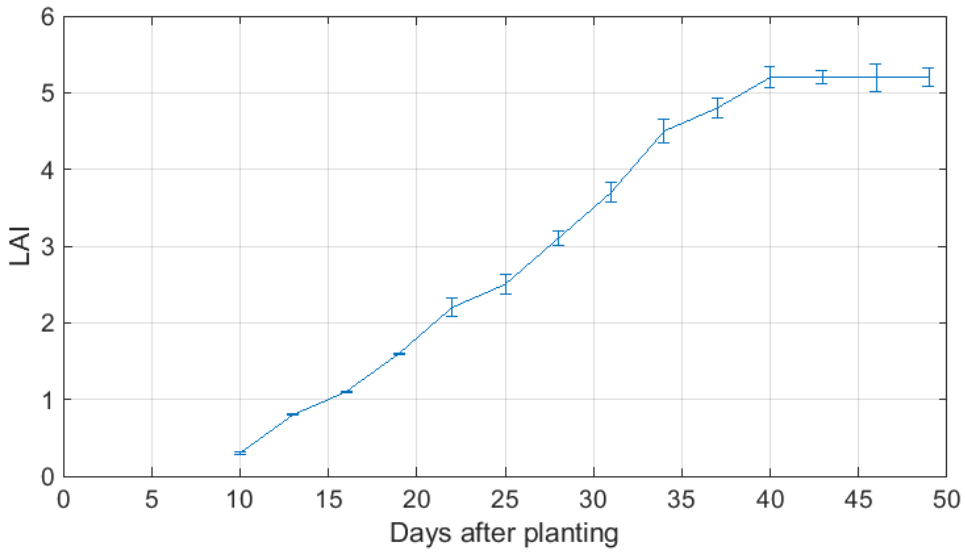

Figure C1. Leaf area index (LAI) evolution during the study period

Table C1. Model parameter estimation (standard errors in brackets) at different leaf area index (LAI) intervals

Baseline temperature	Parameter estimates			LAI interval
	a	b	c	
T_{nws}	0.0043 (0.0003)	0.0018 (0.0002)	0.0060 (0.0004)	0.8 or lower
T_{nws}	0.0055 (0.0004)	0.0032 (0.0003)	0.0094 (0.0003)	0.8 to 1.6
T_{nws}	0.0058 (0.0002)	0.0037 (0.0005)	0.0098 (0.0011)	1.6 to 2.5
T_{nws}	0.0049 (0.0003)	0.0040 (0.0005)	0.0087 (0.0002)	2.5 or higher
T_{dry}	0.0022 (0.0004)	0.0013 (0.0001)	0.0028 (0.0003)	0.8 or lower
T_{dry}	0.0032 (0.0007)	0.0025 (0.0002)	0.0033 (0.0002)	0.8 to 1.6
T_{dry}	0.0037 (0.0001)	0.0031 (0.0004)	0.0038 (0.0003)	1.6 to 2.5
T_{dry}	0.0025 (0.0002)	0.0028 (0.0001)	0.0035 (0.0001)	2.5 or higher

References

Adeyemi, O., Grove, I., Peets, S., Norton, T., 2017. Advanced Monitoring and Management Systems for Improving Sustainability in Precision Irrigation. Sustainability 9, 1–29. https://doi.org/10.3390/su9030353

Agam, N., Cohen, Y., Alchanatis, V., Ben-Gal, A., 2013. How sensitive is the CWSI to changes in solar radiation? Int. J. Remote Sens. 34, 6109–6120. https://doi.org/10.1080/01431161.2013.793873

Agam, N., Cohen, Y., Berni, J.A.J., Alchanatis, V., Kool, D., Dag, A., Yermiyahu, U., Ben-Gal, A., 2013. An insight to the performance of crop water stress index for olive trees. Agric. Water Manag. 118, 79–86. https://doi.org/10.1016/j.agwat.2012.12.004

Al-Faraj, A., Meyer, G.E., Schade, G.R., Horst, G.L., 2000. Dynamic analysis of moisture stress in tall fescue (festuca arundinacea) using canopy temperature, irradaition, and vapor deficit. Trans. ASAE 43, 101–109.

Allen, R., Pereira, L.S., Raes, D., Smith, M., 1998. FAO Irrigation and Drainage Paper No.56, FAO. https://doi.org/10.1016/j.eja.2010.12.001

Ben-Gal, A., Agam, N., Alchanatis, V., Cohen, Y., Yermiyahu, U., Zipori, I., Presnov, E., Sprintsin, M., Dag, A., 2009. Evaluating water stress in irrigated olives: Correlation of soil water status, tree water status, and thermal imagery. Irrig. Sci. 27, 367–376. https://doi.org/10.1007/s00271-009-0150-7

Boonen, C., Joniaux, O., Janssens, K., Berckmans, D., Lemeur, R., Kharoubi, A., Pien, H., 2000. Modeling dynamic behavior of leaf temperature at three-dimensional positions to step variations in air temperature and light. Trans. ASAE-American Soc. Agric. Eng. 43, 1755–1766. https://doi.org/10.13031/2013.3078

Cannavo, P., Bouhoun Ali, H., Chantoiseau, E., Migeon, C., Charpentier, S., Bournet, P.E., 2016. Stomatal resistance of New Guinea Impatiens pot plants. Part 2: Model extension for water restriction and application to irrigation scheduling. Biosyst. Eng. 149, 82–93. https://doi.org/10.1016/j.biosystemseng.2016.07.001

Chai, T., Draxler, R.R., 2014. Root mean square error (RMSE) or mean absolute error (MAE)? -Arguments against avoiding RMSE in the literature. Geosci. Model Dev. 7, 1247–1250. https://doi.org/10.5194/gmd-7-1247-2014

Delgoda, D., Malano, H., Saleem, S.K., Halgamuge, M.N., 2016. Irrigation control based on model predictive control (MPC): Formulation of theory and validation using

weather forecast data and AQUACROP model. Environ. Model. Softw. 78, 40–53. https://doi.org/10.1016/j.envsoft.2015.12.012

Desta, T.Z., Van Brecht, a., Meyers, J., Baelmans, M., Berckmans, D., 2004. Combining CFD and data-based mechanistic (DBM) modelling approaches. Energy Build. 36, 535–542. https://doi.org/10.1016/j.enbuild.2003.12.015

Dhillon, R., Udompetaikul, V., Rojo, F., Slaughter, D., 2014. Detection of Plant Water Stress Using Leaf Temperature and Microclimatic Measurements in Almond, Walnut, and Grape Crops. Trans. ASABE 297–304. https://doi.org/10.13031/trans.57.10319

Fuentes, S., De Bei, R., Pech, P., Tyerman, S., 2012. Computational water stress indices obtained from thermal image analysis of grapevine canopies. Irrig. Sci. 30.

González-Dugo, M.P., Moran, M.S., Mateos, L., Bryant, R., 2006. Canopy temperature variability as an indicator of crop water stress severity. Irrig. Sci. 24, 233–240. https://doi.org/10.1007/s00271-005-0022-8

González, M.G., Ramos, T.B., Carlesso, R., Paredes, P., Petry, M.T., Martins, J.D., Aires, N.P., Pereira, L.S., 2015. Modelling soil water dynamics of full and deficit drip irrigated maize cultivated under a rain shelter. Biosyst. Eng. 132, 1–18. https://doi.org/10.1016/j.biosystemseng.2015.02.001

Grant, O.M., Tronina, L., Jones, H.G., Chaves, M.M., 2007. Exploring thermal imaging variables for the detection of stress responses in grapevine under different irrigation regimes. J. Exp. Bot. 58, 815–825. https://doi.org/10.1093/jxb/erl153

Hedley, C.B., Knox, J.W., Raine, S.R., Smith, R., 2014. Water: Advanced Irrigation Technologies. Encycl. Agric. Food Syst. 5, 378–406. https://doi.org/http://dx.doi.org/10.1016/B978-0-444-52512-3.00087-5

Idso, S.B., Jackson, R.D., Pinter, P.J., Reginato, R.J., Hatfield, J.L., 1981. Normalizing the stress-degree-day parameter for environmental variability. Agric. Meteorol. 24, 45–55. https://doi.org/10.1016/0002-1571(81)90032-7

Jackson, R.D., Idso, S.B., Reginato, R.J., Pinter, P.J., 1981. Canopy temperature as a crop water stress indicator. Water Resour. Res. https://doi.org/10.1029/WR017i004p01133

Jones, H.G., 2014. Plants and Microclimate, Third Edit. ed. Cambridge University Press, New York.

Jones, H.G., 1999. Use of infrared thermometry for estimation of stomatal conductance as

a possible aid to irrigation scheduling. Agric. For. Meteorol. 95, 139–149. https://doi.org/10.1016/S0168-1923(99)00030-1

Jones, H.G., Aikman, D., McBurney, T.A., 1997. Improvements to infra-red thermometry for irrigation scheduling in humid climates. Acta Hortic.

Jones, H.G., Leinonen, I., 2003. Thermal Imaging for the Study of Plant Water Relations. J. Agric. Meteorol. 59, 205–217. https://doi.org/10.2480/agrmet.59.205

Jones, H.G., Schofield, P., 2008. Thermal and other remote sensing of plant stress. Gen. Appl. Plant Physiol. 34, 19–32.

King, B.A., Shellie, K.C., 2016. Evaluation of neural network modeling to predict non-water-stressed leaf temperature in wine grape for calculation of crop water stress index. Agric. Water Manag. 167, 38–52. https://doi.org/10.1016/j.agwat.2015.12.009

Kirchsteiger, H., Pölzer, S., Johansson, R., Renard, E., del Re, L., 2011. Direct continuous time system identification of MISO transfer function models applied to type 1 diabetes. IEEE Conf. Decis. Control Eur. Control Conf. 5176–5181. https://doi.org/10.1109/CDC.2011.6161344

Kuscu, H., Turhan, A., Demir, A.O., 2014. The response of processing tomato to deficit irrigation at various phenological stages in a sub-humid environment. Agric. Water Manag. 133, 92–103. https://doi.org/10.1016/j.agwat.2013.11.008

Lozoya, C., Mendoza, C., Aguilar, A., Román, A., Castelló, R., 2016. Sensor-Based Model Driven Control Strategy for Precision Irrigation. J. Sensors 2016.

Maes, W.H., Steppe, K., 2012. Estimating evapotranspiration and drought stress with ground-based thermal remote sensing in agriculture: a review. J. Exp. Bot. 63, 695–709. https://doi.org/10.1093/jxb/err313

Möller, M., Alchanatis, V., Cohen, Y., Meron, M., Tsipris, J., Naor, A., Ostrovsky, V., Sprintsin, M., Cohen, S., 2007. Use of thermal and visible imagery for estimating crop water status of irrigated grapevine. J. Exp. Bot. 58, 827–838. https://doi.org/10.1093/jxb/erl115

Monaghan, J.M., Daccache, A., Vickers, L.H., Hess, T.M., Weatherhead, E.K., Grove, I.G., Knox, J.W., 2013. More “crop per drop”: Constraints and opportunities for precision irrigation in European agriculture. J. Sci. Food Agric. 93, 977–980. https://doi.org/10.1002/jsfa.6051

Monaghan, J.M., Vickers, L.H., Grove, I.G., Beacham, A.M., 2017. Deficit irrigation

reduces postharvest rib pinking in wholehead Iceberg lettuce, but at the expense of head fresh weight. J. Sci. Food Agric. 97, 1524–1528. https://doi.org/10.1002/jsfa.7895

Oh, M., Carey, E.E., Rajashekar, C.B., 2010. Regulated Water Deficits Improve Phytochemical Concentration in Lettuce. J. Am. Soc. Hortic. Sci. 135, 223–229.

Osroosh, Y., Troy Peters, R., Campbell, C.S., Zhang, Q., 2015. Automatic irrigation scheduling of apple trees using theoretical crop water stress index with an innovative dynamic threshold. Comput. Electron. Agric. 118, 193–203. https://doi.org/10.1016/j.compag.2015.09.006

Payero, J.O., Irmak, S., 2006. Variable upper and lower crop water stress index baselines for corn and soybean. Irrig. Sci. 25, 21–32. https://doi.org/10.1007/s00271-006-0031-2

Qiu, G.Y., Omasa, K., Sase, S., 2009. An infrared-based coefficient to screen plant environmental stress: Concept, test and applications. Funct. Plant Biol. 36, 990–997. https://doi.org/10.1071/FP09132

Quanten, S., De Valck, E., Cluydts, R., Aerts, J.M., Berckmans, D., 2006. Individualized and time-variant model for the functional link between thermoregulation and sleep onset. J. Sleep Res. 15, 183–198. https://doi.org/10.1111/j.1365-2869.2006.00519.x

Rojo, F., Kizer, E., Upadhyaya, S., Ozmen, S., Ko-Madden, C., Zhang, Q., 2016. A Leaf Monitoring System for Continuous Measurement of Plant Water Status to Assist in Precision Irrigation in Grape and Almond crops. IFAC-PapersOnLine 49, 209–215. https://doi.org/10.1016/j.ifacol.2016.10.039

Shao, G.C., Zhang, Z.Y., Liu, N., Yu, S.E., Xing, W.G., 2008. Comparative effects of deficit irrigation (DI) and partial rootzone drying (PRD) on soil water distribution, water use, growth and yield in greenhouse grown hot pepper. Sci. Hortic. (Amsterdam). 119, 11–16. https://doi.org/10.1016/j.scienta.2008.07.001

Shaughnessy, S.A., Evett, S.R., Colaizzi, P.D., Howell, T.A., 2012. A crop water stress index and time threshold for automatic irrigation scheduling of grain sorghum. Agric. Water Manag. 107, 122–132. https://doi.org/10.1016/j.agwat.2012.01.018

Story, D., Kacira, M., 2015. Design and implementation of a computer vision-guided greenhouse crop diagnostics system. Mach. Vis. Appl. 26, 495–506. https://doi.org/10.1007/s00138-015-0670-5

Tanner, C.., 1963. Plant temperatures. Agron. J. 55, 210–211.

Taylor, C.J., Pedregal, D.J., Young, P.C., Tych, W., 2007. Environmental time series analysis and forecasting with the Captain toolbox. Environ. Model. Softw. 22, 797–814. https://doi.org/10.1016/j.envsoft.2006.03.002

Thom, A.S., Oliver, H.R., 1977. On Penman's equation for estimating regional evaporation. Quaterly J. R. Meteorol. Soc. 103, 345–357.

Weber, N., Zupanc, V., Jakopic, J., Veberic, R., Mikulic-Petkovsek, M., Stampar, F., 2016. Influence of deficit irrigation on strawberry (Fragaria x ananassa Duch.) fruit quality. J. Sci. Food Agric. https://doi.org/10.1002/jsfa.7806

Young, P.C., 2006. The data-based mechanistic approach to the modelling, forecasting and control of environmental systems. Annu. Rev. Control 30, 169–182. https://doi.org/10.1016/j.arcontrol.2006.05.002

Young, P.C., Garnier, H., 2006. Identification and estimation of continuous-time, data-based mechanistic (DBM) models for environmental systems. Environ. Model. Softw. 21, 1055–1072. https://doi.org/10.1016/j.envsoft.2005.05.007

Youssef, A., Yen, H.H., Özcan, S.E., Berckmans, D., 2011. Data-based mechanistic modelling of indoor temperature distributions based on energy input. Energy Build. 43, 2965–2972. https://doi.org/10.1016/j.enbuild.2011.06.042

Yuan, G., Luo, Y., Sun, X., Tang, D., 2004. Evaluation of a crop water stress index for detecting water stress in winter wheat in the North China Plain. Agric. Water Manag. 64, 29–40. https://doi.org/10.1016/S0378-3774(03)00193-8

Chapter 4

Dynamic Modelling of Lettuce Transpiration for Water Status Monitoring
.

DOI: https://doi.org/10.1016/j.compag.2018.10.008

Chapter 4 Dynamic Modelling of Lettuce Transpiration for Water Status Monitoring

Abstract

Real-time information on the plant water status is an important prerequisite for the precision irrigation management of crops. The plant transpiration has been shown to provide a good indication of its water status. In this paper, a novel plant water status monitoring framework based on the transpiration dynamics of greenhouse grown lettuce plants is presented. Experimental results indicated that lettuce plants experiencing adequate water supply transpired at a higher rate compared to plants experiencing a shortage in water supply. A data-driven model for predicting the transpiration dynamics of the plants was developed using a system identification approach. Results indicated that a second order discrete-time transfer function model with incoming radiation, vapour pressure deficit, and leaf area index as inputs sufficiently explained the dynamics with an average coefficient of determination of $R_T^2 = 0.93 \pm 0.04$. The parameters of the model were updated online and then applied in predicting the transpiration dynamics of the plants in real-time. The model predicted dynamics closely matched the measured values when the plants were in a predefined water status state. The reverse was the case when there was a significant change in the water status state. The information contained in the model residuals (measured transpiration – model predicted transpiration) was then exploited as a means of inferring the plant water status. This framework provides a simple and intuitive means of monitoring the plant water status in real-time while achieving a sensitivity similar to that of stomatal conductance measurements. It can be applied in regulating the water deficit of greenhouse grown crops, with specific advantages over other available techniques.

1 Introduction

The precise determination of irrigation water requirement and timing is a precursor to the successful precision irrigation management of crops (Kochler et al., 2007). This requires a knowledge of the plant water status in real-time which can then guide in arriving at optimal irrigation scheduling decisions.

Contact monitoring methods such as measurements of stomatal conductance, sap-flow, and leaf turgor pressure have been shown to provide an adequate indication of plant water status. However, these methods are plant-based, requiring large replication to provide an indication of water status at crop level. They also require technical expertise for implementation, laborious and difficult to deploy as a real-time monitoring tool (Jones, 2004). Non-contact measurement of plant canopy temperature (T_c) which is normalized using a crop water stress index (CWSI) also provides a good indication of plant water status (Ben-Gal et al., 2009). Its application as a monitoring tool in commercial crop production is however limited because of the need to know the baseline temperatures which are required for its computation under the same environmental conditions as T_c (Maes and Steppe, 2012). Non-contact monitoring tools which can provide a real-time indication of the plant water status at crop level, with non- laborious implementation, and minimal instrumentation and computation requirements will therefore be beneficial in implementing precision irrigation management in commercial crop production (Adeyemi et al., 2017).

The plant transpiration is perhaps the best indication of plant water status (Jones, 2008; Maes and Steppe, 2012). Plants experiencing unrestricted water supply (well-watered plants) have been shown to transpire at a higher rate when compared to plants experiencing a shortage in water supply (Ben-Gal et al., 2010; Villarreal-Guerrero et al., 2012). This is due to the regulation of water loss by the plant's stomates with the stomates of well-watered plants opening up more in response to atmospheric demand. The stomates of plants experiencing water shortage open up less in response to atmospheric demand in order to limit water loss (Blonquist et al., 2009). Therefore, the water status of a plant can be inferred from measurements of its transpiration rate.

Traditionally, the knowledge of crop transpiration over time has been applied in the dynamic control of water supply to greenhouse crops (Daniel et al., 2013). This is usually in form of an off/off control strategy in which irrigation is applied after the accumulation of a set point cumulative transpiration amount (Davis and Dukes, 2010). These computer-controlled irrigation systems make use of mechanistic or empirical models to estimate crop transpiration based on environmental and physiological factors (Barnard and Bauerle, 2015).

Several models have been developed for the estimation of transpiration from greenhouse cultivated ornamental and vegetable crops (Baptista et al., 2005; Fatnassi et al., 2004; Jolliet and Bailey, 1992; Montero et al., 2001). Most of these models are based on the thermal energy balance equation of the plant canopy and are similar to the Penman-Monteith (PM) equation (Howell and Evett, 2004). These models are able to account for the effect of actual water supply on transpiration through the incorporation of a stomatal resistance component. The stomatal resistance is expressed as a function of several factors including solar radiation, leaf vapour pressure deficit, leaf temperature, CO_2 concentration, photosynthetically active radiation, leaf water potential etc. (Kochler et al., 2007). The development of these models requires the calibration of several hard-to-measure parameters which limit their practical application as an irrigation monitoring tool (Villarreal-Guerrero et al., 2012). Furthermore, these models are unable to account for the time varying nature of the plant system, as their parameters are assumed to remain constant once identified. The response of a plant will vary as a result of growth, biotic and abiotic factors, and adaptation processes (Boonen et al., 2000).

Data-driven modelling approaches based on measured input-output data of a process have been shown to provide robust approximations of various biological processes and often require fewer input parameters when compared to mechanistic models (Navarro-Hellín et al., 2016). The later is difficult to implement as a perfect knowledge of the physical process under consideration is often required (Bennis et al., 2008). Sánchez et al. (2012) applied a system identification approach in predicting the transpiration rate of a greenhouse grown tomato crop. Their approach showed promise in accounting for the time-varying plant response through an online update of the model parameters. Speetjens et al. (2009) also applied an extended Kalman filtering algorithm for the online estimation of model parameters for predicting the transpiration of a greenhouse grown crop. Both studies reported improved prediction of plant transpiration rates when compared to values predicted by mechanistic models. The modelling approach presented in both studies are data-driven making their practical application as an irrigation monitoring tool viable. They also do not require the stomatal behaviour to be modelled explicitly as it is accounted for in the online parameter estimation process.

System identification is a data-driven modelling approach which is applied in modelling dynamic systems (Chen and Chang, 2008). It has been successfully applied in simplifying and modelling complex environmental and biological processes(Taylor et al., 2007; Young, 2006), predicting time-varying biological responses (Kirchsteiger et al., 2011; Quanten et al., 2006) and in many other irrigation decision support applications (Delgoda et al., 2016; Lozoya et al., 2016). It is extensively applied as part of the fault detection methodologies in the advanced process control industry (Young, 2006). During fault detection, a system identification approach is used to build a dynamic model of a process

in a known healthy state. The output predicted by the model can then be compared to the actual real-time measurements from the process. The parameters of the model can also be updated as new data is acquired from the process (Gil et al., 2015). This methodology, which has proven to be successful in the process control industry, can be adapted and applied as part of an adaptive decision support system for irrigation monitoring (Adeyemi et al., 2017).

The objectives of this study are to investigate if the transpiration rates of greenhouse grown lettuce plants (*Lactuca sativa*) maintained at different water deficit levels will differ. This will provide a justification for the application of this measurement as a plant water status monitoring tool. A system identification approach is thereafter applied in developing a model of the transpiration dynamics and predicting the transpiration rate of these plants. Finally, the predicted transpiration rate is used as a tool for monitoring the water status of the lettuce plants and real-time detection of deviations from a defined water status state.

2 Background

2.1 Plant transpiration

Plant transpiration can be described by the Penman-Monteith equation (Monteith, 1973). This equation and other transpiration models derived from it specify that the transpiration ($T_p(gm^{-2}min^{-1})$) is dependent on the incoming solar radiation ($R_{sw}(Wm^{-2})$) and the vapour pressure deficit of the ambient air ($\Delta(kPa)$). This is expressed as

$$T_p = R_{sw}C_A + \Delta C_B \quad (1)$$

Where the coefficients C_A and C_B are crop dependent parameters.

Baille et al. (1994) noted that the coefficient C_B is a function of the plant leaf area index (LAI), and it adopts different values during the day due to oscillations in stomatal resistance.

2.2 System identification

System identification is applied in constructing mathematical models of dynamic systems based on the incoming time-series of input ($u(t)$) and output ($y(t)$) data. The goal is to infer the relationship between the sampled input/output data. During system identification, the model structure is first identified using objective methods of time series analysis based on a given general class of time-series models (here, linear discrete time transfer functions). The resulting model must be able to explain the structure of the observed data. System identification is used to simultaneously linearize and reduce model complexity, so exposing its 'dominant modes' of dynamic behaviour.

In this study, the identification process was conducted based on prior knowledge of the plant transpiration process as shown in equation 1. The vapour pressure deficit and incoming radiation were selected as climatic input, and the LAI was selected as crop

growth input. The identification of the model structure is considered the first step of the identification problem in the present study. An online estimation algorithm is thereafter implemented to update the model parameters based on the real-time data obtained from the process.

In this way, it is possible to detect the changes in the dynamics of the system thus accounting for the time-varying nature of the plant system.

The linear discrete-time transfer function is written as

$$y(t) = \frac{B_1(L)}{A(L)}U_1(t-\delta_1) + \cdots + \frac{B_k(L)}{A(L)}U_k(t-\delta_k) + e(t); e \sim WN(0, \sigma_e^2) \quad (2)$$

Where $y(t)$ is the output (transpiration rate), $U_i(t)$ $(i = 1,2, \ldots\ldots, K)$ are a set of K inputs that affect the output (incoming radiation, vapour pressure deficit), $\delta_i (i = 1,2, \ldots\ldots, K)$ are the delays associated with each input.

In equation 2,

$$A(L) = 1 + \ a_1 L + \cdots + a_n L^n \quad (3)$$

$$B(L) = \ b_0 + b_1 L + \cdots + b_m L^m$$

$A(L)$ and $B(L)$ are polynomials of the order n and m respectively. The backshift operator L is such that $L^j y_t = y_{t-j}$. $a_i (i = 1,2, \ldots\ldots, n)$ and $b_j (j = 1,2, \ldots\ldots, m)$ are coefficients of the polynomials $A(L)$ and $B(L)$. They represent the unknown parameters that are to be identified. The identified model is defined by the triad $[n, m_i, \delta_i]$, where n is the number of denominator parameters; indicating the model order, and m_i is the number of numerator parameters associated with each input. δ_i is defined earlier.

The identification process was conducted using the refined instrumental variable algorithm (Taylor et al., 2007) implemented in the Captain toolbox (Young et al., 2007) on the MATLAB® software.

2.3 Plant water status monitoring framework

The plant water status monitoring algorithm proposed in this paper is data-driven. The algorithm is founded on an estimated dynamic model of the plant transpiration. The model is identified as a time domain model and the parameters of the model are identified online from the real-time measurements of input-output data. The water status monitoring principle is based on a premise that the transpiration dynamics of a plant will vary as a function of the prevailing climatic conditions and its water status. A model of the plant is built at a known water status state and predictions from this model is then compared to real-time output data obtained from the plant. A schematic illustration of the algorithm is presented in Figure 1.

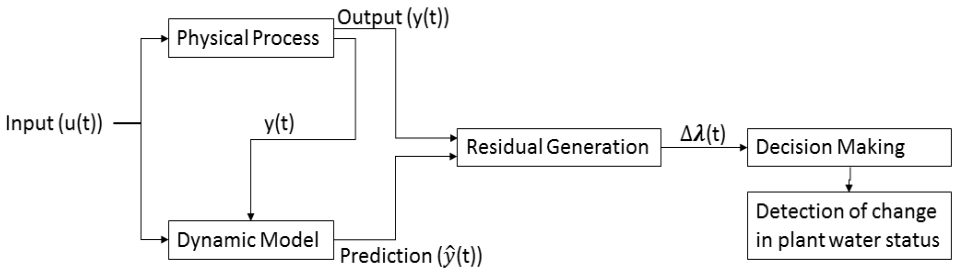

Figure 1. Schematic illustration of the proposed water status monitoring framework

The decision-making module assumes that the residuals (measured transpiration – model predicted transpiration) generated from a healthy mode of the process i.e. non-significant deviation in water status state will conform to an established statistical distribution. A change in this distribution will indicate a significant deviation in the water status state of the plant.

When there is a significant change in plant water status, the model obtained during a particular water status state is unable to predict the observed plant response. This causes the difference between the measured and predicted transpiration rate i.e. the magnitude of the residuals to increase. The decision-making algorithm is further explained in section 2.3.1

2.3.1 Decision-making algorithm

During system identification, the residuals obtained between the measured and modelled output is assumed to be a normally distributed Gaussian sequence (Taylor et al., 2007). For a properly defined model identified during a known process state, the residuals obtained between the measured and predicted output will also conform to this distribution. However, when there is a significant change in the process state, the distribution of the residuals obtained as a function of the predicted output will deviate from the distribution obtained during the modelling phase.

A Gaussian Mixture Model (GMM) can be applied in modelling the distribution of the residuals obtained during the identification process. The GMM assumes we have k normal distributions to describe the data $\{N(\mu_1, \sigma_1) \dots \dots N(\mu_k, \sigma_k)\}$ and estimates the parameters for those individual distributions that when combined best describes the data (Reynolds, 2015). The probability of observing a value X_n^j for a specific data point is expressed as (Reynolds, 2015)

$$p(X_n^j) = \sum_{k=1}^{k} \pi_k \aleph(X_n^j | \mu_k, \sigma_k) \tag{4}$$

With

$\sum_{k=1}^{k} \pi_k = 1$

$\forall_k : 0 \leq \pi_k \leq 1$

Where μ_k and σ_k are the mean and standard deviations of each k distribution and π_k expresses the weight of each distribution.

An expectation maximization algorithm is applied in deriving the parameters that maximize the likelihood of the GMM given the training data, here, the residuals obtained during identification. These parameters are then applied in computing the probability of each observation. The best number of distributions to fit the data is also determined by minimizing the Akaike information criterion (AIC) (Xiao et al., 2016).

Once the GMM is fitted on the training data, a normal or anomalous process state can be identified by computing the probability of observing the residuals computed for that state using the GMM fitted on the residuals obtained during identification. The probabilities of observing the residuals during the anomalous state will be much lower compared to the probability of observing the residuals obtained during the normal process state and also during identification. This methodology has been shown to achieve state of the art performance when detecting faults in rotary machinery and high-voltage electronic equipment (Yan et al., 2017).

3 Materials and Methods

3.1 Greenhouse and experimental setup

Two six week studies were conducted in a climate controlled greenhouse. The heating and ventilation set points were approximately 17 and 23°C respectively. Lettuce plants were planted in individual 2.5 L containers containing a sandy loam soil (FC= 0.186 $m^3 m^{-3}$, PWP= 0.071 $m^3 m^{-3}$). To prevent evaporation, the soil surface of the pots were covered with a 5 cm layer of plastic beads.

During the initial study, the plants were irrigated every two hours. However, four hours prior to the initiation of measurements, four lettuce plants were selected and irrigated to replace 100% of the water lost by transpiration, four plants were irrigated to replace 90% of the water lost by transpiration, and four other plants were irrigated to replace 75% of water lost by transpiration. These irrigation treatments are hereafter referred to as 100ET, 90ET and 75ET respectively. Irrigation volumes corresponding to the treatments was applied every two hours. This approach was used in other to ensure the uniform development of the plant population's leaf area index.

During a follow-up study, after four hours into a diurnal measurement period, irrigation was withheld from four lettuce plants which have been receiving the 100ET irrigation treatment. Four other lettuce plants also received the 100ET irrigation treatment all through the diurnal measurement period. Irrigation was applied every two hours to these set of plants.

3.2 Microclimate measurements

Environmental variables measured at plant canopy level included ambient air temperature and relative humidity using a temperature and humidity probe (Model EE08, E+E Elektronik, Engerwitzdorf, Austria), and incoming radiation using a pyranometer sensor (Model SP-110, Apogee Instruments, Logan, Utah, USA). Wind speed was measured using a hot wire anemometer (Model AM – 4202, Lutron Electronics, London, UK) installed 10cm above the crop canopy. The VPD was calculated using temperature and relative humidity data following the equations outlined in Allen et al. (1998). Sensor readings were obtained at a 5 s interval and averaged online over 1 min periods with a CR1000 data acquisition system (Campbell Scientific, Logan, Utah, USA). All sensors were factory calibrated by their respective manufacturers.

3.3 Transpiration measurements

Crop transpiration of the lettuce plants was measured using three load balance systems (Model ALC, Acculab, Englewood, USA) with a $16\ kg$ capacity and $\pm 0.1\ g$ resolution. Each load balance recorded the mass of the four plants in each treatment group.

The total transpiration for a time period was calculated as the mass difference, ΔM between two consecutive time instants as recorded by the mass balance system. This

was then converted to the units of volume by multiplying ΔM by the density of water ($1000\ kgm^{-3}$). In the various irrigation treatments, a computer controlled irrigation system applied irrigation to replace the predefined percentage of water loss based on the calculated water loss volume. The total irrigation volume calculated for a treatment group was divided equally among the plants assigned to that group.

The transpiration rate was calculated as

$$T_p = \frac{M(t_{i+1}) - M(t_i)}{A.(t_{i+1} - t_i)} \frac{j}{n} \quad (5)$$

Where $M(t_i)$ is the mass (g) given by the balance at time t_i (min), A (m^2) is the area of the shelve on which the plants are placed, n is the number of pots on the balance tray and j is the number of plants on the shelve. During irrigation, the transpiration rate was assumed to be constant. Data from the balance system was directly stored every minute.

3.4 Leaf area index measurements

The leaf area index (LAI) values for the plants placed on the balance were assessed using digital images captured with a mobile phone camera. The LAI values were then extracted from the digital images using the Easy leaf area software (Department of Plant Sciences, University of California).

3.5 Ancillary measurements

The soil moisture status of the plants placed on the balance was measured at hourly intervals using a model GS1 soil moisture sensor (Decagon Devices, Pullman, Washington, USA). The stomatal conductance of the plants was also measured using a diffusion leaf porometer (Model AP4, Delta-T Devices, Cambridge, UK) between 13:00 and 15:00 hrs local standard time.

4 Results and discussion

The night-time transpiration of the plants was negligible all through the study period, with a maximum cumulative transpiration of 3 g being recorded. As such, the daytime transpiration recorded between 8:00 am and 4:00 pm was further explored.

4.1 Dynamics of crop transpiration

The measured typical daily dynamics of the crop transpiration along with prevailing environmental conditions for a sunny and cloudy day are presented in Figure 2 and Figure 3 respectively. It is seen that the 100ET and 90ET plants maintain a higher transpiration rate when compared to the 75ET plants. The transpiration dynamics also seem to follow the dynamics of the incoming radiation. However, there isn't a significant difference in the transpiration rates of the 100ET and 90ET plants $(p > 0.1)$. Stomatal conductance measurements conducted on the plants also didn't indicate a significant difference in their water status $(p > 0.1)$. The reverse was the case for comparisons of stomatal conductance measurements of both the 100ET and 90ET plants with the 75ET plants. In Figure 2 and Figure 3, the datapoints indicating a higher transpiration rate for the 75ET plants are attributed to measurement errors. This anomaly is addressed in section 4.2.

Overall, the difference in transpiration rate between both the 100ET and 90ET plants, and the 75ET plants indicated a significant difference in their plant water status. This is in agreement with the results presented by Agam et al. (2013). They reported a significant difference in the transpiration rates of well-watered and water-stressed olive trees. During the course of the study, a maximum transpiration rate of 1.8 $gm^{-2}min^{-1}$ was recorded for the 75ET plants while a value of 3.2 $gm^{-2}min^{-1}$ was recorded for the 90ET and 100ET plants.

Due to the non-significant difference in the transpiration and water status of the 100ET and 90ET plants, the 100ET and 75ET plants were considered in the subsequent analysis.

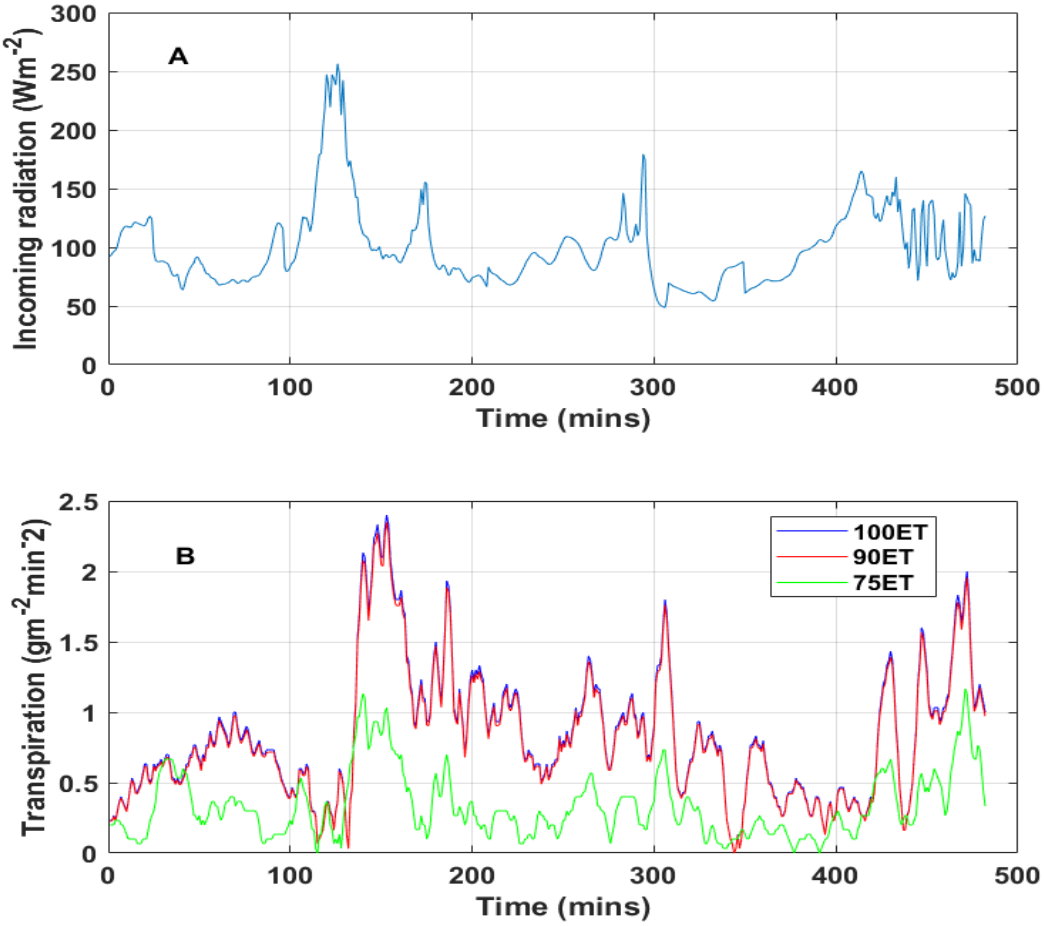

Figure 2. Measured incoming radiation and transpiration dynamics of the lettuce plants during a sunny day (A) incoming radiation (B) transpiration

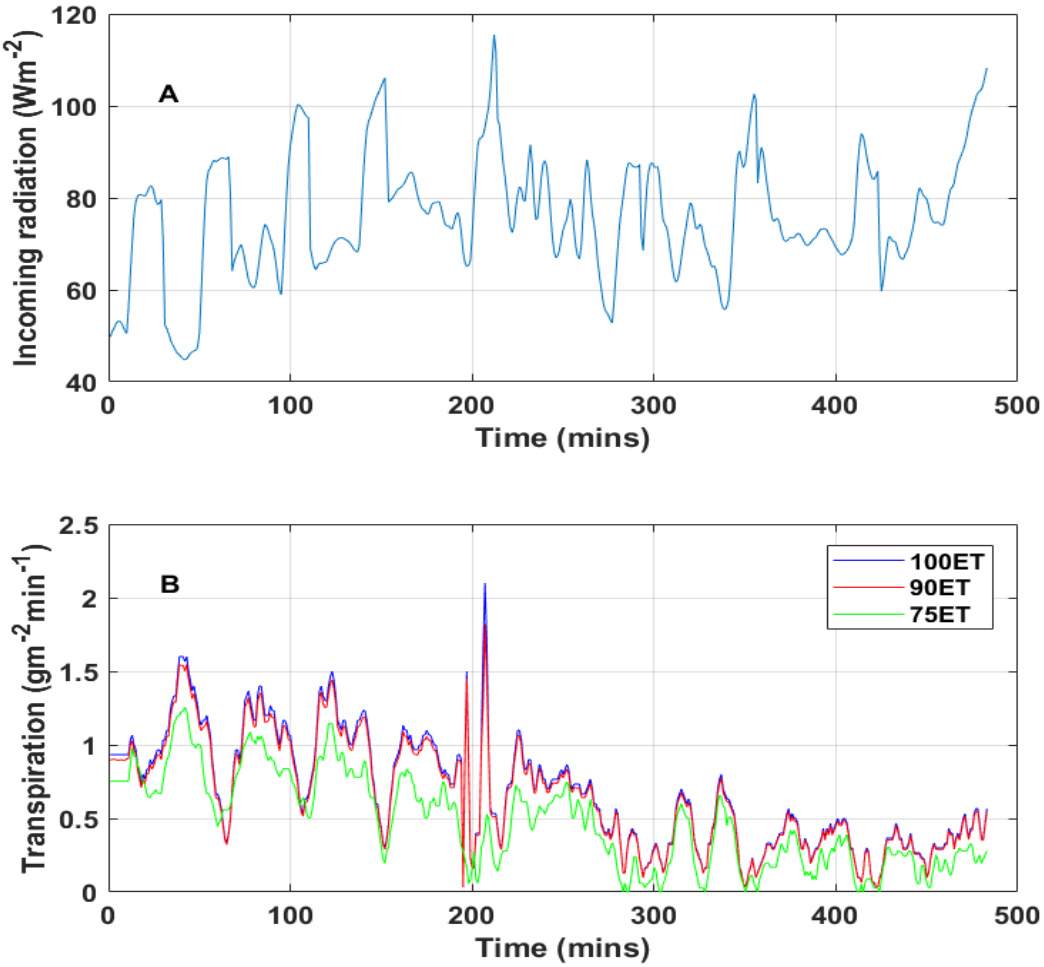

Figure 3. Measured incoming radiation and transpiration dynamics of the lettuce plants during a cloudy day (A) incoming radiation (B) transpiration

4.2 Decoupling and filtering of the transpiration signals

The measured transpiration signals contained different components, some of which were of low amplitude and others characterized by higher amplitudes. The higher amplitude components were determined to be a result of measurement noise and short-term variability in the environment. Such components were decoupled and analysed by calculating the power spectrum of the measured signals using the Fast Fourier transformation algorithm (FFT) (Welch, 1967). Figure 4 shows an example of the power spectrum results obtained from the measured transpiration signals. The results showed that the signals are a combination of different components that have statistical characteristics but which cannot be observed directly (Taylor et al., 2007).

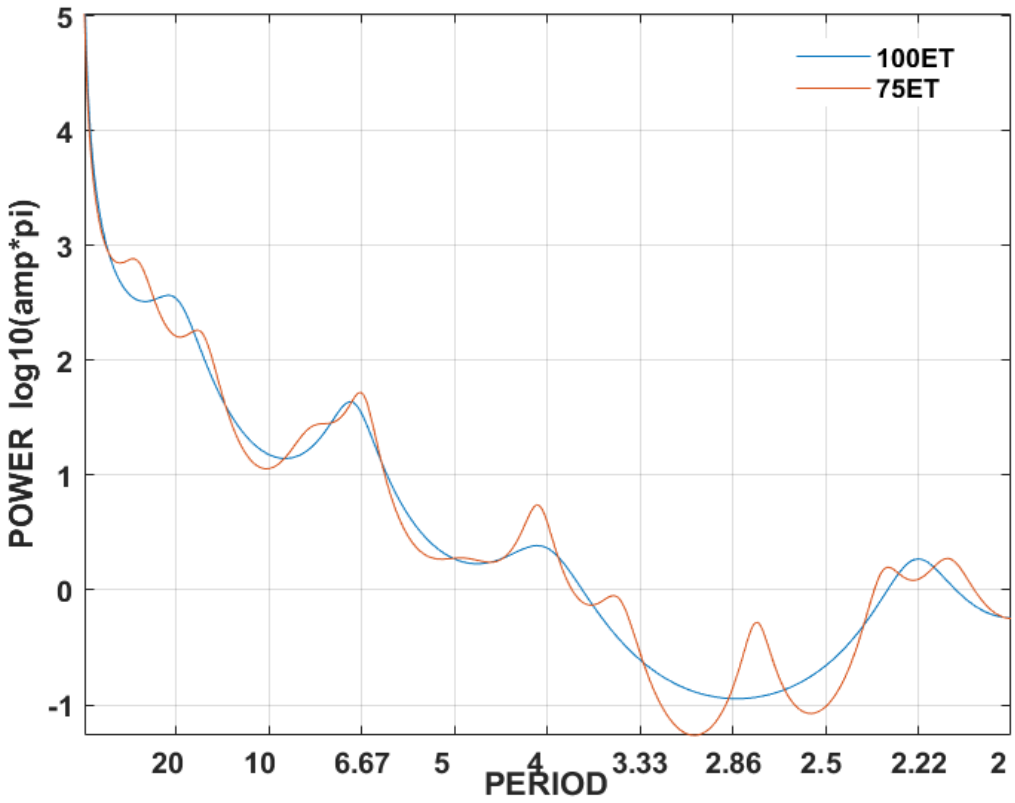

Figure 4. Power spectrum of the measured transpiration signals

The overall transpiration signal $T_p(t)$ as a function of the different components can be represented by the following discrete time equation

$$T_p(t) = T_k + C_k + f_{(uk)} + e_k \quad (6)$$

Where T_k is the trend or low frequency component, C_k is the cyclical or higher frequency component, $f_{(uk)}$ captures the influence of the input variables and e_k is the noise component.

To reduce model complexity, only the T_k and $f_{(uk)}$ components of the transpiration signal were considered. The components are decoupled from the measured transpiration signals and represented as

$$y(k) = T_k + f_{(uk)} \quad (7)$$

Where $y(k)$ is the decoupled transpiration signal. As an example, the decoupled transpiration signals of the 100ET and 75ET plants shown in Figure 3 are presented in

Figure 5. It can be seen that their transpiration dynamics is clearly separated and the measurement noise is sufficiently filtered.

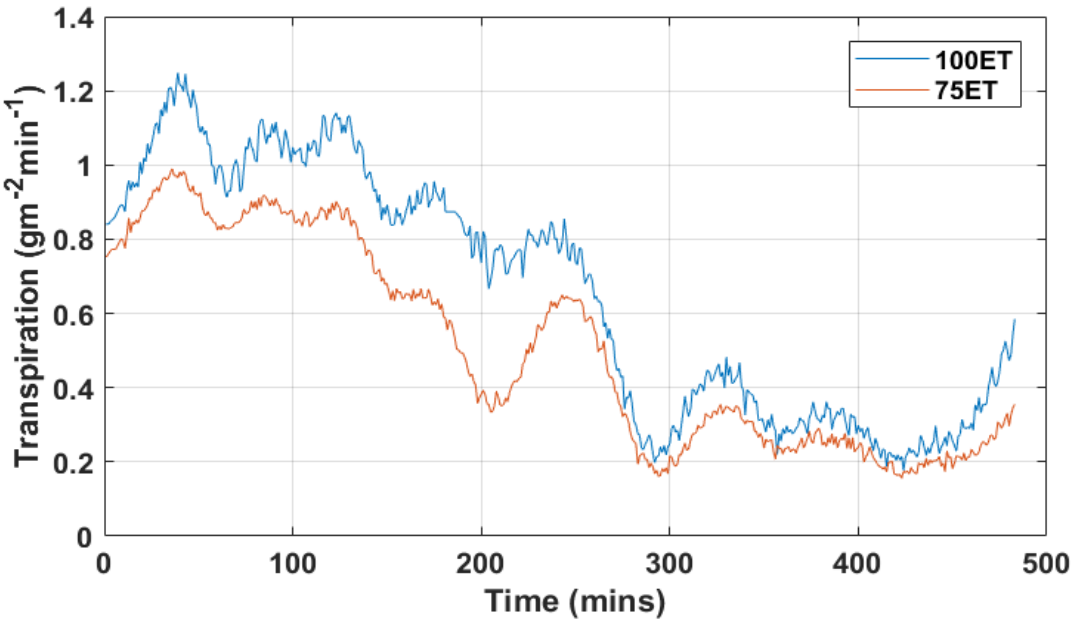

Figure 5. The transpiration signals decoupled from the noisy transpiration measurements presented in Figure 3

4.3 System Identification and dynamic modelling of the plant transpiration

The dynamic model of the plant transpiration was identified online by applying system identification on the incoming time-series data of the measured transpiration rate and environmental variables.

A second-order discrete-time transfer function model was sufficient to describe the transpiration dynamics with an average coefficient of determination $R_T^2 = 0.93 \pm 0.04$ and average Young identification criterion $YIC = -8.00 \pm 3.00$ (Young and Jakeman, 1980).

An example of the measured and modelled transpiration rate for the 100ET and 75ET plants is presented in Figure 6. It is seen that the modelled values closely match that measured values while capturing the dominant dynamics.

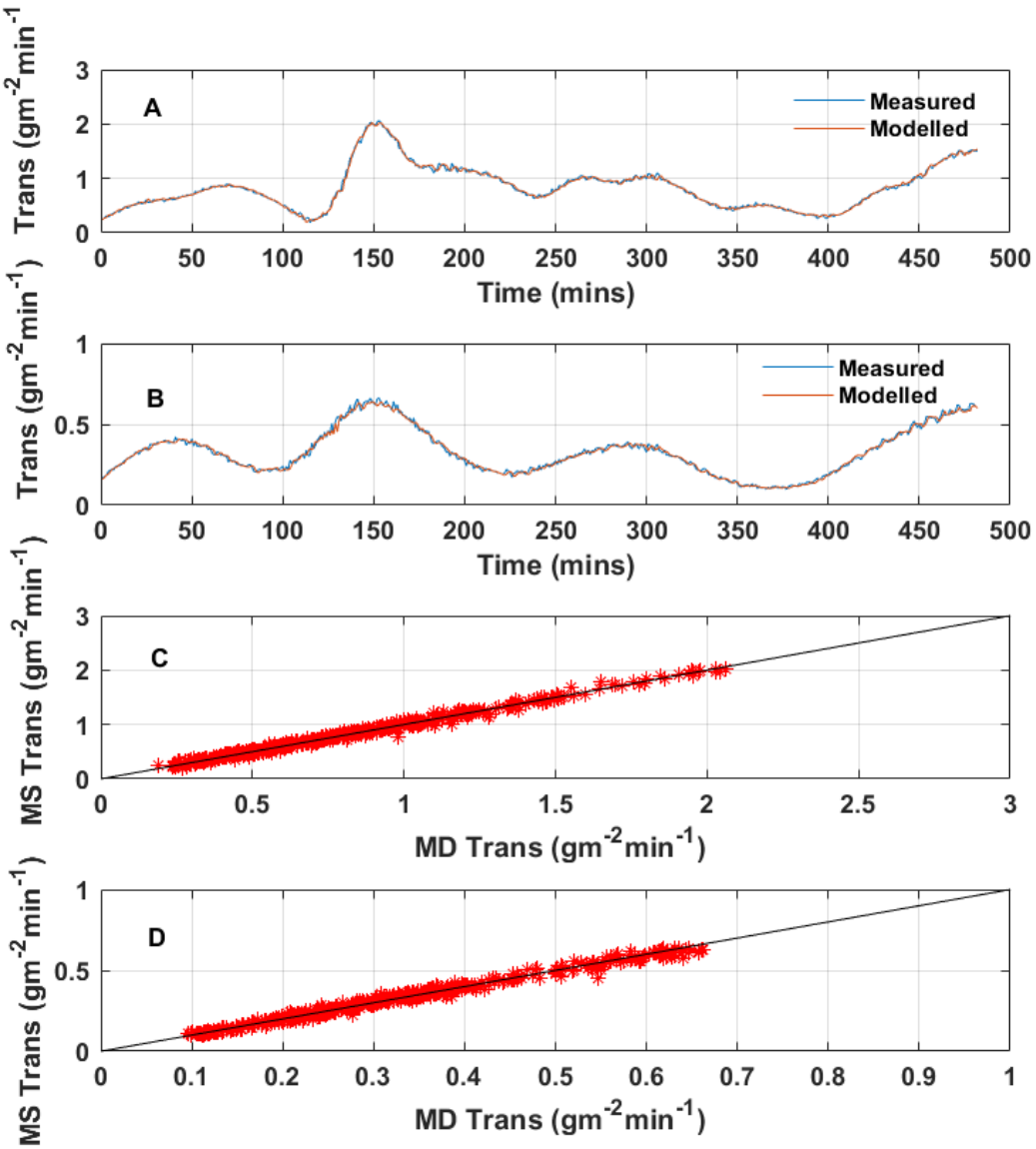

Figure 6. Measured (MS) and modelled (MD) transpiration (Trans) dynamics of the lettuce plants (A) Dynamic plot 100ET (B) Dynamic plot 75ET (C) Scatter plot 100ET (D) Scatter plot 75ET

The time delay associated with the input parameters was however found to vary as a function of plant growth. As such, the LAI was used to divide the model into different intervals as summarized in Table 1. For the division, it is easy to change the LAI into other time units such as days after planting.

Table 1. Results of the model identification as a function of the Leaf area index (LAI) interval. n is the equation's order, m_{SR} is the number of parameters associated with the radiation input, m_{VPD} is the number of parameters associated with the VPD input. δ_{SR} and δ_{VPD} are the time delay associated with the radiation and VPD inputs respectively.

LAI interval	n	m_{SR}	m_{VPD}	δ_{SR}	δ_{VPD}
0.8 or lower	2	2	2	0	0
0.8 to 1.6	2	2	2	2	0
1.6 or higher	2	2	2	4	0

Sánchez et al. (2012) reported that a dynamic model of the transpiration is able to overcome the limitations encountered by steady-state models of crop transpiration. These include the overestimation of transpiration rates at low values of LAI and underestimation at higher values. The steady-state models are also unable to sufficiently capture the dominant dynamics which results in an advancement of the real dynamics over the modelled values.

4.4 Online update of model parameters and prediction of the plant transpiration rate

The biosystem, such as the lettuce plant, is a complex assemblage of interacting physical, chemical and biological processes. As such, its transpiration dynamics will vary from day to day due to changes in the stomatal response, biological adaptation, and the prevailing environment. Accordingly, during the follow-up study, the parameters of the identified models were updated at the start of each diurnal measurement period.

It was found that the incoming time-series measurements of input/output data obtained during the first 120 mins of active transpiration were sufficient to model the transpiration dynamics of the plants in a defined water status state. The parameterized model was then applied in predicting the transpiration dynamics for the subsequent time period and updated after 240 mins. Explained further, at the start of active transpiration at time $t - 120$, the data points recorded during the time period $t - 120$ to t were used for parameter identification and prediction was made during time t to $t + 240$. At time $t + 240$, the model parameters were then updated recursively using data points recorded during t to $t + 240$ which were flagged as conforming to the defined water status state. Predictions are then made for the subsequent time period.

The average prediction performance of the model is summarized in Table 2. Table 2 shows that the models are able to achieve a satisfactory level of performance at all crop growth stages

Table 2. Average prediction performance of the identified models. Standard deviations are included in the brackets

LAI interval	Mean absolute error($gm^{-2}min^{-1}$)	Root mean square error ($gm^{-2}min^{-1}$)
0.8 or lower	0.05 (± 0.0035)	0.06 (± 0.0044)
0.8 to 1.6	0.13 (± 0.0106)	0.15 (± 0.0128)
1.6 or higher	0.09 (± 0.0046)	0.11 (± 0.0059)

Pollet et al. (2000) reported results for a PM type model for estimating the transpiration of greenhouse grown lettuce plants. They reported a 6% overestimation of transpiration by the model. It should also be noted that the parameters of PM type models are fitted for a particular water status state. The dynamic modelling approach presented in the paper can easily be applied to a plant at any water status state. This is because the parametrization of the model can be achieved using routinely measured environmental variables and transpiration measurements. The need to explicitly model the stomatal response is eliminated as this is implicitly accounted for in the online estimated model parameters and time delay. This is in agreement with the conclusions of Sánchez et al. (2012).

4.5 Monitoring of plant water status

The transpiration rate of lettuce plants is dependent on their water status as demonstrated in section 4.1. This suggests that the difference in the transpiration dynamics as a function of water status can be exploited as a means of monitoring the water status of the plants.

As an example, in Figure 7, the model predicted transpiration dynamics of lettuce plants for which irrigation was not withheld along with the measured values during a measurement period is shown. It should be noted that data points applied in parameter identification are not included in the prediction phase. The measured and modelled values closely match each other during this period as irrigation was not withheld from the plants; this period of normal irrigation is defined as state 1. Succinctly, parameter identification was conducted in state 1 and prediction was made at a later period when the plants

remained in state 1. The average stomatal conductance recorded for the plants during this period was 139.22(±1.14) $mmolm^{-2}s^{1}$ and the average soil moisture content was 0.18(±0.002) m^3m^{-3}, a value close to the field capacity of the growing media.

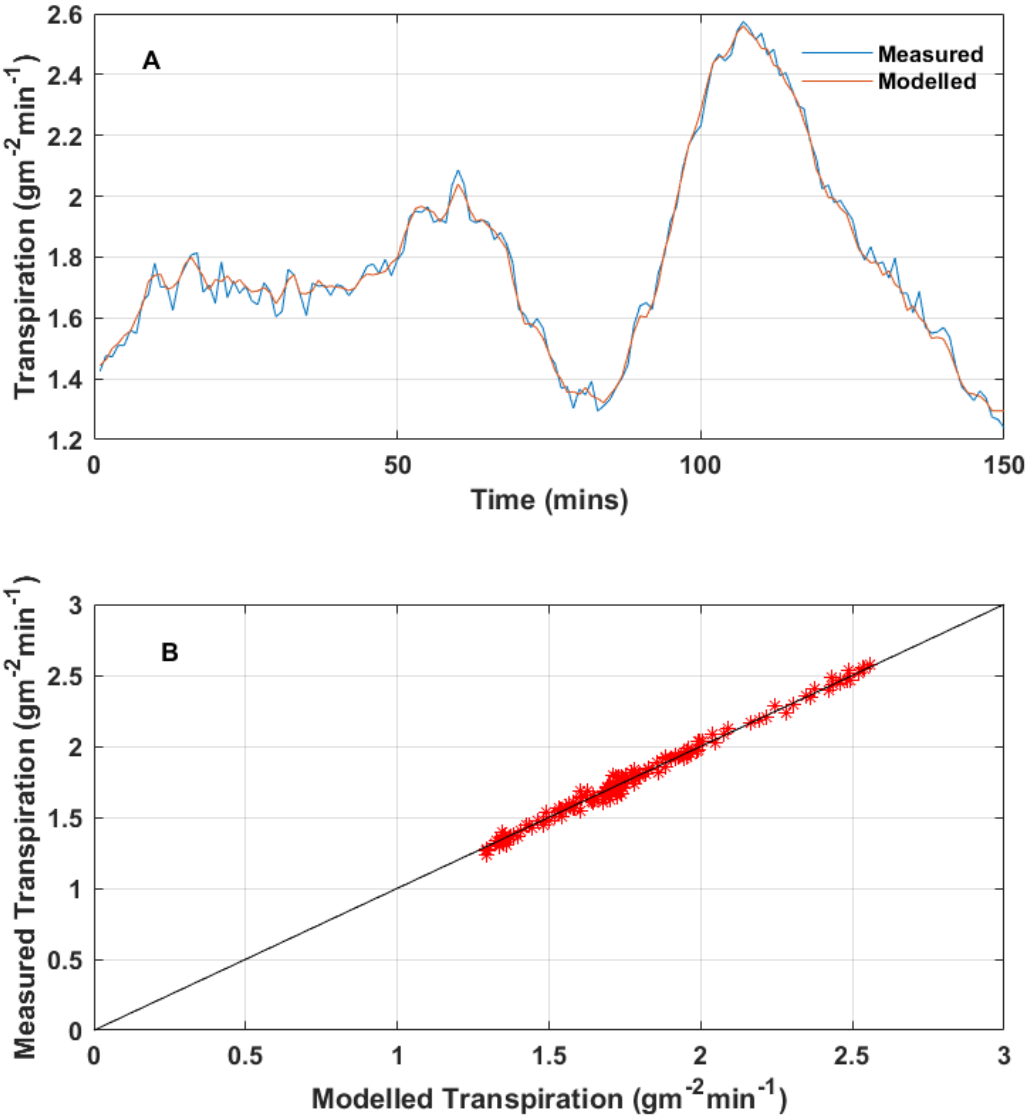

Figure 7. Measured and model predicted transpiration dynamics of the lettuce plants during a period of normal irrigation (A) Dynamic plot (B) Scatter plot

Figure 8 shows the measured and model predicted transpiration dynamics of the set of plants for which irrigation was withheld after a period of normal irrigation, defined as state 2. It is seen that there is a wide deviation between the measured and model predicted values. This is because the model was parameterized for a water status state of the plant during which irrigation was constantly applied to replace transpiration water loss (state 1).

The average stomatal conductance recorded during this period was 116.94(±0.92) $mmolm^{-2}s^{1}$ while the average soil moisture content was 0.16(±0.001) m^3m^{-3}. The stomatal conductance values show a clear significant difference ($p < 0.05$) in water status of the plants in state 1 and state 2. It is interesting to note that this difference in plant water status is also indicated in the measured transpiration rate even though the soil moisture status was above the maximum allowable depletion level of 35% (lower soil moisture target = 0.15 m^3m^{-3}) defined for the lettuce crop.

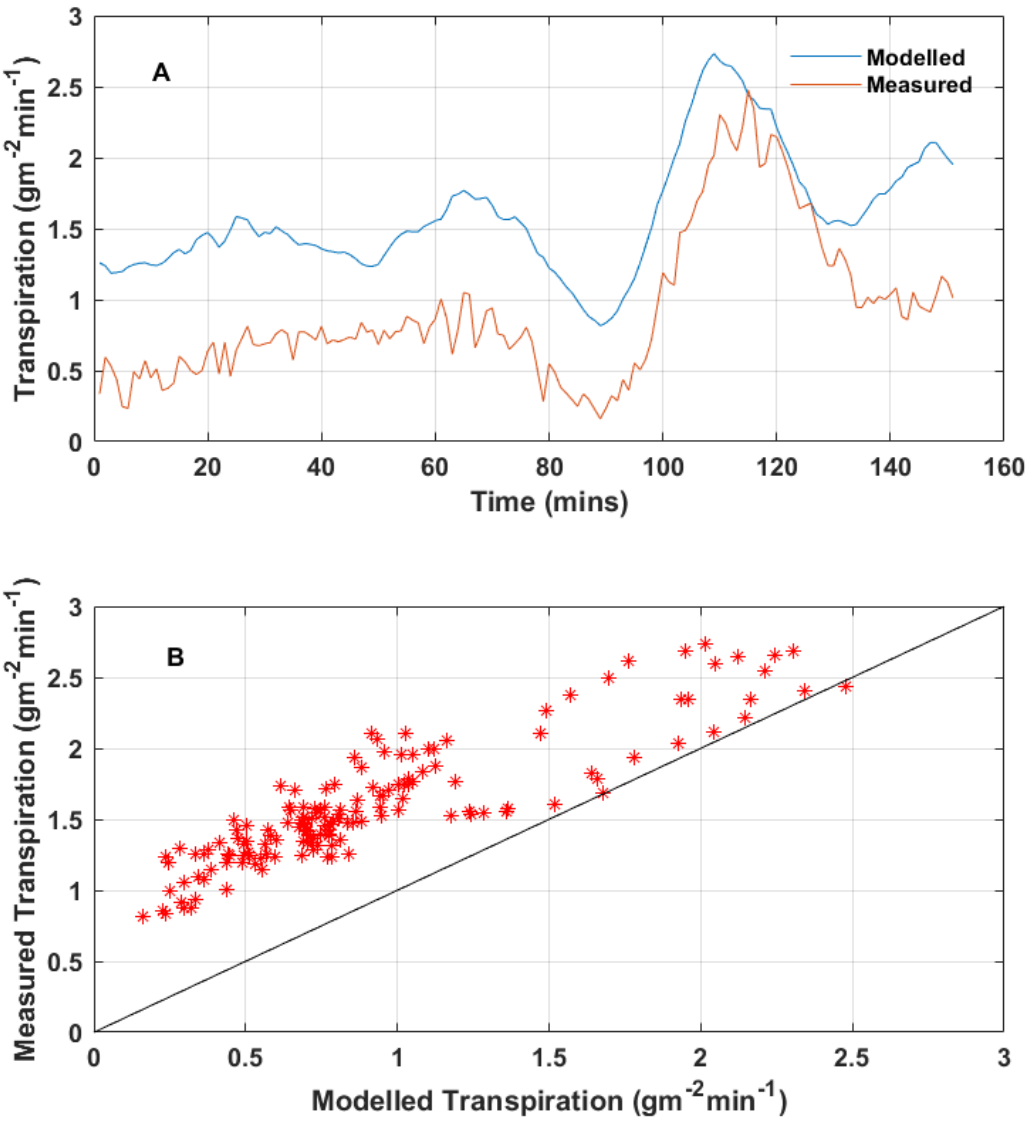

Figure 8. Measured and model predicted transpiration dynamics during a period after which irrigation had been withheld from the lettuce plants (A) Dynamic plot (B) Scatter plot

These results give evidence that the transpiration dynamics can indeed be applied as a tool for monitoring the water status of the lettuce crop. This was consistently shown in the data obtained all through the follow-up study.

Figure 9 shows the distribution of the residuals during the identification phase in state 1 (normal irrigation). The residuals conform to a Gaussian distribution suggesting a well-defined model for the state.

Figure 10 shows the range of the predicted probabilities of observing the data points of the residuals in the identification phase in state 1, during prediction in state 1 and during prediction in state 2.

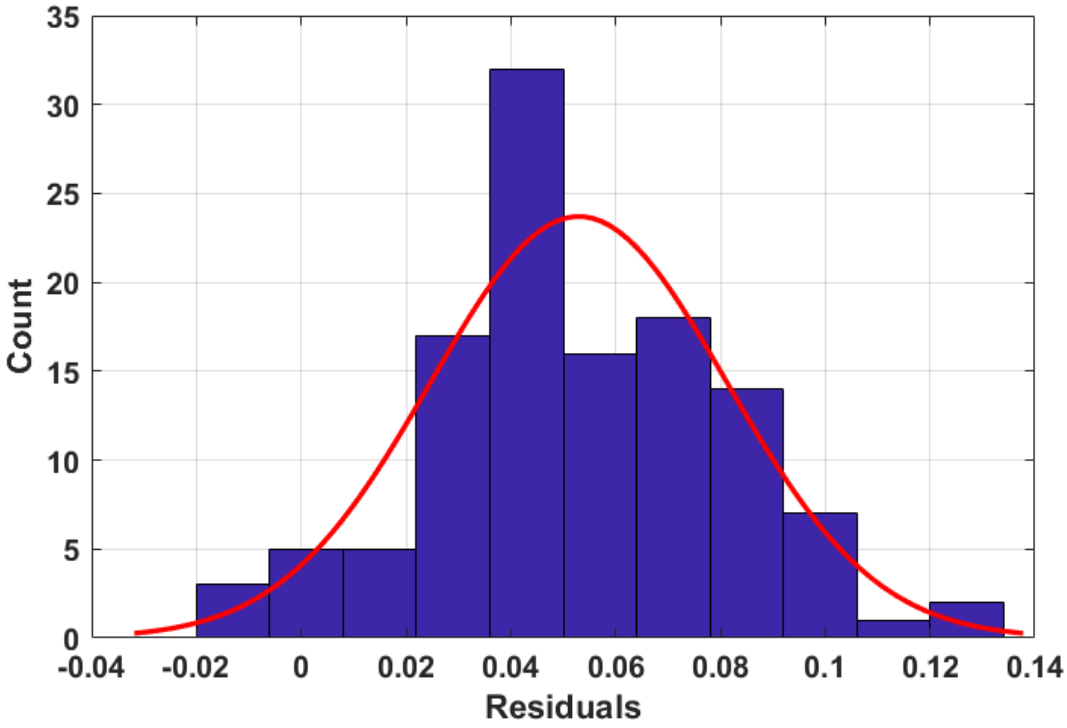

Figure 9. The distribution of the residuals obtained during the system identification phase

These predictions were made using the Gaussian mixture model fitted on the residuals obtained during system identification. Figure 10 shows that there is a high probability of observing the data points during the identification phase and also during prediction in the state for which the model was identified. The lowest probability of observing the data point of the residuals during the prediction in state 1 was 0.8. The reverse was the case during predictions in state 2. Low probabilities were predicted for observing the data points of the residuals in this state, with the highest probability predicted being 0.53. In Figure 10, the notches of the identification and state 1 boxes overlap which indicates that the median of their predicted probabilities is not significantly different at 5% significance level. It can also

be seen that notches of the state 2 box do not overlap with the two other boxes indicating a significant difference in its median value when compared with the other predicted probabilities. The information contained in the predicted probabilities of observing the data points of the residuals provides an adequate indication of the water status state of the plants i.e. high probabilities will be predicted when the plant is in the state for which the model was identified and low probabilities will be predicted when there is a significant change in the water status state.

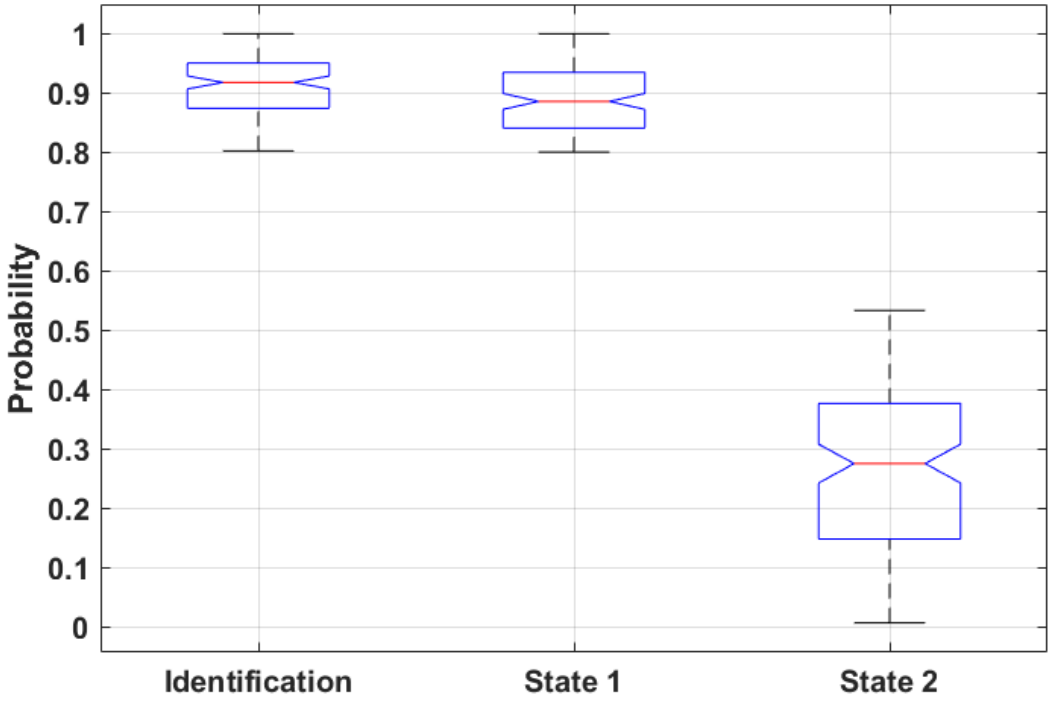

Figure 10. Boxplot of the probabilities predicted by the Gaussian Mixture Model fitted on the residuals obtained during the system identification phase for the identification residuals, state 1 residuals and state 2 residuals

Previous studies e.g. Earl (2003), Prehn et al. (2010), Beeson (2011) have also attempted to use the measured transpiration rate as a tool for monitoring the onset of drought/water stress. They attempt to achieve this by comparing the measured transpiration rate at a particular instance to the initial transpiration rate of the same plant when in a well-watered state. They, however, neglect the influence of the prevailing environment on the transpiration dynamics. The model presented in this paper addresses this drawback by predicting the 'healthy state' transpiration rate as a function of the known water status and real-time measurements of the environmental variables.

The water status monitoring tool proposed in this paper can be applied in regulating the water deficit of greenhouse crops. This can be achieved by applying system identification to identify a model for the plant transpiration at a known water status state and then

comparing the real-time measurements to the model prediction. This approach is used extensively for performing fault detection in the process industry (Das et al., 2012; Sharma et al., 2010).

The intensity of water deficit can be easily quantified by computing the transpiration ratio proposed by Fernández et al. (2008). This is defined as the ratio between the actual transpiration measured on a plant and the transpiration rate expected for a well-watered plant. A value of 1 will indicate the absence of a deficit and a value of zero will indicate a severe deficit. This can be adapted to compute a deficit intensity for any desired reference water status state.

It should be noted that the system identification modelling technique constitutes a data-driven approach in which the dynamic response of the plant transpiration is parametrized for the specific ranges of environmental and crop conditions encountered during model development, and therefore the models are only applicable to the specific crop and environment for which they are developed.

5 Conclusions

A model for predicting the transpiration dynamics of greenhouse cultivated lettuce plants is presented in this paper. The data-driven model has the incoming radiation, vapour pressure deficit as input variables, and its structure varies as a function of plant growth in form of the LAI evolution.

Experimental results indicated that the transpiration dynamics of lettuce plants varied as a function of their water status. This phenomenon was therefore exploited as a tool for monitoring the water status of the plants. A model of the plant transpiration is identified online at a period during which the plant is in a desirable and known water status state. This model is then applied in predicting the crop transpiration. When there is a significant change in the water status state, the identified model is unable to explain the measured transpiration, resulting in a change in the statistical properties of the calculated residuals.

This approach has an advantage over similar approaches which use the plant transpiration as an indicator of its water status because it takes the time-varying nature of the plant system into account through the online adaptation of the model parameters. The difficult to model variation in stomatal response is also implicitly accounted during the online parameter estimation. This makes it a suitable plant water status monitoring tool in commercial greenhouses where the application of mechanistic models has received limited attention, due to their complexity and large input requirements. The implementation of this model in a commercial greenhouse and model development for other high-value crops will be the focus of future research.

References

Adeyemi, O., Grove, I., Peets, S., Norton, T., 2017. Advanced Monitoring and Management Systems for Improving Sustainability in Precision Irrigation. Sustainability 9, 1–29. https://doi.org/10.3390/su9030353

Agam, N., Cohen, Y., Berni, J.A.J., Alchanatis, V., Kool, D., Dag, A., Yermiyahu, U., Ben-Gal, A., 2013. An insight to the performance of crop water stress index for olive trees. Agric. Water Manag. 118, 79–86. https://doi.org/10.1016/j.agwat.2012.12.004

Allen, R., Pereira, L.S., Raes, D., Smith, M., 1998. FAO Irrigation and Drainage Paper No.56, FAO. https://doi.org/10.1016/j.eja.2010.12.001

Baille, M., Baille, A., Laury, J.C., 1994. A simplified model for predicting evapotranspiration rate of nine ornamental species vs. climate factors and leaf area. Sci. Hortic. (Amsterdam). 59, 217–232. https://doi.org/10.1016/0304-4238(94)90015-9

Baptista, F.J., Meneses, J.F., Bailey, B.J., 2005. Measuring and modelling transpiration versus evapotranspiration of a tomato crop grown on soil in a mediterranean greenhouse. Acta Hortic. 691, 313–320.

Barnard, D.M., Bauerle, W.L., 2015. Species-specific irrigation scheduling with a spatially explicit biophysical model: A comparison to substrate moisture sensing with insight into simplified physiological parameterization. Agric. For. Meteorol. 214–215, 48–59. https://doi.org/10.1016/j.agrformet.2015.08.244

Beeson, R.C., 2011. Weighing lysimeter systems for quantifying water use and studies of controlled water stress for crops grown in low bulk density substrates. Agric. Water Manag. 98, 967–976. https://doi.org/10.1016/j.agwat.2011.01.005

Ben-Gal, A., Agam, N., Alchanatis, V., Cohen, Y., Yermiyahu, U., Zipori, I., Presnov, E., Sprintsin, M., Dag, A., 2009. Evaluating water stress in irrigated olives: Correlation of soil water status, tree water status, and thermal imagery. Irrig. Sci. 27, 367–376. https://doi.org/10.1007/s00271-009-0150-7

Ben-Gal, A., Kool, D., Agam, N., van Halsema, G.E., Yermiyahu, U., Yafe, A., Presnov, E., Erel, R., Majdop, A., Zipori, I., Segal, E., Rüger, S., Zimmermann, U., Cohen, Y., Alchanatis, V., Dag, A., 2010. Whole-tree water balance and indicators for short-term drought stress in non-bearing “Barnea” olives. Agric. Water Manag. 98, 124–133. https://doi.org/10.1016/j.agwat.2010.08.008

Bennis, N., Duplaix, J., Enéa, G., Haloua, M., Youlal, H., 2008. Greenhouse climate modelling and robust control. Comput. Electron. Agric. 61, 96–107. https://doi.org/10.1016/j.compag.2007.09.014

Blonquist, J.M., Norman, J.M., Bugbee, B., 2009. Automated measurement of canopy stomatal conductance based on infrared temperature. Agric. For. Meteorol. 149, 2183–2197. https://doi.org/10.1016/j.agrformet.2009.10.003

Boonen, C., Joniaux, O., Janssens, K., Berckmans, D., Lemeur, R., Kharoubi, A., Pien, H., 2000. Modeling dynamic behavior of leaf temperature at three-dimensional positions to step variations in air temperature and light. Trans. ASAE-American Soc. Agric. Eng. 43, 1755–1766. https://doi.org/10.13031/2013.3078

Chen, B.S.E., Chang, Y.T., 2008. A review of system identification in control engineering, signal processing, communication and systems biology. J Biomechatronics Eng 1, 87–109.

Daniel, C., Schmidt, S., Adriano, F., Pereira, D.C., Oliveira, A.S. De, Fonseca, J., Júnior, G., Vellame, L.M., 2013. Design , installation and calibration of a weighing lysimeter for crop evapotranspiration studies para estudos de evapotranspiração de culturas agrícolas 77–85.

Das, A., Maiti, J., Banerjee, R.N., 2012. Process monitoring and fault detection strategies: a review. Int. J. Qual. Reliab. Manag. 29, 720–752. https://doi.org/10.1108/02656711211258508

Davis, S.L., Dukes, M.D., 2010. Irrigation scheduling performance by evapotranspiration-based controllers. Agric. Water Manag. 98, 19–28. https://doi.org/10.1016/j.agwat.2010.07.006

Delgoda, D., Malano, H., Saleem, S.K., Halgamuge, M.N., 2016. Irrigation control based on model predictive control (MPC): Formulation of theory and validation using weather forecast data and AQUACROP model. Environ. Model. Softw. 78, 40–53. https://doi.org/10.1016/j.envsoft.2015.12.012

Earl, H.J., 2003. A Precise Gavimetric Method for Simulating Drought Stress in Pot Experiments. Crop Sci. 43, 1868–1873. https://doi.org/10.2135/cropsci2003.1868

Fatnassi, H., Boulard, T., Lagier, J., 2004. Simple indirect estimation of ventilation and crop transpiration rates in a greenhouse. Biosyst. Eng. 88, 467–478. https://doi.org/10.1016/j.biosystemseng.2004.05.003

Fernández, J.E., Green, S.R., Caspari, H.W., Diaz-Espejo, A., Cuevas, M. V., 2008. The use of sap flow measurements for scheduling irrigation in olive, apple and Asian pear trees and in grapevines. Plant Soil 305, 91–104. https://doi.org/10.1007/s11104-007-9348-8

Gil, P., Santos, F., Palma, L., Cardoso, A., 2015. Recursive subspace system identification for parametric fault detection in nonlinear systems. Appl. Soft Comput. J. 37, 444–455. https://doi.org/10.1016/j.asoc.2015.08.036

Howell, T., Evett, S., 2004. The Penman-Monteith Method, USDA-Agricultural Research Service Conservation & Production Research Laboratory.

Jolliet, O., Bailey, B.J., 1992. The effect of climate on tomato transpiration in greenhouses: measurements and models comparison. Agric. For. Meteorol. 58, 43–62. https://doi.org/10.1016/0168-1923(92)90110-P

Jones, H.G., 2008. Irrigation Scheduling - Comparison of soil, plant and atmosphere monitoring approaches. Acta Hortic. 792, 391–403.

Jones, H.G., 2004. Irrigation scheduling: Advantages and pitfalls of plant-based methods. J. Exp. Bot. 55, 2427–2436. https://doi.org/10.1093/jxb/erh213

Kirchsteiger, H., Pölzer, S., Johansson, R., Renard, E., del Re, L., 2011. Direct continuous time system identification of MISO transfer function models applied to type 1 diabetes. IEEE Conf. Decis. Control Eur. Control Conf. 5176–5181. https://doi.org/10.1109/CDC.2011.6161344

Kochler, M., Kage, H., Stützel, H., 2007. Modelling the effects of soil water limitations on transpiration and stomatal regulation of cauliflower. Eur. J. Agron. 26, 375–383. https://doi.org/10.1016/j.eja.2006.12.003

Lozoya, C., Mendoza, C., Aguilar, A., Román, A., Castelló, R., 2016. Sensor-Based Model Driven Control Strategy for Precision Irrigation. J. Sensors 2016.

Maes, W.H., Steppe, K., 2012. Estimating evapotranspiration and drought stress with ground-based thermal remote sensing in agriculture: a review. J. Exp. Bot. 63, 695–709. https://doi.org/10.1093/jxb/err313

Monteith, J.L., 1973. Principles of Environmental Physics, Principles of Environmental Physics. Edward Arnold, London. https://doi.org/10.1016/B978-0-12-386910-4.00019-6

Montero, J.I., Antón, A., Muñoz, P., Lorenzo, P., 2001. Transpiration from geranium grown

under high temperatures and low humidities in greenhouses. Agric. For. Meteorol. 107, 323–332. https://doi.org/10.1016/S0168-1923(01)00215-5

Navarro-Hellín, H., Martínez-del-Rincon, J., Domingo-Miguel, R., Soto-Valles, F., Torres-Sánchez, R., 2016. A decision support system for managing irrigation in agriculture. Comput. Electron. Agric. 124, 121–131. https://doi.org/10.1016/j.compag.2016.04.003

Pollet, S., Bleyaert, P., Lemeur, R., 2000. Application of the Penman-Monteith model to calculate the evapotranspiration of head lettuce (Lactuca sativa L. var. capitata) in glasshouse conditions. Acta Hortic. 519, 151–161. https://doi.org/10.17660/ActaHortic.2000.519.15

Prehn, A., Owen, J., Warren, S., Bilderback, T., Albano, J.P., dammeri Schneid, C.C., 2010. Comparison of Water Management in Container-Grown Nursery Crops using Leaching Fraction or Weight-Based On Demand Irrigation Control 1 28, 117–123.

Quanten, S., De Valck, E., Cluydts, R., Aerts, J.M., Berckmans, D., 2006. Individualized and time-variant model for the functional link between thermoregulation and sleep onset. J. Sleep Res. 15, 183–198. https://doi.org/10.1111/j.1365-2869.2006.00519.x

Reynolds, D., 2015. Gaussian Mixture Models. Encycl. Biometrics. https://doi.org/10.1007/978-1-4899-7488-4_196

Sánchez, J.A., Rodríguez, F., Guzmán, J.L., Arahal, M.R., 2012. Virtual sensors for designing irrigation controllers in greenhouses. Sensors 12, 15244–15266. https://doi.org/10.3390/s121115244

Sharma, A.B., Golubchik, L., Govindan, R., 2010. Sensor Faults : Detection Methods and Prevalence in Real-World Datasets. ACM Trans. Sens. Networks 6, 23. https://doi.org/10.1145/1754414.1754419

Speetjens, S.L., Stigter, J.D., van Straten, G., 2009. Towards an adaptive model for greenhouse control. Comput. Electron. Agric. 67, 1–8. https://doi.org/10.1016/j.compag.2009.01.012

Taylor, C.J., Pedregal, D.J., Young, P.C., Tych, W., 2007. Environmental time series analysis and forecasting with the Captain toolbox. Environ. Model. Softw. 22, 797–814. https://doi.org/10.1016/j.envsoft.2006.03.002

Villarreal-Guerrero, F., Kacira, M., Fitz-Rodríguez, E., Kubota, C., Giacomelli, G.A., Linker, R., Arbel, A., 2012. Comparison of three evapotranspiration models for a

greenhouse cooling strategy with natural ventilation and variable high pressure fogging. Sci. Hortic. (Amsterdam). 134, 210–221. https://doi.org/10.1016/j.scienta.2011.10.016

Welch, P., 1967. The use of fast Fourier transform for the estimation of power spectra: A method based on time averaging over short, modified periodograms. IEEE Trans. Audio Electroacoust. 15, 70–73. https://doi.org/10.1109/TAU.1967.1161901

Xiao, J., Xu, Q., Wu, C., Gao, Y., Hua, T., Xu, C., 2016. Performance evaluation of missing-value imputation clustering based on a multivariate Gaussian mixture model. PLoS One 11, 1–15. https://doi.org/10.1371/journal.pone.0161112

Yan, H.-C., Zhou, J.-H., Pang, C.K., 2017. Gaussian Mixture Model Using Semisupervised Learning for Probabilistic Fault Diagnosis Under New Data Categories. IEEE Trans. Instrum. Meas. 66, 1–11. https://doi.org/10.1109/TIM.2017.2654552

Young, P., Jakeman, A., 1980. Refined instrumental variable methods of recursive time-series analysis Part III. Extensions. Int. J. Control 31, 741–764. https://doi.org/10.1080/00207178008961080

Young, P.C., 2006. The data-based mechanistic approach to the modelling, forecasting and control of environmental systems. Annu. Rev. Control 30, 169–182. https://doi.org/10.1016/j.arcontrol.2006.05.002

Young, P.C., Taylor, C.J., Pedregal, D.J., 2007. The Captain Toolbox.

Chapter 5 Dynamic Neural Network Modelling of Soil Moisture Content for Predictive Irrigation Scheduling

Abstract

Sustainable freshwater management is underpinned by technologies which improve the efficiency of agricultural irrigation systems. Irrigation scheduling has the potential to incorporate real-time feedback from soil moisture and climatic sensors. However, for robust closed-loop decision support, models of the soil moisture dynamics are essential in order to predict crop water needs while adapting to external perturbation and disturbances. This paper presents a Dynamic Neural Network approach for modelling of the temporal soil moisture fluxes. The models are trained to generate a one-day-ahead prediction of the volumetric soil moisture content based on past soil moisture, precipitation and climatic measurements. Using field data from three sites, a R^2 value above 0.94 was obtained during model evaluation in all sites. The models were also able to generate robust soil moisture predictions for independent sites which were not used in training the models. The application of the Dynamic Neural Network models in a predictive irrigation scheduling system was demonstrated using AQUACROP simulations of the potato-growing season. The predictive irrigation scheduling system was evaluated against a rule-based system which applies irrigation based on predefined thresholds. Results indicate that the predictive system achieves a water saving ranging between 20 – 46% while realizing a yield and water use efficiency similar to that of the rule-based system.

1 Introduction

An increasing world population and climate change have placed a considerable amount of pressure on global freshwater supplies (Adeyemi et al., 2017). Irrigated agriculture is the world's largest consumptive user of fresh water, accounting for over 70% of its global use (Hedley et al., 2014). It is therefore important to develop technologies which enable sustainable and efficient water use for irrigated agriculture while obtaining a healthy plant growth.

It is desirable to irrigate to meet specific plant water demands at the right time while avoiding over and under irrigation. This usually involves irrigation scheduling and control operations on an hourly, daily or a time period usually less than a week (Ali and Talukder, 2001). Precision irrigation aims to accurately determine and quantify plant water needs. The irrigation amount and timing is based on measurements of soil, plant and climatic variables from which the plant water need is inferred (Smith et al., 2009). Precision irrigation has been shown to improve water use efficiency, reduce energy consumption, and enhance crop productivity by leveraging advances in sensor, control and modelling technologies (Hedley and Yule, 2009; Monaghan et al., 2013; Morillo et al., 2015; Ro-Hellín et al., 2015). Such advances include the development of energy efficient and fault-tolerant wireless sensor networks (Nesa Sudha et al., 2011; Parra et al., 2018), intelligent proximal sensing for the detection of plant water stress (Alvino and Marino, 2017; Gonzalez-Dugo et al., 2013; Marin et al., 2018), and variable rate irrigation systems (Evans et al., 2013; Hedley and Yule, 2009; Stone et al., 2015).

The temporal dynamics of field-scale soil moisture is perhaps the most leveraged tool for irrigation scheduling. This is because the soil moisture status is indicative of the water available for uptake by crops (Romano et al., 2013). A number of irrigation scheduling methods estimate crop water needs using soil moisture and climatic data, and rules created by expert agronomists. Most of the commercial automated irrigation systems are programmed to irrigate at specific time intervals and apply a fixed irrigation volume. A number of these systems are also programmed to irrigate after a predefined soil moisture threshold is reached (Pardossi and Incrocci, 2011). Due to their open-loop structure, these methods may not guarantee optimum irrigation scheduling decisions resulting in suboptimal plant health and efficiency in water use (McCarthy et al., 2013). These shortcomings can be alleviated with the use of feedback control where sensor feedback is employed in optimizing irrigation timing and volume (Raine et al., 2007). Although these approaches improve irrigation scheduling decisions, they do not include a model for the process dynamics and as a result, the overall system may not be robust to external perturbations (Park et al., 2009).

Model-based irrigation scheduling systems consist of a calibrated internal model which employs feedback from soil, plant and climatic sensors in order to predict crop water

needs (Park et al., 2009). McCarthy et al. (2014) implemented a model-based control system for predicting the irrigation requirements of cotton with an objective of maximizing crop yield. Their system relied on a complex crop model which requires detailed information on various climatic, soil and crop parameters. Park et al. (2009) developed a model predictive control system for center pivot irrigation which used measured soil and climatic data to calibrate a complex soil-water model. The use of mechanistic models in these systems has many practical limitations because they are data demanding and require time-consuming calibrations during model development.

In recent years, many studies have investigated the applicability of data-driven machine learning models to irrigation decision support. Navarro-Hellín et al. (2016) presented a regression model applied in predicting the weekly irrigation needs of a plantation using climatic and soil data as inputs. Giusti and Marsili-Libelli (2015) applied a fuzzy decision system in predicting the volumetric soil moisture content based on local weather data. King and Shellie (2016) used neural network modelling to estimate the lower threshold (T_{nws}) needed to calculate the crop water stress index for wine grapes. In Delgoda et al. (2014), the authors applied a system identification model in predicting the soil moisture deficit using climatic and soil moisture data as model inputs. These statistical methods explore the spatial and temporal patterns hidden in historical data in order to map input data to an output space. They do not rely on a physical model of the system as they are data-driven (i.e. they learn from data). In many cases, these machine learning methods have been shown to achieve a good prediction performance (Karandish and Šimůnek, 2016). They also have less data requirements when compared to mechanistic models (King and Shellie, 2016; Payero and Irmak, 2006; Young, 2006).

For real-time irrigation scheduling, a model which is able to predict the soil moisture dynamics is desirable (McCarthy et al., 2013). In order to achieve this with traditional machine learning and system identification methods, an extensive physical knowledge of vadose zone hydrology and boundary layer meteorology is required to derive robust input features from soil and climatic data. This is because of the complex nonlinear relationship between the climatic parameters, soil hydraulic properties and the soil moisture dynamics (Mashayekhi et al., 2016). In Lozoya et al. (2016), Delgoda et al. (2014), Giusti and Marsili-Libelli (2015) and Saleem et al. (2013) the authors presented system identification models for the prediction of soil moisture dynamics which are parameterized based on the soil water balance method. This involved assumptions relating to the absence of surface run-off and deep percolation. The estimated evapotranspiration was also used as an input to the models. In practice, the true crop evapotranspiration may be significantly different from the estimated values. Furthermore, these models are only applicable to the site for which they are developed limiting their use for a different environment. This is because models developed using traditional machine learning and system identification

approaches are mostly only applicable to the environment for which they were developed (Navarro-Hellín et al., 2016).

Machine learning approaches such as Support vector machines (SVM) and Adaptive neuro-fuzzy inference systems (ANFIS) are another group of models that have been applied for the prediction of soil moisture dynamics (Deng et al., 2011; Hong et al., 2016; Karandish and Šimůnek, 2016; Liu et al., 2010). These approaches have good prediction capability and limited input requirements. Karandish and Šimůnek (2016) compared various machine learning models including ANFIS and SVM for simulating the time series of soil moisture content using meteorological, precipitation and crop coefficient data as model input. The authors reported that the models achieved a prediction performance comparable to that of a mechanistic physical process-based model; HYDRUS – 2D. However, they noted that these machine learning models are not suitable for the entire range of soil moisture prediction i.e. water stress conditions. It is therefore evident that robust and scalable data-driven models need to be developed for irrigation scheduling applications.

Neural network (NN) methods have a strong learning ability and are able to represent the nonlinear relationship between the inputs and outputs of a system (Capraro et al., 2008). Some specific applications of neural networks to irrigation and water resource management include the prediction of soil moisture to aid irrigation scheduling (Capraro et al., 2008; Tsang and Jim, 2016), crop yield prediction (Gandhi et al., 2016; Guo and Xue, 2014), prediction of irrigation water demand (Pulido-Calvo et al., 2003; Pulido-Calvo and Gutiérrez-Estrada, 2009), rainfall-runoff modelling (Khan and Coulibaly, 2006; Sarkar and Kumar, 2012) and groundwater modelling (Joorabchi et al., 2009; Sun et al., 2016).

A Neural network (NN) method is applied in this study for predicting the soil moisture dynamics because of their ability to produce robust functions approximating complex processes (Goodfellow et al., 2016). However, traditional feedforward neural networks (FFNN) have limited ability to model dynamic data because they are unable to preserve previous information, resulting in suboptimal predictions when they are applied in modelling highly causal systems (Brezak et al., 2012). The learning capability of FFNN's can be improved through additional pre-processing of dynamic data and combining the FFNN with other methods including genetic algorithms (Gu et al., 2017) and fuzzy logic (Tsang and Jim, 2016). For example, Pulido-Calvo and Gutiérrez-Estrada (2009) applied a hybrid FFNN model to generate a one-day-ahead forecast of daily irrigation water demand. The forecast produced by the FFNN was corrected via a fuzzy logic approach whose parameters were adjusted using genetic algorithms. While this sort of hybrid modelling approach can strengthen the ability of a FFNN to learn dynamic data, the long-term generalization ability of such models is limited due to the ad hoc nature of fuzzy logic

rules. Furthermore, the methods which employ additional pre-processing of dynamic data are time-consuming because of the extensive time and frequency domain computations they rely on. The data pre-processing steps also rely on subjective user intervention which limits the scalability of the models to new environments.

This present study focuses on a dynamic modelling task, for which the Recurrent Neural Network (RNN) presents a suitable solution. A RNN has internal self-looped cells, allowing it to preserve information from previous time steps (Funahashi and Nakamura, 1993). The Long Short-Term Memory Network (LSTM), a class of RNN's was selected for this study because of its successful application in the control of nonlinear dynamic systems (Wang et al., 2017; Yu Wang, 2017). The LSTM requires minimal input data pre-processing and it is able to preserve useful information across multiple time steps (Chauhan and Vig, 2015). They have been shown to achieve robust performance in modelling sequential data in fields such as natural language processing (Mikolov et al., 2011), time series classification of chaotic systems (Ordóñez and Roggen, 2016) and speech recognition (Graves et al., 2013).

Zhang et al. (2018) demonstrated a hydrological application of LSTM models for the prediction of water table depth. Time series data on water diversion, evaporation, precipitation and temperature were applied as inputs to the model. The authors reported R^2 scores ranging between 0.789 – 0.952 for the LSTM models, largely outperforming FFNN models which achieved a maximum R^2 score of 0.495. The robust water table depth prediction achieved by the LSTM models highlights their ability to preserve and learn previous information from long-term time series data typical of hydrological application. This ability is particularly desirable in soil moisture based irrigation scheduling where the present soil moisture content is dependent on past soil moisture, precipitation and climatic data.

The objective of this study was to develop LSTM models for the prediction of volumetric soil moisture content for three sites with different soil characteristics. Performance of the LSTM models was evaluated by comparing the LSTM predicted soil moisture content with measured soil moisture content and estimated soil moisture content using traditional Feed Forward Neural Networks (FFNN). The applicability of the LSTM models for prediction in sites not used in model training was also investigated. Finally, the application of the LSTM models in predictive irrigation scheduling was demonstrated using model-based simulations of the potato-growing season.

The rest of the paper is structured as follows. In Section 2, the theoretical background of neural networks is presented, in Section 3, the methodology employed for the study is presented. Section 4 shows the performance evaluation of the neural network models and

the predictive irrigation scheduling system, and in Section 5, the conclusions and recommendations for future work are presented.

2 Background

This section presents a theoretical background on artificial neural networks including the feedforward neural network and the recurrent neural network.

2.1 Neural network preliminaries

The basic building block of neural networks is the neuron. It is a processing element that takes a number of inputs, applies a weight to them, sums them up, includes a bias term and passes the result to an activation function which then produces an output. This activation function implements a nonlinear transformation to the linearly combined input in order to produce a nonlinear output.

Through a combination of these neurons across the input space and connections of the neurons outputs to other neurons, a function can be learned which maps the nonlinear relationship between an input feature space and an output target. The input-output relation of the system can be described by equation 1 (Goodfellow et al., 2016).

$$Z_j^i(k) = f\left(\sum_{i=1}^{N} w_{ij}^i \, x_i^{i-1}(k) + \, \delta^i\right) \tag{1}$$

Where $f(:)$ is the nonlinear activation function, w_{ij}^i is the connection weight of the j th neuron unit in the (i-1) th layer to those of the i th layer. x_i^{i-1} is the input from the (i-1) th layer and δ^i are the respective bias terms.

2.2 Feedforward neural network

The Feedforward neural network (FFNN) also known as the multilayer perceptron (MLP) network is built by ordering neurons in layers and letting each neuron in a layer take as input only the outputs of the units in the previous layer or external inputs. A network with $N = 1,2,3, \ldots \ldots n$ layers is called a n layer network. The FFNN is shown in Figure 1.

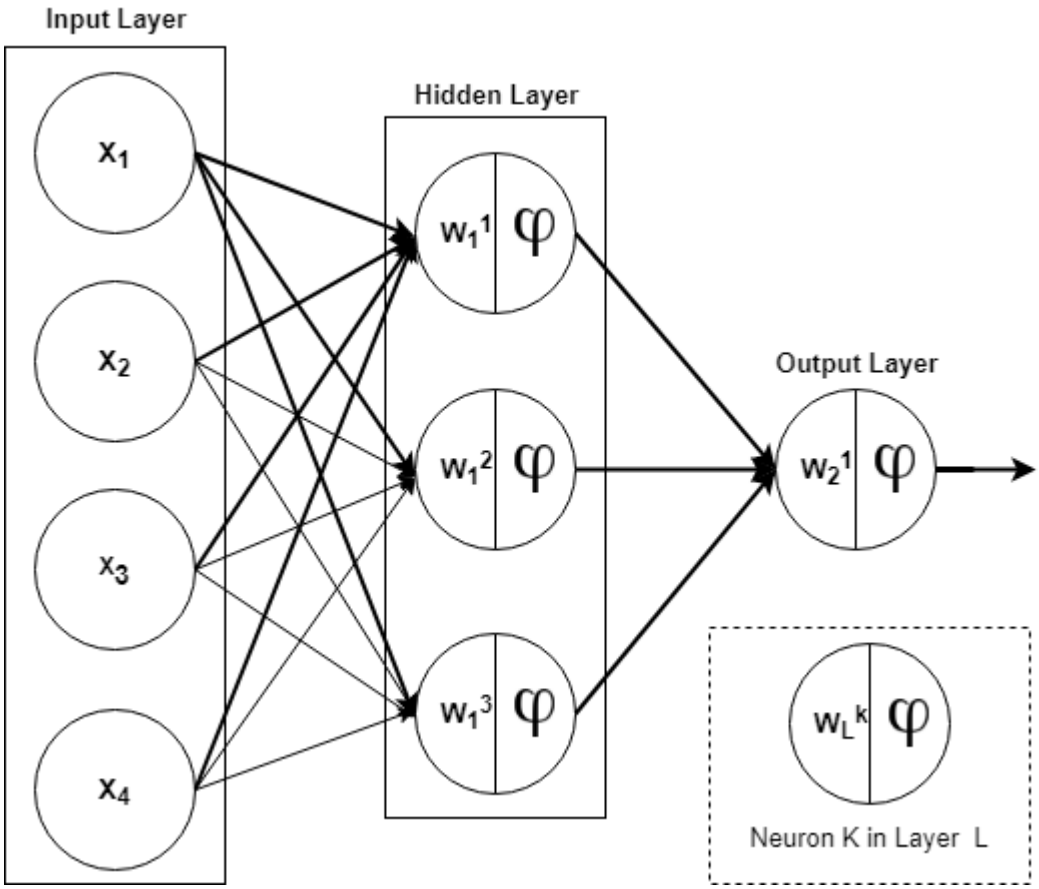

Figure 1. The Feedforward neural network

The second layer in Figure 1 is called the output layer as it produces the output of the network. The first layer is known as the hidden layer since it is located between the external inputs and the output layer. The mathematical formula expressing the FFNN is detailed in equation 2 (Goodfellow et al., 2016)

$$\hat{y}_i = g_i[x, \theta] = F_i \left[\sum_{j=1}^{n_h} \varphi_{i,j} f_j \left(\sum_{l=1}^{n_\varphi} w_{j,lxl} + w_{j,0} \right) + \varphi_{i,0} \right] \quad (2)$$

In equation 2, θ is the parameter vector containing all the adjustable parameters of the network i.e. the weight and the biases $\{w_{j,l}, \varphi_{i,j}\}$ and f_j is the nonlinear activation function. The biases usually take a value of 1.

In order to determine the value of the weights, the network is trained with data containing examples of the inputs x_l and outputs y_i pairs; known as the training set. The weights are chosen to minimize a global loss function which measures the cost of predicting $\hat{y}$ when the true output y is a function over the training set. For regression problems which encompasses dynamic modelling tasks, the cost function to be minimized is the mean-squared error which is computed as shown in equation 3

$$l(\hat{y}, y) = \sum_{k=1}^{K} E(k) = \frac{1}{2n} \sum_{k=1}^{K} \sum_{i=1}^{n} \|\hat{y}_i(k) - y_i(k)\|^2 \quad (3)$$

Where $l(\hat{y}, y)$ is the loss function and n is the number of training examples. The minimization of the loss function and update of weights is achieved using the backpropagation algorithm (Rumelhart et al., 1986).

2.3 Long short-term memory network

The Long short-term memory network (LSTM) is a variant of the Recurrent neural network (RNN), therefore, it is expedient to introduce the RNN before describing the LSTM.

Recurrent neural networks are similar to Feedforward neural networks except that there is a self-feedback of neurons in the hidden layers as illustrated in Figure 2. This gives the network memory and it is able to learn from an entire sequence given portions of the overall sequence i.e. it is a dynamic system.

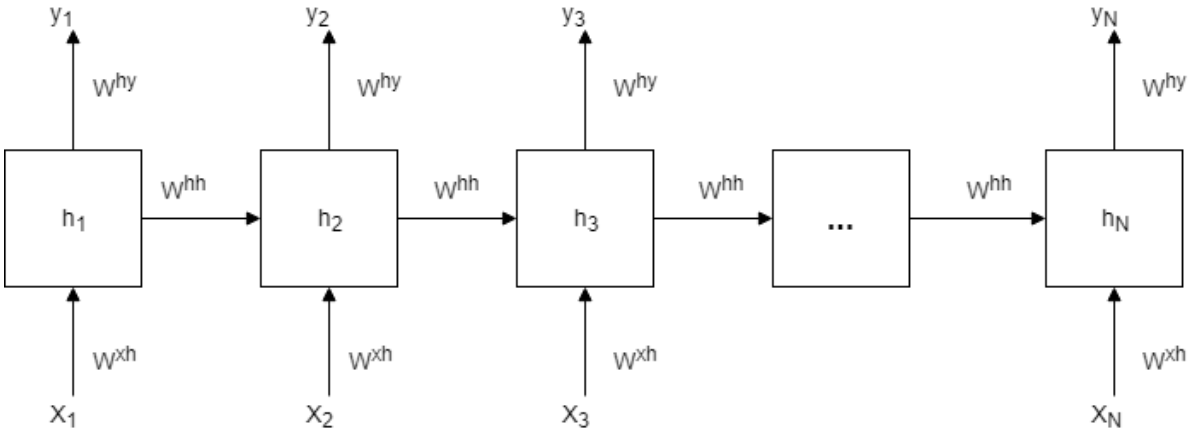

Figure 2. An unrolled recurrent neural network

The hidden nodes $h = (h_1, \ldots\ldots, h_N)$ and output nodes $y = (y_1, \ldots\ldots, y_N)$ are computed by looping through the equations 4 and 5 below (Goodfellow et al., 2016)

$$h_t = \tanh(b_h + Wh_{t-1} + Ux_t) \quad (4)$$

$$y_t = b_o + Vh_t \quad (5)$$

Where x_t is the input vector at time t and h_{t-1} is the hidden cell state at time $t-1$, b_o and b_h are the vectorised bias terms and U, W, V are the weight matrices for input-to-hidden, hidden-to-hidden and hidden-to-output connections respectively.

The loss is calculated as the total loss for each time-step and the gradients are computed via Back-Propagation Through Time (BPTT) (Werbos, 1990).

However, BPTT is not able to learn a pattern from long-term dependency because of the gradient vanishing problem (Hochreiter, 1998). The RNN's use their back-coupling

connections to memorize short-term dependency in a sequence and as a result, the backpropagated error signals in time can become infinitely high or vanish (Pascanu et al., 2013). Hochreiter and Schmidhuber (1997) proposed the LTSM which is able to solve the exploding or vanishing gradients problem by enforcing constant error flows through constant error carousels within special multiplicative units. These units regulate the error flow in the network by learning how to open or close specialized gates in the network. The constant error carousels (CEC), the multiplicative and gates units form the memory block of the LSTM (Zhang et al., 2018).

The CEC loops through the network without an activation function and thus the vanishing gradient problem doesn't occur when BPTT is applied to train an LSTM (Goodfellow et al., 2016). Therefore, LSTM's are able to approximate long-term information because the information can flow easily along the cells unchanged. The input, forget and output gates of the memory block control the input into the CEC cell, the information retained in the cells and the output from the cell into other blocks in the network. A schematic representation of the LSTM memory block along with its associated components is shown in Figure 3.

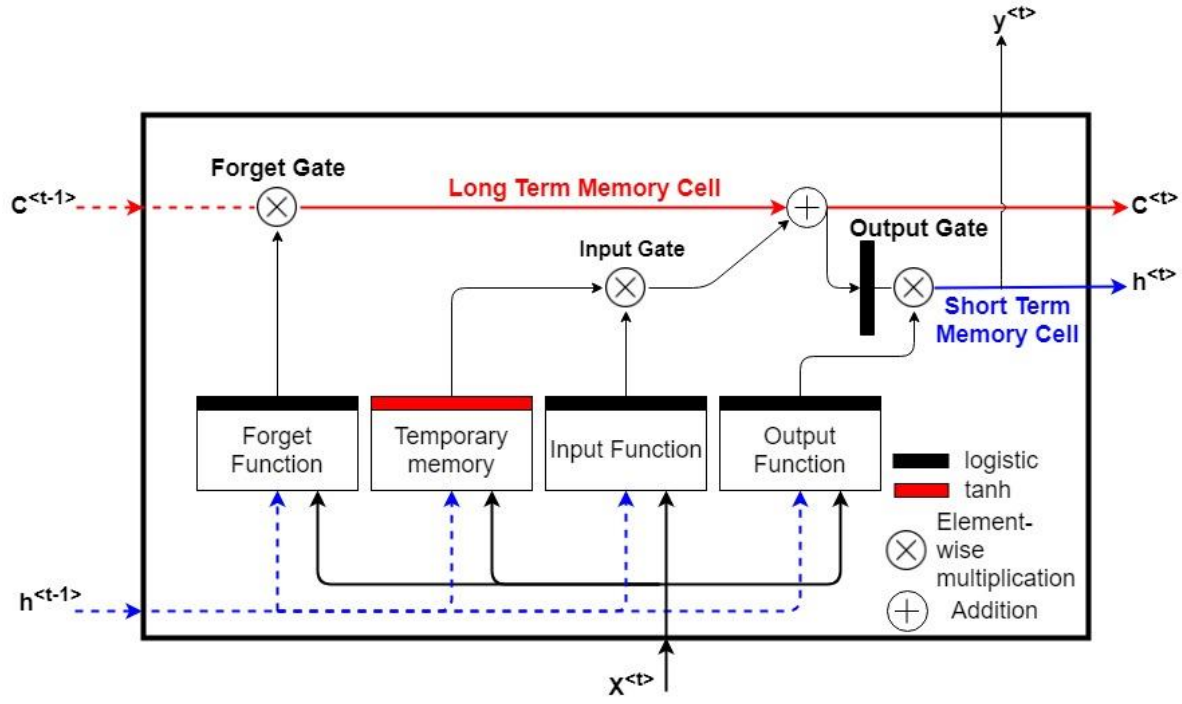

Figure 3. The long short-term network memory block

The LSTM computes the mapping from an input sequence x to the output by looping through equations 6 – 11 with initial values $C_o = 0$ and $h_o = 0$ (Goodfellow et al., 2016)

$$i_t = \sigma(w_i x_t + U_i h_{t-1} + b_i) \tag{6}$$

$$f_t = \sigma\left(w_f x_t + U_f h_{t-1} + b_f\right) \quad (7)$$

$$\sigma_t = \sigma(w_o x_t + U_o h_{t-1} + b_o) \quad (8)$$

$$\tilde{C}_t = \tanh(w_c x_t + U_c h_{t-1} + b_c) \quad (9)$$

$$C_t = f_t \otimes C_{t-1} + i_t \otimes \tilde{C}_t \quad (10)$$

$$h_t = o_t \otimes \tanh(C_t) \quad (11)$$

Where w_i, w_f, w_o are the weight matrices from the input, forget and output gates to the input respectively, U_i, U_f, U_o are the matrices of the weights from the input, forget and output gates to the hidden layer respectively, b_i, b_f, b_o are the bias vectors associated with the input, forget and output gates, σ is the nonlinear sigmoid activation function $\sigma(x) = \frac{1}{1+e^{-x}}$, and i_t, f_t, o_t, C_t are the input, forget, output gate and the cell state vectors at time t respectively. The element-wise vector multiplication is denoted with $\otimes$.

3 Methodology

The methodology employed for this study is presented in this section. This includes an overview of the data applied for developing the soil moisture prediction models, the structure of the neural network models and the structure of the predictive irrigation scheduling system.

3.1 Study sites and data source

The data applied in developing the neural network (NN) models for soil moisture prediction were obtained from three study sites which are part of the Cosmic-ray Soil Moisture Observing System (COSMOS) monitoring project in the United Kingdom (Shuttleworth et al., 2010). Briefly, the COSMOS project is a soil moisture and climate monitoring network operating in the UK, USA, Australia and China. The project provides near real-time soil moisture and climatic data for use in a variety of applications including agriculture, water resources management, flood prediction and land-surface modelling.

The data obtained for the three study sites included hourly measurements of windspeed, rainfall, air temperature, net radiation, relative humidity, and volumetric soil moisture content. Details of the three sites are summarized in Table 1.

Table 1. Details of the sites used for model training

Site name	Soil type	Land cover	Date range
Baluderry	Sandy loam	Farmland	May 2014 – September 2017
Stoughton	Loam	Arable	August 2015 – September 2017
Waddeston	Clay	Grassland	December 2013 – September 2017

The volumetric soil moisture content in all sites is measured using the cosmic-ray soil moisture sensor (Model CRS-1000/B, Hydroinnova LLC, Albuquerque, USA) deployed using a site-specific calibration. The cosmic-ray soil moisture sensor consists of a non-invasive probe which measures the neutron emitted by cosmic rays within the air and soil. These neutrons are moderated by hydrogen atoms emitted from soil water into the atmosphere. The neutrons and hydrogen atoms combine instantaneously and its density is inversely correlated with soil moisture (Zreda et al., 2012). A calibration function defines the relationship between the neutron intensity and soil moisture. This calibration function is simple, monotonic and invariant with soil texture and chemical composition (Desilets et al., 2010). The sensor has a horizontal measurement range of 200m and an effective measurement depth of up to 60m. The sensor is reported to have an accuracy of $\pm 2\ \%$ measured volumetric soil moisture content (Franz et al., 2013). Full details on the operating principle of the sensor can be found in Shuttleworth et al. (2010). The meteorological variables (e.g. air temperature, relative humidity, net radiation, windspeed and precipitation) in all sites are measured by a MetPak Pro Base automatic weather station (Gill Instruments, Hampshire, UK).

The NN models trained on data from the sites listed in Table 1 were also applied in predicting the soil moisture content in two independent sites with soil characteristics similar to that of the sites for which the models were trained. This was done to evaluate the applicability of the models for prediction in new sites which were not used in model training. A summary of the independent sites is presented in Table 2.

Table 2. The independent sites corresponding to each model training site

Training site		Independent site 1			Independent site 2	
	Name	Land cover	Soil type	Name	Land cover	Soil type
Baluderry	Bunny Park	Arable	Sandy loam	Bickley Hall	Grassland	Sandy loam
Stoughton	Morley	Arable	Loam	Cockle Park	Grassland	Loam
Waddeston	Hollin Hill	Grassland	Clay	Chimney Meadows	Grassland	Clay

3.2 Data cleaning and pre-processing

The hourly data was resampled to daily (24 hours) intervals as this is a time period applicable for field scale irrigation scheduling (Delgoda et al., 2016). The daily averages of the climatic variables were calculated during the resampling while the daily precipitation was calculated as the sum of daily rainfall and irrigation depths. The volumetric soil moisture content was also resampled to its average daily value. The data cleaning steps included imputing of missing values and removal of outliers.

The pre-processing steps applied for the data modelled with the FFNN included a box-cox transform (Box and Cox, 1964) of the soil moisture and air temperature data in order to stabilize their variance. The transformed data were thereafter deseasonalized using the seasonal and trend decomposition using loess (STL), as proposed by Cleveland et al. (1990). Several studies have shown that deseasonalizing dynamic data which exhibits seasonality prior to modelling is necessary in order to produce robust predictions with a FFNN model (Ben Taieb et al., 2012; Crone et al., 2011). The STL technique decomposes the soil moisture and air temperature data into their trend, seasonal and residual components. Thereafter, the sums of the trend and level were passed to the next step of the data pre-processing. An example of the transformed and decomposed soil moisture data is shown in Figure 4. In the next data pre-processing step, the climatic, precipitation and soil moisture data were standardized by computing the z-score of their data points. In the post-processing stage, the soil moisture predictions were back-transformed to their actual scale through an inverse z-score transformation, addition of the seasonal component and an inverse box-cox transformation.

For the LSTM, the only data pre-processing step applied was a standardization of the climatic, precipitation and soil moisture data. This was accomplished by computing the z-score of their data points. In the post-processing stage, the soil moisture predictions were back-transformed to their actual scale through an inverse z-score transformation.

For the model training sites, the dataset was divided into a 70:30 ratio for the purpose of model training and evaluation. The division was done such that the temporal nature of the data was accounted for i.e. the evaluation dataset is posterior to the training dataset.

Data spanning 2016 – 2017 for the independent sites (Table 2) was applied in evaluating the prediction performance of the trained NN models on those sites.

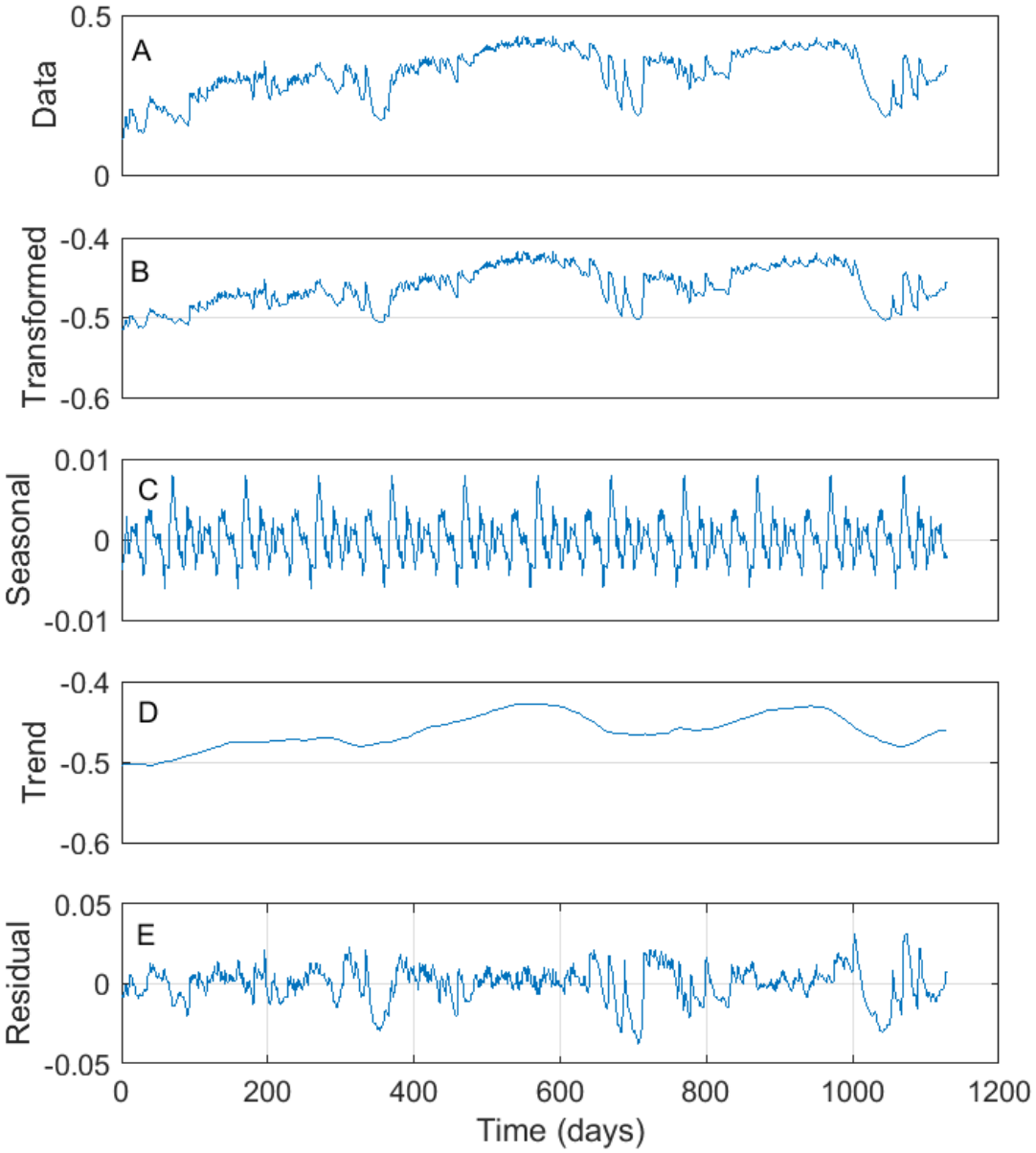

Figure 4. Soil moisture data transformation and decomposition prior to modelling (A) Observed data (B) Box-cox transformed data (C) Seasonal component (D) Trend component (E) Residual component

3.3 Proposed Model Framework

For predictive irrigation scheduling, a one-day-ahead prediction of the soil moisture content is required.

The soil moisture content at time $t + 1$ is a nonlinear function of past and present climatic, and precipitation inputs. It is also influenced by the past and present soil moisture content values. This is a Multiple Input and Single Output (MISO) system. The FFNN and LSTM networks are encoded in various suitable architectures appropriate for the learning task. The neural networks were developed using the Keras Deep Learning library on the Python programming platform (Chollet, 2015).

3.3.1 Feedforward neural network structure

The FFNN is straightforward to employ for discrete-time modelling of dynamic systems for which there is a nonlinear relationship between the system's inputs and output. The soil moisture dynamics can be modelled as a Nonlinear Autoregressive with Exogenous Input System (NARX) as shown in equation 12

$$y(t+1) = S[y(t),, \dots\dots, y(t-j), u(t), \dots\dots, u(t-n), p(t), \dots\dots, p(t-m)] \quad (12)$$

Where $y(t+1)$ is the one day ahead prediction of the volumetric soil moisture content, $y(t = 0 \dots j)$ are the present and past soil moisture content at day $t = 0 \dots j$, $u(t = 0 \dots n)$ are the climatic inputs at day $t = 0 \dots n$, $p(t = 0 \dots m)$ are the precipitation inputs at day $t = 0 \dots m$ and S is a nonlinear function which is approximated using the FFNN.

The time lags m, n and j are determined through experimentation. The number of hidden layers in the network and the number of neurons in each hidden layer are also determined through experimentation. The soil moisture prediction is framed as a regression problem, and as such, an appropriate activation function is required for the hidden layers of the FFNN. For regression problems, the most robust nonlinear activation function is the point-wise rectified linear units (RELU), $\max(0, x)$ where x is the input into the neuron. The RELU activation function is reported to provide easier optimization, faster convergence and better generalization with the added bonus of being computationally efficient (Dahl et al., 2013).

During the study, the RELU nonlinearity was applied in the hidden layers while the network loss was minimized using the adaptive moment estimation (ADAM) optimization algorithm which is reported to improve network convergence (Kingma and Ba, 2015).

3.3.2 Long short-term memory network structure

For modelling dynamic systems, the LSTM introduces a nonlinearity from the input to system states followed by a dynamic linearity from the states to the output. This can be represented in the state space form as shown in equations $13a$ and $13b$

$$x(t+1) = NNi[x(t) \dots x(t-k), u(t) \dots u(t-n), y(t) \dots y(t-j), p(t) \dots p(t-m); V] \quad (13a)$$

$$y(t+1) = NNo[x(t+1); W] \quad (13b)$$

Where $x(t+1)$ is the future state of the network at day $t+1$, $x(t=0 \dots k)$ are the present and past network states at day $t=0 \dots k$, $y(t=0 \dots j)$ are the present and past soil moisture content at day $t=0 \dots j$, $u(t=0 \dots n)$ are the climatic inputs at day $t=0 \dots n$, $p(t=0 \dots m)$ are the precipitation inputs at day $t=0 \dots m$ and $y(t+1)$ is the one day ahead prediction of the volumetric soil moisture content. V is the parameter set of the network that corresponds to the states and W is the parameter set of the network that corresponds to the output.

The time lags m, n and j are determined through experimentation while the time delay k for the states is learned implicitly by the network during training. The network is designed as an LSTM nonlinear element (NNi) followed by a linear output layer (NNo). The number of LSTM layers and the number of memory blocks in each layer are also determined through experimentation. During the study, the network loss was minimized using the ADAM optimization algorithm (Kingma and Ba, 2015).

3.4 Irrigation scheduling

A predictive irrigation scheduling system is enabled by a model which uses feedback from soil and climatic sensors to predict the crop water demand (Park et al., 2009). A trained neural network model is able to generate soil moisture predictions and presents an opportunity for implementing predictive irrigation scheduling.

In order to demonstrate the applicability of a trained LSTM for predictive irrigation scheduling, the AQUACROP model developed by the Food and Agricultural Organization was used in simulating soil-plant-atmosphere interactions for the potato crop (Hsiao et al., 2009; Raes et al., 2009; Steduto et al., 2009). The AQUACROP model has been widely validated and it is able to simulate soil moisture dynamics and crop response to water deficits across various soil types as a function of climatic inputs and water availability (Akumaga et al., 2017; Kim and Kaluarachchi, 2015; Linker et al., 2016; Perez-Ortola et al., 2015).

Climatic and rainfall data for the model training sites were used as inputs into the AQUACROP model. The LSTM models trained for each site was applied in generating a one-day-ahead prediction of soil moisture content using the climatic data and

AQUACROP simulated soil moisture as inputs. Thereafter, the prediction was used to determine the irrigation depth and timing during the AQUACROP simulations. This formed the basis of the predictive irrigation system described in section 3.4.1. The AQUACROP soil file was modified to represent the soil types and characteristics for the model training sites as summarized in Table 3. The crop characteristics of the default Lima potato file was used during the simulations.

Table 3. Soil characteristics of the model development sites applied in the AQUACROP simulation

Site	Field capacity (m^3m^{-3})	Permanent wilting point (m^3m^{-3})	Profile
Baluderry	0.22	0.10	Sandy loam
Stoughton	0.31	0.15	Deep uniform loam
Waddeston	0.33	0.138	Clay

The predictive irrigation system was compared to a rule-based irrigation scheduling system set up on AQUACROP. The rule-based system was programmed to apply irrigation based on specified soil moisture thresholds and applied water depths to refill the soil moisture content to field capacity. It was set up as an open-loop system, which does not consider soil moisture feedback after irrigation events.

It should be noted that only data from the evaluation dataset set of the model training sites was applied in the simulations.

3.4.1. Predictive irrigation scheduling system

The goal of irrigation scheduling is to maintain the soil moisture content between an upper and lower bound. The upper bound is usually defined as the field capacity while the lower bound is a point above the permanent wilting point expressed a function of the management allowable depletion (MAD).

In irrigation, it is common practice to express the amount of water retained in the plant root zone (W_r) as an equivalent depth of soil water (mm of water). This is expressed as shown in equation 14

$$W_r = 1000\theta Z_r \tag{14}$$

Where θ is the volumetric soil moisture content and Z_r is the thickness of the root zone is meters.

The water deficit at time t (DP_t) is expressed as shown in equation 15

$$DP_t = W_{r,FC} - W_{r,t} \quad (15)$$

Where $W_{r,FC}$ is the water depth at field capacity and $W_{r,t}$ is the water depth at time t. It is evident from equation 15 that the water deficit at the upper bound (DP_U) will be zero i.e. ($W_{r,FC} - W_{r,FC}$). The deficit at the lower bound (DP_L) is determined from a knowledge of the soils available water and the crops MAD. This is expressed as shown in equations $16a$ and $16b$

$$DP_L = W_{r,FC} - W_{r,LB} \quad (16a)$$

with

$$W_{r,LB} = W_{r,FC} - MAD\left(W_{r,FC} - W_{r,PWP}\right) \quad (16b)$$

Where $W_{r,LB}$ is the water depth at the lower bound and $W_{r,PWP}$ is the water depth at permanent wilting point. DP_L will vary over the growth season as a result of root growth.

If a prediction of the soil volumetric soil moisture content at time $t+1$ is available from the LSTM model, the deficit at time $t+1$ (DP_{t+1}) can be easily calculated. The irrigation amount is computed as the water application depth that will replenish the water deficit to the upper bound i.e. Irrigation = (DP_{t+1}). For close-loop irrigation scheduling, the irrigation threshold is set at a safe point below DP_L. The advantage of this simplified irrigation scheduling system is the inclusion of a time variable lower bound. Delgoda et al. (2016) noted that this is difficult to achieve with the optimization schemes applied in model predictive control systems. A block diagram of the proposed irrigation scheduling system is presented in Figure 5. Figure 5 shows that soil moisture, precipitation, irrigation and climatic data are applied as inputs into a trained LSTM model in order to generate a prediction of the soil moisture content. The predicted soil moisture content is then used in conjunction with information on crop water requirement and soil water retention to determine the irrigation timing and amount.

During the simulations, for both the predictive and rule-based irrigation scheduling system, a MAD of 30% was assumed for the potato crop and the lower bound was dynamically adjusted as a function of rooting depth growth during the simulated growing season.

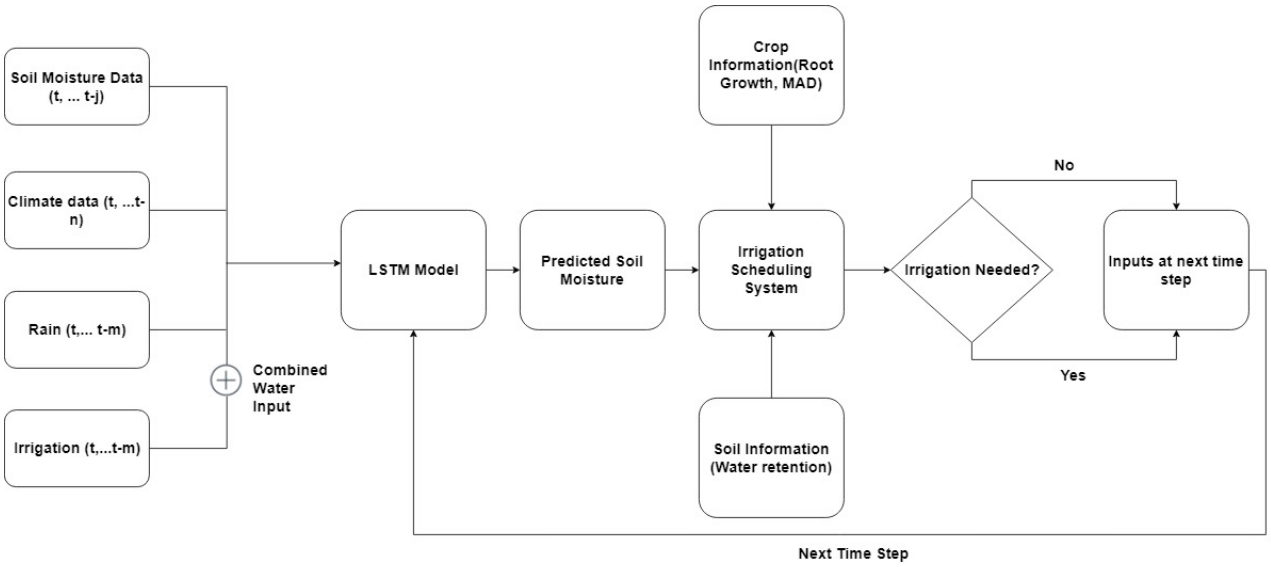

Figure 5. Block diagram of the predictive irrigation scheduling system. t is the time in days, m,n, and j are past time steps.

3.5 Model evaluation criteria

To assess the performance of the trained models for the prediction of the soil moisture content during the model evaluation, several measures of accuracy were applied. The model's accuracy between the observed and predicted soil moisture content was evaluated using the coefficient of determination (R^2), root mean squared error ($RMSE$) and the mean absolute error (MAE).

The R^2 describes the proportion of the total variance in the observed data that is explained by the model and ranges between $[-\infty, 1]$. A R^2 close to 1 indicates that the model explains well the variance of observations. It is expressed as R^2 in equation 17

$$R^2 = \frac{\sum_{i=1}^{N}(y_i - \bar{y})^2 - \sum_{i=1}^{N}(y_i - \hat{y}_i)^2}{\sum_{i=1}^{N}(y_i - \bar{y})^2} \quad (17)$$

where y_i is the measured value at time i, $\bar{y}$ is the mean of y_i $(i = 1 \ldots . N)$ and $\hat{y}_i$ is the predicted value at time i.

However, the $RMSE$ strongly penalizes large outliers and as such, it is preferable to compliment it with the MAE (Chai and Draxler, 2014). $RMSE$ and MAE values close to zero indicate good model predictions. The MAE and RMSE are defined as

$$\mathrm{MAE} = \frac{1}{n}\sum_{i=1}^{n}|y_i - \hat{y}_i| \quad (18)$$

$$\mathrm{RMSE} = \left[\frac{\sum_{i=1}^{n}(y_i - \hat{y}_i)^2}{n}\right]^{0.5} \quad (19)$$

In equations 18 and 19, y_i and $\hat{y}_i$ are observed and predicted value at time i $(i = 1,2,\ldots\ldots n)$ respectively.

4 Results and Discussion

The structure of the neural network models, their predictive performance and the performance of the predictive irrigation scheduling system are presented and evaluated in this section.

4.1 Model structure

The model structure and hyper-parameters of the neural network (NN) models were determined through a five-fold cross-validation on the training dataset. The model structures which achieved the best performance for the one-day-ahead prediction of the soil moisture content across the different sites are summarized in Table 4.

Table 4. The identified model structure with the best one-day ahead prediction performance across the training sites.

Site	Model	FFNN					LSTM					
	N	M	J	Neurons	Layers	R^2	N	M	J	Blocks	Layers	R^2
Baluderry	1	1	1	40	1	0.95	1	1	1	20	1	0.95
Stoughton	1	1	1	20	1	0.97	1	1	1	20	1	0.97
Waddeston	1	2	2	20	1	0.99	1	2	2	40	1	0.99

N is the time lag associated with the climatic inputs, M is the time lag associated with the precipitation input, and J is the time lag associated with the past soil moisture content input.

Table 4 shows that a first-order model taking the precipitation, climatic variables and soil moisture content at the present day as inputs is able to predict the soil moisture content of the next day for the sandy loam (Baluderry) and loam (Stoughton) sites. For the heavier textured clay site (Waddeston), the soil moisture content at the next day is dependent on the precipitation and soil moisture during the present and previous day. This can be explained by the low infiltration capacity of heavier textured soils. The precipitation input on any day may take a time period greater than a day to completely infiltrate into the soil column.

It was also found that a single layer of neurons and memory blocks in both the feedforward neural network (FFNN) and long short-term memory network (LSTM) respectively is able to satisfactorily model the soil moisture dynamics across all the sites. Additional layers could not further improve the learning capabilities of both networks. As an example, the performance of NN models with the same model structure with those listed in Table 4 but with two hidden layers is presented in Table 5. It is seen that the two-layer models achieve a lower prediction accuracy across all sites. Moreover, as part of the model training experiments, the best cross-validation performance achieved by a FFNN which included only a z-score transformation of the modelled data was a R^2 value of 0.68.

Table 5. Training Cross-validation performance of two-layer neural network models

Site	FFNN	LSTM
	R^2	R^2
Baluderry	0.93	0.91
Stoughton	0.92	0.95
Waddeston	0.95	0.97

4.2 Soil moisture content prediction

The prediction capability of a model is exemplified by its performance on data not seen by the model during training. As such, the prediction capability of the models was tested on the evaluation dataset set aside for each of the model training sites.

The prediction performance of a non-machine learning baseline which predicts the soil moisture content at a particular day as the average soil moisture content of the three previous days is presented in Table 6. This is presented along with the prediction performance of the trained NN models. A model will only be accepted as skillful if its performance surpasses that of the non-machine learning baseline. This is considered a good practice for approaching predictive modelling tasks (Géron, 2017).

Table 6. Prediction performance of the non-machine learning (naïve) and neural network models when tested on the evaluation dataset for all the model training sites

Site	Model	Naive			FFNN			LSTM	
	R^2	MAE (m^3m^{-3})	$RMSE$ (m^3m^{-3})	R^2	MAE (m^3m^{-3})	$RMSE$ (m^3m^{-3})	R^2	MAE (m^3m^{-3})	$RMSE$ (m^3m^{-3})
Baluderry	0.89	0.02	0.03	0.94	0.01	0.01	0.95	0.01	0.01
Stoughton	0.88	0.02	0.03	0.97	0.01	0.01	0.97	0.01	0.01
Waddeston	0.92	0.01	0.02	0.99	0.01	0.01	0.99	0.01	0.01

Table 6 shows that both the FFNN and LSTM outperform the non-machine learning (naïve) baseline across all the sites. Therefore, the NN models can be accepted as being skillful. The FFNN and LSTM models are also shown to achieve a comparable prediction performance across all the sites. However, it is interesting that the LSTM achieves a comparable performance to the FFNN without extensive pre-processing of input data. This highlights the ability of the LSTM to sufficiently learn the underlying function approximating dynamic data (Chauhan and Vig, 2015). This ability is particularly desirable because the data pre-processing pipeline applied for the FFNN required subjective human intervention which may not lead to an improvement in model performance for more complex dynamic systems.

The soil moisture predicted by the FFNN and LSTM models along with the observed soil moisture content for the evaluation dataset is presented in Figure 6. Figure 6 shows that the LSTM models are able to accurately model the soil moisture dynamics while capturing its dominant modes. The LSTM models are also able to respond to perturbation from the precipitation input shown in the stem plots. Again, it is clear that the LSTM model is able to achieve a performance comparable to that of the FFNN with minimal input data pre-processing.

There have been previous attempts in literature to model the soil moisture dynamics and predict the soil moisture content in order to aid irrigation scheduling. In Delgoda et al. (2014) the authors presented a linear dynamic model with assumptions made on the absence of saturation flows. This lead to a degradation in the modelling results. The saturation flows are a nonlinear function of the soils hydraulic properties (Mashayekhi et al., 2016). The LSTM models presented in this study are able to implicitly learn such nonlinear relations during training. This is done during the adjustment of the network weights in order to define a function relating the climatic and precipitation inputs to the soil

moisture content. Since soil moisture depends on the balance between water input and output, saturation flows have been incorporated in the LSTM model. In Lozoya et al. (2016) the authors highlighted the need to parametrize several linear dynamics models for the prediction of soil moisture content for any particular site. This was attributed to the differing dynamics at saturation, available water content and below the permanent wilting point. The LSTM models are able to model these nonlinearities for the entire range of a sites soil moisture content. The use of a single model for the entire range of operation of a process is usually favored for decision support purposes because of the need to ensure simple debugging and test procedures (Qin and Badgwell, 2003). This may become complex when several models are used as part of a decision support system. This gives further evidence in favor of the application of the LSTM models for the purpose of soil moisture prediction and irrigation scheduling.

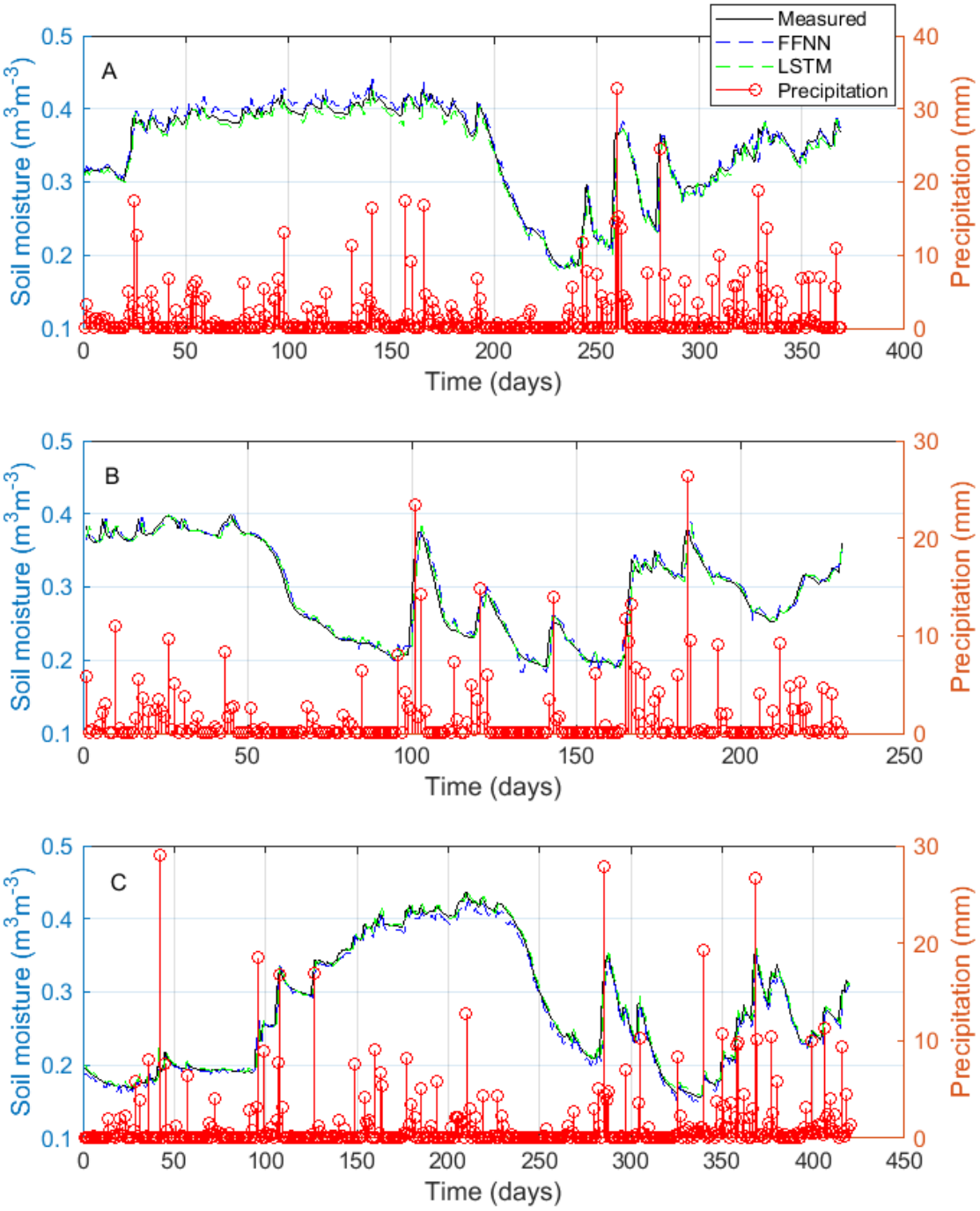

Figure 6. Measured soil moisture content and soil moisture content predicted by the feedforward neural network (FFNN) and the long short-term memory network (LSTM) using the evaluation dataset for the three training sites (A) Baluderry (B) Stoughton (C) Waddeston

4.3 Prediction performance in the independent sites

For the purpose of irrigation scheduling, it may be necessary to predict the soil moisture content for a new site for which historical data required to train a NN model is not available. The predictions will be generated using the climatic and soil variables of the new site as input into a model trained exclusively with data from another site. As such, the ability of the LSTM models to generate soil moisture predictions for independent sites using models from the training sites was evaluated. The prediction performance of the trained LSTM and FFNN models for these independent sites is presented in Table 7.

Table 7. Prediction performance of the neural network models for the independent sites

		Independent Site 1			Independent Site 2		
Models	Training Site	R^2	MAE (m^3m^{-3})	$RMSE$ (m^3m^{-3})	R^2	MAE (m^3m^{-3})	$RMSE$ (m^3m^{-3})
FFNN	Baluderry	0.74	0.04	0.07	0.93	0.01	0.01
	Stoughton	0.94	0.01	0.01	0.96	0.01	0.01
	Waddeston	0.95	0.01	0.01	0.94	0.01	0.01
LSTM	Baluderry	0.92	0.01	0.01	0.98	0.01	0.01
	Stoughton	0.96	0.01	0.01	0.98	0.01	0.01
	Waddeston	0.98	0.01	0.01	0.97	0.01	0.01

Table 7 shows that the LTSM models generate accurate predictions for the independent sites and these predictions outperform those generated by the FFNN in terms of R^2 scores. This is because of the dynamic nature of the LSTM which enables it to generate predictions as a function of model inputs and state maintained for a learned past time period. Table 7 also shows that the FFNN is unable to achieve a good prediction performance when the model trained in Baluderry was applied for prediction in independent site 1. This may be because the data pre-processing steps applied on the training data were not applicable to the data of independent site 1. This further highlights the robustness of the LSTM model which is able to sufficiently learn the underlying function approximating the dynamic data. The data in Table 7 demonstrates the excellent approximation ability of the LSTM which makes them useful for generating prediction for processes with an underlying dynamics similar to the process they were trained on. This approximation ability of the LSTM has been widely exploited in the field of time series

forecasting where a single LSTM model is trained to predict data points for a group of time series belonging a common cluster (Kobayashi and Shirayama, 2017).

The applicability of data-driven models trained for a particular site for prediction in a different site will further enhance the precision water management of various crops. Navarro-Hellín et al. (2016) showed that models which are able to generalize to new sites not included in the model development are difficult to realize using traditional machine learning methods. The excellent generalization ability of the LSTM presents an opportunity for the development of multi-site soil moisture prediction models as demonstrated by the robust performance of the LSTM models presented in this study when tested on the independent sites.

4.4 Application in predictive irrigation scheduling

In this study, the purpose of modelling the soil moisture dynamics is to generate predictions of the volumetric soil moisture content which is required for predictive irrigation scheduling. As such, the LSTM model developed for each of the training sites was applied as part of a predictive irrigation scheduling system, which was evaluated alongside a rule-based system using AQUACROP simulations of the potato-growing season. The resulting soil moisture deficit for the predictive and rule-based systems, and the lower bound deficit during simulations for the three training sites are shown in Figure 7.

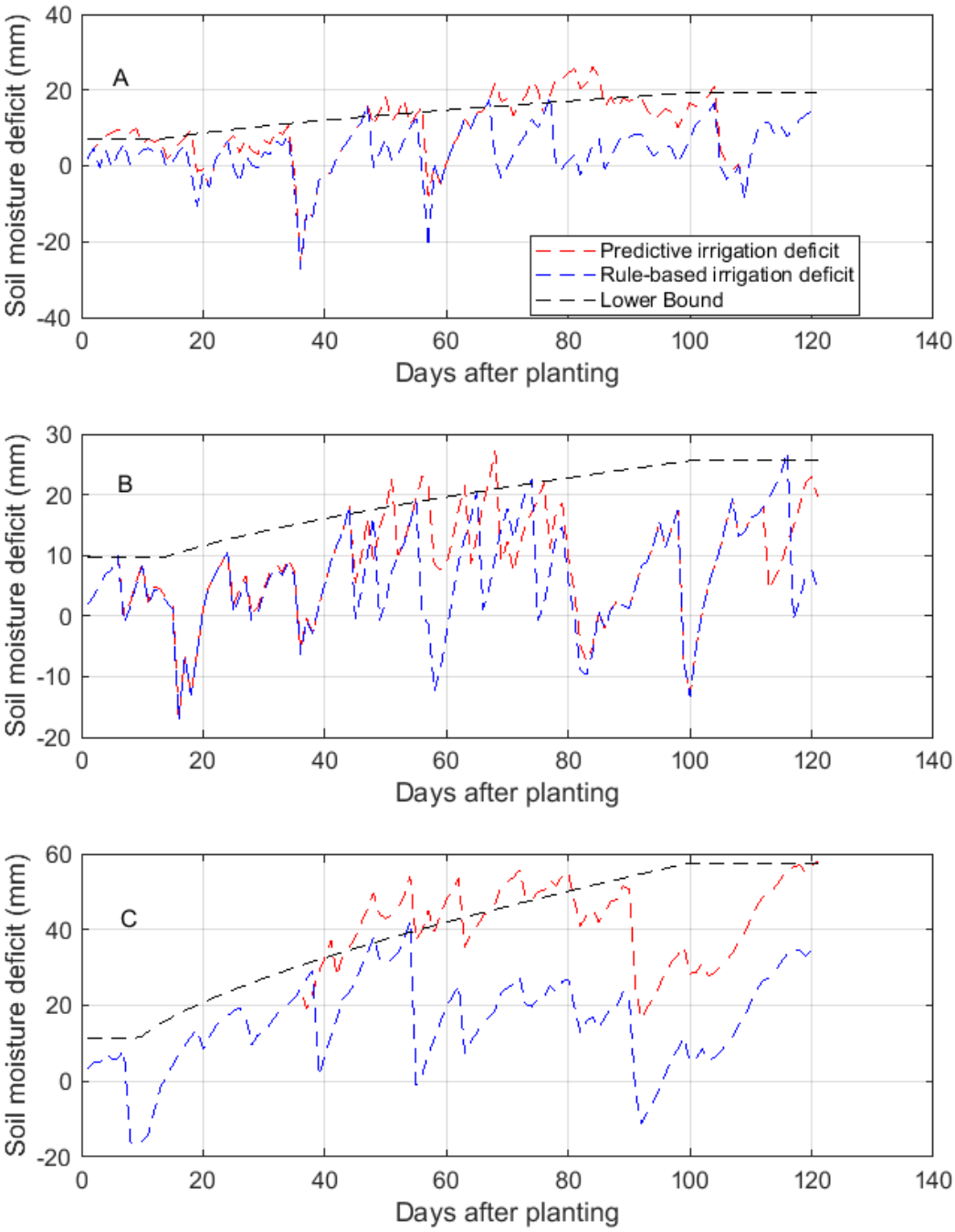

Figure 7. Comparison between the predictive and rule-based irrigation scheduling system for AQUACROP simulations of the potato-growing season on the three model training sites. (A) Baluderry (B) Stoughton (C) Waddeston

It should be noted that the negative deficit values in Figure 7 indicate soil moisture values above the field capacity, hence overwatering. Figure 7 shows that in the heavy textured clay site (Waddeston), the predictive system violates the lower bound threshold during the mid-growing season. This occurred because the LSTM model applied in predicting the soil moisture content was not trained specifically for the potato crop. The high mid-season

water demand of potato altered the dynamics learned by the model. Nevertheless, it is seen that the deficits are close to the lower bound threshold and they are later minimized. It can also be seen that across all sites, the rule-based system tends to over-irrigate as indicated by the negative deficit values. Overall, the predictive system is able to maintain the soil moisture deficits within the allowable range and it is able to account for the change in crop water requirements over the growing season.

The total water applied during the growing season along with the simulated crop yield and water use efficiency (WUE) is summarized in Table 8.

Table 8. Total irrigation application depth along with the simulated crop yield and water use efficiency for the potato growing season

Site	Total irrigation (mm)		Yield (ton/ha)		WUE (kgm^{-3})	
	Predictive system	Rule-based system	Predictive system	Rule-based system	Predictive system	Rule-based system
Baluderry	69.50	129.80	12.64	12.64	4.08	3.93
Stoughton	141	177.20	12.64	12.64	3.68	3.68
Waddeston	55	79.90	12.64	12.64	3.82	3.85

It can be seen from Table 8 that the predictive system consistently applied less irrigation depths when compared with the rule-based system. The predictive system achieved a water saving of 46% in Baluderry, 20% in Stoughton and 31% in Waddeston. The predictive system also achieved a yield and water use efficiency (WUE) similar to that of the rule-based system. These results confirm that the predictive system is suitable for irrigation scheduling and it is able to improve water conservation.

5 Conclusions

The precise water management of crops will immensely benefit from automated decision support systems which integrate climatic and soil moisture measurements with a robust data-driven model of the soil moisture dynamics. This technology development will facilitate the prediction of crop water needs and an improvement in water conservation.

This paper has presented a dynamic neural network approach for modelling the time series of soil moisture content. The performance of the long short-term memory network (LSTM) for the prediction of soil moisture content was evaluated for three sites with

different soil characteristics. Using an independent evaluation dataset, the LSTM models developed for the sites achieved accuracies ($R^2 > 0.94$) for a one-day ahead prediction. The LSTM models also generated accurate soil moisture predictions for independent sites not used in training the models.

The use of the LSTM models in predictive irrigation scheduling was also demonstrated using AQUACROP simulations of the potato-growing season. The performance of the proposed predictive irrigation scheduling system was evaluated by comparing its irrigation policies to those of a rule-based system. The predictive system was able to maintain the soil moisture deficit within allowable limits for the most part of the simulated growing season while minimizing over-irrigation. Furthermore, the predictive system was able to achieve a yield and WUE similar to that achieved by the rule-based system using less irrigation application depths.

For future research, the predictive system should be extended to include rainfall forecasts. This will ensure that irrigation is optimized to further increase water savings through the maximum utilization of forecasted rainfall depths. The development of crop specific LSTM models trained on a rich dataset obtained from sites with similar soil types will enhance the adoption of data-driven soil moisture models for use in irrigation scheduling applications.

References

Adeyemi, O., Grove, I., Peets, S., Norton, T., 2017. Advanced Monitoring and Management Systems for Improving Sustainability in Precision Irrigation. Sustainability 9, 1–29. https://doi.org/10.3390/su9030353

Akumaga, U., Tarhule, A., Yusuf, A.A., 2017. Validation and testing of the FAO AquaCrop model under different levels of nitrogen fertilizer on rainfed maize in Nigeria, West Africa. Agric. For. Meteorol. 232, 225–234. https://doi.org/10.1016/j.agrformet.2016.08.011

Ali, M.H., Talukder, M.S.U., 2001. Methods or Approaches of Irrigation Scheduling – An Overview. J. Inst. Eng. 28, 11–23.

Alvino, A., Marino, S., 2017. Remote Sensing for Irrigation of Horticultural Crops. Horticulturae 3, 40. https://doi.org/10.3390/horticulturae3020040

Ben Taieb, S., Bontempi, G., Atiya, A.F., Sorjamaa, A., 2012. A review and comparison of strategies for multi-step ahead time series forecasting based on the NN5 forecasting competition. Expert Syst. Appl. 39, 7067–7083. https://doi.org/10.1016/j.eswa.2012.01.039

Box, G.E.P., Cox, D.R., 1964. An Analysis of Transformations. J. R. Stat. Soc. 26, 211–252.

Brezak, D., Bacek, T., Majetic, D., Kasac, J., Novakovic, B., 2012. A comparison of feed-forward and recurrent neural networks in time series forecasting, in: 2012 IEEE Conference on Computational Intelligence for Financial Engineering & Economics (CIFEr). New York, USA, pp. 1–6. https://doi.org/10.1109/CIFEr.2012.6327793

Capraro, F., Patiño, D., Tosetti, S., Schugurensky, C., 2008. Neural network-based irrigation control for precision agriculture, in: Proceedings of 2008 IEEE International

Conference on Networking, Sensing and Control, ICNSC. Sanya, China, pp. 357–362. https://doi.org/10.1109/ICNSC.2008.4525240

Chai, T., Draxler, R.R., 2014. Root mean square error (RMSE) or mean absolute error (MAE)? -Arguments against avoiding RMSE in the literature. Geosci. Model Dev. 7, 1247–1250. https://doi.org/10.5194/gmd-7-1247-2014

Chauhan, S., Vig, L., 2015. Anomaly detection in ECG time signals via deep long short-term memory networks, in: Proceedings of the 2015 IEEE International Conference on Data Science and Advanced Analytics, DSAA 2015. Paris, France. https://doi.org/10.1109/DSAA.2015.7344872

Chollet, F., 2015. Keras.

Cleveland, R.B., Cleveland, W.S., McRae, J.E., Terpenning, I., 1990. STL: A seasonal-trend decomposition procedure based on loess. J. Off. Stat. https://doi.org/citeulike-article-id:1435502

Crone, S.F., Hibon, M., Nikolopoulos, K., 2011. Advances in forecasting with neural networks? Empirical evidence from the NN3 competition on time series prediction. Int. J. Forecast. 27, 635–660. https://doi.org/10.1016/j.ijforecast.2011.04.001

Dahl, G.E., Sainath, T.N., Hinton, G.E., 2013. Improving deep neural networks for LVCSR using rectified linear units and dropout, in: 2013 IEEE International Conference on Acoustics, Speech and Signal Processing. IEEE, Vancouver, BC, Canada. https://doi.org/10.1109/icassp.2013.6639346

Delgoda, D., Malano, H., Saleem, S.K., Halgamuge, M.N., 2016. Irrigation control based on model predictive control (MPC): Formulation of theory and validation using weather forecast data and AQUACROP model. Environ. Model. Softw. 78, 40–53. https://doi.org/10.1016/j.envsoft.2015.12.012

Delgoda, D., Saleem, S.K., Malano, H., Halgamuge, M.N., 2014. Root zone soil moisture prediction models based on system identification: Formulation of the theory and validation using field and AQUACROP data. Agric. Water Manag. 163, 344–353. https://doi.org/10.1016/j.agwat.2015.08.011

Deng, J., Chen, X., Du, Z., Zhang, Y., 2011. Soil Water Simulation and Predication Using Stochastic Models Based on LS-SVM for Red Soil Region of China. Water Resour. Manag. 25, 2823–2836. https://doi.org/10.1007/s11269-011-9840-z

Desilets, D., Zreda, M., Ferré, T.P.A., 2010. Nature's neutron probe: Land surface hydrology at an elusive scale with cosmic rays. Water Resour. Res. 46, 1–7. https://doi.org/10.1029/2009WR008726

Evans, R.G., LaRue, J., Stone, K.C., King, B.A., 2013. Adoption of site-specific variable rate sprinkler irrigation systems. Irrig. Sci. 31, 871–887. https://doi.org/10.1007/s00271-012-0365-x

Franz, T.E., Zreda, M., Rosolem, R., Ferre, T.P.A., 2013. A universal calibration function for determination of soil moisture with cosmic-ray neutrons. Hydrol. Earth Syst. Sci. 17, 453–460. https://doi.org/10.5194/hess-17-453-2013

Funahashi, K., Nakamura, Y., 1993. Approximation of dynamical systems by continuous time recurrent neural networks. Neural Networks 6, 801–806. https://doi.org/10.1016/S0893-6080(05)80125-X

Gandhi, N., Petkar, O., Armstrong, L.J., 2016. Rice crop yield prediction using Artificial Neural Networks, in: IEEE International Conference on Technological Innovations in ICT For Agriculture and Rural Development. Chennai, India, pp. 105–110.

Géron, A., 2017. Hands-On Machine Learning with Scikit-Learn and TensorFlow, 1st ed. O'Reilly Media, Sebastopol. https://doi.org/10.3389/fninf.2014.00014

Giusti, E., Marsili-Libelli, S., 2015. A Fuzzy Decision Support System for irrigation and water conservation in agriculture. Environ. Model. Softw. 63, 73–86. https://doi.org/10.1016/j.envsoft.2014.09.020

Gonzalez-Dugo, V., Zarco-Tejada, P., Nicolás, E., Nortes, P.A., Alarcón, J.J., Intrigliolo, D.S., Fereres, E., 2013. Using high resolution UAV thermal imagery to assess the variability in the water status of five fruit tree species within a commercial orchard. Precis. Agric. 14, 660–678. https://doi.org/10.1007/s11119-013-9322-9

Goodfellow, I., Bengio, Y., Courville, A., 2016. Deep Learning. MIT Press, Cambridge, MA.

Graves, A., Mohamed, A. R., Hinton, G., 2013. Speech recognition with deep recurrent neural networks, in: 2013 IEEE International Conference on Acoustics, Speech and Signal Processing. Vancouver, BC, Canada, pp. 6645–6649. https://doi.org/10.1109/ICASSP.2013.6638947

Gu, J., Yin, G., Huang, P., Guo, J., Chen, L., 2017. An improved back propagation neural network prediction model for subsurface drip irrigation system. Comput. Electr. Eng. 60, 58–65. https://doi.org/10.1016/j.compeleceng.2017.02.016

Guo, W.W., Xue, H., 2014. Crop yield forecasting using artificial neural networks: A comparison between spatial and temporal models. Math. Probl. Eng. 2014. https://doi.org/10.1155/2014/857865

Hedley, C., Yule, I., 2009. Soil water status mapping and two variable-rate irrigation scenarios. Precis. Agric. 10, 342–355. https://doi.org/10.1007/s11119-009-9119-z

Hedley, C.B., Knox, J.W., Raine, S.R., Smith, R., 2014. Water: Advanced Irrigation Technologies. Encycl. Agric. Food Syst. 5, 378–406. https://doi.org/http://dx.doi.org/10.1016/B978-0-444-52512-3.00087-5

Hochreiter, S., 1998. The Vanishing Gradient Problem During Learning Recurrent Neural Nets and Problem Solutions. Int. J. Uncertainty, Fuzziness Knowledge-Based Syst. 06, 107–116. https://doi.org/10.1142/s0218488598000094

Hochreiter, S., Schmidhuber, J., 1997. Long Short-Term Memory. Neural Comput. 9, 1735–1780. https://doi.org/10.1162/neco.1997.9.8.1735

Hong, Z., Kalbarczyk, Z., Iyer, R.K., 2016. Using a wireless sensor network and machine learning techniques, in: 2016 IEEE International Conference on Smart Computing (SMARTCOMP). St. Louis, MO.

Hsiao, T.C., Heng, L., Steduto, P., Rojas-Lara, B., Raes, D., Fereres, E., 2009. Aquacrop-The FAO crop model to simulate yield response to water: III. Parameterization and testing for maize. Agron. J. 101, 448–459. https://doi.org/10.2134/agronj2008.0218s

Joorabchi, A., Zhang, H., Blumenstein, M., 2009. Application of artificial neural networks to groundwater dynamics in coastal aquifers. J. Coast. Res. 2009, 966–970.

Karandish, F., Šimůnek, J., 2016. A comparison of numerical and machine-learning modeling of soil water content with limited input data. J. Hydrol. 543, 892–909. https://doi.org/10.1016/j.jhydrol.2016.11.007

Khan, M.S., Coulibaly, P., 2006. Bayesian neural network for rainfall-runoff modeling. Water Resour. Res. 42, 1–18. https://doi.org/10.1029/2005WR003971

Kim, D., Kaluarachchi, J., 2015. Validating FAO AquaCrop using Landsat images and regional crop information. Agric. Water Manag. 149, 143–155. https://doi.org/10.1016/j.agwat.2014.10.013

King, B.A., Shellie, K.C., 2016. Evaluation of neural network modeling to predict non-water-stressed leaf temperature in wine grape for calculation of crop water stress index. Agric. Water Manag. 167, 38–52. https://doi.org/10.1016/j.agwat.2015.12.009

Kingma, D.P., Ba, J., 2015. Adam: A Method for Stochastic Optimization, in: International Conference on Learning Representations. San Diego, USA.

Kobayashi, S., Shirayama, S., 2017. Time Series Forecasting with Multiple Deep Learners: Selection from a Bayesian Network. J. Data Anal. Inf. Process. 05, 115–130. https://doi.org/10.4236/jdaip.2017.53009

Linker, R., Ioslovich, I., Sylaios, G., Plauborg, F., Battilani, A., 2016. Optimal model-based deficit irrigation scheduling using AquaCrop: A simulation study with cotton, potato and tomato. Agric. Water Manag. 163, 236–243. https://doi.org/10.1016/j.agwat.2015.09.011

Liu, D., Yu, Z., Lü, H., 2010. Data assimilation using support vector machines and ensemble Kalman filter for multi-layer soil moisture prediction. Water Sci. Eng. 3, 361–377. https://doi.org/10.3882/j.issn.1674-2370.2010.04.001

Lozoya, C., Mendoza, C., Aguilar, A., Román, A., Castelló, R., 2016. Sensor-Based Model Driven Control Strategy for Precision Irrigation. J. Sensors 2016.

Marin, J., Parra, L., Rocher, J., Sendra, S., Lloret, J., Mauri, P. V, Masaguer, A., 2018. Urban Lawn Monitoring in Smart City Environments. J. Sensors 2018. https://doi.org/10.1155/2018/8743179

Mashayekhi, P., Ghorbani-Dashtaki, S., Mosaddeghi, M.R., Shirani, H., Nodoushan, A.R.M., 2016. Different scenarios for inverse estimation of soil hydraulic parameters from double-ring infiltrometer data using HYDRUS-2D/3D. Int. Agrophysics 30, 203–210. https://doi.org/10.1515/intag-2015-0087

McCarthy, A.C., Hancock, N.H., Raine, S.R., 2014. Simulation of irrigation control strategies for cotton using Model Predictive Control within the VARIwise simulation framework. Comput. Electron. Agric. 101, 135–147. https://doi.org/10.1016/j.compag.2013.12.004

McCarthy, A.C., Hancock, N.H., Raine, S.R., 2013. Advanced process control of irrigation: The current state and an analysis to aid future development. Irrig. Sci. 31, 183–192. https://doi.org/10.1007/s00271-011-0313-1

Mikolov, T., Kombrink, S., Burget, L., Černocký, J., Khudanpur, S., 2011. Extensions of recurrent neural network language model, in: 2011 IEEE International Conference on Acoustics, Speech and Signal Processing (ICASSP). Prague, Czech Republic, pp. 5528–5531. https://doi.org/10.1109/ICASSP.2011.5947611

Monaghan, J.M., Daccache, A., Vickers, L.H., Hess, T.M., Weatherhead, E.K., Grove, I.G., Knox, J.W., 2013. More “crop per drop”: Constraints and opportunities for precision irrigation in European agriculture. J. Sci. Food Agric. 93, 977–980. https://doi.org/10.1002/jsfa.6051

Morillo, J.G., Martín, M., Camacho, E., Díaz, J. A. R., Montesinos, P., 2015. Toward precision irrigation for intensive strawberry cultivation. Agric. Water Manag. 151, 43–51. https://doi.org/10.1016/j.agwat.2014.09.021

Navarro-Hellín, H., Martínez-del-Rincon, J., Domingo-Miguel, R., Soto-Valles, F., Torres-Sánchez, R., 2016. A decision support system for managing irrigation in agriculture. Comput. Electron. Agric. 124, 121–131. https://doi.org/10.1016/j.compag.2016.04.003

Nesa Sudha, M., Valarmathi, M.L., Babu, A.S., 2011. Energy efficient data transmission in automatic irrigation system using wireless sensor networks. Comput. Electron. Agric. 78, 215–221. https://doi.org/10.1016/j.compag.2011.07.009

Ordóñez, J.F., Roggen, D., 2016. Deep Convolutional and LSTM Recurrent Neural Networks for Multimodal Wearable Activity Recognition. Sensors . https://doi.org/10.3390/s16010115

Pardossi, A., Incrocci, L., 2011. Traditional and New Approaches to Irrigation Scheduling in Vegetable Crops. Horttechnology 21, 309–313.

Park, Y., Shamma, J.S., Harmon, T.C., 2009. A Receding Horizon Control algorithm for adaptive management of soil moisture and chemical levels during irrigation. Environ. Model. Softw. 24, 1112–1121. https://doi.org/10.1016/j.envsoft.2009.02.008

Parra, L., Rocher, J., García, L., Lloret, J., Tomás, J., Romero, O., Rodilla, M., Falco, S., Sebastiá, M.T., Mengual, J., González, J.A., Roig, B., 2018. Design of a WSN for smart irrigation in citrus plots with fault-tolerance and energy-saving algorithms. Netw. Protoc. Algorithms 10, 95–115. https://doi.org/10.5296/npa.v10i2.13205

Pascanu, R., Mikolov, T., Bengio, Y., 2013. On the difficulty of training Recurrent Neural Networks, in: Proceedings of the 30th International Conference on Ma- Chine Learning. Georgia, USA. https://doi.org/10.1109/72.279181

Payero, J.O., Irmak, S., 2006. Variable upper and lower crop water stress index baselines for corn and soybean. Irrig. Sci. 25, 21–32. https://doi.org/10.1007/s00271-006-0031-2

Perez-Ortola, M., Daccache, A., Hess, T.M., Knox, J.W., 2015. Simulating impacts of irrigation heterogeneity on onion (Allium cepa L.) yield in a humid climate. Irrig. Sci. 33, 1–14. https://doi.org/10.1007/s00271-014-0444-2

Pulido-Calvo, I., Gutiérrez-Estrada, J.C., 2009. Improved irrigation water demand forecasting using a soft-computing hybrid model. Biosyst. Eng. 102, 202–218. https://doi.org/10.1016/j.biosystemseng.2008.09.032

Pulido-Calvo, I., Roldan, J., Lopez-Luque, R., Gutierrez-Estrada, J.C., 2003. Demand Forecasting for Irrigation Water Distribution Systems. Irrig. Drain. Eng. 129, 270–277. https://doi.org/10.1061/(ASCE)0733-9437(2003)129

Qin, J., Badgwell, T., 2003. A survey of industrial model predictive control technology. Control Eng. Pract. 11, 733–764.

Raes, D., Steduto, P., Hsiao, T.C., Fereres, E., 2009. Aquacrop-The FAO crop model to simulate yield response to water: II. main algorithms and software description. Agron. J. 101, 438–447. https://doi.org/10.2134/agronj2008.0140s

Raine, S.R., Meyer, W.S., Rassam, D.W., Hutson, J.L., Cook, F.J., 2007. Soil-water and solute movement under precision irrigation: Knowledge gaps for managing sustainable root zones. Irrig. Sci. 26, 91–100. https://doi.org/10.1007/s00271-007-0075-y

Ro-Hellín, H., Torres-Sánchez, R., Soto-Valles, F., Albaladejo-Pérez, C., López-Riquelme, J. A., Domingo-Miguel, R.N., 2015. A wireless sensors architecture for efficient irrigation water management. Agric. Water Manag. 151, 64–74. https://doi.org/10.1016/j.agwat.2014.10.022

Romano, N., D'Urso, G., Severino, G., Chirico, G.B., Palladino, M., Majone, B., Viani, F., Filippi, E., Bellin, a., Massa, a., Toller, G., Robol, F., Salucci, M., 2013. Wireless Sensor Network Deployment for Monitoring Soil Moisture Dynamics at the Field Scale. Procedia Environ. Sci. 19, 426–435. https://doi.org/10.1016/j.proenv.2013.06.049

Rumelhart, D.E., Hinton, G.E., Williams, R.J., 1986. Learning representations by back-propagating errors. Nature 323, 533–536. https://doi.org/10.1038/323533a0

Saleem, S.K.., Delgoda, D.., Ooi, S.K.., Dassanayake, K.B.., Yue, L.., Halmamuge, M.., Malano, H., 2013. Model Predictive Control for Real-Time Irrigation Scheduling, in: IFAC Conference on Modelling and Control in Agriculture, Horticulture and Post Harvest Industry. IFAC, Espoo, Finland, pp. 299–304. https://doi.org/10.3182/20130828-2-SF-3019.00062

Sarkar, A., Kumar, R., 2012. Artificial Neural Networks for Event Based Rainfall-Runoff Modeling. J. Water Resour. Prot. 04, 891–897. https://doi.org/10.4236/jwarp.2012.410105

Shuttleworth, W.J., Zreda, M., Zeng, X., Zweck, C., Ferré, T.P.A., 2010. The COsmic-ray Soil Moisture Observing System (COSMOS): a non-invasive, intermediate scale soil moisture measurement network, in: Proceedings of the British Hydrological Society's Third International Symposium:"Role of Hydrology in Managing Consequences of a Changing Global Environment",. Newcastle, UK, pp. 19–23. https://doi.org/10.7558/bhs.2010.ic111

Smith, R.J., Baillie, J.N., Futures, I., 2009. Defining precision irrigation : A new approach to irrigation management, in: Irrigation and Drainage Conference. Victoria, Australia, pp. 18–21.

Steduto, P., Hsiao, T.C., Raes, D., Fereres, E., 2009. Aquacrop-the FAO crop model to simulate yield response to water: I. concepts and underlying principles. Agron. J. 101, 426–437. https://doi.org/10.2134/agronj2008.0139s

Stone, K.C., Bauer, P.J., Busscher, W.J., Millen, J.A., Evans, D.E., Strickland, E.E., 2015. Variable-rate irrigation management using an expert system in the eastern coastal plain. Irrig. Sci. 33, 167–175. https://doi.org/10.1007/s00271-014-0457-x

Sun, Y., Wendi, D., Kim, D.E., Liong, S.-Y., 2016. Technical note: Application of artificial neural networks in groundwater table forecasting - a case study in a Singapore swamp forest. Hydrol. Earth Syst. Sci. 20, 1405–1412. https://doi.org/10.5194/hess-20-1405-2016

Tsang, S.W., Jim, C.Y., 2016. Applying artificial intelligence modeling to optimize green roof irrigation. Energy Build. 127, 360–369. https://doi.org/10.1016/j.enbuild.2016.06.005

Wang, Y., Kirubakaran, V., Biao, H., 2017. A Long-Short Term Memory Recurrent Neural Network Based Reinforcement Learning Controller for Office Heating Ventilation and Air Conditioning Systems. Processes 5, 1–18. https://doi.org/10.3390/pr5030046

Werbos, P.J., 1990. Backpropagation through time: what it does and how to do it. Proc. IEEE 78, 1550–1560. https://doi.org/10.1109/5.58337

Young, P.C., 2006. The data-based mechanistic approach to the modelling, forecasting and control of environmental systems. Annu. Rev. Control 30, 169–182. https://doi.org/10.1016/j.arcontrol.2006.05.002

Yu Wang, 2017. A new concept using LSTM Neural Networks for dynamic system identification. 2017 Am. Control Conf. 5324–5329. https://doi.org/10.23919/ACC.2017.7963782

Zhang, J., Zhu, Y., Zhang, X., Ye, M., Yang, J., 2018. Developing a Long Short-Term Memory (LSTM) based model for predicting water table depth in agricultural areas. J. Hydrol. 561, 918–929. https://doi.org/10.1016/j.jhydrol.2018.04.065

Zreda, M., Shuttleworth, W.J., Zeng, X., Zweck, C., Desilets, D., Franz, T., Rosolem, R., 2012. COSMOS: The cosmic-ray soil moisture observing system. Hydrol. Earth Syst. Sci. 16, 4079–4099. https://doi.org/10.5194/hess-16-4079-2012

Chapter 6 General Conclusions

Precision irrigation holds the promise for the conservation of the world's scarce freshwater resources. However, there is a need to further improve the sustainability potential of this technology. This research focused on the critical elements of precision irrigation (measurement, monitoring, and management) and showed that adaptive decision support tools can leverage a synergistic combination of these critical elements to realize a robust precision irrigation scheduling system. Below are the general conclusions of this research.

Measurement

Monitoring of soil moisture content is perhaps the most leveraged measurement for scheduling irrigation both in field-scale and protected crop cultivation (Romano, 2014). Therefore, the availability of reliable data from soil moisture sensors is an important requirement for the realization of robust irrigation scheduling decisions. Chapter 2 of this study has shown that the reliability of data acquired from dielectric soil moisture sensors is only assured when the various factors affecting their performance is considered prior to their deployment.

The results presented in the study shows that the accuracy of dielectric soil moisture sensors in various soil types can be improved when they are deployed using soil specific calibration equations developed in either the field or laboratory. Overall, this process will improve the reliability of data available to inform precision irrigation scheduling decisions.

Significant variations in bulk density due to compaction will reduce the accuracy of dielectric soil moisture sensors. However, calibration equations developed at the compaction level obtainable in the field in which they will be deployed will generally improve their accuracy.

The dielectric soil moisture sensors tested in this study were marginally affected by increasing temperature in a non-saline light and heavy textured soil respectively. However, an empirical temperature compensation procedure was demonstrated to improve their overall accuracy. The temperature compensation procedure is important, as the range of soil moisture values where the sensors exhibited the highest sensitivity to temperature increase is critical for irrigation scheduling decisions. The data of the present study shows that these sensors are unable to achieve the accuracy required for agricultural purposes when operated in soils experiencing high temperature and salinity conditions. Therefore, in saline soils, a temperature compensation procedure is beneficial when deploying dielectric soil moisture sensors in order to assure data quality.

This study focused on the evaluation of dielectric soil moisture sensors under laboratory conditions. Further investigation is required in order to characterize the response of the sensors to dynamics wetting and drying events. This will form a basis for assessing the performance of the sensors during high-frequency irrigation events and applications where the soil moisture content experiences relatively short time constants. In such

applications, the availability of robust temporal soil moisture data sampled at high frequencies is required to guide irrigation scheduling decisions.

Adaptive monitoring and decision support systems

Adaptive monitoring and decision support tools are an important component of a robust precision irrigation system. These tools ensure that the overall precision irrigation system is able to account for the time-varying and stochastic crop response in order to adequately fulfill crop water requirements. Adaptive monitoring and decision support systems have been shown to improve the performance of manufacturing and chemical process systems (Qin and Badgwell, 2003). This gives evidence in favor of their application as technological tools for improving agricultural water management.

Chapter 3 of this study demonstrated a novel application of dynamic modelling for the prediction of the baseline temperatures which are required for the computation of the crop water stress index (CWSI). The baseline temperatures will vary as a result of crop growth limiting the application of the empirical CWSI proposed by Idso et al. (1981). The theoretical CWSI proposed by Jackson et al. (1981) however addresses the time-varying plant response by including an aerodynamic resistance parameter in its computation. This aerodynamic resistance is dependent on the plant and environmental temporal response, hence, making it a time-varying parameter. The computation of the theoretical CWSI requires extensive instrumentation and knowledge of crop physiology. These factors limit its practical application for irrigation scheduling (Maes and Steppe, 2012). Nevertheless, it has been demonstrated to provide an adequate indication of the plant water status (Osroosh et al., 2015).

The dynamic modelling approach presented in this study is able to account for the time-varying plant response in the prediction of the baseline temperatures. Results also show that the CWSI values computed using the predicted baseline temperatures are well correlated with theoretical CWSI values. The dynamic model requires easily measured plant and environmental variables (Leaf area index, solar radiation, vapour pressure deficit, air temperature) as inputs. This makes it a promising tool for irrigation scheduling applications where it is important to monitor the plant response to aid finely tuned water management. The CWSI has previously been demonstrated as a tool for guiding spatially varied water application (Shaughnessy et al., 2014). This suggests that the dynamic modelling approach for baseline temperature prediction is amenable for variable rate irrigation applications. The modelling approach can be adapted for field data. It is, however, important to account for the influence of varying wind speeds in such applications.

Chapter 4 of this study presents a novel data-driven dynamic modelling framework for real-time monitoring of the plant water status. This framework utilizes measurements and

model predictions of the crop transpiration to infer the plant water status. The dynamic modelling approach employed in the framework is able to account for the time-varying plant response. The proposed framework provides an intuitive means of monitoring the plant response to water deficits in order to aid irrigation scheduling decisions. It is directly applicable to protected crop production systems where the real-time transpiration dynamics can be monitored with lysimeters.

For field-scale deployment, a robust means of measuring the real-time spatiotemporal plant transpiration dynamics is required. Surface renewal analysis fulfills the temporal resolution requirements but it is unable to provide transpiration measurements at low spatial dimensions associated with irrigation management units. Fernández et al. (2008) demonstrated the use of sap-flow sensors for monitoring the plant transpiration dynamics in orchards. These sensors can be deployed in different irrigation management units due to their portability. The authors further demonstrated the potential of using the transpiration ratio as an irrigation scheduling tool. The transpiration ratio is obtained by dividing the transpiration measured on a target plant by the model predicted transpiration for a similar-sized well-watered plant. They, however, noted that the development of simplified transpiration prediction models is a requirement for the adoption of the transpiration ratio approach for scheduling irrigation. The dynamic modelling approach presents a simplified method for predicting crop transpiration.

The dynamic model can be parameterized for a crop at a desired water deficit level and the model predictions can be applied for irrigation management of other target plants to maintain that desired deficit. This will be beneficial for deficit irrigation applications. It should be noted that for spatially varied irrigation applications, a dynamic model would be parametrized for each of the identified irrigation management zones. Transpiration measurements would also be acquired in each management zone.

Management

The predictive irrigation scheduling system presented in chapter 5 demonstrates the use of data-driven models for improving irrigation management. The dynamic neural network model presented in this chapter is able to generate a one-day-ahead prediction of the soil moisture content. The predicted soil moisture content is then applied in predictive irrigation scheduling. The model inputs include routinely measured climatic variables that can be acquired from local weather stations. Furthermore, the dynamic neural network models are applicable to other sites with soil characteristics similar to the sites used in training the models. The availability of robust and scalable data-driven soil moisture prediction models will further contribute to the development of precision irrigation systems that are capable of the proactive fulfillment of crop water needs. Model-based irrigation scheduling systems have been shown to improve water management and crop growth (Delgoda et al., 2016; Giusti and Marsili-Libelli, 2015; McCarthy et al., 2014). This is

because the underlying models are able to assure a closed-loop control structure that adapts to soil and weather perturbations. This suggests that the adoption of model-based decision support systems will further contribute to the conservation of scarce freshwater resources.

The dynamic neural network model presented in this study has been demonstrated as robust to the stochastic soil-plant-atmosphere interactions. For variable rate irrigation applications, such models can be independently applied for predicting the soil moisture content in each irrigation management zone. Each management zone would be defined according to differing soil and crop properties across the field.

Collectively, this study has shown that

- The accuracy of dielectric soil moisture sensors can be improved with soil specific calibration equations. The negative effect of varying bulk density, salinity and temperature on sensor performance can be mitigated using empirical calibration procedures.
- A dynamic modelling approach can be applied for developing models which are able to predict the plant response to water supply in form of canopy temperature and transpiration. These models are able to account for the time-varying plant response. The dynamic models require minimal input parameters and are amenable for irrigation scheduling in commercial crop production.
- Dynamic neural network models can be used as part of a field scale predictive irrigation scheduling system. These models require minimal pre-processing of input data and are able to generate accurate volumetric soil moisture content predictions. Using model based simulations of the potato growing season, it was demonstrated that a dynamic neural network based predictive irrigation scheduling system is able to reduce irrigation water use without an adverse effect on crop yield

In conclusion, this study has demonstrated the applicability of data-driven dynamic models for adaptive monitoring, decision support and management purposes. The proposed adaptive monitoring and decision support tools can be combined to realize a synergistic sustainable precision irrigation system. This can be viewed as a real-time decision-making system that combines field variability, plant response, plant growth, atmospheric demand, and predictions of soil water availability to increase crop yield and water use efficiency while lowering the costs associated with irrigation and the corresponding environmental impacts (Veraa et al., 2017).

Recommendations for future study

The dynamic model for the prediction of the baseline temperatures presented in chapter 3 of this study was developed under greenhouse conditions. The modelling methodology is applicable to different environments and crops. Therefore, future research should focus on

the development of dynamic baseline temperature prediction models for field conditions. The simplicity and robustness associated with such models will further enhance the adoption of the CWSI as an irrigation scheduling tool.

The water status monitoring framework presented in chapter 4 can also be adapted for field conditions. However, this will be dependent on the availability of transpiration measurement sensors with high spatial and temporal resolutions. Presently, the sap flow sensor partly fulfills this requirement but a dense sensor deployment is required to achieve a high spatial resolution. Furthermore, commercial sap flow sensors are mostly designed for deployment on tree crops. Therefore, future research should focus on the development of robust and cost-effective sap flow sensors that can be deployed on various high-value crops.

The predictive irrigation scheduling system presented in chapter 5 was evaluated using simulations. The evaluation of similar systems adapted for various soil types and crops will be beneficial for further quantification of their sustainability potential. Future research should also focus on the development of crop and soil specific data-driven soil moisture prediction models. The predictive irrigation scheduling system presented in this study was designed to assure a short-term objective of maintaining a suitable soil moisture deficit. Based on the simulation results of McCarthy et al. (2014), field evaluation of predictive irrigation scheduling systems which are designed to maximize an end of season objective (e.g. final yield) will be beneficial for overall quantification of the sustainability improvement potential of model-based irrigation decision support.

References

Delgoda, D., Malano, H., Saleem, S.K., Halgamuge, M.N., 2016. Irrigation control based on model predictive control (MPC): Formulation of theory and validation using weather forecast data and AQUACROP model. Environ. Model. Softw. 78, 40–53. https://doi.org/10.1016/j.envsoft.2015.12.012

Fernández, J.E., Green, S.R., Caspari, H.W., Diaz-Espejo, A., Cuevas, M. V., 2008. The use of sap flow measurements for scheduling irrigation in olive, apple and Asian pear trees and in grapevines. Plant Soil 305, 91–104. https://doi.org/10.1007/s11104-007-9348-8

Giusti, E., Marsili-Libelli, S., 2015. A Fuzzy Decision Support System for irrigation and water conservation in agriculture. Environ. Model. Softw. 63, 73–86. https://doi.org/10.1016/j.envsoft.2014.09.020

Idso, S.B., Jackson, R.D., Pinter, P.J., Reginato, R.J., Hatfield, J.L., 1981. Normalizing the stress-degree-day parameter for environmental variability. Agric. Meteorol. 24, 45–55. https://doi.org/10.1016/0002-1571(81)90032-7

Jackson, R.D., Idso, S.B., Reginato, R.J., Pinter, P.J., 1981. Canopy temperature as a crop water stress indicator. Water Resour. Res. https://doi.org/10.1029/WR017i004p01133

Maes, W.H., Steppe, K., 2012. Estimating evapotranspiration and drought stress with ground-based thermal remote sensing in agriculture: a review. J. Exp. Bot. 63, 695–709. https://doi.org/10.1093/jxb/err313

McCarthy, A.C., Hancock, N.H., Raine, S.R., 2014. Simulation of irrigation control strategies for cotton using Model Predictive Control within the VARIwise simulation framework. Comput. Electron. Agric. 101, 135–147. https://doi.org/10.1016/j.compag.2013.12.004

Osroosh, Y., Troy Peters, R., Campbell, C.S., Zhang, Q., 2015. Automatic irrigation scheduling of apple trees using theoretical crop water stress index with an innovative dynamic threshold. Comput. Electron. Agric. 118, 193–203. https://doi.org/10.1016/j.compag.2015.09.006

Qin, J., Badgwell, T., 2003. A survey of industrial model predictive control technology. Control Eng. Pract. 11, 733–764.

Romano, N., 2014. Soil moisture at local scale: Measurements and simulations. J. Hydrol. 516, 6–20. https://doi.org/10.1016/j.jhydrol.2014.01.026

Shaughnessy, S.A.O., Evett, S.R., Colaizzi, P.D., 2014. Infrared Thermometry as a Tool for Site-Specific Irrigation Scheduling, in: Proceedings of the 26th Annual Central Plains Irrigation Conference. pp. 136–145.

Veraa, J., Abrisqueta, I., Conejero, W., Ruiz-Sánchez, M.C., 2017. Precise sustainable irrigation: A review of soil-plantatmosphere Monitoring. Acta Hortic. 1150, 195–200. https://doi.org/10.17660/ActaHortic.2017.1150.28